



M. H. Groschup  
H. A. Kretzschmar (eds.)

Prion Diseases

Diagnosis  
and Pathogenesis

**Springer-Verlag Wien GmbH**

Dr. Martin H. Groschup  
Institut für Immunologie,  
Bundesforschungsanstalt für Viruskrankheiten der Tiere,  
Tübingen, Germany

Prof. Dr. Hans A. Kretzschmar  
Institut für Neuropathologie, Ludwig-Maximilians-Universität,  
München, Germany

This work is subject to copyright.  
All rights are reserved, whether the whole or part of the material is concerned,  
specifically those of translation, reprinting, re-use of illustrations, broadcasting,  
reproduction by photocopying machines or similar means,  
and storage in data banks.

© 2000 Springer-Verlag Wien

Typesetting: Scientific Publishing Services (P) Ltd., Madras  
Printing: A. Holzhausens Nfg., A-1070 Wien  
Binding: Papyrus, A-1100 Wien

Graphic design: Ecke Bonk

Printed on acid-free and chlorine-free bleached paper

SPIN: 10772976

With 89 partly coloured Figures

CIP data applied for

**ISBN 978-3-211-83529-6      ISBN 978-3-7091-6308-5 (eBook)**  
**DOI 10.1007/978-3-7091-6308-5**

## **Preface**

More than fourteen years ago the first cases of bovine spongiform encephalopathy (BSE) were diagnosed in British cattle. In the course of a large epidemic, almost a million animals were infected and the majority were slaughtered in the preclinical stage. Thus the consumer was exposed to BSE infectivity until effective sanitary measures were implemented in the United Kingdom and elsewhere.

When the first cases of a new variant form of Creutzfeldt–Jakob disease (vCJD) were diagnosed in March 1996, transmission of BSE to humans was considered the most likely explanation because of its coincidence in time and geographical distribution in Europe. In the meantime, mouse transmission experiments and the molecular analysis of pathological prion protein deposited in the central nervous system of vCJD victims clearly support this hypothesis. Hence, BSE has been treated as a zoonotic disease since 1996, and additional measures have been implemented to protect consumer health.

A comprehensive understanding of prion diseases and their infectious agents is crucial for risk assessment as regards both animals and man, as well as for working out adequate control strategies. To further the communication of the current knowledge and the exchange of diagnostic technologies in the scientific community, a symposium on the ‘Characterization and Diagnosis of Prion Diseases’ was held from September 23–25, 1999 in Tübingen, Germany. This symposium was supported by funds made available by the EU Commission.

The overwhelming interest and the participation of more than 500 scientists from 26 countries at the symposium made it a success. Thirty-seven speakers were invited by the members of the Editorial Board (A. Aguzzi, J. Collinge, D. Dormont, M.H. Groschup, H.A. Kretzschmar and C. Weissmann) to give lectures on their most recent experimental results. More than 170 posters were displayed. Sixteen posters were selected for platform presentation.

In particular the following questions were addressed:

1. What are the key features of the pathogenesis of prion diseases in humans and animals?
2. Which molecular mechanisms determine prion transmissibility across species barriers?

3. What are the factors that influence susceptibility of the host species to disease?
4. Which animal and in-vitro models are currently available for the detection and quantification of prion infectivity?
5. Which diagnostic techniques allow the reliable investigation and confirmation of suspect cases in animals and humans?
6. What are the molecular and biological characteristics of prion strains?

In this volume, twenty-seven invited speakers comprehensively summarize answers to these questions. Although this selection cannot reflect the enormous spectrum and depth of prion research, it certainly illustrates the current state of the art in the field.

*Martin H. Groschup*  
*Hans A. Kretzschmar*

## Contents

### *Pathogenesis of Prion Diseases*

<b>Glatzel, M., Klein, M. A., Brandner, S., Aguzzi, A.:</b> Prions: from neurografts to neuroinvasion. . . . .	3
<b>Brown, K. L., Stewart, K., Ritchie, D., Fraser, H., Morrison, W. I., Bruce, M. E.:</b> Follicular dendritic cells in scrapie pathogenesis. . . . .	13
<b>Jeffrey, M., McGovern, G., Martin, S., Goodsir, C. M., Brown, K. L.:</b> Cellular and sub-cellular localisation of PrP in the lymphoreticular system of mice and sheep . . . . .	23
<b>Beringue, V., Lamoury, F., Adjou, K. T., Maignien, T., Demoy, M., Couvreur, P., Dormont, D.:</b> Pharmacological manipulation of early PrP <sup>res</sup> accumulation in the spleen of scrapie-infected mice . . . . .	39
<b>van Keulen, L. J. M., Schreuder, B. E. C., Vromans, M. E. W., Langeveld, J. P. M., Smits, M. A.:</b> Pathogenesis of natural scrapie in sheep. . . . .	57

### *Animal Models for Prion Diseases*

<b>Buschmann, A., Pfaff, E., Reifenberg, K., Müller, H. M., Groschup, M. H.:</b> Detection of cattle-derived BSE prions using transgenic mice overexpressing bovine PrP <sup>C</sup> . . . . .	75
<b>Campbell, S., Dench, U., Telling, G.:</b> Analyzing the influence of PrP primary structure on prion pathogenesis in transgenic mice . . . . .	87
<b>Manson, J. C., Barron, R., Jamieson, E., Baybutt, H., Tuzi, N., McConnell, I., Melton, D., Hope, J., Bostock, C.:</b> A single amino acid alteration in murine PrP dramatically alters TSE incubation time. . . . .	95
<b>Harris, D. A., Chiesa, R., Drisaldi, B., Quaglio, E., Migheli, A., Piccardo, P., Ghetti, B.:</b> A transgenic model of a familial prion disease . . . . .	103
<b>Scott, M. R., Supattapone, S., Nguyen, H.-O. B., DeArmond, S. J., Prusiner, S. B.:</b> Transgenic models of prion disease . . . . .	113

### *Epidemiology and Diagnosis of Prion Diseases*

<b>Heim, D., Wilesmith, J. W.:</b> Surveillance of BSE . . . . .	127
--	-----

<b>Budka, H.:</b> Histopathology and immunohistochemistry of human transmissible spongiform encephalopathies (TSEs) . . . . .	135
<b>Ironside, J. W.:</b> Pathology of variant Creutzfeldt–Jakob disease . . . . .	143
<b>Poser, S., Zerr, I., Schroeter, A., Otto, M., Giese, A., Steinhoff, B. J., Kretzschmar, H. A.:</b> Clinical and differential diagnosis of Creutzfeldt–Jakob disease . . . . .	153
<b>Giese, A., Bieschke, J., Eigen, M., Kretzschmar, H. A.:</b> Putting prions into focus: application of single molecule detection to the diagnosis of prion diseases. . . . .	161
<b>Schulz-Schaeffer, W. J., Fatzer, R., Vandeveld, M., Kretzschmar, H. A.:</b> Detection of PrP <sup>Sc</sup> in subclinical BSE with the paraffin-embedded tissue (PET) blot. . . . .	173
<b>Hunter, N., Goldmann, W., Marshall, E., O'Neill, G.:</b> Sheep and goats: natural and experimental TSEs and factors influencing incidence of disease. . . . .	181
<b>Oesch, B., Doherr, M., Heim, D., Fischer, K., Egli, S., Bolliger, S., Biffiger, K., Schaller, O., Vandeveld, M., Moser, M.:</b> Application of Prionics Western blotting procedure to screen for BSE in cattle regularly slaughtered at Swiss abattoirs. . . . .	189
<b>Grassi, J., Créminon, C., Frobert, Y., Frétier, P., Turbica, I., Rezaei, H., Hunsmann, G., Comoy, E., Deslys, J.-P.:</b> Specific determination of the proteinase K-resistant form of the prion protein using two-site immunometric assays. Application to the post-mortem diagnosis of BSE . . . . .	197
<i>Characterization of the Infectious Agent</i>	
<b>Chen, S. G., Zou, W., Parchi, P., Gambetti, P.:</b> PrP <sup>Sc</sup> typing by N-terminal sequencing and mass spectrometry . . . . .	209
<b>Groschup, M. H., Kuczius, T., Junghans, F., Sweeney, T., Bodemer, W., Buschmann, A.:</b> Characterization of BSE and scrapie strains/isolates .	217
<b>Safar, J., Cohen, F. E., Prusiner, S. B.:</b> Quantitative traits of prion strains are enciphered in the conformation of the prion protein . . . . .	227
<i>Structure and Function of PrP</i>	
<b>Kretzschmar, H. A., Tings, T., Madlung, A., Giese, A., Herms, J.:</b> Function of PrP <sup>C</sup> as a copper-binding protein at the synapse . . . . .	239
<b>Billeter, M., Wüthrich, K.:</b> The prion protein globular domain and disease-related mutants studied by molecular dynamics simulations .	251
<b>Post, K., Brown, D. R., Groschup, M. H., Kretzschmar, H. A., Riesner, D.:</b> Neurotoxicity but not infectivity of prion proteins can be induced reversibly in vitro . . . . .	265

*PrP Conversion*

**Demaimay, R., Chesebro, B., Caughey, B.:** Inhibition of formation of protease-resistant prion protein by Trypan Blue, Sirius Red and other Congo Red analogs . . . . . 277

**Vorberg, I., Pfaff, E., Groschup, M. H.:** The use of monoclonal antibody epitopes for tagging PrP in conversion experiments . . . . . 285

*Listed in Current Contents*

## **Pathogenesis of Prion Diseases**

## **Prions: from neurografts to neuroinvasion**

**M. Glatzel, M. A. Klein, S. Brandner, and A. Aguzzi**

Institute of Neuropathology, University Hospital Zurich, Zurich

**Summary.** Spongiform encephalopathies are infectious neurodegenerative diseases caused by pathogens that seem to be devoid of any informational nucleic acids. Histopathologically, these diseases are characterized by spongiform degeneration of the central nervous system. Although the main pathological changes during the course of the disease occur in the brain, the infectious agent accumulates early in lymphoid tissue. The consecutive development of clinical disease depends on the presence of an intact immune system including mature B-cells and follicular dendritic cells. In this article we review the state of knowledge on the routes of neuroinvasion used by the infectious agent in order to gain access to the central nervous system upon entry into extracerebral sites.

### **Introduction**

Prion diseases typically result in spongiform degeneration of the central nervous system (CNS), yet the entry point of the infectious agent (termed prion) is often through peripheral sites like the gastrointestinal tract. In this article we review the transport mechanisms of prions within the CNS and from the periphery to the CNS. Special emphasis is put on the role of the lymphoreticular system (LRS) and the peripheral nervous system (PNS).

### **Neurografts in prion research**

*Prnp*<sup>0/0</sup> mice show normal development and behavior [12, 36]. This fact has led to the hypothesis that scrapie pathology may come about because PrP<sup>Sc</sup> deposition is neurotoxic [17], rather than by depletion of cellular PrP<sup>C</sup> [14]. To study the question of neurotoxicity of PrP<sup>Sc</sup>, we exposed brain tissue of *Prnp*<sup>0/0</sup> mice to a continuous source of PrP<sup>Sc</sup>. This was done by grafting neural tissue overexpressing PrP<sup>C</sup> into the brain of PrP<sup>C</sup>-deficient mice using well-established protocols [25–27]. These mice were then intracerebrally inoculated with scrapie prions. As a result neuroectodermal grafts accumulated high levels of PrP<sup>Sc</sup> and infectivity and developed severe histopathological changes characteristic for scrapie (Fig. 1). In mice that

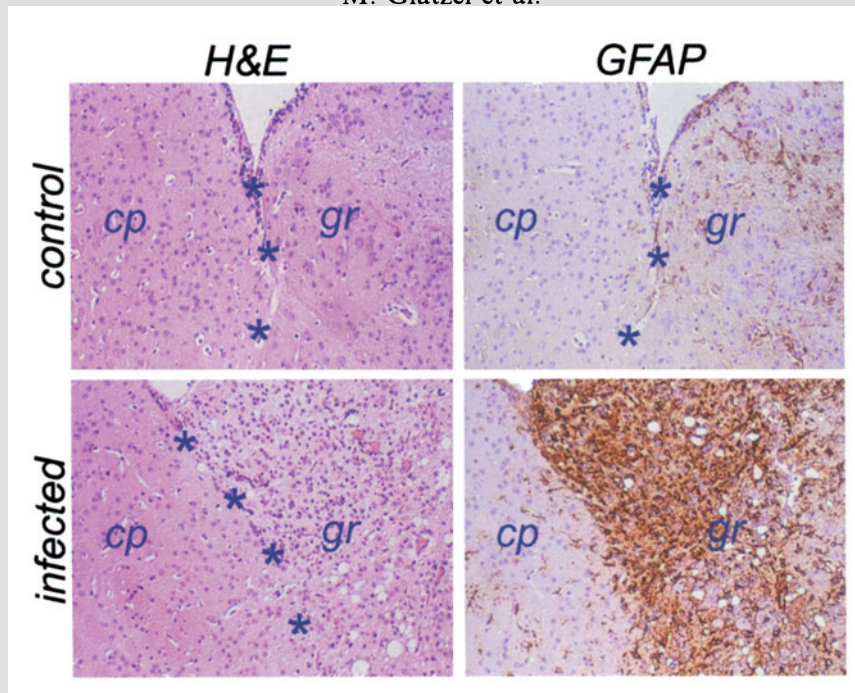


**Fig. 1.** Typical histological appearance of a PrP<sup>C</sup>-expressing graft (*gr*) (left) at the interface to the knockout host brain (*cp*) (right). Note the spongiform microcystic changes (left: hematoxylin-eosin) and the brisk astrocytic reaction evidenced by the immunocytochemical stain for glial fibrillary acidic protein (right: GFAP)

were sacrificed at later time points substantial amounts of graft-derived PrP<sup>Sc</sup> migrated into the host brain and even in areas distant from the grafts, substantial amounts of infectivity were detected [8, 16]. Nonetheless, even 16 months after transplantation and infection with prions, no pathological changes were detected in the PrP<sup>C</sup>-deficient tissue, not even in the immediate vicinity of the grafts or the PrP<sup>C</sup> deposits. These results suggest that PrP<sup>Sc</sup> is inherently non-toxic and opens the possibility that PrP<sup>Sc</sup> plaques found in spongiform encephalopathies may be an epiphenomenon rather than a cause of neuronal damage [1].

Because mice harboring a chronically scrapie-infected neural graft did not develop any signs of disease, they gave us the possibility to study changes occurring during the progression of scrapie disease in neuroectodermal tissue and were also an ideal model to assess the effects of prions on the surrounding tissue. Studying extremely late time points after infection with the scrapie agent was useful in order to observe phenomena that cannot be seen in PrP<sup>C</sup>-expressing mice because these mice develop clinical symptoms eventually leading to death earlier. With increasing length of the incubation time, grafts underwent progressive astrogliosis and spongiosis which was accompanied by loss of neuronal processes within the grafts and subsequent destruction of the neuropil. At the latest studied time point, 435 days after inoculation, grafts showed an increase of cellular density

probably due to astroglial proliferation and a complete loss of neurons [7]. The outcome of these studies confirmed several predictions about the pathogenesis of spongiform encephalopathies. In particular it appears that scrapie leads to selective neuronal loss, while astrocytes and perhaps other neuroectodermal cells can survive and maintain their phenotypic characteristics for very long periods of time.

### **Spread of prions in the central nervous system**

Intracerebral inoculation of scrapie-infected brain homogenates into suitable recipients is the most effective method for transmission of spongiform encephalopathies and may even facilitate circumvention of the species barrier. In the CNS axonal transport in the retino-tectal pathway was investigated by injecting prions intraocularly. This is a convenient and elegant way of studying neural spread of the agent within the CNS because the retina is a part of the CNS and intraocular injection does not cause direct physical trauma to the brain. Following intraocular injection of prions the first lesions were observed in the contralateral projections of the retino-tectal pathway [18]. The rate of spread within the CNS was calculated to be around 1 mm/day [30]. This speaks in favor of a common mechanism of transport operating in the PNS and CNS. The neurografting technique whereby a PrP<sup>C</sup>-expressing graft is placed in the brain of a PrP<sup>0/0</sup> mouse proved that PrP<sup>C</sup> expression is necessary for transport of the scrapie agent within the CNS. The graft did not develop pathological changes after intraocular injection of prions [9]. In one instance, the graft of an intraocularly inoculated mouse was assayed and found to be devoid of infectivity [9]. These results suggest that the intracerebral spread of prions is based on a PrP<sup>C</sup> paved chain of cells, perhaps because they are capable of supporting prion replication. In the case of a PrP<sup>0/0</sup> mouse this chain is interrupted and propagation can no longer take place. Whether the mode of transport is axonal or rather a domino stone-like spread occurs in which spreading of prions in the CNS occurs *per continuitatem* through conversion of PrP<sup>C</sup> to PrP<sup>Sc</sup> [2] is still unclear.

### **Spread of prions from extracerebral sites to the CNS, role of the LRS**

From an epidemiological point of view oral uptake of prions may be more relevant than intracerebral transmission, because it is thought to be responsible for the bovine spongiform encephalopathy epidemic and for transmission of bovine spongiform encephalopathy to a variety of species including humans [11, 23]. One of the main characteristics of prion diseases is the long incubation time. A possible explanation for this clinically silent incubation time is the multiplication of prions in 'reservoirs'. Likely candidates that could constitute this reservoir are parts of the PNS or the LRS.

Many studies point to the importance of prion replication in lymphoid organs which always precedes prion replication in the CNS, even if

infectivity is administered intracerebrally [15]. Infectivity can accumulate in all components of the LRS, including lymph nodes and intestinal Peyer's patches, where, in mice, prions replicate almost immediately after oral administration [31]. Recently, it was shown that new variant Creutzfeldt–Jakob disease prions accumulate in the lymphoid tissue of tonsils in such large amounts that PrP<sup>Sc</sup> can easily be detected with antibodies on histological sections [24]. A wealth of studies points to the importance of prion replication in lymphoid organs yet little is known about which cells support prion propagation in the LRS. Because treating mice with whole-body ionizing radiation after intraperitoneal infection does not change the incubation times it was suggested that the critical cells are long-lived [19]. The follicular dendritic cells (FDC) would be a prime candidate, and indeed PrP<sup>Sc</sup> accumulates in such cells of wild type and nude mice (which have a selective T-cell defect) [33]. Moreover, intraperitoneal infection does not lead to replication of prions in the spleen nor to cerebral scrapie in mice with severe combined immunodeficiency whose FDC are thought to be functionally impaired [38]. In a recently published study the essential role of FDC was demonstrated by creating chimeric mice with a mismatch in the PrP<sup>C</sup> status between FDC and other cells of the immune system. In this study it was demonstrated that replication of prions in the spleen depends on PrP<sup>C</sup> expressing FDC [10]. Reconstitution of severe combined immunodeficiency mice with wild-type spleen cells restores susceptibility to scrapie after peripheral infection [35]. These findings suggest that components of the immune system are required for efficient transfer of prions from the site of peripheral infection to the CNS.

To study the role of the immune system in more detail we used a panel of immune-deficient mice which were inoculated intraperitoneally with prions. We found that defects affecting T cells had no apparent effect, but that all mutations that disrupted the differentiation of B cells prevented the development of clinical scrapie [34]. These results argue for a crucial role of B cells in the development of scrapie after peripheral infection. The observation that B cells are important for the development of scrapie does not tell anything about the exact function of B cells in this process. The possible functions of B cells are so diverse that it would be far-fetched to conclude that B cells actually transport prions from the periphery to the CNS. The fact that lymphocytes do not normally cross the blood brain barrier and up to 30% of B-cell deficient mice contain prions in their brains yet show no signs of clinical disease also argue against a direct transport of prions to the CNS via B cells [20].

### **Spread of prions from extracerebral sites to the CNS, role of the PNS**

The question of whether accumulation of prions in the LRS is necessary to obtain neuroinvasion is still under discussion. There is substantial evidence for both lines of argumentation. The fact that splenectomy prolongs the

incubation time and the key role of the LRS including the FDC in neuroinvasion clearly speaks in favour of an essential role of the LRS in neuroinvasion [10, 32, 34]. On the other hand several studies have shown that neuroinvasion can be achieved in mice devoid of an intact immune system or in mice without PrP<sup>C</sup> expression on cells of the LRS [35, 39]. It was shown that PrP<sup>Sc</sup> is detectable in enteric ganglia after oral infection of hamsters with the scrapie agent [37]. In a different experimental setup PrP<sup>Sc</sup> was detectable after intraperitoneal infection of hamsters and sheep in ganglia belonging to the autonomous nervous system like enteric and dorsal root ganglia [22]. A possible conclusion from all these studies could be that the PNS constitutes the above mentioned reservoir function.

A question of high importance in this respect is the function of PrP<sup>C</sup> in this process. Indirect evidence points to a crucial role of PrP<sup>C</sup> expression on the PNS in neuroinvasion via the PNS. PrP<sup>C</sup>-expressing neurografts in *Prnp<sup>0/0</sup>* mice do not develop scrapie histopathology after intraperitoneal or intravenous inoculation with prions and no infectivity is detectable in spleens. Following reconstitution of the host lymphohemopoietic system with PrP<sup>C</sup>-expressing cells, prion titers in the spleen are restored to wild-type levels but, surprisingly, PrP<sup>C</sup>-expressing grafts fail to develop scrapie upon intraperitoneal or intravenous infection with prions (Fig. 2) [5].

In order to study the role of the PNS and especially the function of PrP<sup>C</sup> expression on the PNS we have developed a method to express genes of interest in the PNS. We are using this system to express PrP<sup>C</sup> selectively in the sciatic nerve of a PrP<sup>C</sup> knockout mouse (Fig. 3) [21]. With this system one should be able to answer some of the open questions concerning neuroinvasion and the role of PrP<sup>C</sup> expression in the PNS.

Even if the accumulation of prions within the LRS is essential to achieve neuroinvasion, one common pathway for neuroinvasion could be via the PNS. How the transfer of infectivity from cells belonging to the LRS to peripheral nerves is accomplished is still a matter of discussion. Access to peripheral nerves is facilitated if myelination of the nerves is reduced or absent [28]. Therefore the mantle zone of lymph follicles which are innervated by terminal unmyelinated nerve fibres could be the entry point of the scrapie agent into the PNS. Possibly this is a region where processes belonging to FDC could be in close contact with nerve fibres. Once invasion of the PNS has taken place the agent probably travels along the peripheral nerves to the CNS. The exact mode of transport within the PNS remains to be discovered: axonal and non-axonal modes of transport are conceivable. For PrP<sup>C</sup> transport in the fast axonal pathway was shown [6]. For PrP<sup>Sc</sup> the mode of transport has only been studied in an indirect fashion by comparing the incubation times of mice inoculated intraneurally to mice that were inoculated extraneurally or intracerebrally. In the case of intraneural injection of the agent, transport of the scrapie agent to the CNS occurred faster than in extraneurally injected mice. The actual rate of spread within the PNS was calculated to be around 1 to 2 mm/day [28].

### No graft pathology upon restoration of PrP<sup>+</sup> hematopoietic cells

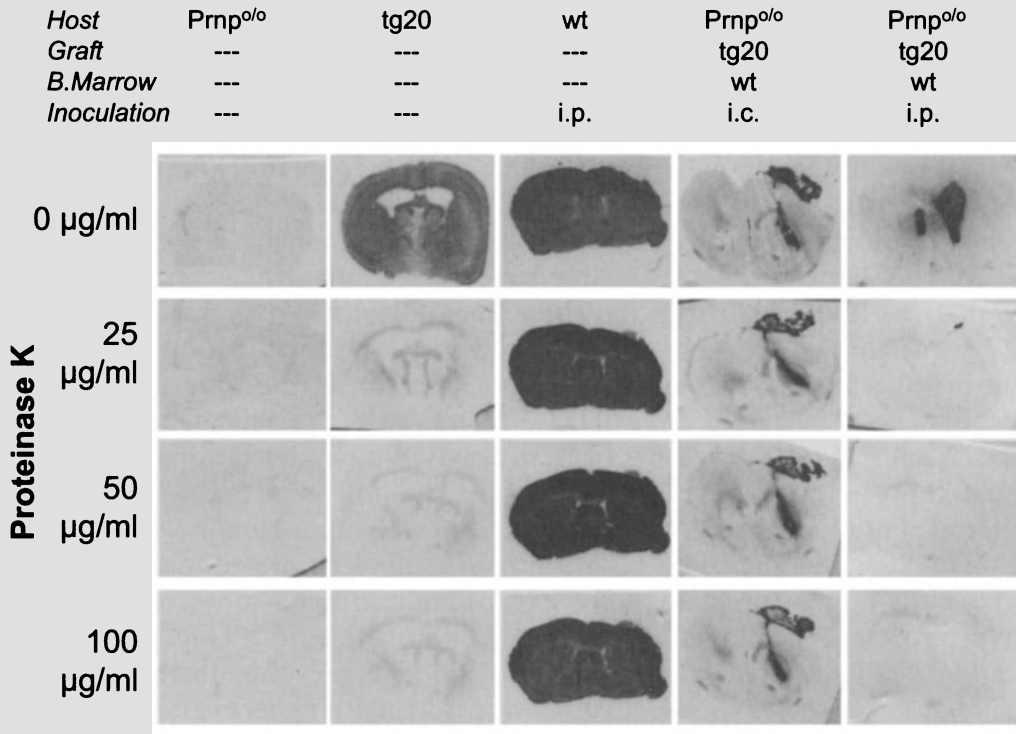


**Fig. 2.** Accumulation of PrP<sup>Sc</sup> in brain grafts. Histoblots showing immunoreactive PrP<sup>C</sup> in brain sections natively (first row) and after digestion with increasing levels of proteinase K (second through fourth row). *Prnp*<sup>0/0</sup> mice (first column) show no immunoreactivity, while mock-inoculated *tg20* mice (which overexpress PrP<sup>C</sup>) show proteinase K-sensitive PrP<sup>C</sup> (second column), but no proteinase K-resistant PrP<sup>Sc</sup>. Terminally sick scrapie-infected wild-type mice contain large amounts of both PrP<sup>C</sup> and PrP<sup>Sc</sup> (third column). *Prnp*<sup>0/0</sup> whose bone marrow has been reconstituted with wild-type FLCs accumulate PrP<sup>Sc</sup> in their PrP<sup>C</sup>-overexpressing grafts after i.c. (fourth column) but not after i.p. prion administration (fifth column)

Obviously this rate of spread does not correspond to the fast axonal transport. Recently, data was presented that PrP<sup>Sc</sup> localizes adaxonally within the PNS of intraperitoneally infected hamsters and sheep: this speaks in favour of a non-axonal transport mechanism within the PNS [22]. Considering the advances in visualisation of axonal and non-axonal transport mechanism, clarification of the exact transport mechanism of PrP<sup>Sc</sup> should be possible in the near future.

Based on the assumption that prions are transported in the PNS, a very important question relates to the anatomical identity of the nerves in which transport occurs. In the case of direct intraneural injection of prions, transport of infectivity to the CNS is accomplished via the injected nerve. Following intraperitoneal or oral infection prions accumulate in lymphatic

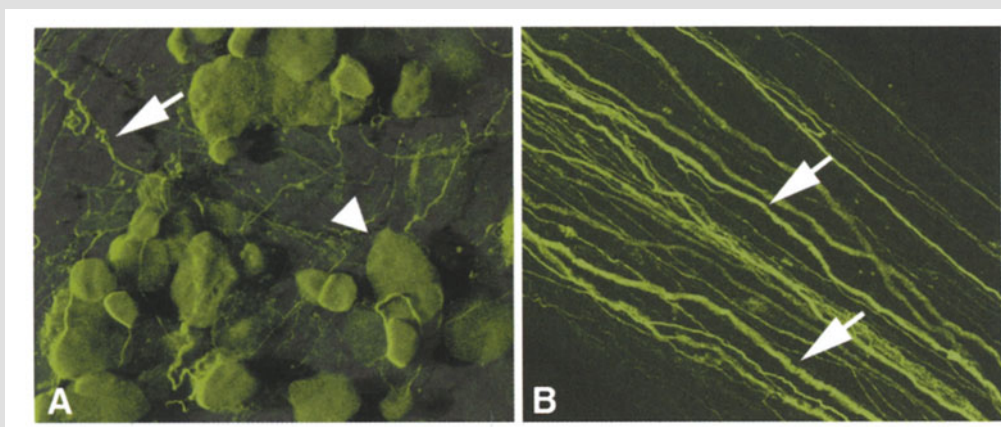


**Fig. 3.** Confocal laser scanning microscopy pictures showing the expression of enhanced green fluorescent protein in the dorsal root ganglia (A) and the sciatic nerve (B) 45 days after injection of a recombinant adeno-associated-virus containing DNA encoding enhanced green fluorescent protein under a neuron specific promoter. The expression is confined to dorsal root ganglia (block arrow) and axons protruding from dorsal root ganglia (arrow). We are currently expressing PrP<sup>C</sup> selectively in one sciatic nerve using the same method

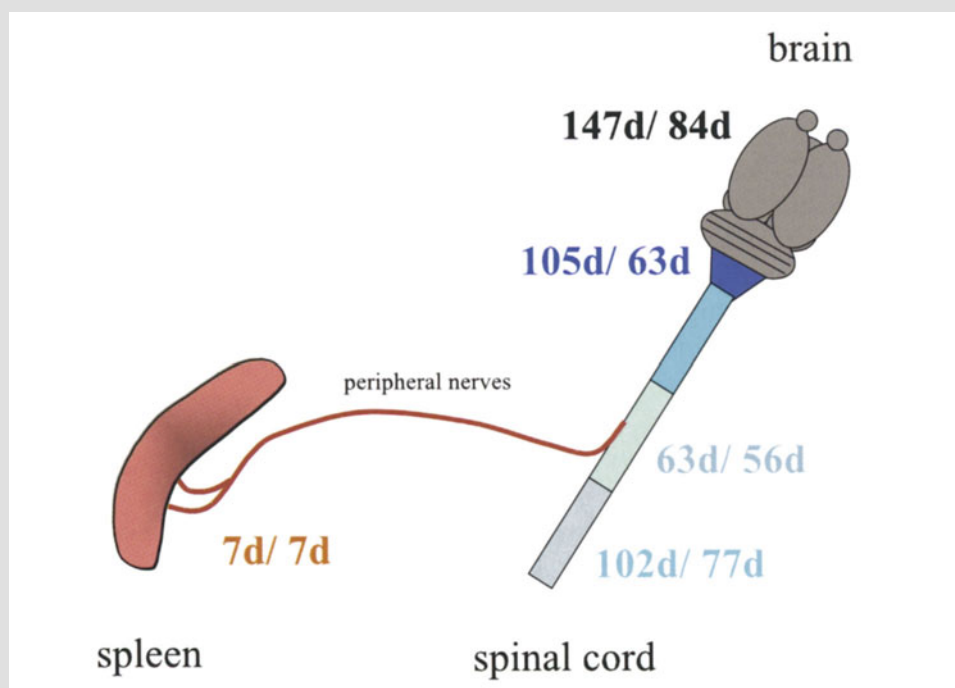


**Fig. 4.** Detection of PrP<sup>Sc</sup> or detection of pathological changes in the spleen, the spinal cord (first number) and detection of replication of the infectious agent (second number) in the spleen, the spinal cord and the CNS of mice following intraperitoneal administration of the infectious agent. Infectivity and PrP<sup>Sc</sup> can be detected in the LRS at very early time points. The first pathological changes and detection of infectivity within the CNS can be observed in the thoracic spinal cord [13]

organs. Lymphatic organs are predominantly innervated by nerve fibres belonging to the sympathetic nervous system (SNS). The first hints that the scrapie agent might invade the CNS using nerve fibres of the SNS came from studies aiming to unravel the dynamics of vacuolation and replication in the CNS. Following peripheral inoculation of the scrapie agent the first pathological changes like spongiosis as well as replication of the infectious agent appear in the mid thoracal spinal cord in the same level where nerves from the SNS enter the spinal cord (Fig. 4) [13, 29]. More recent studies describe an additional access route which bypasses the spinal cord using nerves of the parasympathetic nervous system, namely the vagal nerve. This alternative route seems to be highly significant when animals are challenged via the oral route of infection [3, 4].

### Conclusion

The process of neuroinvasion occurring in prion diseases starting with the contact of the infectious agent with extracerebral sites and eventually resulting in brain disease occurs in distinct sequential phases. The first and very early event in disease progression is certainly accumulation of prions in the LRS. This process is dependent upon components of the host immune system. Whether prions replicate or merely accumulate in the LRS is not known with certainty. FDC play a major role in this process but the details are still under discussion. In order to achieve efficient neuroinvasion either B cells or B cell-dependent processes are essential. One B cell-dependent event that is of relevance is the acquisition of a functional FDC network within the germinal centres of peripheral lymphoid tissue.

The second phase of neuroinvasion appears to encompass transfer of prions from lymphoid tissue to nerve endings of the peripheral nervous system. Because lymphoid organs are predominantly innervated by nerve fibres of the SNS, this part of the peripheral nervous system is a prime candidate.

### References

1. Aguzzi A (1998) Grafting mouse brains: from neurocarcinogenesis to neurodegeneration. *Embo J* 17: 6107–6114
2. Aguzzi A (1997) Neuro-immune connection in spread of prions in the body? *Lancet* 349: 742–743
3. Baldauf E, Beekes M, Diringer H (1997) Evidence for an alternative direct route of access for the scrapie agent to the brain bypassing the spinal cord. *J Gen Virol* 78: 1187–1197
4. Beekes M, McBride PA, Baldauf E (1998) Cerebral targeting indicates vagal spread of infection in hamsters fed with scrapie. *J Gen Virol* 79: 601–607
5. Blättler T, Brandner S, Raeber AJ, Klein MA, Voigtländer T, Weissmann C, Aguzzi A (1997) PrP-expressing tissue required for transfer of scrapie infectivity from spleen to brain. *Nature* 389: 69–73

6. Borchelt DR, Koliatsos VE, Guarnieri M, Pardo CA, Sisodia SS, Price DL (1994) Rapid anterograde axonal transport of the cellular prion glycoprotein in the peripheral and central nervous systems. *J Biol Chem* 269: 14711–14714
7. Brandner S, Isenmann S, Kuhne G, Aguzzi A (1998) Identification of the end stage of scrapie using infected neural grafts. *Brain Pathol* 8: 19–27
8. Brandner S, Isenmann S, Raeber A, Fischer M, Sailer A, Kobayashi Y, Marino S, Weissmann C, Aguzzi A (1996) Normal host prion protein necessary for scrapie-induced neurotoxicity. *Nature* 379: 339–343
9. Brandner S, Raeber A, Sailer A, Blattler T, Fischer M, Weissmann C, Aguzzi A (1996) Normal host prion protein (PrP<sup>C</sup>) is required for scrapie spread within the central nervous system. *Proc Natl Acad Sci USA* 93: 13148–13151
10. Brown KL, Stewart K, Ritchie DL, Mabbott NA, Williams A, Fraser H, Morrison WI, Bruce ME (1999) Scrapie replication in lymphoid tissues depends on prion protein-expressing follicular dendritic cells. *Nature Med* 5: 1308–1312
11. Bruce ME, Will RG, Ironside JW, McConnell I, Drummond D, Suttie A, McCordle L, Chree A, Hope J, Birkett C, Cousens S, Fraser H, Bostock CJ (1997). Transmissions to mice indicate that ‘new variant’ CJD is caused by the BSE agent. *Nature* 389: 498–501
12. Büeler HR, Fischer M, Lang Y, Bluethmann H, Lipp HP, DeArmond SJ, Prusiner SB, Aguet M, Weissmann C (1992) Normal development and behaviour of mice lacking the neuronal cell-surface PrP protein. *Nature* 356: 577–582
13. Cole S, Kimberlin RH (1985) Pathogenesis of mouse scrapie: dynamics of vacuolation in brain and spinal cord after intraperitoneal infection. *Neuropathol Appl Neurobiol* 11: 213–227
14. Collinge J, Whittington MA, Sidle KC, Smith CJ, Palmer MS, Clarke AR, Jefferys JG (1994) Prion protein is necessary for normal synaptic function. *Nature* 370: 295–297
15. Eklund CM, Kennedy RC, Hadlow WJ (1967) Pathogenesis of scrapie virus infection in the mouse. *J Infect Dis* 117: 15–22
16. Fischer M, Rülcke T, Raeber A, Sailer A, Moser M, Oesch B, Brandner S, Aguzzi A, Weissmann C (1996) Prion protein (PrP) with amino-proximal deletions restoring susceptibility of PrP knockout mice to scrapie. *EMBO J* 15: 1255–1264
17. Forloni G, Angeretti N, Chiesa R, Monzani E, Salmona M, Bugiani O, Tagliavini F (1993) Neurotoxicity of a prion protein fragment. *Nature* 362: 543–546
18. Fraser H, Dickinson AG (1985) Targeting of scrapie lesions and spread of agent via the retino-tectal projection. *Brain Res* 346: 32–41
19. Fraser H, Farquhar CF (1987) Ionising radiation has no influence on scrapie incubation period in mice. *Vet Microbiol* 13: 211–223
20. Frigg R, Klein MA, Hegyi I, Zinkernagel RM, Aguzzi A (1999) Scrapie pathogenesis in subclinically infected B-cell-deficient mice [In Process Citation]. *J Virol* 73: 9584–9588
21. Glatzel M, Flechsig E, Navarro B, Klein MA, Paterna JC, Bueler H, Aguzzi A (2000) Adenoviral and adeno-associated viral transfer of genes to the peripheral nervous system. *Proc Natl Acad Sci USA* 97: 442–447
22. Groschup MH, Beekes M, McBride PA, Hardt M, Hainfellner JA, Budka H (1999) Deposition of disease-associated prion protein involves the peripheral nervous system in experimental scrapie. *Acta Neuropathol (Berl)* 98: 453–457
23. Hill AF, Desbruslais M, Joiner S, Sidle KC, Gowland I, Collinge J, Doey LJ, Lantos P (1997) The same prion strain causes vCJD and BSE. *Nature* 389: 448–504

24. Hill AF, Zeidler M, Ironside J, Collinge J (1997) Diagnosis of new variant Creutzfeldt-Jakob disease by tonsil biopsy. *Lancet* 349: 99
25. Isenmann S, Brandner S, Aguzzi A (1996) Neuroectodermal grafting: a new tool for the study of neurodegenerative diseases. *Histol Histopathol* 11: 1063–1073
26. Isenmann S, Brandner S, Kuhne G, Boner J, Aguzzi A (1996) Comparative in vivo and pathological analysis of the blood–brain barrier in mouse telencephalic transplants. *Neuropathol Appl Neurobiol* 22: 118–128
27. Isenmann S, Brandner S, Sure U, Aguzzi A (1996) Telencephalic transplants in mice: characterization of growth and differentiation patterns. *Neuropathol Appl Neurobiol* 21: 108–117
28. Kimberlin RH, Hall SM, Walker CA (1983) Pathogenesis of mouse scrapie. Evidence for direct neural spread of infection to the CNS after injection of sciatic nerve. *J Neurol Sci* 61: 315–325
29. Kimberlin RH, Walker CA (1980) Pathogenesis of mouse scrapie: evidence for neural spread of infection to the CNS. *J Gen Virol* 51: 183–187
30. Kimberlin RH, Walker CA (1982) Pathogenesis of mouse scrapie: patterns of agent replication in different parts of the CNS following intraperitoneal infection. *J R Soc Med* 75: 618–624
31. Kimberlin RH, Walker CA (1989) Pathogenesis of scrapie in mice after intragastric infection. *Virus Res* 12: 213–220
32. Kimberlin RH, Walker CA (1989) The role of the spleen in the neuroinvasion of scrapie in mice. *Virus Res* 12: 201–211
33. Kitamoto T, Muramoto T, Mohri S, Dohura K, Tateishi J (1991) Abnormal isoform of prion protein accumulates in follicular dendritic cells in mice with Creutzfeldt-Jakob disease. *J Virol* 65: 6292–6295
34. Klein MA, Frigg R, Flechsig E, Raeber AJ, Kalinke U, Bluethmann H, Bootz F, Suter M, Zinkernagel RM, Aguzzi A (1997) A crucial role for B cells in neuroinvasive scrapie. *Nature* 390: 687–690
35. Lasmezias CI, Cesbron JY, Deslys JP, Demaimay R, Adjou KT, Rioux R, Lemaire C, Loch C, Dormont D (1996) Immune system-dependent and -independent replication of the scrapie agent. *J Virol* 70: 1292–1295
36. Manson JC, Clarke AR, Hooper ML, Aitchison L, McConnell I, Hope J (1994) 129/Ola mice carrying a null mutation in PrP that abolishes mRNA production are developmentally normal. *Mol Neurobiol* 8: 121–127
37. McBride PA, Beekes M (1999) Pathological PrP is abundant in sympathetic and sensory ganglia of hamsters fed with scrapie. *Neurosci Lett* 265: 135–138
38. Muramoto T, Kitamoto T, Hoque MZ, Tateishi J, Goto I (1993) Species barrier prevents an abnormal isoform of prion protein from accumulating in follicular dendritic cells of mice with Creutzfeldt–Jakob disease. *J Virol* 67: 6808–6810
39. Race R, Oldstone M, Chesebro B (2000) Entry versus blockade of brain infection following oral or intraperitoneal scrapie administration: role of prion protein expression in peripheral nerves and spleen. *J Virol* 74: 828–833

Authors' address: Dr. A. Aguzzi, Institute of Neuropathology, Schmelzbergstr. 12, CH-8091 Zürich, Switzerland.

## Follicular dendritic cells in scrapie pathogenesis

K. L. Brown<sup>1</sup>, K. Stewart<sup>1</sup>, D. Ritchie<sup>1</sup>, H. Fraser<sup>1</sup>, W. I. Morrison<sup>2</sup>, and M. E. Bruce<sup>1</sup>

<sup>1</sup>Institute for Animal Health, Neuropathogenesis Unit, Edinburgh, U.K.

<sup>2</sup>Institute for Animal Health, Compton, Newbury, U.K.

**Summary.** Scrapie pathogenesis was studied in chimaeric mice that carried the prion protein (PrP) gene only in particular cells of the immune system. These mice were produced by grafting bone marrow from PrP expressing donors into PrP deficient recipients and vice versa. As follicular dendritic cells are not replaced significantly from the bone marrow in adult mice, this procedure resulted in a mismatch in PrP genotype between these cells and bone marrow derived cells such as lymphocytes. Using these models we obtained strong evidence that follicular dendritic cells produced high levels of the normal form of PrP in uninfected mice. Furthermore, the replication of a mouse-passaged scrapie strain in the spleen depended only on the presence of PrP expressing follicular dendritic cells. PrP expression by lymphocytes or other bone marrow derived cells had no influence on replication in spleen or on neuroinvasion in these models. These results indicate that the follicular dendritic cell is a potential target for prophylactic or therapeutic intervention in transmissible spongiform encephalopathies.

### Introduction

The great majority of accidental transmissions of transmissible spongiform encephalopathies (TSEs) have resulted from peripheral exposure to infection, for example from feed. It is important to understand the events in peripheral tissues which precede invasion of infection into the central nervous system (CNS), as therapeutic and preventative strategies are most likely to be effective at this stage. Replication of TSE agents outside the CNS occurs predominantly in the spleen and lymph nodes in both experimentally and naturally infected animals [11]. In mice infected by peripheral challenge, a major route of entry of infection into the CNS is from the spleen, probably via its sympathetic innervation [11]. Previous experiments involving  $\gamma$ -irradiation of mice before or after peripheral infection indicated that the progression of the disease depends on a non-dividing long-lived cell type [8]. This would exclude most lymphocytes and myeloid cells, but one cell that fulfills these criteria is the follicular dendritic cell (FDC). FDCs

have also been suspected of participating in TSE pathogenesis because high levels of the host “prion protein” (PrP) have been detected immunocytochemically on these cells in mice experimentally infected with scrapie [19] or CJD [12], sheep with natural scrapie [24] and humans with “new variant” CJD [9]. The normal form of PrP has also been detected on FDCs in uninfected mice [19]. However, lower levels of PrP have been demonstrated on the surface of lymphocytes from uninfected mice [17] and humans [5].

Severe combined immunodeficiency (SCID) mice carry a mutation, *scid*, which blocks the rearrangement of immunoglobulin and T cell receptor genes, resulting in a profound deficiency of both T and B lymphocytes [2]. As FDCs require signals from B cells for their maturation, SCID mice also lack functional FDCs. Bone marrow grafts from immunocompetent donors restore T and B cell populations, leading to germinal centre formation and the maturation of FDCs from resident precursor cells in the spleen and lymph nodes (Fig. 1) [10]. SCID mice are fully susceptible to TSE infection when challenged by the intracerebral route, but relatively resistant to challenge by peripheral routes [6]. This resistance is related to an inability of the SCID spleen to support TSE replication [7, 20]. Bone marrow grafts induce the SCID spleen to support TSE replication and render the mice susceptible to peripheral challenge [7]. These previous results suggest that infection is established in mature FDCs within germinal centres, but do not preclude a direct role for lymphocytes. This paper describes a series of studies aimed at defining the separate roles of FDCs and lymphocytes in pathogenesis in a mouse scrapie model.

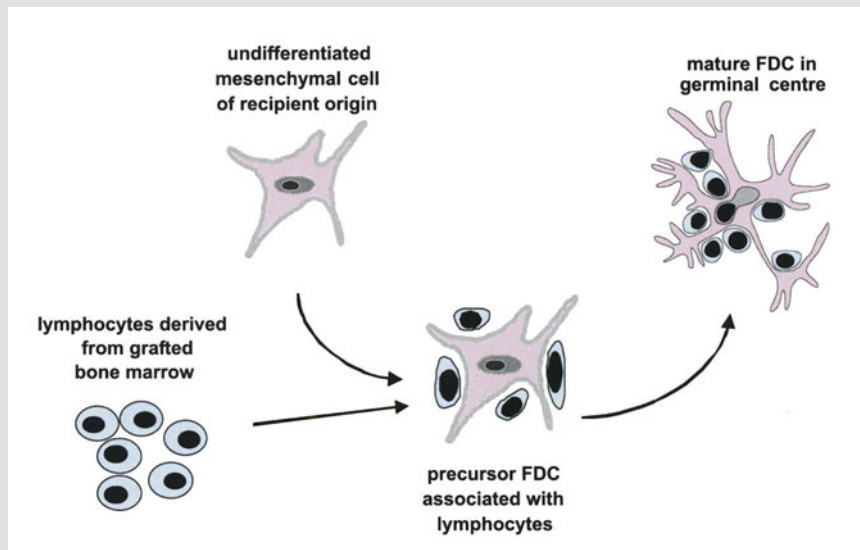


**Fig. 1.** Induction of FDC maturation in lymphoid tissues following bone marrow grafting. Lymphocytes derived from the graft interact with resident FDC precursor cells of recipient origin, leading to FDC maturation and the formation of germinal centres. Grafting PrP<sup>+/+</sup> bone marrow into PrP<sup>-/-</sup> mice and the converse produces a mismatch in PrP genotype between FDCs and lymphocytes

### **Production of PrP-chimaeric mice by bone marrow grafting**

PrP “knockout” mice, produced by disruption of the PrP gene by gene targeting techniques, are resistant to scrapie challenge and fail to replicate infectivity in any of their tissues, indicating that the PrP protein is necessary for scrapie replication [4, 18]. To test the hypothesis that mature FDCs support scrapie replication in lymphoid tissues, we studied pathogenesis in mice with chimaeric immune systems with respect to PrP expression [3]. These experiments depended on the fact that FDCs are not replaced significantly from the bone marrow in adult mice [23] and involved the transfer of bone marrow from PrP-expressing (PrP<sup>+/+</sup>) donors into PrP-deficient (PrP<sup>-/-</sup>) recipients and vice versa. Two types of chimaeric model were employed. In the first type of model, bone marrow grafting into SCID mice induced the maturation of FDCs of recipient origin in the presence of lymphocytes of graft origin (Fig. 1). This approach required, as a first step, the introduction of the *scid* mutation by selective breeding into PrP<sup>-/-</sup> and histocompatible PrP<sup>+/+</sup> mouse lines [3]. In the second type of chimaeric model, PrP<sup>+/+</sup> or PrP<sup>-/-</sup> immunocompetent mice were subjected to a dose of  $\gamma$ -radiation (950 rads) that destroys lymphocyte and myeloid precursor cells, but leaves FDCs intact. They were then rescued by grafting bone marrow from appropriate donors, a procedure that replaces both lymphocytes and myeloid cells, but not FDCs. Using these two approaches it was possible to produce mice in which there was a mismatch in PrP genotype between FDCs and lymphocytes/myeloid cells [3].

### **Cellular association of PrP in uninfected spleens**

The first question to be addressed using these chimaeric models was whether PrP is produced by FDCs in uninfected animals. Spleen sections from SCID/PrP<sup>-/-</sup> or SCID/PrP<sup>+/+</sup> mice, grafted respectively with PrP<sup>+/+</sup> or PrP<sup>-/-</sup> bone marrow, were examined immunocytochemically for the presence of PrP, mature FDCs and B cells, at intervals up to 28 days (Table 1). B cells were first detected at 10–14 days after bone marrow transfer, coincident with increased immunoglobulin levels. Labelling of FDCs with FDC-M1 (a monoclonal antibody specific for mouse FDCs [15]) was observed in both grafted groups from 10–21 days onwards. PrP labelling, confined to FDC networks, was demonstrated in SCID/PrP<sup>+/+</sup> mice reconstituted with PrP<sup>-/-</sup> bone marrow, also from 21 days. In contrast, no PrP labelling was seen in spleens of SCID/PrP<sup>-/-</sup> mice reconstituted with PrP<sup>+/+</sup> bone marrow, even in mice with well-developed FDC networks. In the course of this study we developed an immunofluorescence method for the detection of PrP and FDCs in the same tissue section [22]. Confocal imaging of double stained sections confirmed a close colocalisation between PrP and the FDC marker in SCID/PrP<sup>+/+</sup> mice grafted with PrP<sup>-/-</sup> bone marrow, in contrast to an absence of PrP labelling on FDCs of SCID/PrP<sup>-/-</sup> mice grafted with PrP<sup>+/+</sup> bone marrow (Fig. 2) [3].

**Table 1.** Immunolabelling of B cells, FDC networks and PrP on FDCs in uninfected PrP chimaeric mice at intervals after bone marrow reconstitution.<sup>a</sup> Two spleens were examined at each time point

Recipient mouse line	PrP genotype of bm graft	Days post reconstitution	B cells	FDC networks	PrP on FDCs
SCID/PrP <sup>+/+</sup>	PrP <sup>-/-</sup>	7	+ -	- -	- -
		10	- -	- -	- -
		14	+ +	- -	(+) -
		21	+ +	+ +	+ +
		28	+ +	+ +	+ +
SCID/PrP <sup>-/-</sup>	PrP <sup>+/+</sup>	7	- -	- -	- -
		10	+ +	+ +	- -
		14	+ +	+ -	- -
		21	+ +	+ -	- -
		28	+ +	+ +	- -

+ strong, (+) weak, - no immunolabelling

<sup>a</sup>PrP was detected in paraffin-embedded, PLP-fixed tissues, using the 1B3 polyclonal antibody. FDC networks and B cells were visualised in acetone-fixed frozen sections, using, respectively, the FDC-M1 [15] and B-220 (Caltag Laboratories) monoclonal antibodies. All labelling was carried out by the avidin-biotin complex technique

Similarly, PrP was detected on FDCs of irradiation chimaeras only if the recipient of the graft carried an intact PrP gene, irrespective of the PrP genotype of the graft. As FDCs will have retained the PrP status of the recipient, these results provide strong evidence that the high levels of PrP detected on these cells by immunocytochemistry are produced by the FDCs themselves, rather than by surrounding lymphocytes or myeloid cells.

### Scrapie infection in PrP chimaeric mice

PrP chimaeric mice, together with control non-chimaeric mice, were challenged with the ME7 scrapie strain by intracerebral (i.c.) or intraperitoneal (i.p.) routes and their spleens collected at intervals after injection. As in unchallenged mice, immunocytochemical detection of PrP on FDC networks depended only on the PrP genotype of the FDCs themselves and not at all on the PrP genotype of grafted lymphocytes and/or myeloid cells [3]. When tissues were bioassayed by injection into groups of wild type mice, high levels of infectivity were detected in spleens of all PrP<sup>+/+</sup> mice grafted with either PrP<sup>+/+</sup> or PrP<sup>-/-</sup> bone marrow (Tables 2 and 3) [3]. However, very little or no infectivity could be detected in the spleens of PrP<sup>-/-</sup> mice, even when they were grafted with PrP<sup>+/+</sup> bone marrow. Furthermore, in i.p. challenged irradiation chimaeras, the PrP genotype of the graft had very little effect on the incubation period of the disease (Table 3) (it was not

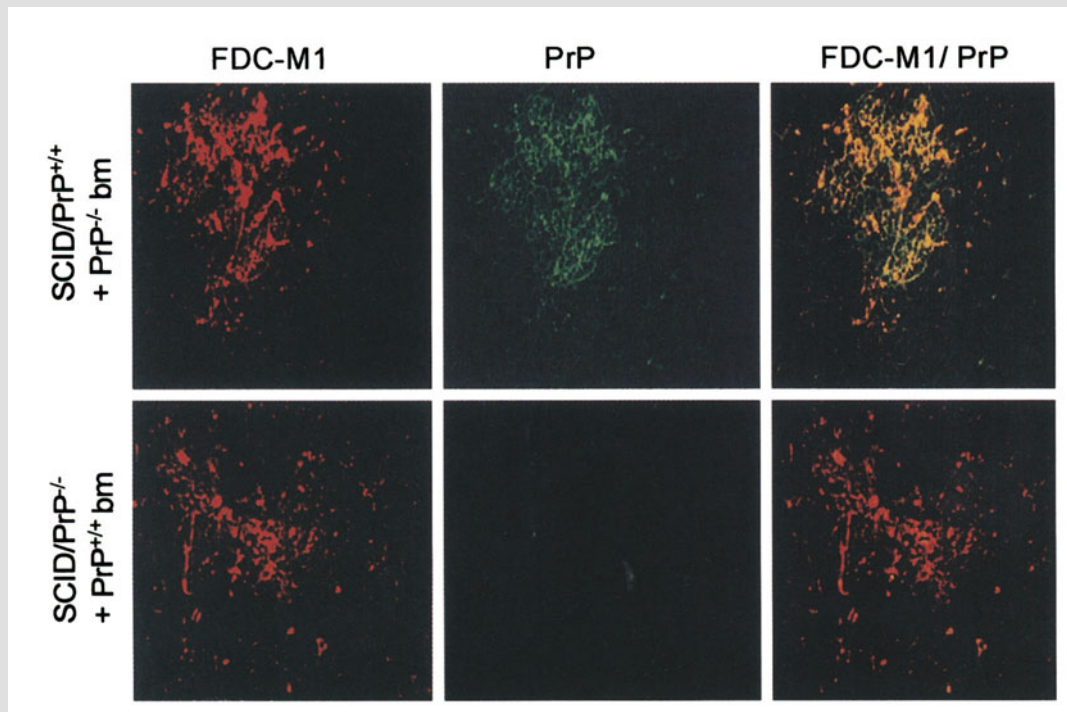


**Fig. 2.** Fluorescent immunolabelling of FDCs and PrP, separately and combined, in spleen sections from uninfected mice with PrP chimaeric immune systems. Although both types of chimaeric mice had mature FDCs, PrP was demonstrated on FDCs only when the recipient of the graft (that is, the FDCs themselves) carried a functional PrP gene. This figure has appeared in a previous publication [3]

possible to make this comparison in the SCID chimaeras because of their poor survival). These results give a strong indication that replication of the ME7 strain of scrapie in lymphoid tissues depends on the presence of PrP-expressing FDCs. They give no indication of any direct involvement of lymphocytes or myeloid cells, either in replication or in neuroinvasion. A crucial role for FDCs in pathogenesis is supported by the observation that TNF- $\alpha$  knockout mice, which possess T and B cells but lack mature FDCs, are relatively resistant to challenge with ME7 scrapie by peripheral injection [3].

### Conclusions

This study confirmed a central role for mature FDCs in the replication of scrapie in lymphoid tissues. We found no evidence that bone marrow derived cells modulate this process directly in the ME7 scrapie model, although it is known that B cells are required for the maturation of FDCs and so play an indirect role in scrapie pathogenesis. However, our results contrast with those obtained elsewhere, using a different mouse scrapie isolate. In these studies, replication of RML scrapie was observed in spleens of irradiated PrP deficient mice grafted with PrP expressing bone marrow [1],

**Table 2.** Scrapie incidence, incubation periods and spleen infectivity titres in SCID PrP chimaeric mice and in non-chimaeric control mice (based on previously published data [3])

Recipient mouse	Bone marrow graft	Route of challenge	Scrapie incidence	Mean incubation period (days) $\pm$ SEM	Individual spleen titres (log i.c.ID <sub>50</sub> /g) <sup>a</sup> at		
					10 weeks	15 weeks	24 weeks
SCID/PrP <sup>+/+</sup>	PrP <sup>+/+</sup>	i.c.	4/4	163 $\pm$ 11	6.0, 5.7	6.0, 5.8	6.2, 4.6
SCID/PrP <sup>+/+</sup>	PrP <sup>-/-</sup>	i.c.	5/5	177 $\pm$ 4	5.5, 5.9	5.4, 5.3	5.6, 5.3
SCID/PrP <sup>+/+</sup>	none	i.c.	4/4	137 $\pm$ 6	<i>ud, ud</i>	<i>ud, ud</i>	<i>ud, ud</i>
SCID/PrP <sup>-/-</sup>	PrP <sup>+/+</sup>	i.c.	0/5	–	<i>ud, ud</i>	not tested	<i>ud, ud</i>
SCID/PrP <sup>-/-</sup>	PrP <sup>-/-</sup>	i.c.	0/9	–	< 1.6, <i>ud</i>	not tested	<i>ud, ud</i>
SCID/PrP <sup>-/-</sup>	none	i.c.	0/9	–	<i>ud, ud</i>	not tested	<i>ud, ud</i>

*ud* Infectivity undetectable, bioassay mice negative up to 350 days post injection

<sup>a</sup>Two individual spleens bioassayed at each time point

**Table 3.** Scrapie incidence, incubation periods and spleen infectivity titres in PrP irradiation chimaeric mice and in non-chimaeric control mice (based on previously published data [3])

Recipient mouse	Bone marrow graft	Route of challenge	Scrapie incidence	Mean incubation period (days) $\pm$ SEM	Individual spleen titres (log i.c.ID <sub>50</sub> /g) <sup>a</sup> at		
					5 weeks	10 weeks	15 weeks
$\gamma$ PrP <sup>+/+</sup>	PrP <sup>+/+</sup>	i.c.	9/9	157 $\pm$ 2	6.0, 6.2	6.0, 6.0	6.2, 6.7
$\gamma$ PrP <sup>+/+</sup>	PrP <sup>-/-</sup>	i.p.	11/11	252 $\pm$ 2		5.7, 6.2	
$\gamma$ PrP <sup>+/+</sup>	PrP <sup>-/-</sup>	i.c.	8/8	153 $\pm$ 3	5.5, 6.6	5.9, 6.0	5.9, 6.0
PrP <sup>+/+</sup>	none	i.p.	10/10	239 $\pm$ 3		5.8, 6.5	
PrP <sup>+/+</sup>	none	i.c.	9/9	161 $\pm$ 2	4.9, 4.6	6.1, 6.3	6.7, 6.4
$\gamma$ PrP <sup>-/-</sup>	PrP <sup>+/+</sup>	i.p.	10/10	256 $\pm$ 3		5.7, 6.2	
$\gamma$ PrP <sup>-/-</sup>	PrP <sup>+/+</sup>	i.c.	0/7	-	< 1.6, ud	< 1.6, ud	< 1.8, ud
$\gamma$ PrP <sup>-/-</sup>	PrP <sup>-/-</sup>	i.p.	0/7	-		ud, ud	
$\gamma$ PrP <sup>-/-</sup>	PrP <sup>-/-</sup>	i.c.	0/7	-	ud, ud	ud, ud	ud, ud
$\gamma$ PrP <sup>-/-</sup>	PrP <sup>-/-</sup>	i.p.	0/7	-		ud, ud	
PrP <sup>-/-</sup>	none	i.c.	0/9	-	ud, ud	ud, ud	< 1.6, ud
PrP <sup>-/-</sup>	none	i.p.	0/13	-		ud, ud	

*ud* Infectivity undetectable, bioassay mice negative up to 350 days post injection

<sup>a</sup>Two individual spleens bioassayed at each time point

implying that a bone marrow derived cell type can support replication of this isolate. Further studies using RML scrapie have implicated B cells in pathogenesis [13], although their exact role remains unclear [14, 21]. This discrepancy between results for ME7 and RML scrapie may suggest that different strains of TSE agent target different cell populations in lymphoid tissues.

The major function of FDCs is to trap and retain antigen in the form of immune complexes on their cell surface. This leads to the formation of germinal centres, which support avidity maturation of antibody and generation of B cell memory [16]. The high levels of PrP on mature FDCs suggest that PrP may play a functional role in these processes. It is also possible that TSE agents exploit the normal function of PrP to focus infectivity to the FDCs. These results provide the basis for future studies to dissect the early events in infection of lymphoid tissues. They also indicate a potential target cell for prophylactic or therapeutic intervention, for example in “new variant” CJD.

### Acknowledgements

This paper is based largely on a previously published study [3]. The authors thank I. McConnell, M. Brady and L. Gray for their excellent technical support, C. Farquhar for the PrP-specific 1B3 antibody, M. Kosco-Vilbois for the FDC-M1 antibody and J. Manson for PrP knockout mice. This work was supported by the BBSRC and MRC.

### References

1. Blattler T, Brandner S, Raeber AJ, Klein MA, Volgtlander T, Weissmann C, Aguzzi A (1997) PrP-expressing tissue required for transfer of scrapie infectivity from spleen to brain. *Nature* 389: 69–73
2. Bosma GC, Custer RP, Bosma MJ (1983) A severe combined immunodeficiency mutation in the mouse. *Nature* 301: 527–530
3. Brown KL, Stewart K, Ritchie DL, Mabbott NA, Williams A, Fraser H, Morrison WI, Bruce ME (1999) Scrapie replication in lymphoid tissues depends on prion protein-expressing follicular dendritic cells. *Nature Med* 5: 1308–1312
4. Bueler H, Aguzzi A, Sailer A, Greiner R-A, Autenried P, Aguet M, Weissmann C (1993) Mice devoid of PrP are resistant to scrapie. *Cell* 73: 1339–1347
5. Cashman NR, Loertscher R, Nalbantoglu J, Shaw I, Kascsak RJ, Bolton DC, Bendheim PE (1990) Cellular isoform of the scrapie agent protein participates in lymphocyte activation. *Cell* 61: 185–192
6. Fraser H, Brown K (1994) Peripheral pathogenesis of scrapie in normal and immunocompromised mice. *Animal Technol* 45: 21–23
7. Fraser H, Brown KL, Stewart K, McConnell I, McBride P, Williams A (1996) Replication of scrapie in spleens of SCID mice follows reconstitution with wild-type mouse bone marrow. *J Gen Virol* 77: 1935–1940
8. Fraser H, Farquhar CF (1987) Ionising radiation has no influence on scrapie incubation period in mice. *Vet Microbiol* 13: 211–223
9. Hill AF, Butterworth RJ, Joiner S, Jackson G, Rossor MN, Thomas DJ, Frosh A, Tolley N, Bell JE, Spencer M, King A, Al-Sarraj S, Ironside JW, Lantos PL,

- Collinge J (1999) Investigation of variant Creutzfeldt-Jakob disease and other human prion diseases with tonsil biopsy samples. *Lancet* 353: 183–189
10. Kapasi ZF, Burton GF, Shultz LD, Tew JG, Szakal AK (1993) Induction of functional follicular dendritic cell development in severe combined immunodeficiency mice: influence of B and T cells. *J Immunol* 150: 2648–2658
  11. Kimberlin RH, Walker CA (1979) Pathogenesis of mouse scrapie: dynamics of agent replication in spleen, spinal cord and brain after infection by different routes *J Comp Pathol* 89: 551–562
  12. Kitamoto T, Muramoto T, Mohri S, Doh-ura K, Tateishi J (1991) Abnormal isoform of prion protein accumulates in follicular dendritic cells in mice with Creutzfeldt–Jakob disease. *J Virol* 65: 6292–6295
  13. Klein MA, Frigg R, Flechsig E, Raeber AJ, Kalinke U, Bluethmann H, Bootz F, Suter M, Zinkernagel RM, Aguzzi A (1997) A crucial role for B cells in neuro-invasive scrapie. *Nature* 390: 687–690
  14. Klein MA, Frigg R, Raeber AJ, Flechsig E, Hegyi I, Zinkernagel RM, Weissmann C, Aguzzi A (1998) PrP expression in B lymphocytes is not required for prion neuroinvasion. *Nature Med* 4: 1429–1433
  15. Kosco MH, Pflugfelder E, Gray D (1992) Follicular dendritic cell-dependent adhesion and proliferation of B cells in vitro. *J Immunol* 148: 2331–2339
  16. Kosco-Vilbois MH, Zentgraf H, Gerdes J, Bonnefoy J-Y (1997) To ‘B’ or not to ‘B’ a germinal center? *Immunol Today* 18: 225–230
  17. Mabbott NA, Brown KL, Manson J, Bruce ME (1997) T-lymphocyte activation and the cellular form of the prion protein. *Immunol* 92: 161–165
  18. Manson JC, Clarke AR, McBride PA, McConnell I, Hope J (1994) PrP gene dosage determines the timing but not the final intensity or distribution of lesions in scrapie pathology. *Neurodegen* 3: 331–340
  19. McBride PA, Eikelenboom P, Kraal G, Fraser H, Bruce ME (1992) PrP protein is associated with follicular dendritic cells of spleens and lymph nodes in uninfected and scrapie-infected mice. *J Pathol* 168: 413–418
  20. O’Rourke KI, Huff TP, Leathers CW, Robinson MM, Gorham JR (1994) SCID mouse spleen does not support scrapie agent replication. *J Gen Virol* 75: 1511–1514
  21. Raeber AJ, Klein MA, Frigg R, Flechsig E, Aguzzi A, Weissmann C (1999) PrP-dependent association of prions with splenic but not circulating lymphocytes of scrapie-infected mice. *EMBO J* 18: 2702–2706
  22. Ritchie DL, Brown KL, Bruce ME (1999) Visualisation of PrP protein and follicular dendritic cells in uninfected and scrapie infected spleen. *J Cell Pathol* 4: 3–10
  23. Tkachuk M, Bolliger S, Ryffel B, Pluschke G, Banks TA, Herren S, Gisler RH, Kosco-Vilbois MH (1998) Crucial role of tumor necrosis factor receptor 1 expression on nonhematopoietic cells for B cell localization within the splenic white pulp. *J Exp Med* 187: 469–477
  24. van Keulen LJM, Schreuder BEC, Meloen RH, Mooij-Harkes G, Vromans MEW, Langeveld JPM (1996) Immunohistochemical detection of prion protein in lymphoid tissues of sheep with natural scrapie. *J Clin Microbiol* 34: 1228–1231

Authors’ address: Dr. M. E. Bruce, Institute for Animal Health, Neuropathogenesis Unit, Ogston Building, West Mains Road, Edinburgh EH9 3JF, U.K.

## **Cellular and sub-cellular localisation of PrP in the lymphoreticular system of mice and sheep**

**M. Jeffrey, G. McGovern, S. Martin, C. M. Goodsir, and K. L. Brown**

Lasswade Veterinary Laboratory, Penicuik, Scotland, U.K.

**Summary.** Using immunocytochemistry or immunogold electron microscopy, abnormal PrP accumulation was found in lymphoreticular tissues of Suffolk sheep naturally exposed to scrapie and in the spleens of ME7 infected C57 BL mice at 70 days after infection and at the terminal stage of disease at 170 days. Clinically diseased scrapie affected sheep show widespread PrP accumulation within tingible body macrophages (TBMs) and follicular dendritic cells (FDCs) of secondary lymphoid follicles. Serial tonsillar biopsies taken from 171ARQ/ARQ sheep at 4 months of age did not contain abnormal PrP accumulations but 80% of biopsies were positive by 14 months. In contrast, whole body necropsies of sheep not previously biopsied failed to detect PrP in the tonsil of sheep at 4, 8, 12 or 16 months of age. These findings suggest that the biopsy procedure of susceptible sheep but not resistant sheep may induce tonsillar infection. In spleen of mice both at 70 and 170 dpi, accumulations of PrP were found within lysosomes of TBMs and also at the plasma-lemma of FDCs. In the light zone of follicles of terminally diseased mice, all FDC dendrites were arranged in the form of highly reactive or hyperplastic labrynthine glomerular complexes. PrP was consistently seen between FDC dendrites in association with abundant electron dense antigen-antibody complexes. At 70 days after challenge, labrynthine complexes were rare and invariably labelled for PrP. However, sparse PrP labelling was also seen on simple FDC dendrites at this stage. These observations suggests that scrapie infected FDCs continually release PrP from the cell surface where it accumulates in excess in association with trapped immune complexes and dendritic extension. It is likely that TBMs acquire lysosomal PrP following phagocytosis of effete FDC processes or from the extracellular space. We suggest that the normal function of PrP may involve cell process extension or immune complex trapping.

### **Introduction**

Many studies indicate that the lymphoreticular system is important for scrapie pathogenesis. Within a few weeks of scrapie infection, agent

replication can be detected in a variety of lymphoid tissues [27] and, initial neuroinvasion is thought to occur following retrograde transportation of infectivity to the spinal cord via splanchnic nerves which innervate the spleen [20].

Studies employing a variety of experimental approaches, including the use of cell fractionation techniques, severe combined immunodeficient (SCID) mice and whole body  $\gamma$  irradiation, suggest that the follicular dendritic cell (FDC) is important for scrapie pathogenesis [6, 7, 12, 13, 24]. Procedures which deplete mitotic cells, such as  $\gamma$  irradiation as well as genetic athymia or surgical thymectomy do not significantly alter incubation periods [12, 13] suggesting that scrapie replication does not depend upon T cells but requires radioresistant mitotically inactive cells. Disease specific accumulations of PrP are also seen in association with FDCs of TSE infected mice, sheep and human beings [16, 22, 27, 33]. PrP<sup>sen</sup> can be detected in association with FDCs of the murine spleen [27].

SCID mice lack B and T cells and FDCs fail to mature [2]. They are relatively resistant to scrapie challenge by peripheral routes and fail to replicate infectivity in their spleens [4, 6]. Following reconstitution by bone marrow grafting these mice become fully susceptible to peripheral challenge and capable of supporting replication in their spleens. In further studies, chimaeric mice have been produced by bone marrow grafting either SCID or  $\gamma$ -irradiated mice, which express PrP in FDCs but not lymphocytes, and vice versa. This has been possible because, in adult mice, FDCs probably derive from a stromal cell within the lymphoreticular system and are not replaced significantly from the bone marrow. Following ME7 scrapie infection, replication has been shown in the spleens of mice with a functional PrP gene (PrP<sup>+/+</sup>) reconstituted with PrP<sup>+/+</sup> or PrP null (PrP<sup>-/-</sup>) bone marrow but not in the spleens of PrP<sup>-/-</sup> mice reconstituted with either PrP<sup>+/+</sup> or PrP<sup>-/-</sup> bone marrow [4, 5]. These observations indicate that mature PrP expressing FDCs are necessary for scrapie replication. However, other studies using a different murine scrapie strain have suggested that B cells may be involved [1] although this now appears to be in some doubt [23]. Nevertheless, it has been clearly shown that some lymphocytes express PrP<sup>sen</sup> on their cell surface [8, 25].

These studies were undertaken to try and better understand the role of the LRS in the peripheral pathogenesis of scrapie.

## Materials and methods

### *Animals*

Sequential tonsillar biopsies or necropsies were performed on lambs taken from a flock of Suffolk sheep which had experienced frequent cases of scrapie over a period of several years. All but 2 of 106 scrapie cases examined between 1990 and 1996 in this flock were homozygous for glutamine at codon 171 of the PrP gene with a mean age to clinical disease of 30 months. Clinically affected sheep had widespread PrP

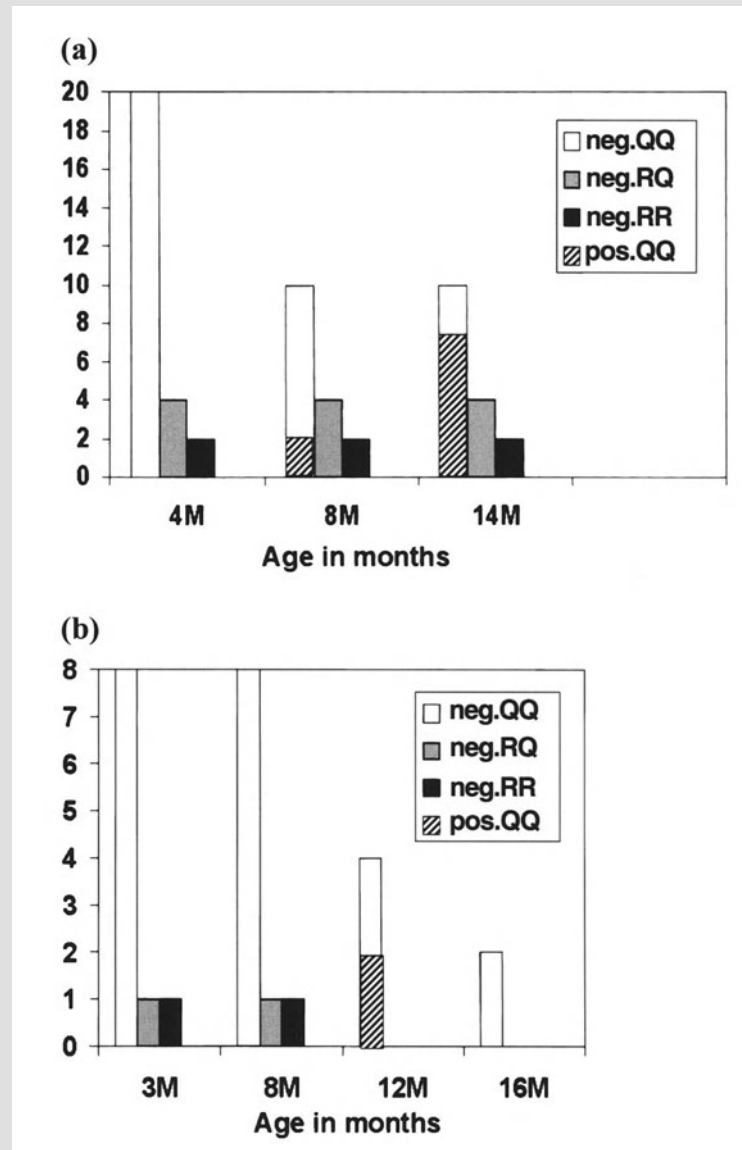


**Fig. 1. a** Numbers of positive and negative tonsillar biopsies by age and genotype; **b** numbers of positive necropsies with positive or negative immunostaining in viscera by genotype and age of sheep

accumulation in the lymphoreticular system and peripheral ganglia. Lambs born in Spring of 1998 were serially biopsied from tonsils or were subjected to whole body necropsy at selected time intervals (Fig. 1).

C57 BL mice infected with the ME7 scrapie strain by intracerebral injection of 20  $\mu$ l of a 1% brain homogenate were available for electron microscopy studies. Forty-seven spleen tissue blocks were taken from two scrapie infected mice at 70 days after infection and 33 spleen tissue blocks were taken from three mice at terminal stages of the disease (mean incubation period approximately 170 days). From five age matched normal brain inoculated control mice, 70 blocks of spleen tissue were available for examination.

*Light and electron microscopical immunohistochemical staining procedure*

Details of light and electron microscopical techniques for immunostaining are as previously described [20]. Spleens were immersion fixed in 2% PLP, 0.5% paraformaldehyde/0.5% glutaraldehyde or in a variety of concentrations of paraformaldehyde/glutaraldehyde for 24 h at 4 °C. Primary antibody (1A8) at a 1:500 dilution in incubation buffer or pre-immune serum were then applied for 15 h. After rinsing extensively, sections were incubated with Auroprobe 1 nm colloidal gold diluted 1:50 in incubation buffer for 2 hours.

Tonsillar biopsies were prepared as described by van Keulen et al. [33] and stained using both the 521.2 antibody (kindly supplied by Dr. van Keulen) and a polyclonal rabbit anti-sheep PrP peptide antibody R482. None of the above antibodies can distinguish between PrP<sup>scn</sup> and PrP<sup>res</sup>. However, under the conditions of fixation and embedding employed in this study no staining was seen in control tissues. Immunocytochemically detected PrP therefore represents accumulation of abnormal amounts of PrP of unknown protease sensitivity.

## Results

*Natural sheep scrapie*

Clinically affected sheep showed PrP accumulation in virtually all follicles of all lymph nodes. The numbers of secondary lymphoid follicles appeared to be more frequent than in controls and often penetrated into the medulla of the node. PrP was found in cells of the light zone which resembled mature FDCs and in serial sections co-localised with CD21 staining. Other cells which resembled TBMs were also immunostained and were found in light zone, dark zone, mantle zone and, in smaller numbers in the paracortex.

Serial tonsillar biopsies taken from lambs at 4, 8 and 14 months of age did not show any PrP accumulation in germinal centres of two ARR/ARR or four ARQ/ARR sheep. In serial biopsies from ARQ/ARQ lambs disease specific PrP accumulation was not seen in 20 lambs at 4 months of age, but was found in 2 of 10 lambs at 8 months and in 7 of 10 lambs at 14 months (Figs. 1 and 2). Initially, the earliest disease specific PrP accumulation seen was in TBMs within germinal centres and only later was it detected in a reticular pattern in the light zone of germinal centres. As in clinically diseased sheep, the latter staining was found to co-localise with CD21 suggesting that PrP was present in FDCs. At 12 months some immunostained TBMs were found in paracortical areas.

Eight ARQ/ARQ lambs necropsied at 3 or 8 months of age had no visceral PrP accumulations but at 12 months of age two of four ARQ/ARQ lambs had PrP accumulation in mesenteric lymph nodes alone. Other lymphoreticular tissues including tonsil were not affected. The remaining two 12-month-old ARQ/ARQ and two ARQ/ARQ sheep at 16 months had no CNS or visceral PrP (Fig. 1).

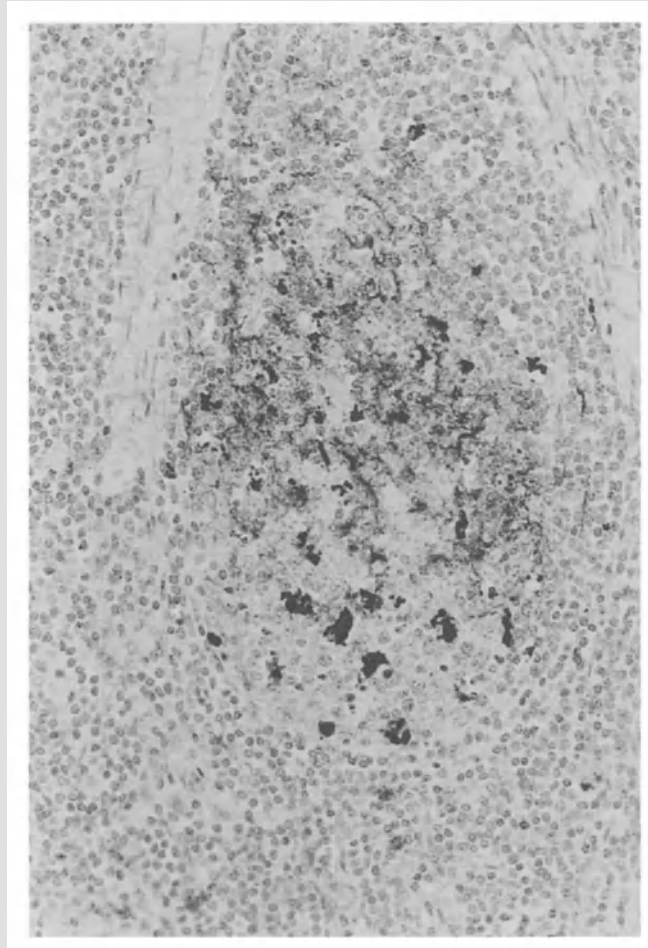


**Fig. 2.** Tonsillar biopsy of a 14-month-old sheep. The follicle shows marked immunostaining of cells with intense granular intracytoplasmic staining (Tingible body macrophages) throughout all regions of the follicle and diffuse punctate staining within the light zone (presumed FDCs). ABC staining for PrP

*Murine scrapie infected spleen: light microscopy*

In 1  $\mu\text{m}$  thick sections of the spleens of mice at terminal stages of disease, PrP was detected in the white pulp in a proportion of macrophage like cells as multiple intense puncta of intracytoplasmic staining as described in sheep. These cells were located throughout the white pulp and occasionally in red pulp in the mantle zones and in both the dark and light zones of secondary lymphoid follicles and were provisionally interpreted as TBMs. All germinal centres were affected. A further cell type presumptively identified as the FDC, showed a diffuse pattern of staining in association with cytoplasmic processes which extended for considerable distances from the cell body.

At 70 days post inoculation (dpi) the overall amount of immunostaining was considerably lower and not all follicles showed evidence of PrP

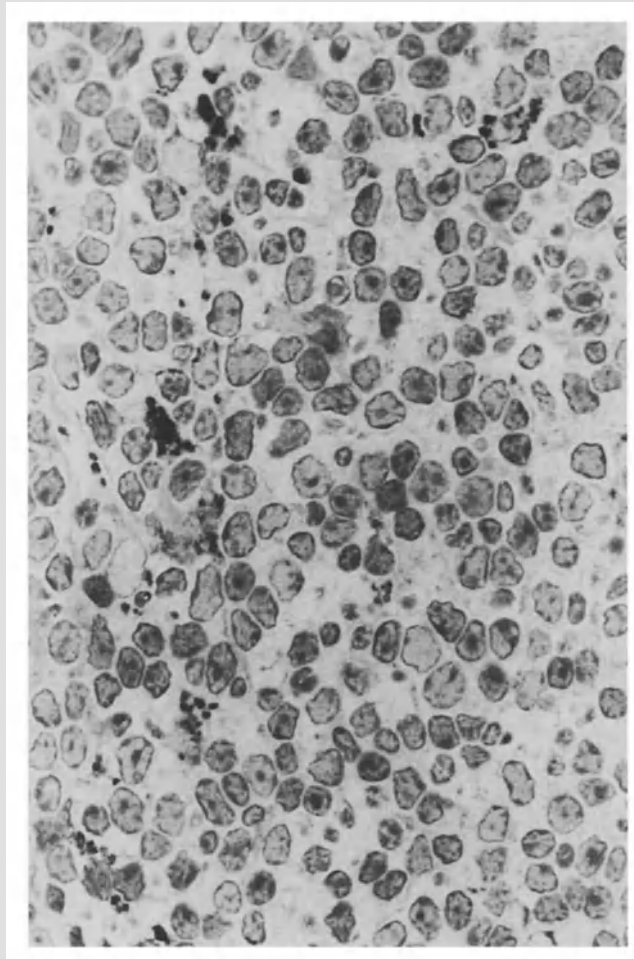


**Fig. 3.** Murine spleen. 70 days postinoculation showing staining of cells and processes.  
1  $\mu$ m thick section PAP for PrP

accumulation. Although more subtle in amount, the patterns of staining at 70 days post inoculation was essentially the same as in terminal diseased mice (Fig. 3). No immunostaining was seen in the red or white pulp of age matched normal brain inoculated controls.

#### *Electron microscopy*

Control tissues did not show any immunostaining when examined by electron microscopy. The dark zones of germinal centres contained lymphocytes between which were small filiform dendritic processes of FDCs. At the centre of some foci of white pulp, secondary lymph follicles could be identified. In part of these follicles lymphocytes were large often with indented nuclei, (the germinal centre light zone) and between them, arranged in small knots were more complex branching processes (labyrinthine glomerular complexes) of FDCs. At the plasmalemma of these dendrites

was electron dense material. TBMs were identified in white pulp and less frequently in red pulp.

In tissues obtained from ME7 infected mice at 70 dpi and at terminal disease, a proportion of TBMs showed marked immunogold affinity for PrP within membrane bound electron dense structures resembling lysosomes (Fig. 4). Only a proportion of TBMs showed immunogold staining.

Immunogold labelling was also associated with a second population of cells found only in the light zone and characterised by complex branching processes (dendrites), sometimes containing desmosome-like membrane specialisations, which identified them as FDCs (Fig. 5). In the light zone of follicles examined from the spleens of 170 dpi mice, the FDC dendrites invariably formed large and complex labyrinthine glomeruli (Figs. 5 and 6) [31] indicating a highly reactive response to stimulation. At the plasma-lemma of dendrites there was an amorphous electron dense material (Figs. 5 and 6). Immunogold staining was seen in the extracellular space surrounding the dendritic processes of FDCs and was associated with the electron dense deposit. The immunogold staining intensity and the complexity of branching of dendritic processes within the glomeruli increased in

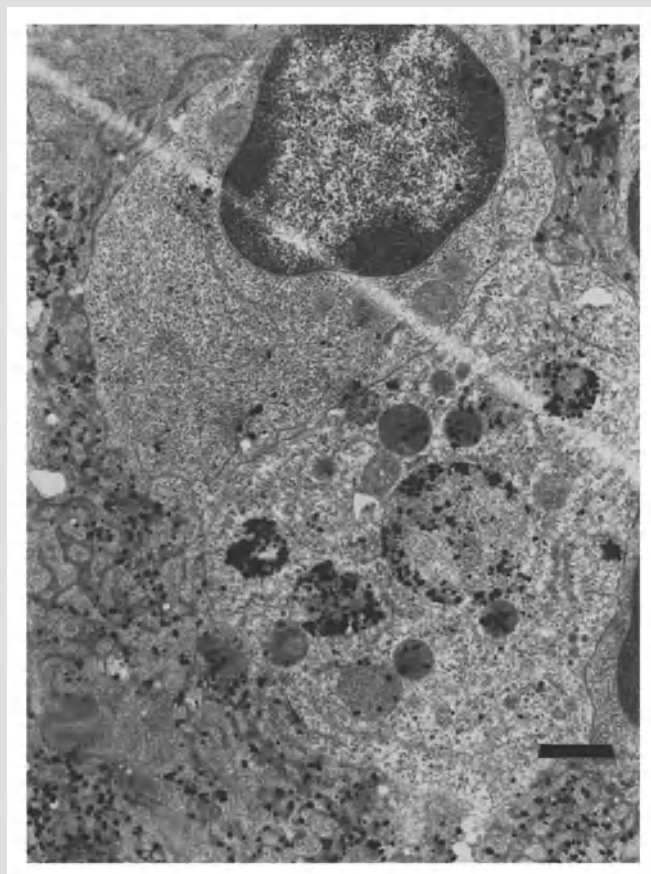


**Fig. 4.** Murine spleen. 70 days postinoculation. Tingible body macrophage showing intra-lysosomal PrP accumulation. Bar: 0.75  $\mu$ m

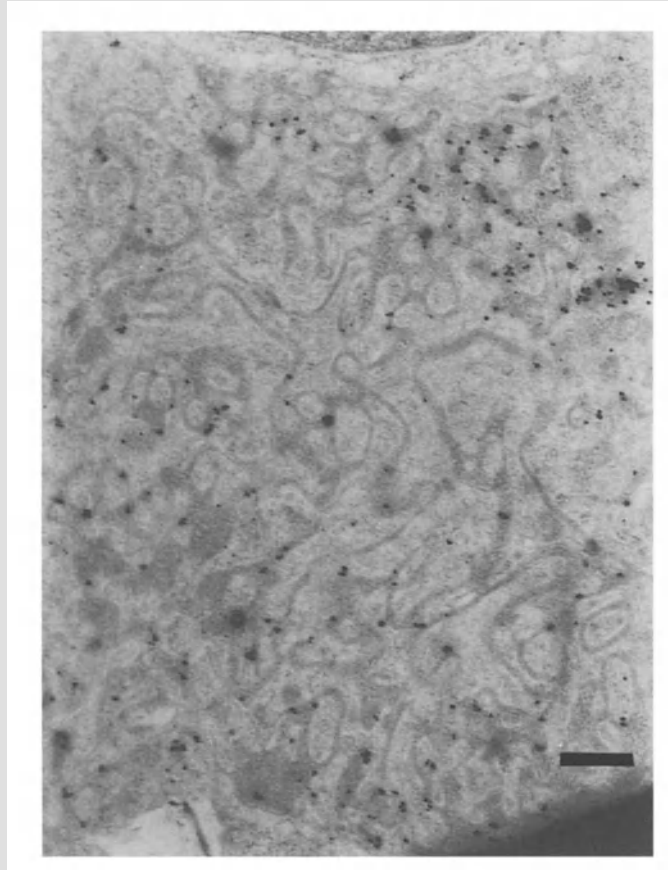


**Fig. 5.** Murine spleen. Terminal disease. Foci of immunoreactivity are present between lymphocyte cell nuclei in association with a FDC labyrinthine glomerular complex containing highly convoluted dendrites. Bar: 0.45  $\mu\text{m}$

proportion to the amount of electron dense material within the extracellular space (Figs. 5 and 6). In some areas amyloid fibrils were present within the extracellular space and were associated with the electron dense deposit (Fig. 6). Immunogold reaction was present in electron dense material associated with FDC dendrites surrounding (emperipolesis) plasmablasts with dilated endoplasmic reticulum. When compared with control material the frequency of plasmablast transformation within germinal centres was increased. Degenerate FDCs with condensation and fragmentation of nuclear chromatin and cytoplasmic vacuolation were also found in germinal centres of scrapie infected tissues but not in controls.

In terminal disease affected mice, most or all germinal centres in light zones were characterised by frequent reactive FDCs with highly complex labyrinthine glomeruli. FDCs were recognised by electron microscopy in areas lacking PrP immunostaining at light microscopy (the dark zone and periarteriolar sheath). FDCs in this region had a primitive morphology with few filiform dendrites and did not show immunogold staining.

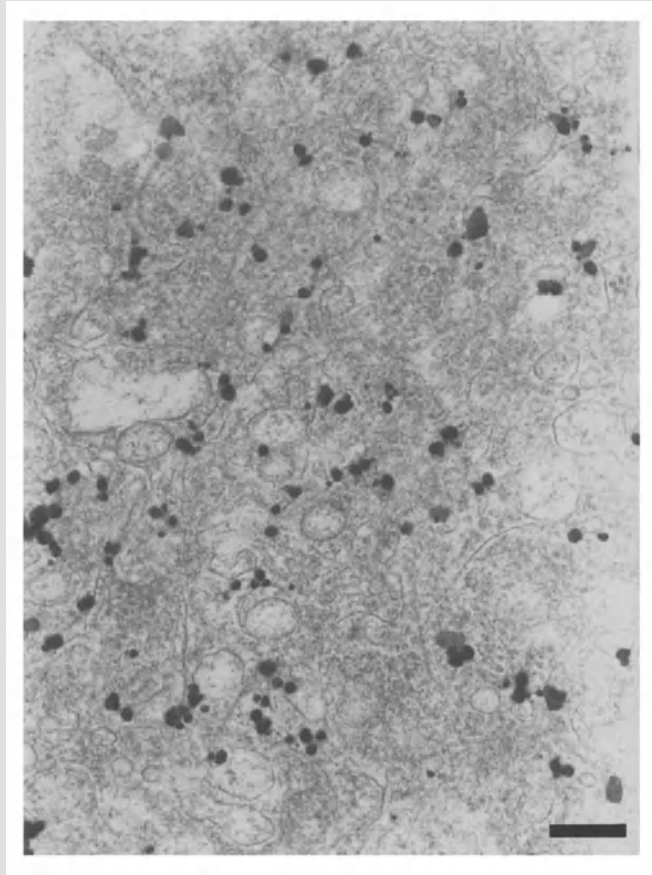


**Fig. 6.** Murine spleen. Terminal disease. FDC processes associated with intense immunogold reaction. There are frequent short filaments present within the extracellular space. Bar: 0.28  $\mu\text{m}$

At 70 days post inoculation most FDCs in the follicular light zones had relatively inconspicuous dendrites that formed small knots of labyrinthine complexes interspersed between lymphocytes and thus were similar to controls. Relatively smaller amounts of amorphous electron dense deposit were present at the plasmalemma. Weak immunostaining was seen within electron dense material around some mildly reactive FDC dendrites of a minority of cells (Fig. 7). FDCs with large labyrinthine glomerular complexes similar to those found in terminal diseased mice were occasionally detected and invariably associated with intense immunogold staining (Fig. 8). Some such areas showed amyloid fibril formation with increased numbers of coated pits.

### Discussion

Although the study of sequential tonsillar biopsies and necropsies within our Suffolk flock are still incomplete, abnormal PrP accumulation has not been detected in tissues of sheep with ARR/ARR or ARQ/ARR

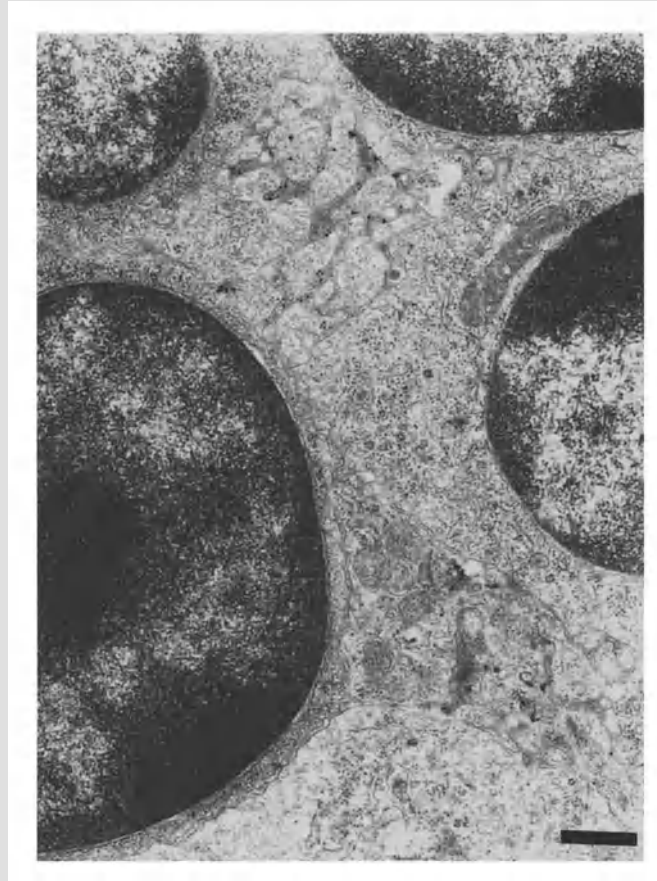


**Fig. 7.** Murine spleen. 70 days postinoculation. Small areas of immunogold reaction are present. These are located at the surface of FDC processes extending between lymphocytes. The dendrites are simple and do not have conspicuous electron dense deposits at the plasmalemma. Bar: 0.63  $\mu\text{m}$

genotypes. In contrast to the results of Dutch Texel and Swifter sheep reported by Schreuder and others [34], susceptible sheep up to 16 months of age have only low levels of immunohistochemically detectable PrP. This may reflect lower levels of susceptibility in Suffolk sheep generally when compared with Texel and Swifter sheep, or lower levels of infection within this flock compared to those studied by van Keulen et al. [33]. The disparity between abnormal PrP detection in tonsils at necropsy and following multiple tonsil biopsy is interesting. The results suggest that the biopsy procedure of susceptible sheep but not resistant sheep may increase susceptibility of FDCs within the remainder of the tonsil to infection.

The studies of murine spleen confirm previous light microscopy studies showing that disease specific accumulations of PrP occur in secondary follicles of spleen. Although the antibodies used do not distinguish between the protease sensitive and protease resistant isoforms of PrP, we would anticipate that at least some of the excess PrP accumulations, particularly

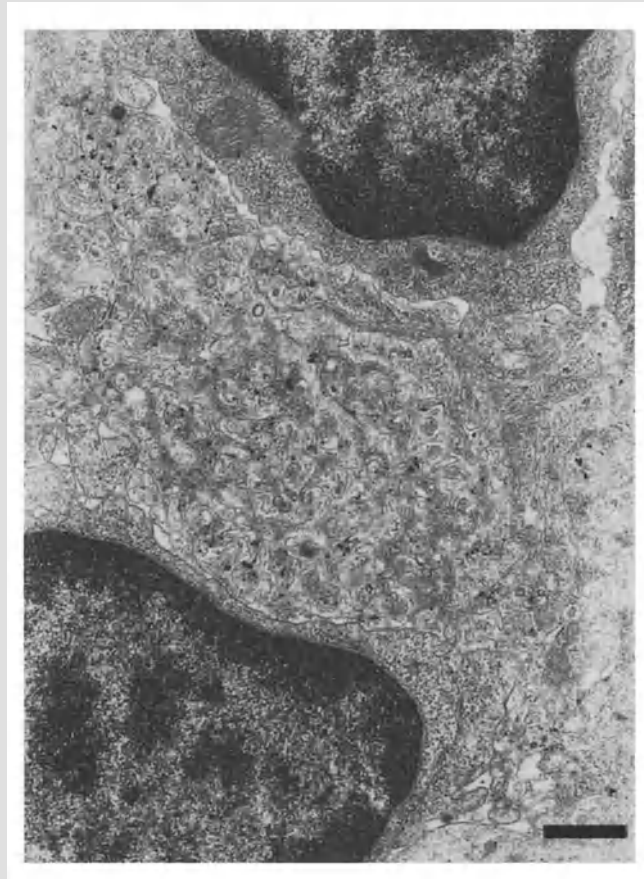


**Fig. 8.** Murine spleen. 70 days postinoculation. An intense immunogold reaction associated with the electron dense deposit overlying complex labyrinthine convolutions of FDCs similar to those seen in terminal mice. Frequent fibrils are present in the extracellular space. Frequent coated pits are also present in association with these fibrils. Bar: 0.53  $\mu\text{m}$

those in fibrillar forms, would be protease resistant. In agreement with transmission and light microscopy studies of Brown et al. [5], our observations do not suggest that PrP accumulation occurs within B lymphocytes in ME7 scrapie affected spleens. Rather, the presence of PrP within TBMs in the paracortical zone or peri-follicular areas in spleen suggests that these cells or dendritic cells rather than plasma cells may possibly be responsible for transporting infection throughout the LRS.

Secondary follicles are divided into a mantle zone of small re-circulating lymphocytes surrounding the dark and light zones of germinal centres [15]. In the light zone there are large lymphoid cells (centrocytes) and FDCs with extensive cytoplasmic extensions. FDCs in the dark zone have immature processes. During the development of germinal centres, FDCs produce specific surface antigens. As increasing quantities of immune complexes are retained, the surfaces of FDCs enlarge, form plicae and dendrites develop [15]. Immune complexes are bound to the cytoplasmic extensions

(dendrites) of FDCs where they may remain for weeks or months. These complexes are not endocytosed but are held at the surface of the dendrite by C3b or Fc receptors [3, 31]. Free antigens are not bound to the surface of FDCs. Antigen-antibody complexes serve to periodically restimulate B and perhaps T cells.

Immature FDCs corresponding to those found in the dark zone were morphologically similar in controls and in infected mice. However, in light zones, all FDCs at terminal stages of disease and a proportion of FDCs at 70 dpi had large and highly complex labyrinthine glomeruli. This appears to represent an abnormal reactive or hyperplastic change of FDCs compared to controls. In addition, excess plasmablast differentiation and FDC degeneration were abnormal. These features show that pathological responses to scrapie infection are not confined to the CNS.

Transmission studies using chimaeric mice [5] in which some immune system cells carry the PrP gene and some do not, and light microscopy immunocytochemical studies of spleen and lymph nodes, suggest that mature FDCs accumulate PrP [5, 22, 27]. The sub-cellular localisation of disease specific PrP accumulations described above confirms that mature FDCs are associated with this accumulation. Outwith the light zone of the follicle, immature FDCs with poorly developed processes do not contain immunoreactive PrP. The disease specific PrP accumulation is not intracytoplasmic but is found at the cell surface of FDCs. This is similar to the plasmalemmal and extracellular localisation of PrP around neurons in the brains of scrapie infected mice [17, 18]. The continued accumulation of PrP both in brain and in spleen appears to lead to the formation of amyloid fibrils within the extracellular space [17–19], a feature consistent with other conventional amyloid diseases.

In this study, an increase in the complexity of FDC dendritic branching was associated with both an increase in the amount of electrondense deposit at the FDC dendrite plasmalemma and the intensity of immunostaining for PrP. As attachment of immune complexes are the trigger for a marked increase in the complexity of dendritic processes [14, 31], the pattern of dendritic branching and distribution of immunogold deposit in terminally diseased mice indicates that the FDCs were highly stimulated by abundant or abnormal PrP, or by excess trapping of immune complexes. In scrapie infected sheep tonsil and lymph nodes, PrP co-localised with CD 21, a marker confined to fully mature FDCs with well developed processes. The sites of accumulation of excess disease specific PrP and the morphological responses of the FDCs may reflect the normal function of PrP<sup>sen</sup>. We suggest that PrP<sup>sen</sup> is involved in dendritic process elongation or assisting in the adhesion of immune complexes to the cell surface. In the present study, the uncomplicated nature of most FDC dendrites at 70 dpi and the paucity of plasmalemma associated electron dense deposits suggest that early disease specific PrP accumulation may occur initially in the absence of antigen-antibody complex trapping.

PrP immunostaining in FDC plasmalemma associated electron dense material could also be interpreted as possible trapped antibody-PrP complexes. However, host antibodies to PrP<sup>sen</sup> would not be anticipated. Antibodies to PrP are not detected in TSE infected animals although parenteral injection does cause an immunological response in PrP null mice. It is therefore possible that low levels of antibodies may be formed to abnormal PrP<sup>res</sup> as a result of structural changes, aggregation and fibrillation. Recent evidence using chimaeric SCID-PrP null mice irradiated and then re-constituted with either PrP null or PrP<sup>+/+</sup> bone marrow, indicate that scrapie replication and accumulation of PrP on FDCs [5] depends on PrP<sup>sen</sup> expressing FDCs. These findings would suggest that most of the PrP detected at the cell surface of FDCs and within electron dense material at the cell surface, was initially expressed at the surface of FDCs and then released into the extracellular space to aggregate and form fibrils.

If increased surface expression of PrP increases the ability of FDCs to scavenge circulating immune complexes, then a breakdown in antibody homeostasis and a heightened non-specific polyclonal antibody response might be anticipated. The large number of lymphoid follicles with some penetrating into the medullary zones of lymph nodes in clinically diseased sheep <sup>1</sup> suggests an abnormal response of lymph nodes to scrapie infection. Sub-cellular pathology <sup>2</sup> including FDC degeneration, plasmablast differentiation, magnitude and ubiquity of labyrinthine glomerular complexes of FDCs in light zones of terminally diseased ME7 infected mice <sup>3</sup> further indicate an altered immunological response. Alterations in immunoglobulin levels have been described in some scrapie-host model systems [7, 9, 10] including natural scrapie of sheep [10] but they are clearly not an essential aspect of disease as most models do not exhibit changes in immunoglobulin levels. In some models immunoglobulin levels may be altered at early stages of infection. The widespread distribution of the hyperplastic form of FDCs with emperipolesis, and the marked increase in amounts of immunocomplexes suggests that scrapie infection may induce an enhanced trapping capacity of immunocomplexes. PrP may therefore be involved in non-specific binding of antigen-antibody complexes. Increased trapping of immune complexes caused by excess PrP at the FDC dendritic plasmalemma may elicit alterations in homeostasis of antibody responses and an increased host polyclonal antibody response. These observations suggest that the immunological response in scrapie is more complex than previously supposed and further investigation of the immune system interactions with PrP may be of interest, not least as a potential for disease intervention strategies and diagnosis.

TBMs ingest apoptotic cells, mostly B cells which are not selected to form clones of globulin producing cells. However, they also scavenge the ends of FDC processes and perhaps effete FDCs themselves [28, 30]. TBMs containing intra-lysosomal PrP were found adjacent to PrP accumulation associated with FDCs and as individual stained cells distant from other foci

of immunostaining. Intra-lysosomal PrP accumulation has also been seen within phagocytic cells of the CNS, including microglia [16], astroglia [16] and Kohler cells (unpubl. obs.). We suggest that TBMs ingest excess or abnormal PrP following phagocytosis of entire degenerate FDCs or their processes or by scavenging the extracellular space.

In the light of recent reports indicating that PrP accumulates within the tonsil of clinical [16] and pre-clinical CJD patients, the importance in understanding the role of the lymphoreticular system in TSE pathogenesis has been greatly increased. The present study indicates that natural and experimental scrapie induced pathological changes are not confined to the CNS. It also provides an insight into the cellular and sub-cellular involvement of FDCs in the peripheral pathogenesis of scrapie and also suggests possible functions of PrP<sup>sen</sup>.

### Acknowledgements

We gratefully acknowledge the assistance of Drs. J.R. Thomson and I. Begara-McGorum for tonsillar biopsies. The EU commission provided part funding of this work under grant 97/6013; UK MAFF provided part funding under SE1928.

### References

1. Blattler T, Brandner S, Raeber AJ, Klein MA, Voigtlander T, Weissmann C, Aguzzi A (1997) PrP-expressing tissue required for transfer of scrapie infectivity from spleen to brain. *Nature* 389: 69–73
2. Bosma GC, Fried M, Custer RP, Carroll A, Gibson DM, Bosma MJ (1983) A severe combined immunodeficiency mutation in the mouse. *Nature* 301: 527–530
3. Bosseloir A, Bouzahzah F, Simar L, Heinen E (1995) B cells in contact with FDC. In: Heinen E (ed) *Follicular dendritic cells in normal and pathological conditions*. Springer, Berlin Heidelberg New York Tokyo, pp 53–78
4. Brown KL, Stewart K, Bruce ME, Fraser H (1997) Severely combined immunodeficient (SCID) mice resist infection with bovine spongiform encephalopathy. *J Gen Virol* 78: 2707–2710
5. Brown KL, Stewart K, Ritchie D, Mabbott NA, Williams A, Fraser H, Morrison WI, Bruce ME (2000) Scrapie replication in lymphoid tissues depends on prion PrP-expressing follicular dendritic cells. *Nature Med* 11: 1308–1311
6. Brown KL, Stewart K, Bruce ME, Fraser H (1996) Scrapie in immunodeficient mice. In: Court L, Dodet B (eds) *Transmissible subacute spongiform encephalopathies*. Elsevier, Paris, pp 159–166
7. Carp RI, Callaghan SM, Patrick BA, Mehta PD (1994) Interaction of scrapie agent and cells of the lymphoreticular system. *Arch Virol* 136: 255–268
8. Cashman NR, Loertscher R, Nalbantoglu J (1990) Cellular isoform of the scrapie agent protein participates in lymphocyte activation. *Cell* 61: 185
9. Collis CS, Kimberlin RH (1985) Long term persistence of scrapie infection in mouse spleens in the absence of clinical disease. *FEMS Microbiol Lett* 29: 111–114
10. Collis SC, Kimberlin RF (1983) Further studies on changes in immunoglobulin G in the sera and CSF of Herdwick sheep with natural and experimental scrapie. *J Comp Pathol* 93: 331–338

11. Diringer H, Gelderblom H, Hilmert H, Ozel M, Edelbluth C (1983) Scrapie infectivity, fibrils and low molecular weight protein. *Nature* 306: 476–478
12. Fraser H, Dickinson AG (1978) Studies of lymphoreticular system in the pathogenesis of scrapie. The role of spleen and thymus. *J Comp Pathol* 88: 563–573
13. Fraser H, Farquhar C (1987) Ionising radiation has no influence on scrapie incubation period in mice. *Vet Microbiol* 13: 211–223
14. Harris DA (1999) Cell biological studies of the prion protein. In: Harris DA (ed) *Prions: molecular and cellular biology*. Horizon Scientific Press, Norfolk, pp 53–66
15. Heinen E, Bosseloir A, Bouzahzah F (1995) Follicular dendritic cells: origin and function. *Curr Top Microbiol Immunol* 201: 15–47
16. Hill AF, Zeidler M, Ironside J, Collinge J (1997) Diagnosis of new variant Creutzfeldt–Jakob disease by tonsil biopsy. *Lancet* 349: 99–100
17. Jeffrey M, Goodsir CM, Bruce ME, McBride PA, Scott JR, Halliday WG (1994) Correlative light and electron microscopy studies of PrP localisation in 87V scrapie. *Brain Res* 656: 329–343
18. Jeffrey M, Goodsir CM, Bruce ME, McBride PA, Fowler N, Scott JR (1994) Murine scrapie-infected neurons in vivo release excess PrP into the extracellular space. *Neurosci Lett* 174: 39–42
19. Jeffrey M, Goodsir CM, Fowler N, Hope J, Bruce ME, McBride PA (1996) Ultrastructural immunolocalisation of synthetic prion protein peptide antibodies in 87V murine scrapie. *Neurodegeneration* 5: 101–109
20. Jeffrey M, McGovern G, Goodsir CM, Brown KL, Bruce ME (2000) Sites of prion protein accumulation in scrapie-infected mouse spleen revealed by immunoelectron microscopy. *J Pathol* (in press)
21. Kimberlin RH, Walker CA (1988) Incubation periods in six models of intraperitoneally injected scrapie depend mainly on the dynamics of agent replication within the nervous system and not the lymphoreticular system. *J Gen Virol* 69: 2953–2960
22. Kitamoto T, Muramoto T, Mohri S, Doh-ura K, Tatieishi J (1991) Abnormal isoform of prion protein accumulates in follicular dendritic cells in mice with Creutzfeldt–Jakob Disease. *J Virol* 65: 6292–6295
23. Klein MA, Frigg R, Raeber AJ, Flechsig E, Hegyi I, Zinkernagel RM, Weissmann C, Aguzzi A (1998) PrP expression in B lymphocytes is not required for prion invasion. *Nature Med* 4: 1429–1433
24. Laszemas CI, Cesbron J-Y, Deslys J-P, Demaimay R, Adjou KT, Rioux R, Lemaire C, Loch C, Dormont D (1996) Immune system-dependent and independent replication of the scrapie agent. *J Virol* 70: 1292–1295
25. Mabbott NA, Brown KL, Manson J, Bruce ME (1997) T lymphocyte activation and the cellular form of the prion protein. *Immunology* 92: 161–165
26. Manson J, McBride P, Hope J (1992) Expression of the PrP gene in the brain of sinc congenic mice and its relationship to the development of scrapie. *Neurodegeneration* 1: 45–52
27. McBride PA, Eikelenboom P, Kraal G, Fraser H, Bruce ME (1992) PrP protein is associated with follicular dendritic cells of spleens and lymph nodes in uninfected and scrapie-infected mice. *Pathol* 168: 413–418
28. Ritchie DL, Brown KL, Bruce ME (2000) Visualisation of PrP protein and follicular dendritic cells in uninfected and scrapie infected spleen. *J Cell Pathol* 1: 3–10

29. Shyng S-L, Heuser JE, Harris DA (1994) A glycolipid-anchored prion protein is endocytosed via clathrin coated pits. *J Cell Biol* 124: 1239–1250
30. Szakal AK, Kosco MH, Tew JG (1988) A novel in vivo follicular dendritic cell-dependent iccosome-mediated mechanism for delivery of antigen to antigen-processing cells. *J Immunol* 140: 342–353
31. Terashima K, Dobashi M, Maeda K, Imai Y (1992). Follicular dendritic cell and iccosomes in germinal centre reactions. *Semin Immunol* 4: 267–274
32. Tew JG, Kosco MH, Szakal AK (1989) The alternative antigen pathway. *Immunol Today* 10: 229–231
33. van Keulen LJM, Schreuder BEC, Meloen RH, MooijHarkes G, Vromans MEW, Langeveld JPM (1996) Immunohistochemical detection of prion protein in lymphoid tissues of sheep with natural scrapie. *J Clin Microbiol* 34: 1228–1231
34. Schreuder BEC, van Keulen LJM, Vromans MEW, Langeveld JPM, Smits M (1998) Tonsillar biopsy and PrP<sup>Sc</sup> detection in the preclinical diagnosis of scrapie. *Vet Rec* 142: 564–568

Authors' address: Dr. M. Jeffrey, Lasswade Veterinary Laboratory, Pentlands Science Park, Bush Loan, Penicuik, Midlothian, Scotland, EH26 0PZ, U.K.

## Pharmacological manipulation of early PrP<sup>res</sup> accumulation in the spleen of scrapie-infected mice

V. Beringue<sup>1</sup>, F. Lamoury<sup>1</sup>, K. T. Adjou<sup>1</sup>, T. Maignien<sup>1</sup>,  
M. Demoy<sup>2</sup>, P. Couvreur<sup>2</sup>, and D. Dormont<sup>1</sup>

<sup>1</sup>CEA, Service de Neurovirologie, DRM/DSV, CRSSA,  
Fontenay aux Roses, France

<sup>2</sup>Laboratoire de Physico-chimie, Pharmacotechnie et Biopharmacie,  
Université Paris XI, Chatenay-Malabry, France

**Summary.** In most experimental models of scrapie and in some naturally infected species, the lymphoreticular system and the spleen in particular play a major role in the pathogenesis of the disease. Previous studies demonstrated scrapie infectivity in peripheral organs from the day of infection up to the terminal stage. The discovery of the abnormal prion protein, PrP<sup>res</sup>, as a specific molecular hallmark of scrapie should permit enhanced study of scrapie pathogenesis and has some pharmacological applications. In this study, PrP<sup>res</sup> accumulation was followed day by day in peripheral organs. Four different phases were identified: the circulation of scrapie inoculum, a clearance phase, the peripheral accumulation of PrP<sup>res</sup> and a plateau phase. This kinetics was then pharmacologically modified (i) by applying the macrophage “suicide” technique to unveil the cellular types involved in scrapie pathogenesis and (ii) with anti-scrapie drugs such as polyene antibiotics, polyanions and Congo red to investigate their mode and site of action.

### Introduction

The emergence of a new variant of Creutzfeldt–Jakob disease (vCJD) is thought to originate from a bovine spongiform encephalopathy (BSE) epidemic [13]. Patients infected with vCJD strikingly accumulate abnormal prion protein (PrP<sup>res</sup>) in tissues of the immune system, unlike other forms of sporadic, familial or infectious CJD [2, 13]. PrP<sup>res</sup> is an abnormal protease-resistant isoform of the normal prion protein (PrP<sup>C</sup>), which accumulates during the development of TSE [21–22] proportionally to infectivity. The peripheral contamination is similar to other TSE, such as natural scrapie in sheep and goats, as well as experimental scrapie in mice,

in which the lymphoreticular system (LRS) and the spleen in particular are infectious soon after infection and long before neuroinvasion occurs [2, 17, 19]. A partly or totally functional immune system is required for scrapie propagation from the periphery to the central nervous system after intraperitoneal infection. The disease is delayed in splenectomized mice and does not or only rarely occur in a panel of immunodeficient mice with deficits in B/T, B lymphocytes and follicular dendritic cell (FDC) development, such as SCID mice, *Rag*<sup>0/0</sup> or  $\mu$ *MT* mice [2, 17, 19]. But the relative importance of individual cell types remains to be more precisely determined, as there is some controversy among the experimental models used [2, 7, 17, 19]. Replication does not exclusively occur in T cells since thymectomized mice, *nude* mice and transgenic mice lacking functional T cells are fully susceptible to experimental scrapie infection [2, 19]. However, splenic T cells have been shown to contain substantial amounts of scrapie infectivity when they express PrP<sup>C</sup> at their surface [2]. Whole body irradiation, splenocyte fractionation and spleen immunostaining have suggested that the cells may be FDC, which are non-dividing stromal cells [2, 7, 19]. In addition, the presence of mature B cells is necessary for scrapie propagation, most probably because they are involved in FDC maturation [2]. Macrophages might also be involved in the pathogenesis of experimental TSE. Their phagocytic capacity might theoretically interfere with TSE agent replication. In contrast they might also permit replication since they are radioresistant, express PrP<sup>C</sup> and are distributed throughout LRS tissues. Therefore, as regards vCJD, there is an urgent need to develop a sensitive and rapid way to detect TSE agent in peripheral organs, as well as to understand precisely which immune cells are involved in TSE pathogenesis.

To date no treatments are available for vCJD and TSE in general. However, some molecules have been shown to prolong survival in experimental models of scrapie and BSE [1]. These include polyene antibiotics such as amphotericin B and its less toxic derivative MS-8209, polyanions such as dextran sulfate 500 (DS500), heteropolyanions or sulfated polyanions and Congo red [1, 3, 16, 19]. Infectivity and PrP<sup>res</sup> accumulation are reduced in vivo in the brain of scrapie-infected rodents after treatment with polyene antibiotics and polyanions [1, 3, 14, 19], and in vitro in scrapie-infected mouse neuroblastoma cell lines after polyanion and Congo red (CR) administration [10–11]. Therefore, these drugs probably interfere with the formation of PrP<sup>res</sup>. Consequently, as polyanions and CR are sulfated glycosaminoglycan analogues, they have been proposed to specifically inhibit PrP<sup>res</sup> accumulation by impairing the association of PrP<sup>res</sup> with endogenous glycosaminoglycans, a necessary step in PrP amyloid plaque formation [11]. A more direct interaction of CR with PrP<sup>res</sup> has also been suggested because this drug binds to PrP<sup>res</sup> fibrils [22]. In vitro incubation of CR with PrP<sup>res</sup> seems to overstabilize the conformation of the protein, therefore impairing the formation of new PrP<sup>res</sup> molecules [9]. Moreover,

the anti-scrapie efficiency of these molecules is linked to their time of administration, and consequently to their site of action. Polyanions and CR are merely efficient when administered around the time of scrapie infection [19]. Polyene antibiotics are also efficient at this time and are the only drugs exerting benefits when given at a later stage [1, 3, 14]. Polyanions, due to their effects on the immune system, probably act via the LRS [19]. The sites of action of polyene antibiotics and CR remain undetermined. Understanding both mechanism and site of action of these drugs has become more crucial for later application in a rationale therapeutic development for vCJD.

In view of these questions, the kinetics of PrP<sup>res</sup> accumulation in mouse peripheral organs was established. Its pharmacological manipulation was performed with (i) liposome-encapsulated dichloromethylene diphosphate (Cl<sub>2</sub>MDP) or clodronate, which is known to deplete macrophage populations of the spleen [12] and to modify cellular homeostasis in mouse spleen, and (ii) anti-TSE drugs such as the polyene antibiotic MS-8209, the polyanion DS500 and Congo red.

## Materials and methods

### *Chemicals*

Cl<sub>2</sub>MDP was obtained from Boehringer Mannheim. Cl<sub>2</sub>MDP-containing liposomes were prepared as described elsewhere [5]. In each experiment throughout the study, spleen macrophages were depleted by a single intravenous injection of 200 µl of a solution containing about 2 mg of liposome-entrapped Cl<sub>2</sub>MDP. MS-8209 is the N-methyl glucamine (NMG) salt of 1-deoxy-1-amino-4,6,0-benzylidene-D-fructosyl-amphotericin B (Mayoly-Spindler laboratories, France). MS-8209 and NMG (Sigma) were suspended in a 5% glucose (wt/vol) sterile solution. The sodium salt DS500 (Pharmacia) was resuspended in a 0.9% NaCl sterile solution. Ninety-nine percent pure Congo Red (Sigma) was dissolved in sterile distilled water.

### *PrP<sup>res</sup> detection in peripheral organs*

The mouse scrapie strain C506M3 was obtained from brain homogenates of terminally ill animals. Eight-week-old C57BL/6 females were intraperitoneally inoculated with 100 µl of a 2% (wt/vol) brain homogenate. Sacrifices were performed in triplicate at different days post-inoculation (dpi), by cervical column disruption. Various organs were immediately removed, frozen in liquid nitrogen, and kept at -80 °C until PrP<sup>res</sup> analysis.

### *Clodronate administration to scrapie-infected mice*

Cl<sub>2</sub>MDP-containing liposomes were injected 2 days before or 1 day after intraperitoneal scrapie inoculation of C57BL/6 mice with 100 µl of 2% (wt/vol) brain homogenate. Controls were untreated or injected with empty liposomes. Mice were sacrificed at various days post-infection. Spleens were removed and immediately

frozen in liquid nitrogen. They were kept at  $-80^{\circ}\text{C}$  until use. In parallel, immunohistochemical studies were performed on the spleen of C57BL/6 mice injected with clodronate [5]. Frozen spleen sections (10  $\mu\text{m}$  thick) were stained with dilutions of monoclonal antibodies against mouse CD90.2/Thy1.2 (Pharmingen), CD45R/B220 (Southern Biotechnology Associates), CD35/CR1 (clone 8C12, Pharmingen), as markers of T lymphocytes, B lymphocytes and FDC, respectively. Acid-phosphatase activity in spleen sections was tested as a pan macrophage marker [5].

*Pre-incubation of scrapie inoculum with anti-scrapie drugs before administration to mice*

Equal doses of either MS-8209, DS500 or CR (100  $\mu\text{l}$  of a 7.5 mg/ml solution, i.e. 25 mg/kg for mice) were incubated with the C506M3 inoculum (100  $\mu\text{l}$  of a 2% brain homogenate), 2 h at room temperature under slight stirring. The solution (200  $\mu\text{l}$ ) was then inoculated intraperitoneally into 8-week-old C57BL/6 mice. As a control, 5% glucose was pre-incubated with the scrapie inoculum. Day 0 is the day of inoculation. Spleens were harvested in triplicate at various dpi, from day 0 up to day 100.

*Repetitive administration of Congo red to scrapie-infected mice*

The intraperitoneal route was used to infect C57BL/6 mice with 100  $\mu\text{l}$  of a 2% brain homogenate. 0.5 mg CR was then intraperitoneally administered twice weekly during 5 weeks after inoculation. Spleens were removed and PrP<sup>res</sup> analysis was performed every week. Control mice were untreated.

*Direct incubation of CR with scrapie inoculum*

Congo red (100  $\mu\text{l}$  of a 7.5 mg/ml solution) was incubated with C506M3 scrapie inoculum (100  $\mu\text{l}$  of a 2% brain homogenate), 2 h at room temperature under slight stirring. PrP<sup>res</sup> from the inoculum was then purified by a scrapie-associated fibrils (SAF) protocol (see below) or only by proteinase K ([PK]; 10  $\mu\text{g}/\text{ml}$ ) digestion. Samples were then resuspended in loading buffer before denaturation and Western blotting procedure [4–6]. Equivalents of 50  $\mu\text{g}$  brain homogenate were run on the 12% polyacrylamide gel for PrP<sup>res</sup> detection.

*PrP<sup>res</sup> detection and quantification*

Tissues were homogenised at 20% (wt/vol) in a 5% glucose (wt/vol) sterile solution with a Ribolyser (Hybaid). PrP<sup>res</sup> was extracted from 100–200  $\mu\text{l}$  tissue homogenate using a SAF protocol previously reported [4–6, 18]. PK was used at 10  $\mu\text{g}/\text{ml}$ . Samples were denatured in loading buffer for 5 min at  $100^{\circ}\text{C}$  before acetone purification and Western blotting procedure. Ten to 40 mg equivalent of tissue were run on 12% polyacrylamide gels. Immunoblotting was performed with a 1/5000 dilution of the polyclonal anti-PrP antibody JB007 [14]. Immunoreactivity was visualized with an enhanced chemiluminescence kit on autoradiographic films (Amersham). The quantity of PrP<sup>res</sup> present in the tissue was expressed as an equivalent of terminally ill scrapie brain mass and was denoted  $\mu\text{g}$  brain equivalent [4–6, 18].

## Results and discussion

### *Early detection of PrP<sup>res</sup> in peripheral organs*

We investigated whether PrP<sup>res</sup> could be used as a sensitive predictor of early scrapie pathogenesis in the spleen and other peripheral organs. PrP<sup>res</sup> was detected in the spleen of C57BL/6 mice as soon as 45 min after intraperitoneal scrapie infection, until 6 h (Table 1 and Fig. 1). PrP<sup>res</sup> was also evidenced in liver and pancreas 15 and 45 min after scrapie infection, respectively, to 6 h post-infection but not in the thymus or in salivary glands (Table 1 and Fig. 1). On day 1, PrP<sup>res</sup> was not detected in these

**Table 1.** PrP<sup>res</sup> detection in peripheral organs of mice infected intraperitoneally with scrapie

Time pi	No. of mice positive for PrP <sup>res</sup> detection/no. of mice tested				
	Spleen	Liver	Pancreas	Thymus	Salivary glands <sup>a</sup>
<i>C57BL/6 mice</i>					
15 min	0/3	1/3	0/3	0/3	0/3
30 min	0/3	1/3	nd	0/3	0/3
45 min	1/3	2/3	1/3	0/3	0/3
1 h	1/3	2/3	3/3	0/3	0/3
2 h	2/3	3/3	3/3	0/3	0/3
3 h	3/3	3/3	3/3	0/3	0/3
4 h	3/3	3/3	3/3	0/3	0/3
6 h	2/3	2/3	2/2	0/3	0/3
Day 1 to 4	0/3	0/3	0/3	0/3	nd
Day 5	3/3	0/3	0/3	0/3	nd
Day 55	3/3	0/3	3/3 <sup>b</sup>	3/3	nd
TS	3/3	0/3	3/3	3/3	3/3
<i>SCID mice</i>					
2 h	3/3	nd	nd	nd	nd
4 h	3/3	3/3	3/3	nd	nd
6 h	3/3	nd	nd	nd	nd
Day 1	2/3	nd	nd	nd	nd
Day 2	1/3	nd	nd	nd	nd
Day 2 to TS	0/3	0/3	0/3	0/3	0/3
<i>PrP<sup>0/0</sup> mice</i>					
3 h	2/2	nd	nd	nd	nd
6 h	2/2	nd	nd	nd	nd
Day 1	1/2	nd	nd	nd	nd
Day 2 to 28	0/2	0/2	0/2	0/2	nd

<sup>a</sup> Salivary glands were pooled and homogenized in 200 µl of a 5% glucose solution

<sup>b</sup> PrP<sup>res</sup> detection in the pancreas was inconstant

TS Terminal stage of the disease

nd Not determined

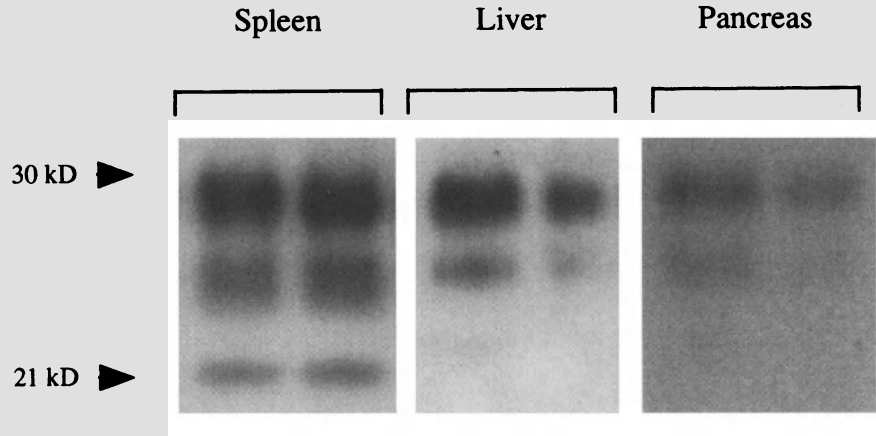


**Fig. 1.** Detection of PrP<sup>res</sup> in peripheral mouse organs on the day of scrapie infection. C57BL/6 mice were intraperitoneally infected with the C506M3 scrapie strain. PrP<sup>res</sup> present in scrapie inoculum was detected in spleen, liver and pancreas harvested 4, 3 and 6 h after inoculation, respectively

organs (Table 1). PrP<sup>res</sup> was again detected on day 5, and increasing amounts accumulated in the spleen until 30 dpi, when a plateau level was reached that remained until the terminal stage of the disease (Table 1 and Fig. 2). Among the experiments and the volume injected into the animals (see experiments below with anti-TSE drugs), PrP<sup>res</sup> reached its plateau in the spleen between 30 and 70 dpi. The maximum amounts of PrP<sup>res</sup> detected at this time were 30 to 150 times less than the maximum amounts found in the brain/per gram. In other organs, PrP<sup>res</sup> was detected in the thymus and occasionally in the pancreas from 55 dpi to the terminal stage of the disease. Little PrP<sup>res</sup> was found in a pool of salivary glands at the terminal stage (Table 1). In another study, we found that PrP<sup>res</sup> was detected in mesenteric lymph nodes from day 21, in Peyer's patches and axillary lymph nodes from day 35. These tissues were then PrP<sup>res</sup>-positive until the animal's death [20]. As a control, the presence of PrP<sup>res</sup> was assessed in the spleen of PrP<sup>0/0</sup> and severely combined immunodeficient (SCID) mice. This organ is not involved in scrapie pathogenesis in SCID mice [4] and PrP<sup>0/0</sup> mice are not susceptible to the infection [19]. PrP<sup>res</sup> was detected in the spleen, liver and pancreas of SCID mice and in the spleen of PrP<sup>0/0</sup> mice a few hours after scrapie infection (Table 1). In contrast to C57BL/6 mice, spleen PrP<sup>res</sup> was also evidenced on day 1 and day 2 but not later (Table 1). The detection of PrP<sup>res</sup> in organs involved in the capture of non-host particles shortly after the inoculation, and independently of mouse status, indicates that PrP<sup>res</sup> associated to the brain inoculum was detected on the day of scrapie infection. When the LRS was immunologically impaired (in SCID mice) or did not express PrP<sup>C</sup> (in PrP<sup>0/0</sup> mice), inoculum-associated PrP<sup>res</sup> was quickly eliminated. In contrast, when the LRS is functional and expresses

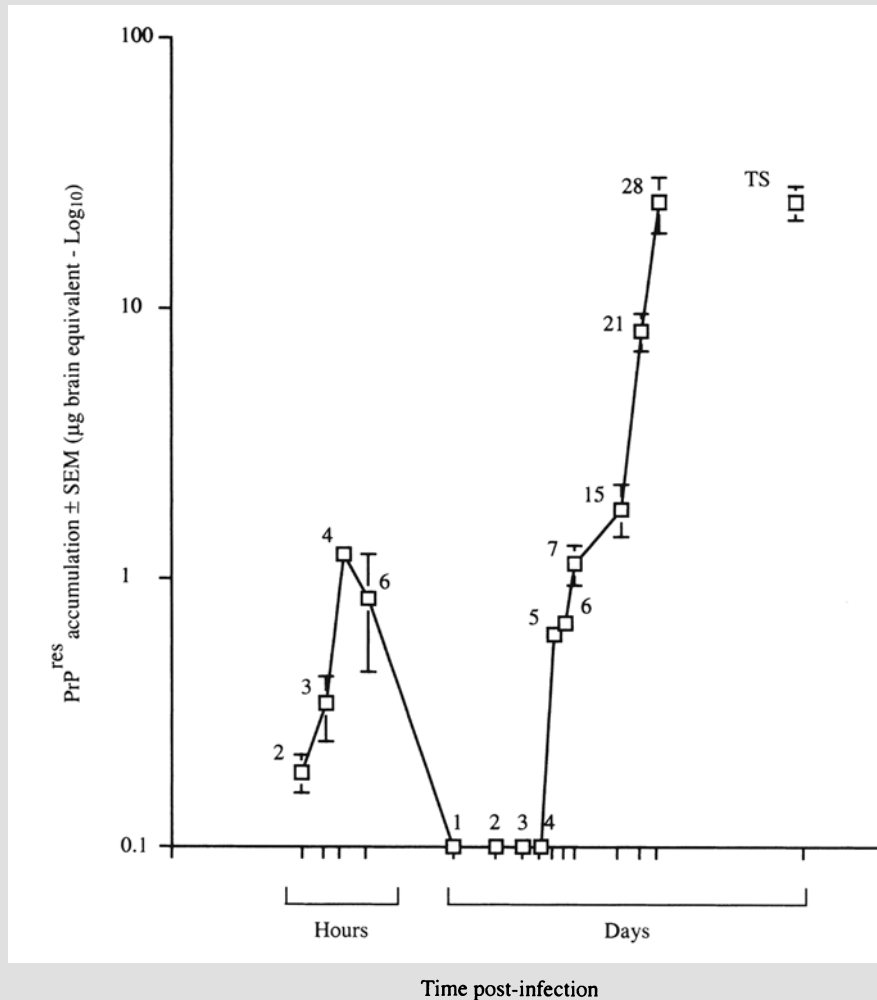


**Fig. 2.** PrP<sup>res</sup> accumulation in the spleen of intraperitoneally scrapie-infected mice. C57BL/6 mice were infected with 100  $\mu$ l of a 2% scrapie brain homogenate. Spleen PrP<sup>res</sup> was quantified (logarithmic scale) from day 0 until the terminal stage of the disease (TS). Results are expressed as an equivalent of scrapie brain mass ( $\mu$ g brain equivalent). The standard deviations for results without error bars were too small to be represented

PrP<sup>C</sup>, inoculum-associated PrP<sup>res</sup> clearance also occurred but PrP<sup>res</sup> reappeared in the spleen on day 5. This probably represents newly synthesized PrP<sup>res</sup>. Lymph nodes, Peyer's patches, thymus, pancreas and salivary glands may represent secondary replication centres, as PrP<sup>res</sup> is detected in them later. This pattern of PrP<sup>res</sup> detection fits with infectivity studies [17], which suggests that PrP<sup>res</sup> may permit enhanced study of scrapie pathogenesis.

The kinetics of PrP<sup>res</sup> accumulation in the spleen of C57BL/6 mice was used to study the molecular effects of clodronate and of anti-TSE drugs.

*Effect of clodronate on spleen PrP<sup>res</sup> accumulation*

## Depletion of spleen macrophages after clodronate administration

The status of spleen macrophages was first assessed after clodronate treatment by measuring acid-phosphatase activity on spleen cryostat sections. Within 1 day after administration, the intravenous injection of liposome-encapsulated clodronate strongly reduced this activity [5] and after 3 days, elimination of all spleen macrophage subpopulations was nearly complete (Fig. 3). Macrophages reappeared on day 10 (Fig. 3) and all macrophage subsets had fully repopulated the spleen 1–2 months after clodronate administration [5]. This description is in accordance with previously published data [12].

## Involvement of macrophages in scrapie inoculum clearance

The first clodronate treatment, performed 2 days before scrapie inoculation, ensured depletion of splenic macrophages on the day of infection (Fig. 4a). (i) More PrP<sup>res</sup> was associated with the scrapie inoculum in the

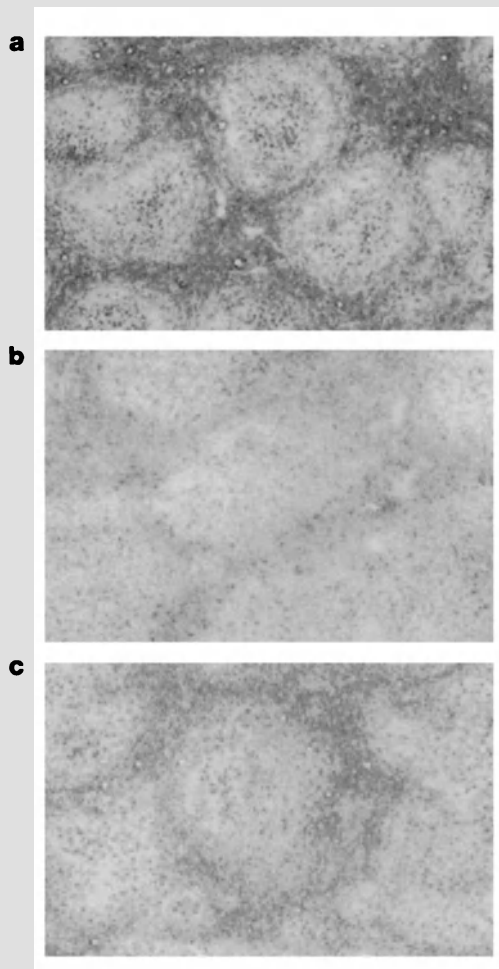


**Fig. 3.** Depletion of spleen macrophages induced by liposome-encapsulated clodronate administration. Macrophage depletion was assessed on frozen spleen sections by measuring acid-phosphatase activity 3 days (**b**) or 10 days (**c**) after intravenous clodronate injection. Control mice were untreated or treated with empty liposomes (**a**).  $\times 40$

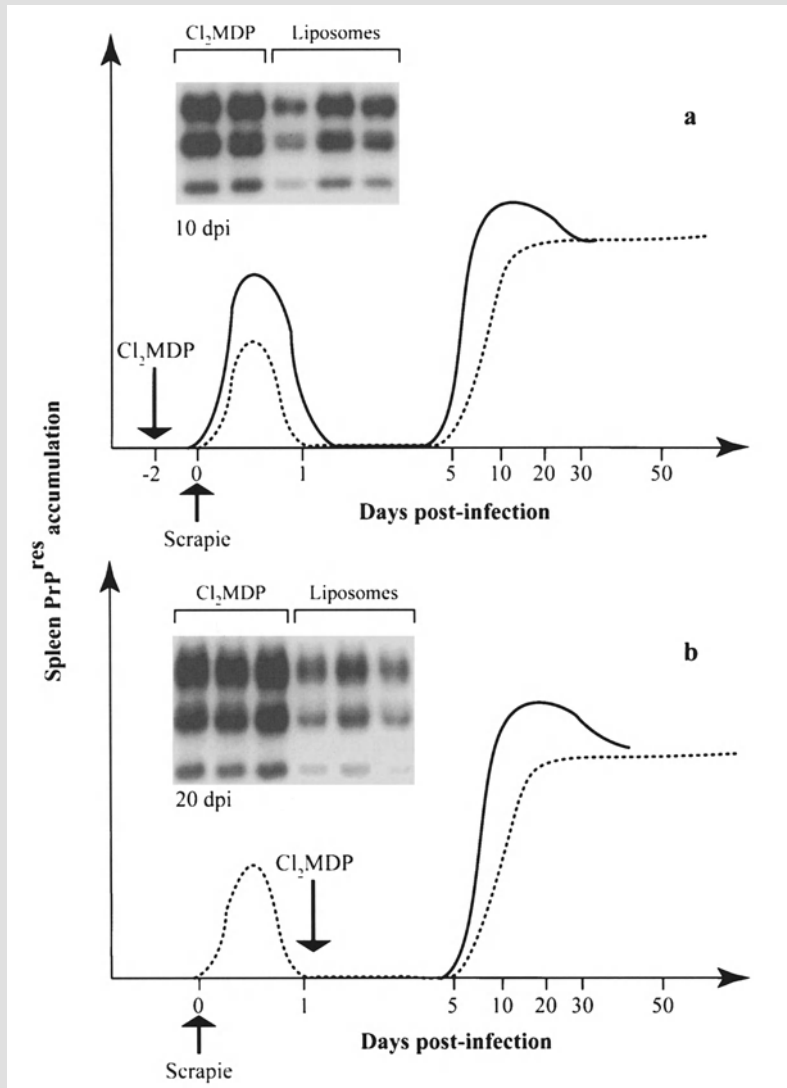


**Fig. 4.** PrP<sup>res</sup> accumulation in the spleen of scrapie-infected mice, following clodronate-containing liposomes administration. Clodronate was injected either 2 days before (a) or 1 day after (b) scrapie inoculation (plain line). Representative spleen PrP<sup>res</sup> detection is presented at 10 (a) and 20 (b) days post-inoculation (dpi). Mice treated with empty liposomes and untreated mice were used as controls (dotted line)

spleen on the day of infection. (ii) A significant increase in newly synthesized PrP<sup>res</sup> during 20 days post-inoculation ( $p < 0.05$ , Mann-Whitney test; Fig. 4) was observed. Therefore, macrophage depletion, induced prior to scrapie inoculation, increased the amount of detectable inoculum in the spleen on the day of infection. This excess of inoculum consequently induced a transient increase in newly synthesized PrP<sup>res</sup>. This study illustrates the involvement of splenic macrophages in the clearance of scrapie inoculum on the day of infection, most probably resulting from their ability to phagocytose insoluble PrP<sup>res</sup>. It is noteworthy that, *in vitro*,

macrophages have also been reported to reduce the infectivity of scrapie inoculum [8].

#### Involvement of macrophages in PrP<sup>res</sup> catabolism

We next assessed the outcome of macrophage depletion for PrP<sup>res</sup> synthesis at the end of the inoculum clearance phase. Mice were treated one day after scrapie infection (Fig. 4b). This regimen also led to a significant increase of PrP<sup>res</sup> accumulation in the spleen ( $p < 0.05$ , Mann-Whitney test; Fig. 4b). This suggests that, in untreated mice, macrophages have the capacity to eliminate newly synthesized PrP<sup>res</sup> molecules that are produced in small amounts just after the post-clearance phase.

In addition, both treatments revealed that, in our scrapie mouse model, macrophages were not directly involved in PrP<sup>res</sup> neosynthesis in the spleen. However, due to the strong resistance of PrP<sup>res</sup> to proteolysis [21], they could also passively contribute to scrapie agent propagation, if they were unable to destroy PrP<sup>res</sup>.

#### Cells involved in scrapie replication after clodronate administration

Using standard immunohistochemistry we also studied, whether other cells in the spleen were depleted by intravenous clodronate administration, particularly those reported to be involved in TSE pathogenesis. This was necessary to ensure that the effects observed with clodronate were indeed specific to macrophage depletion. T lymphocytes were unaffected by the treatment (Table 2). B lymphocytes were, however, strongly depleted during the 6–16-day period after clodronate administration but repopulated very rapidly (Table 2). FDC numbers were also reduced between the 3–16 day period, the strongest effect was observed on day 10; thereafter, the number of FDC slowly increased (Table 2). These alterations were specific for clodronate administration. The injection of liposomes alone did not modify the immunohistochemical staining of the cell populations studied (Table 2). Our observations are consistent with previous studies reporting a similar reduction of marginal zone B cells after clodronate administration without affecting T cells of the white pulp, immunohistochemically or functionally [5]. Moreover, the delay observed between macrophage death, which was almost immediate, and B cell or FDC disappearance suggests that these cells were probably not damaged by Cl<sub>2</sub>MDP directly but by the lysosomal contents released by dying macrophages. Also, *in vitro* incubation of cell suspensions from lymphoid tissues with the drug did not damage lymphocytes [5]. FDC and possibly also B cells have been reported to be involved in scrapie agent replication in the spleen [2, 7, 19]. The depletion of these cells after clodronate administration, suggests the existence of compensatory mechanisms on the cellular or tissue level which

**Table 2.** Changes in immune cell populations of the spleen after clodronate treatment

Cell type	Staining	Analysis day of mice injected with clodronate at day 0								
		Controls <sup>a</sup>	1	3	6	10	16	28	50	
T lymphocytes	Anti-Thy 1.2	++	++	±	++	++	++	++	++	++
B lymphocytes	Anti-B220	++	++	++	-	-	++	++	++	++
Follicular dendritic cells	8C12	++	++	±	±	-	±	±	±	++

<sup>a</sup>Controls were untreated and empty liposome-treated mice

*nd* Not determined

++ Normal number of cells

± Reduced number of cells

- Absence of cells

allow the scrapie agent to persist and even replicate in the absence of B cells and FDC. As T cells were not affected by clodronate administration, it is tempting to suggest that they become target cells in situations where the preferential targets are not available [2, 19]. In situations of T and B lymphocyte and FDC impairment, such as observed in SCID mice, no synthesis of PrP<sup>res</sup> was detectable in the spleen early in the infection (this study and [4]).

#### *Effect of anti-TSE drugs on spleen PrP<sup>res</sup> accumulation*

As the precise mechanisms of action of polyene antibiotics, polyanions and Congo red as well as their site of intervention remain unclear, modifications of the kinetics of PrP<sup>res</sup> accumulation induced by the pre-incubation of these drugs with scrapie inoculum or by treatments performed before or after scrapie infection were studied.

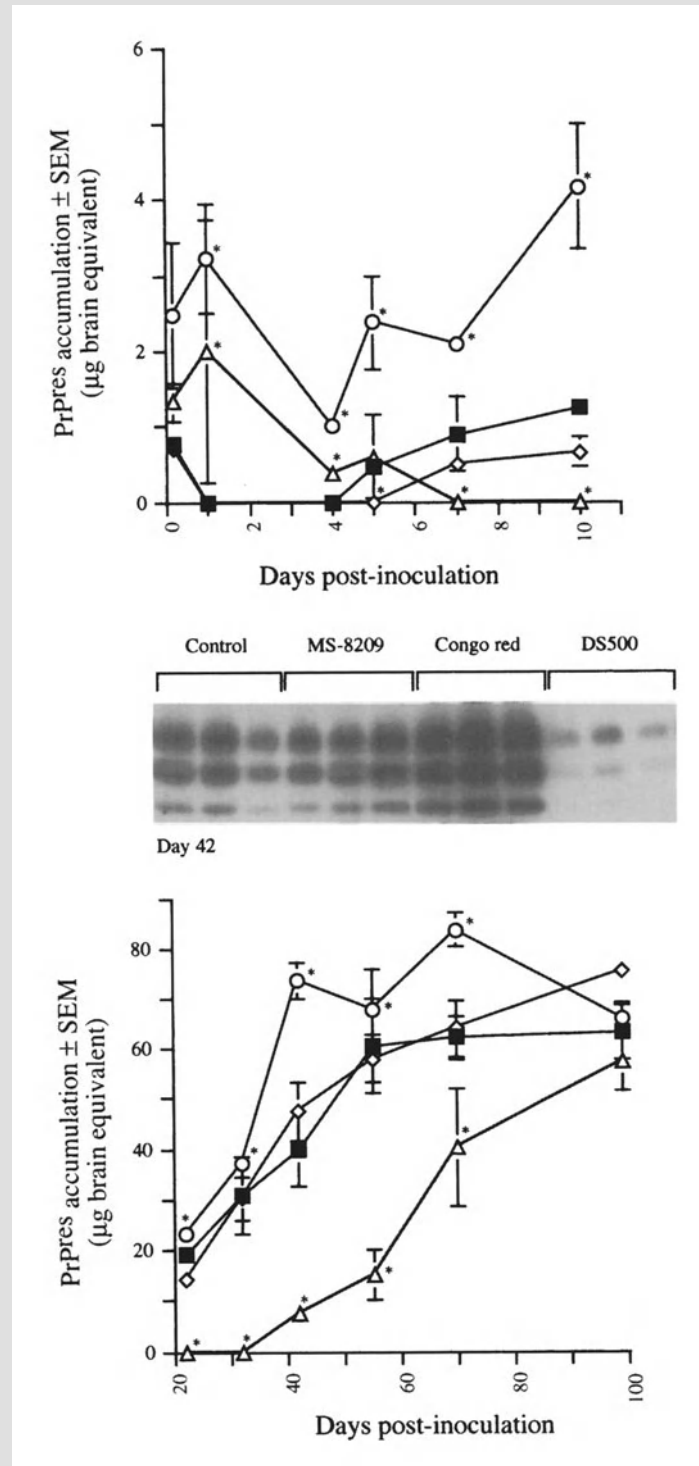
The polyene antibiotic MS-8209 did not involve mainly the spleen

We first studied MS-8209, as it represents one of the most efficient anti-scrapie drugs [1, 3, 14]. Pre-incubation of MS-8209 with scrapie inoculum did not modify spleen PrP<sup>res</sup> detection on the day of inoculation or during the following 4 days when compared to control mice (Fig. 5). MS-8209 only significantly reduced spleen PrP<sup>res</sup> on day 5, compared to its solvent (NMG) or to the 5% glucose control ( $p < 0.05$ , Mann-Whitney test; Fig. 5). After this period, similar amounts of PrP<sup>res</sup> were present in both groups (Fig. 5). A similar effect, restricted to one week after scrapie infection, was observed when the drug was administered 2 h before scrapie inoculation [6]. It is noteworthy that longer treatment periods with MS-8209 slightly increased its anti-PrP<sup>res</sup> accumulation effects in the spleen (unpublished data), but the reduction induced did not account for the benefits observed on survival time [1, 3, 14]. Therefore, the anti-scrapie effects of MS-8209 do mainly not depend on spleen interactions, at least during the early stages of infection. Moreover, treatment of scrapie-infected SCID mice with MS-8209 has shown that the drug was efficient in the absence of a functional LRS, further suggesting that the spleen was not involved [4]. As MS-8209 is

---

**Fig. 5.** PrP<sup>res</sup> accumulation in the spleen of scrapie-infected mice, following inoculation with scrapie inoculum pre-incubated with either MS-8209, DS500 and Congo red. MS-8209 (◇), DS500 (△) or Congo red (○) solutions (7.5 mg/ml) were incubated with mouse scrapie inoculum before intraperitoneal injection. Control mice (■) were infected with inoculum incubated with 5% glucose. Amounts of PrP<sup>res</sup> were statistically compared (Mann-Whitney test). Asterisks indicate when the difference between treated and untreated mice was statistically significant. The standard deviations for results without error bars were too small to be represented. A representative immunoblot is shown 42 days post-infection

also efficient when neuroinvasion has occurred and in transgenic mice expressing only PrP<sup>C</sup> in neurones [14–15], all these data indicate that MS-8209 effects may mainly not involve scrapie replication in the spleen.



### Strong impairment of PrP<sup>res</sup> accumulation in the spleen with the polyanion DS500

DS500 strongly reduced spleen PrP<sup>res</sup> accumulation for long periods of time ( $p < 0.05$ , Mann-Whitney test): spleen PrP<sup>res</sup> concentration decreased slowly in the early stages after inoculation with the DS500-inoculum mixture and was undetectable from day 7 to day 42 (Fig. 5). This suggests, as in SCID mice (Table 1), that pre-incubation of scrapie agent with DS500 induced the clearance of the majority of inoculum-associated PrP<sup>res</sup>. On 42 dpi, spleen PrP<sup>res</sup> was again detected (Fig. 5). Subsequently PrP<sup>res</sup> accumulation increased gradually, reaching concentrations that were similar to those of controls on day 100 (Fig. 5). A similar and transient inhibition of PrP<sup>res</sup> accumulation was observed when the drug was injected 2 h before scrapie infection [6]. When treatment with DS500 was delayed, the efficiency of the drug was more limited on PrP<sup>res</sup> accumulation [6] as well as on infectivity [19] in the spleen. Therefore, DS500 seems to involve the very early stage of scrapie replication in the spleen. How it could modulate scrapie pathogenesis on the cellular level remains to be determined. DS500 exerts pleiotropic effects on immune splenic cells [19]. Therefore, it is likely that PrP<sup>res</sup>-cellular interactions may be altered.

### Congo red transiently increased PrP<sup>res</sup> accumulation in the spleen

Finally, the effects of Congo red were tested. We expected a reduction in spleen PrP<sup>res</sup> accumulation since this drug inhibits PrP<sup>res</sup> accumulation in scrapie-infected cell lines, exerts some benefits in hamster scrapie and has been frequently compared to polyanions [10–11, 16]. CR pre-incubation with scrapie inoculum before mouse infection was important because CR action has often been linked to a binding with PrP<sup>res</sup> [9, 11, 22]. Surprisingly, the pre-incubation of CR with mouse scrapie inoculum transiently increased PrP<sup>res</sup> accumulation in the spleen (Fig. 5). Decreased amounts of PrP<sup>res</sup> were detected in the spleen from day 1 to day 4, but thereafter the spleen accumulated significantly more PrP<sup>res</sup> in CR-treated mice than in control mice until day 70 ( $p < 0.05$ , Mann-Whitney test; Fig. 5). Mice were also treated twice weekly from day 0 to day 35 with 0.5 mg CR per mouse to ensure that the absence of PrP<sup>res</sup> inhibition was not linked to the treatment regimen. Again, CR transiently increased PrP<sup>res</sup> accumulation during 4 weeks ( $p < 0.05$  Mann-Whitney test; Fig. 6). This suggests that, in our mouse model, CR may not exert any benefit. Moreover, the pattern of PrP<sup>res</sup> accumulation observed after CR preincubation with scrapie inoculum could indicate that the drug renders inoculum PrP<sup>res</sup> more resistant to the 0–4 day clearance period and is consequently present in higher amounts.

Congo red overstabilized mouse PrP<sup>res</sup> and increased its protease resistance

To support this hypothesis, the direct effects of CR on inoculum-associated PrP<sup>res</sup> were studied. Equal volumes of CR and 2% mouse scrapie

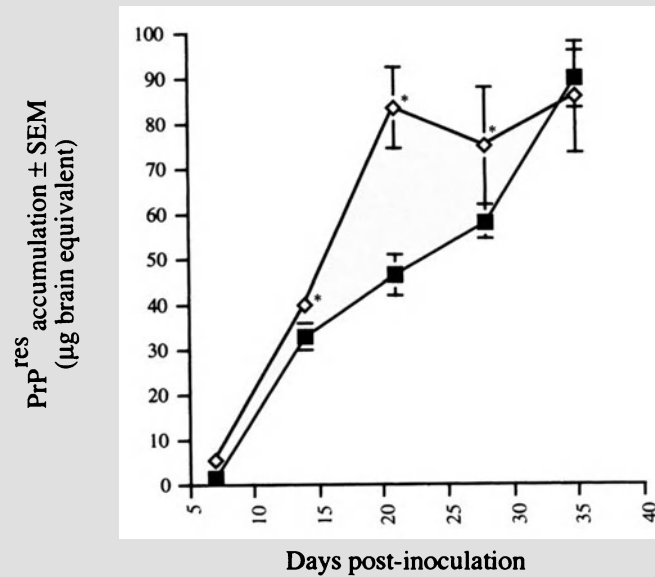


**Fig. 6.** PrP<sup>res</sup> accumulation in the spleen of scrapie-infected mice, following repetitive administration of Congo red. 0.5 mg of Congo red per mouse (◇) was administered twice weekly during 5 weeks. Amounts of PrP<sup>res</sup> were compared to those obtained in untreated scrapie-infected mice (■). Asterisks indicate when the difference between treated and untreated mice was statistically significant ( $p < 0.05$ , Mann-Whitney test). The standard deviations for results without error bars were too small to be represented

inoculum were incubated for 2 h at room temperature. After incubation, PrP<sup>res</sup> was purified following the SAF protocol. The detection of inoculum-associated PrP<sup>res</sup> was enhanced at a dose of 750 µg, i.e. 25 mg/kg (Fig. 7a). This enhancement was dose-dependant until the dose of 37 µg [6] was reached. A similar increase was also observed when PrP<sup>res</sup> was purified only by PK digestion (Fig. 7b). When CR was added after PK cleavage but before denaturation the profile of PrP<sup>res</sup> detection was not modified (Fig. 7c), indicating that the drug directly increased the PK resistance of PrP<sup>res</sup>. CR is known to intercalate into β-sheets of proteins and PrP<sup>res</sup> is characterized by a high β-sheet content [22]. Thus, CR may directly bind to PrP<sup>res</sup> and, thereby overstabilize the complex, making it more resistant to proteolysis.

Congo red “disrupted” hamster PrP<sup>res</sup> and decreased its protease resistance

To assess the scrapie-strain specificity of CR, we investigated the effects of the drug on PrP<sup>res</sup> present in a homogenate of scrapie-infected hamster brain (263K strain). Unlike mouse scrapie, hamster PrP<sup>res</sup> detection after SAF purification was strongly decreased (Fig. 7d), as previously described [9], suggesting that CR effects on PrP<sup>res</sup> are strain-specific. Thus, among the scrapie strain and the host, CR could either stabilize or disrupt inoculum-associated PrP<sup>res</sup>. It is noteworthy that CR was efficient in

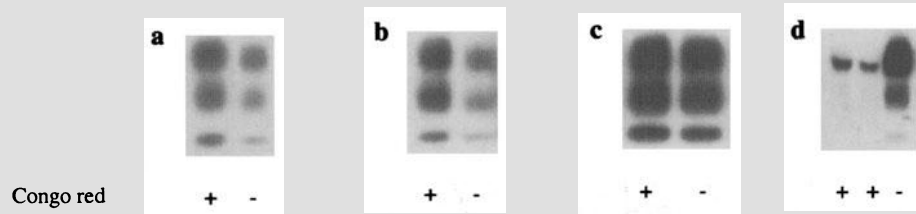


**Fig. 7.** Effects of Congo red (CR) on the detection of PrP<sup>res</sup> associated to scrapie inoculum. 750 µg of CR were incubated with mouse scrapie inoculum (C506M3 strain) 2 h at room temperature before PrP<sup>res</sup> purification by a scrapie-associated fibrils protocol. CR increased inoculum PrP<sup>res</sup> detection (a). A similar increase was also observed when PrP<sup>res</sup> was purified with proteinase K digestion only (b), but not when CR was added after the scrapie-associated fibrils protocol (c). CR was similarly incubated with 2% brain homogenate from scrapie-infected golden hamsters (263K strain). In this case, PrP<sup>res</sup> signal was weakly detected (d). Controls were incubated with 5% glucose

prolonging survival time in hamster scrapie [16]. Taken together, these data suggest that CR binds to PrP<sup>res</sup> and the effects observed in scrapie-infected animals may be its direct consequence.

### Conclusion

Pharmacological manipulation of early PrP<sup>res</sup> accumulation in the spleen suggests that macrophages can interact and interfere with scrapie agent propagation. These effects are probably more prominent in the very early stage of infection in the periphery because late treatment with clodronate did not modify the course of PrP<sup>res</sup> accumulation in the spleen [5]. It also indicated the complexity of the involvement of immune cells in scrapie pathogenesis. FDC and lymphoid cells might act co-operatively and one population could be able to take the relay of the other one in case of the modification cellular homeostasis.

Moreover, it has permitted going further into the mechanism of action of some anti-scrapie drugs. Polyene antibiotics and polyanions may have complementary sites of action, as the first is probably related to neuroinvasion and the second to scrapie replication in spleen. Congo red effect seems to be specifically linked to the PrP<sup>res</sup> protein itself. This is the first drug exhibiting such a tight specificity for scrapie. Studies involving the incubation of Congo red with other TSE agent strains would be of particular interest to confirm if this link is a general phenomenon.

### Acknowledgements

We gratefully acknowledge Pr. M. Seman for the gift of MS-8209 and Pr. C. Weissmann for providing us with PrP<sup>0/0</sup> mice. This project was supported by the “Programme interministériel sur les ESST et les prions”. V.B. is a recipient of a fellowship from the Fondation pour la Recherche Medicale (Paris, France).

### References

1. Adjou KT, Deslys JP, Demaimay R, Seman M, Dormont D (1998) Prospects for the pharmacological treatment of human prion diseases. *CNS Drugs* 10: 83–89
2. Aguzzi A (2000) Prion diseases, blood and the immune system: concerns and reality. *Haematologica* 85: 3–10
3. Beringue V, Demaimay R, Adjou KT, Demart S, Lamoury F, Seman M, Lasmézas CI, Deslys JP, Dormont D (1998) Polyene antibiotics in experimental transmissible subacute spongiform encephalopathies, In: Morrison DRO (ed) *Prions and brain diseases in animals and humans*. Plenum Press, New York, pp 177–185
4. Beringue V, Lasmézas CI, Adjou KT, Demaimay R, Lamoury F, Deslys JP, Seman M, Dormont D (1999) Inhibiting scrapie neuroinvasion by polyene antibiotic treatment of SCID mice. *J Gen Virol* 80: 1873–1877
5. Beringue V, Demoy M, Lasmézas CI, Gouritin B, Weingarten C, Deslys JP, Andreux JP, Couvreur P, Dormont D (2000) Role of spleen macrophages in the clearance of scrapie agent early in the pathogenesis. *J Pathol* 190: 495–502
6. Beringue V, Adjou KT, Lamoury F, Maignien T, Deslys JP, Race R, Dormont D (2000) Opposite effects of dextran sulfate 500, the polyene antibiotic MS-8209 and Congo red on accumulation of the protease-resistant isoform of PrP in the spleens of mice inoculated intraperitoneally with the scrapie agent. *J Virol* 74: 5432–5440
7. Brown KL, Stewart K, Ritchie DL, Mabbott NA, Williams A, Fraser H, Morrison WI, Bruce ME (1999) Scrapie replication in lymphoid tissues depends on prion protein-expressing follicular dendritic cells. *Nature Med* 5: 1308–1312
8. Carp RI, Callahan SM (1982) Effect of mouse peritoneal macrophages on scrapie infectivity during extended in vitro incubation. *Intervirology* 17: 201–207
9. Caspi S, Halimi M, Yanai A, BenSasson S, Taraboulos A, Gabizon R (1998) The anti-prion activity of Congo red. Putative mechanism. *J Biol Chem* 273: 3484–3489
10. Caughey B, Race RE (1992) Potent inhibition of scrapie-associated PrP accumulation by Congo Red. *J Neurochem* 59: 768–771
11. Caughey B, Brown K, Raymond GJ, Katenstein GE, Thresher W (1994) Binding of the protease-sensitive form of prion protein PrP to sulfated glycosaminoglycan and Congo red. *J Virol* 68: 2135–2141
12. Claassen I, Van Rooijen N, Claassen E (1990) A new method for removal of mononuclear phagocytes from heterogeneous cell populations in vitro, using the liposome-mediated macrophage “suicide” technique. *J Immunol Methods* 134: 153–161
13. Collinge J (1999) Variant Creutzfeldt–Jakob disease. *Lancet* 354: 317–323
14. Demaimay R, Adjou KT, Beringue V, Demart S, Lasmézas CI, Deslys JP, Seman M, Dormont D (1997) Late treatment with polyene antibiotics can prolong the survival time of scrapie-infected animals. *J Virol* 71: 9685–9689
15. Demaimay R, Race R, Chesebro B (1999) Effectiveness of polyene antibiotics in treatment of transmissible spongiform encephalopathy in transgenic mice expressing syrian hamster PrP only in neurons. *J Virol* 73: 3511–3513
16. Ingrosso L, Ladogana A, Pocchiari M (1995) Congo red prolongs the incubation period in scrapie-infected hamsters. *J Virol* 69: 506–508
17. Kimberlin RH, Walker CA (1988) Pathogenesis of experimental scrapie. *Ciba Found Symposium* 135: 37–62

18. Lasmézas CI, Deslys JP, Robain O, Jaegly A, Beringue V, Peyrin JM, Fournier JG, Hauw JJ, Rossier J, Dormont D (1997) Transmission of the BSE agent to mice in the absence of detectable abnormal prion protein. *Science* 275: 402–405
19. Mabbott NA, Farquhar CF, Brown KL, Bruce ME (1998) Involvement of the immune system in TSE pathogenesis. *Immunol Today* 19: 201–203
20. Maignien T, Lasmézas CI, Beringue V, Dormont D, Deslys JP (1999) Pathogenesis of the oral route of infection of mice with scrapie and bovine spongiform encephalopathy agents. *J Gen Virol* 80: 3035–3042
21. Prusiner SB (1982) Novel proteinaceous infectious particles cause scrapie. *Science* 216: 136–144
22. Prusiner SB, McKinley MP, Bowman KA, Bolton DC, Bendheim PE, Groth DF, Glenner GG (1983) Scrapie prions aggregate to form amyloid-like birefringent rods. *Cell* 35: 349–358

Authors' address: Dr. V. Beringue, Neuroimmunology Group/Department of Neurogenetics, Imperial College School of Medicine at St Mary's, Norfolk Place, London W2 1PG, U.K.

## Pathogenesis of natural scrapie in sheep

L. J. M. van Keulen, B. E. C. Schreuder, M. E. W. Vromans,  
J. P. M. Langeveld, and M. A. Smits

Institute for Animal Science and Health, Lelystad, The Netherlands

**Summary.** Although scrapie has been known for a long time as a natural disease of sheep and goats, the pathogenesis in its natural host still remains unclear. To study the pathogenesis of natural scrapie, we used immunohistochemistry to monitor the deposition of PrP<sup>Sc</sup> in various tissues, collected during a natural scrapie infection from sheep with the PrP<sup>VRQ</sup>/PrP<sup>VRQ</sup> genotype which were purposely bred for their short incubation period for natural scrapie. PrP<sup>Sc</sup> was present in the lymphoid tissues of all animals from the age of 5 months onwards. At this age, PrP<sup>Sc</sup> was detected in the neural tissues only in the enteric nervous system (ENS) at the level of the duodenum and ileum. At the age of 10 months, PrP<sup>Sc</sup> was not only found in the ENS but also in the ganglion mesentericum cranialis/coeliacum, the dorsal motor nucleus of the vagus, and the intermediolateral column of the thoracic segments T8–T10. PrP<sup>Sc</sup> was detected for the first time in the nucleus tractus solitarius and ganglion nodosus at 17 months of age and in the ganglion trigeminale and several spinal ganglia at 21 months of age. Since the scrapie agent consists largely, if not entirely of PrP<sup>Sc</sup>, these results indicate that the ENS acts as a portal of entry to the neural tissues for the scrapie agent followed by centripetal and retrograde spread through sympathetic and parasympathetic efferent fibers of the autonomic nervous system to the spinal cord and medulla oblongata respectively. PrP<sup>Sc</sup> accumulation in sensory ganglia occurs after infection of the CNS and is therefore probably due to centrifugal and anterograde spread of the scrapie agent from the CNS through afferent nerve fibers.

### Introduction

Scrapie has been known for decades as a natural disease of sheep and goats in many countries throughout the world. Although scrapie has been studied extensively in experimental animal models, relatively little attention has been paid to scrapie as a natural disease in sheep and goats. Therefore

many questions regarding e.g. transmission and pathogenesis of natural scrapie remain to be answered [10]. The need to answer these questions is felt even more urgently as several countries are attempting to control or eradicate scrapie from their sheep population.

In the past several problems have hampered pathogenetic studies of scrapie in its natural host, for example the impossibility of identifying pre-clinically scrapie-infected sheep, the lack of knowledge on the relationship between the incubation period of natural scrapie and PrP genotype and the lack of convenient methods to detect scrapie infectivity other than by the laborious bio-assay in mice. Recently, important progress has been made in these areas enabling pathogenesis studies to be conducted on the natural disease. It is currently possible to identify pre-clinically scrapie-infected sheep by detection of PrP<sup>Sc</sup> in tonsil biopsies [26]. In addition, more knowledge has become available on the relationship between PrP genotype and scrapie susceptibility and scrapie incubation period [5, 6, 12–14, 18]. Unfortunately, no easy way of detecting scrapie infectivity other than by bio-assay has been developed yet. Instead PrP<sup>Sc</sup>, which is closely associated with the scrapie agent and therefore widely used as a marker for scrapie infectivity, can now be detected quite easily and rapidly by means of immunohistochemistry and Western blotting [7–9, 15, 16, 20–23, 25, 28–30]. Although detection of PrP<sup>Sc</sup> by immunohistochemistry has the major drawback that it is difficult to quantify, it has the additional advantage of revealing the cellular and neuro-anatomical localization of PrP<sup>Sc</sup> in the tissues thereby providing valuable information on the neuro-anatomical pathways in scrapie pathogenesis studies.

In a previous study on the distribution of PrP<sup>Sc</sup> within the gastrointestinal tract, we detected PrP<sup>Sc</sup> in the enteric nervous system (ENS) of sheep in the end phase of natural scrapie [31]. Because the ENS is richly innervated by sympathetic and parasympathetic neurons of the CNS (Fig. 1) a possible pathogenetic route of the scrapie agent to reach the CNS along autonomic nerves from the gut was postulated. However, the ENS could also become infected through the reverse route: centrifugal spread of the scrapie agent from the CNS to the gut. Since pathogenetic mechanisms cannot be proven by studying end point cases alone, a sequential time point study in sheep was set up to clarify the role of the ENS in scrapie pathogenesis. In this paper, we report the results of this study using sheep with a highly scrapie susceptible genotype that were naturally infected with the scrapie agent. The sheep were sequentially killed during the course of natural scrapie infection to collect a large range of tissues with special emphasis on the enteric, autonomic and central nervous system. The sequential appearance of PrP<sup>Sc</sup> in these tissues was monitored by means of immunohistochemistry to identify the pathogenetic route(s) of the scrapie agent.

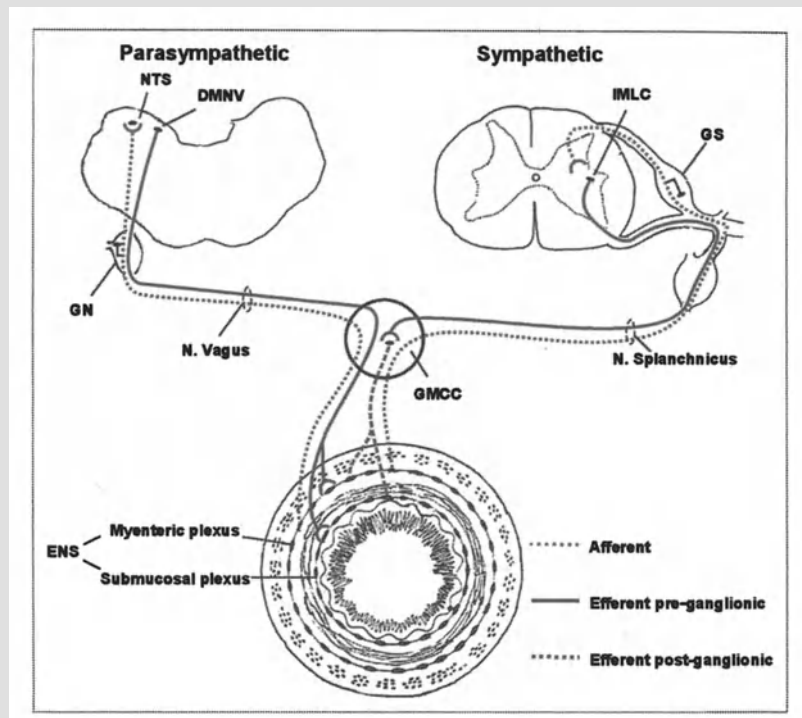


**Fig. 1.** Schematic representation of the parasympathetic (shown on the left) and sympathetic (shown on the right) innervation of the enteric nervous system (*ENS*). The cell bodies of the parasympathetic efferent nerve fibers are located in the dorsal motor nucleus of the vagus (*DMNV*) in the medulla oblongata (pre-ganglionic) and in the enteric nervous system (*ENS*) within the gut wall (post-ganglionic); cell bodies of the sympathetic efferent nerve fibers are located in the intermediolateral column (*IMLC*) in the spinal cord (pre-ganglionic) and in the ganglion mesentericum cranialis/coeliacum (*GMCC*) (post-ganglionic). The afferent parasympathetic nerve fibers have cell bodies in the ganglion nodosum (*GN*) and terminate in the nucleus tractus solitarius (*NTS*). The cell bodies of the afferent sympathetic fibers are located in the ganglia spinalis (*GS*)

## Materials and methods

### *Sheep*

Ten Swifter × Texel crossbreds were purposely bred for high scrapie susceptibility and short incubation period. In these sheep breeds, high susceptibility to natural scrapie is associated with the PrP<sup>VRQ</sup>/PrP<sup>VRQ</sup> genotype (expressed as the triplet sequence present at codons 136, 154 and 171) with a survival time of approximately 2 years [5, 6]. The animals were born and raised at premises where scrapie had been occurring with a high incidence for several years. Tonsillar biopsies were taken between the age of 5 and 10 months and examined immunohistochemically for the presence of PrP<sup>Sc</sup> [27]. All animals were confirmed to be infected with scrapie at this stage. Sheep were sequentially killed at pre-determined timepoints which were based on an expected incubation period of approximately 2 years. Two sheep were killed at 5, 10, and 14 months of age and 1 sheep at 17 and 21 months of age. The two remaining animals

were kept alive until the end point of clinical scrapie and were killed at 26 months of age after having shown signs of clinical scrapie for several weeks. Two animals of the PrP<sup>VRQ</sup>/PrP<sup>ARR</sup> genotype associated with increased resistance to natural scrapie [5, 6] which were born and raised on the same premises were used as negative control animals and were killed at 14 and 26 months of age.

#### *Necropsy*

Sheep were anaesthetized with sodium pentobarbital and killed by exsanguination. Samples were collected in duplo from a range of tissues (Table 1). One set of tissue samples was fixed for 24 h in periodate-lysine-paraformaldehyde (PLP) containing 2% paraformaldehyde, trimmed to a thickness of 2–3 mm, fixed for another 24 h in PLP and then routinely dehydrated and embedded in paraffin. The other set of samples was frozen at  $-70^{\circ}\text{C}$ . The brain was dissected sagittally and the larger part was used for histopathology/immunohistochemistry while the smaller part was frozen at  $-70^{\circ}\text{C}$ .

#### *Immunohistochemistry*

Sections (5  $\mu$ ) were immunostained with antipeptide antisera R505 and R521 as described in detail elsewhere [29–31]. In short, tissue sections were deparaffinized and pretreated with formic acid and hydrated autoclaving. After inactivation of endogenous peroxidase activity, tissue sections were incubated sequentially with antipeptide

**Table 1.** Tissues sampled from each sheep at necropsy

<i>Gastro-intestinal tract</i>	<i>Brain</i>
Oesophagus	Cerebral cortex
Rumen (ventral and dorsal sac)	Septal area and head of the caudate nucleus
Reticulum	Hippocampus
Omasum	Vermis cerebelli
Abomasum	(Hypo)thalamus <sup>a</sup>
Duodenum	Mesencephalon <sup>a</sup>
Jejunum at 25, 50, and 75% of its total length	Pons <sup>a</sup>
Ileum	Medulla oblongata <sup>a</sup>
Caecum	
Mid colon spirale	
Rectum	
<i>Spinal cord (including spinal ganglia)</i>	<i>Lymphoid tissues</i>
C <sub>1</sub> –C <sub>8</sub>	Spleen
T <sub>1</sub> –T <sub>13</sub>	Palatine tonsil
L <sub>1</sub> –L <sub>6</sub>	Pharyngeal tonsil
<i>Autonomic ganglia</i>	Medial retropharyngeal lymph node
Ganglion trigeminale	Superficial cervical lymph node
Ganglion nodosum	Subiliac lymph node
Ganglion mesentericum cranialis/coeliacum	Ileo-caecal lymph node
	Tracheobronchial lymph node

<sup>a</sup>Multiple successive samples taken spanning the entire brain region

antisera, biotinylated secondary antiserum and streptavidin-peroxidase with extensive rinsing between steps. Diaminobenzidine containing 0.1 M imidazole was used as substrate. Pre-immune sera of R505 and R521 served as negative control sera.

When PrP<sup>Sc</sup> was detected in a tissue for the first time, the entire tissue block (with the exception of the spinal ganglia) from the animal(s) of the previous kill was screened for the presence of PrP<sup>Sc</sup>. For this purpose the tissue block was completely trimmed up into serial sections of 5 µ and multiple sections at 50 µm intervals were immunostained for PrP<sup>Sc</sup>.

## Results

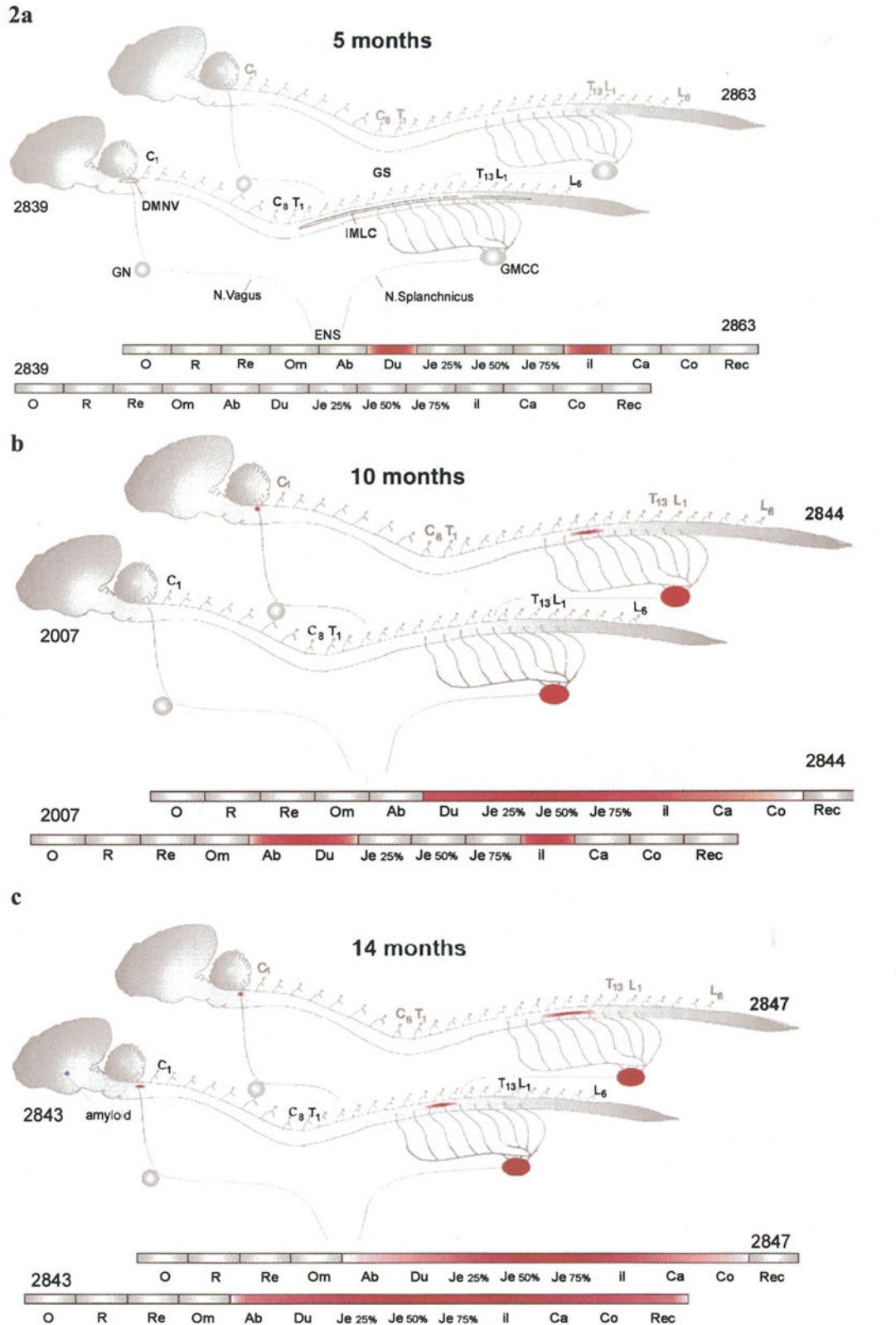
PrP<sup>Sc</sup> was detected in all lymphoid tissues (including peyer's patches) of all scrapie susceptible animals at the age of 5 months and older but not in the PrP<sup>VRQ</sup>/PrP<sup>ARR</sup> sheep. The pattern of PrP<sup>Sc</sup> deposition in the lymphoid tissues was similar to what has been described previously [30]. Amongst all neural tissues examined from the animals of 5 months of age, PrP<sup>Sc</sup> could only be detected in the enteric nervous system (ENS) at the level of the duodenum and ileum in one of the two animals killed at this age (sheep no. 2863 Figs. 2a and 3).

In the animals of 10 months of age, PrP<sup>Sc</sup> was not only seen in the ENS but also in the ganglion mesentericum cranialis/coeliacum (GMCC) (Figs. 2b and 4a). In addition, in one of these animals (sheep no. 2844) PrP<sup>Sc</sup> was found in single neurons of the dorsal motor nucleus of the vagus (DMNV) in the medulla oblongata at the level of the obex (Fig. 4b) and in the intermediolateral column (IMLC) of the thoracic segments T8–T10 of the spinal cord (Fig. 4c).

In the animals killed at 14 months of age, PrP<sup>Sc</sup> was distributed more widespread within the ENS extending from the abomasum to the rectum and was again detected in the GMCC (Fig. 2c). In sheep 2847, PrP<sup>Sc</sup> was seen within single neurons of the DMNV at the level of the obex and in the IMLC of the spinal cord segments T8–T12. In sheep number 2843, PrP<sup>Sc</sup> was detected in the DMNV (mainly in the ventral part) extending from the obex to the caudal pole of the nucleus (Fig. 5) and in the IMLC of the spinal cord segments T8–T10. PrP<sup>Sc</sup> in the form of vascular amyloid was present in the thalamus within the endothelium of several capillaries and

---

**Fig. 2.** Schematic representation of PrP<sup>Sc</sup> accumulation (in red) in the ENS and CNS in naturally scrapie-affected sheep of the PrP<sup>VRQ</sup>/PrP<sup>VRQ</sup> genotype at **a** 5 months; **b** 10 months; **c** 14 months; **d** 17 months; **e** 21 months and **f** 26 months of age. Abbreviations : *DMNV* dorsal motor nucleus of the vagus; *IMLC* intermediolateral column; *C*, *T* and *L* cervical, thoracic and lumbal segments of the spinal cord; *GN* ganglion nodosum; *GMCC* ganglion mesentericum cranialis/coeliacum; *GS* Ganglia spinalis; *O* Oesophagus; *R* Rumen; *Re* Reticulum; *Om* Omasum; *Ab* Abomasum; *Du* Duodenum; *Je* Jejunum; *il* Ileum; *Ca* Caecum; *Co* Colon; *Rec* Rectum. Animal numbers are indicated on the left and on the right: the ENS and CNS of the same animal are aligned to the left or to the right. Only efferent nerve fibers are shown



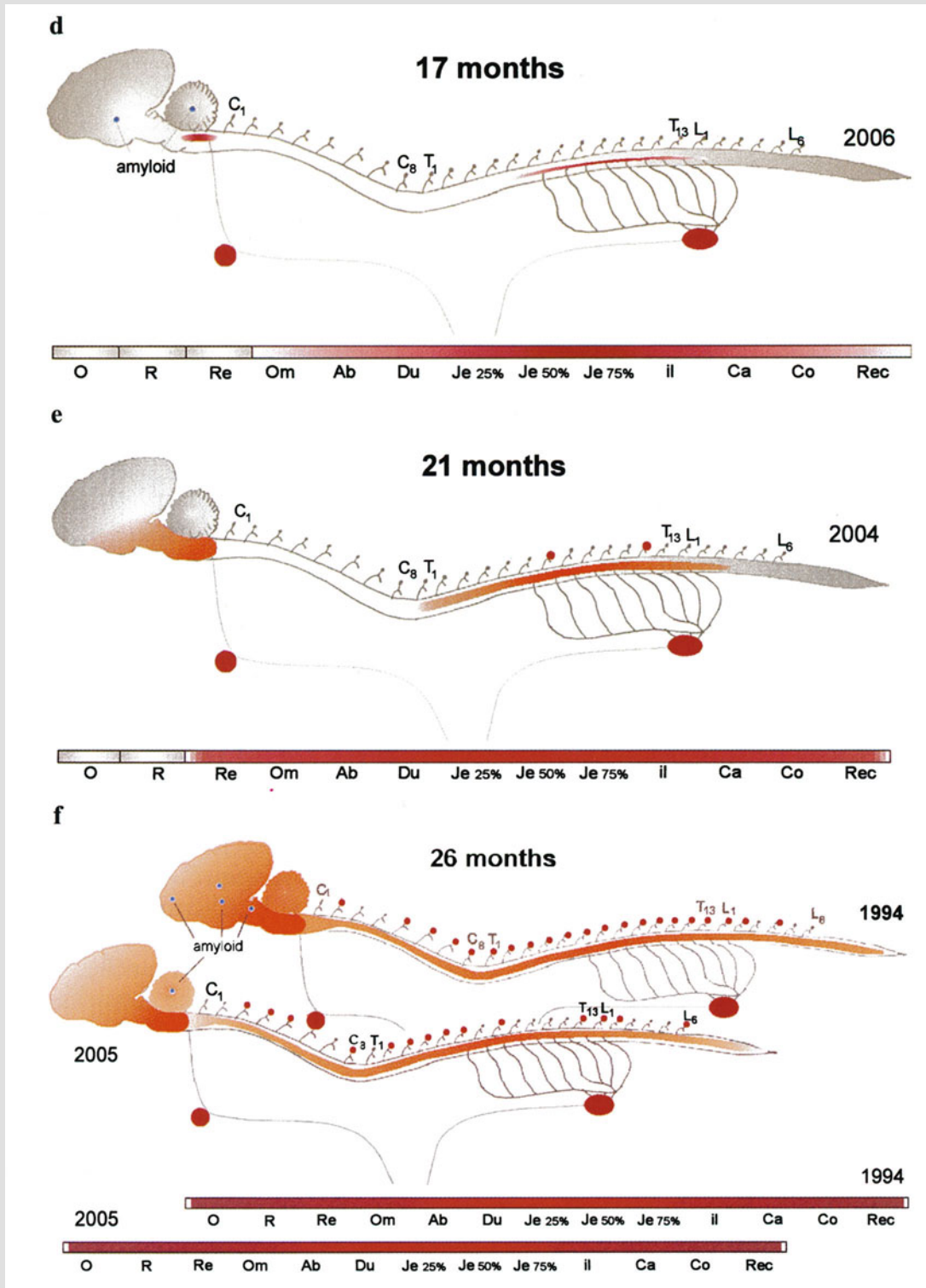
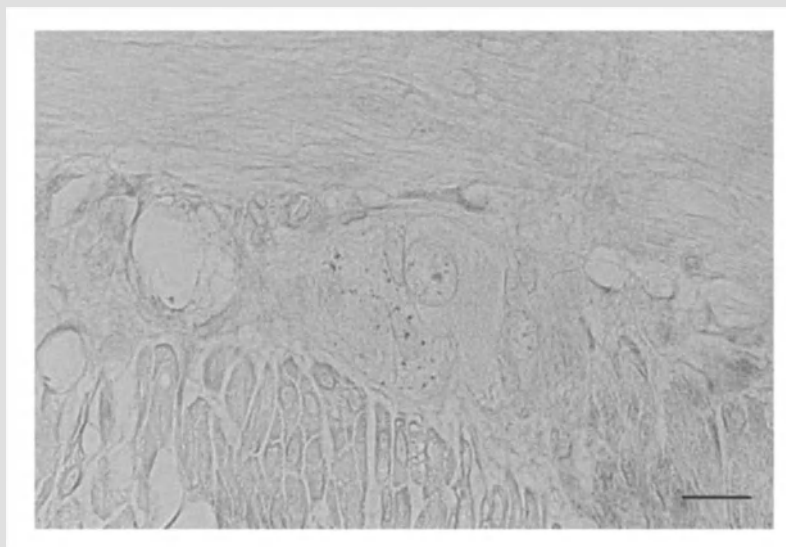


Fig. 2. (continued)



**Fig. 3.** Sheep 2863 (5 months of age). Granules of PrP<sup>Sc</sup> in the cytoplasm of a neuron in the myenteric plexus of the enteric nervous system at the level of the duodenum. Bar: 15  $\mu$ m

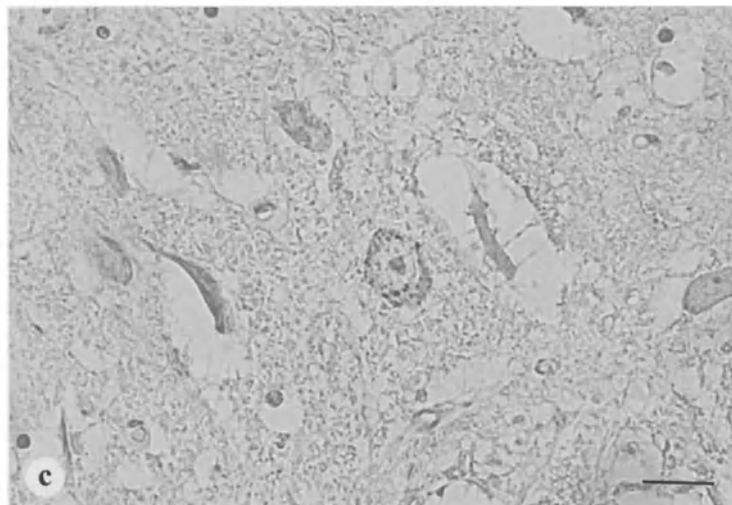
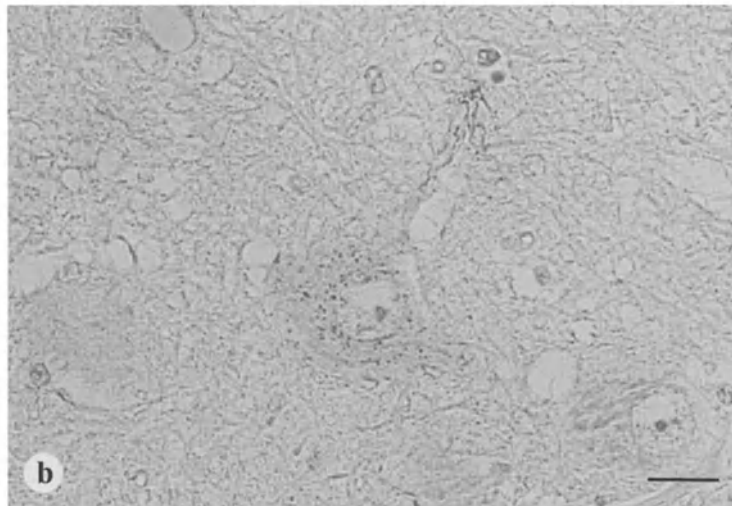
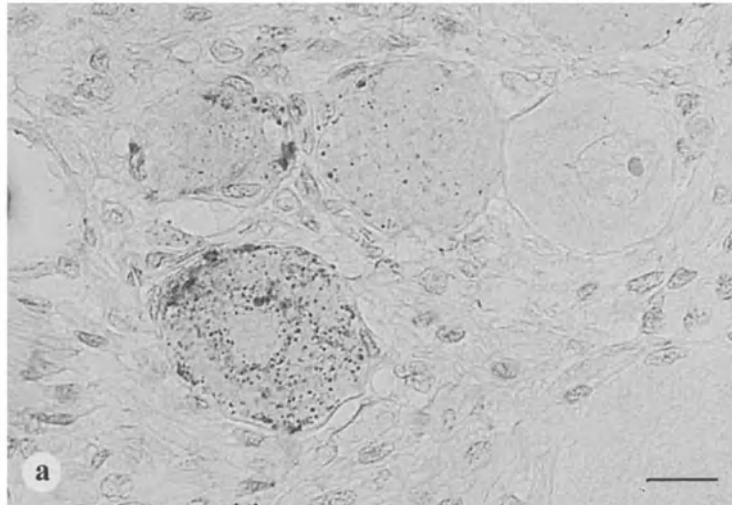
in the surrounding peri-capillary space. In serial sections, PrP<sup>Sc</sup> was not detected in the neurons or the neuropil in the vicinity of these capillaries.

In sheep 2006, killed at 17 months of age, PrP<sup>Sc</sup> was present in the ENS extending from the omasum to the rectum and in the GMCC (Fig. 2d). In the spinal cord, PrP<sup>Sc</sup> was seen in the neurons of the IMLC of the segments T5–L1. In the medulla oblongata the entire nucleus of the DMNV stained positive for PrP<sup>Sc</sup> (Fig. 6) with small branches of PrP<sup>Sc</sup> extending into the area postrema (AP) and the nucleus tractus solitarius (NTS). In addition, PrP<sup>Sc</sup> was found in the nucleus ambiguus (NA) and the descending vestibular nucleus (DVN). Several neurons within the ganglion nodosum (GN) showed some granular staining of PrP<sup>Sc</sup> within their cytoplasm. Furthermore, PrP<sup>Sc</sup> occurred as vascular amyloid in and around capillaries in the thalamus and in the granular layer of the vermis cerebelli. Small granules and branches of PrP<sup>Sc</sup> were seen in the neuropil of the thalamus and between the cerebellar granular cells surrounding these foci of vascular amyloid. A low grade neuronal and neuropil vacuolation was present in the DMNV at this stage.

At 21 months of age, PrP<sup>Sc</sup> was observed in the ENS of the reticulum, omasum, abomasum and small and large intestines (Fig. 2e). In addition, PrP<sup>Sc</sup> was detected in the GMCC and GN, and for the first time in the ganglion trigeminale and the spinal ganglia of segment T7 and T12. Apart from an intense staining of the DMNV, PrP<sup>Sc</sup> was now widely distributed

---

**Fig. 4.** Sheep 2844 (10 months of age). Neuronal PrP<sup>Sc</sup> accumulation in **a** the ganglion mesentericum cranialis/coeliacum; **b** the dorsal motor nucleus of the vagus at the level of the obex; **c** the intermediolateral column at the level of T10. Bar: 15  $\mu$ m



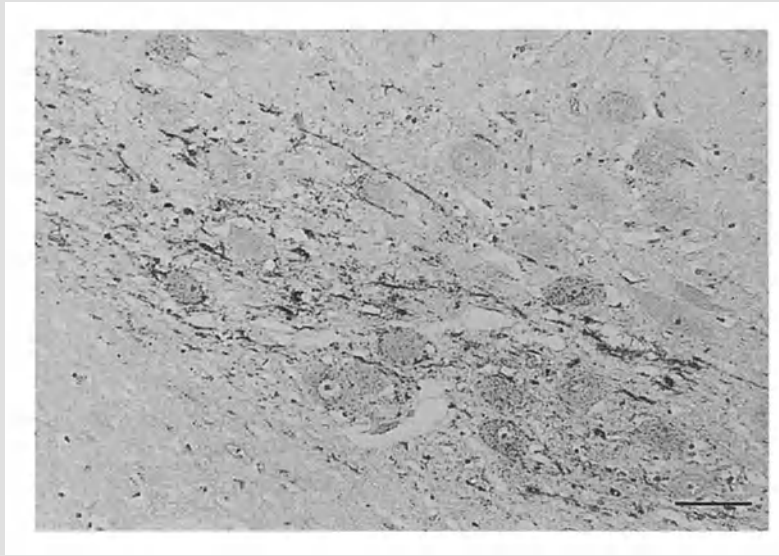


**Fig. 5.** Sheep 2843 (14 months of age). PrP<sup>Sc</sup> accumulation concentrated in the ventral part of the dorsal motor nucleus of the vagus at the level of the obex. Bar: 100  $\mu$ m



**Fig. 6.** Sheep 2006 (17 months of age). PrP<sup>Sc</sup> accumulation throughout the dorsal motor nucleus of the vagus at the level of the obex. Bar: 100  $\mu$ m

in the brain from the obex to the thalamic area and in the spinal cord in the grey matter of segments T1–L3. In the medulla oblongata, vacuolation was prominently present in the DMNV but minimal to absent outside the DMNV.

In the two animals killed in the end stage of natural scrapie at 26 months of age, PrP<sup>Sc</sup> was widely distributed in the brain and spinal cord covering all cervical, thoracic and lumbal segments (Fig. 2f). At this stage,

PrP<sup>Sc</sup> was not only present in the autonomic ganglia but also in the majority of spinal ganglia collected from the cervical, thoracic and lumbar regions. Vacuolation was now widespread throughout the brain but most severe in the medulla oblongata.

In the two sheep that were killed at 14 and 26 months of age and that carried the PrP<sup>VRQ</sup>/PrP<sup>ARR</sup> genotype, no PrP<sup>Sc</sup> could be found in any of the lymphoid or neural tissues examined. No immunostaining was found in any of the tissues of the scrapie-infected animals when pre-immune sera were used as negative control primary antisera.

### Discussion

Oral infection is likely to be the natural route of scrapie infection in sheep [11]. The pathogenesis of scrapie after intragastric or oral inoculation has thus far only been studied in mice and in hamsters [2–4, 17, 19]. These studies showed onset of infectivity and/or first appearance of the scrapie-associated prion protein (PrP<sup>Sc</sup>) in the thoracic spinal cord between the segments T4–T9 indicating to neuroinvasion via the sympathetic fibres of the splanchnic nerve. An alternative route was suggested in orally infected hamsters in which the scrapie agent was found to spread through the vagus nerve to the DMNV and then to the solitary nucleus in the medulla oblongata [4]. However, it is still unclear whether these pathogenetic findings in scrapie challenged mice and hamsters also apply to scrapie as a natural disease in sheep and goats.

In this study we report that in sheep infected with natural scrapie, PrP<sup>Sc</sup> accumulation appears first at multiple sites within the ENS before any PrP<sup>Sc</sup> can be detected in the autonomic ganglia, brain or spinal cord. Next, PrP<sup>Sc</sup> spreads within the ENS and appears in the post-ganglionic sympathetic neurons of the GMCC and in the pre-ganglionic sympathetic neurons in the IMLC of the spinal cord segments T8–T10 indicating the spread of the scrapie agent through efferent sympathetic fibers of the splanchnic nerve. At the same time, PrP<sup>Sc</sup> is seen in the pre-ganglionic parasympathetic neurons in the DMNV of the medulla oblongata which suggest an additional spread of the scrapie agent through the efferent fibers of the vagus nerve. The initial appearance of PrP<sup>Sc</sup> in the ENS indicates that the ENS acts as the portal of entry for the scrapie agent followed by centripetal, retrograde spread to the brain and spinal cord through parasympathetic and sympathetic efferent nerve fibres of the vagus and splanchnic nerve, respectively. After PrP<sup>Sc</sup> had accumulated in the DMNV, it appeared in other nuclei of the medulla oblongata namely the nucleus tractus solitarius, area postrema, nucleus ambiguus and the descending vestibular nucleus. This latter finding is consistent with spread of infectivity through neuronal pathways originating or terminating in the DMNV [32]. Neuro-anatomical connections between the DMNV/NTS and the descending vestibular nucleus have been demonstrated in rats, rabbits and cats as part

of the autonomic influence on vestibular functions and could also exist in sheep [1, 24, 33]. PrP<sup>Sc</sup> accumulation in the sensory ganglia (dorsal spinal ganglia, ganglion nodosum and ganglion trigeminale) was detected after PrP<sup>Sc</sup> had already accumulated in the CNS and is therefore probably due to centrifugal and anterograde spread of the scrapie agent from the CNS along afferent nerve fibres.

In this study, we focused on the neural spread of the scrapie agent with the emphasis on the ENS as a possible portal of entry as was suggested by the results from a previous study [31]. The present study, however, does not exclude unambiguously the possibility of other additional pathogenetic routes in natural scrapie. For instance, scrapie infection could also spread from the lymphoid tissues (which are infected in the very early stage of scrapie infection) to the CNS along autonomic nerve fibers some of which might be identical to the neural pathways identified in this study. However in sheep of the PrP<sup>VRQ</sup>/PrP<sup>ARR</sup> genotype with clinical scrapie, we previously could not detect PrP<sup>Sc</sup> in the lymphoid tissues whilst PrP<sup>Sc</sup> was detected in the ENS and the CNS [29–31]. This means that, at least in sheep with the PrP<sup>VRQ</sup>/PrP<sup>ARR</sup> genotype, scrapie pathogenesis can be completely independent of infection of the lymphoid tissues. Although probably not a prerequisite for scrapie pathogenesis, infection of the lymphoid tissues could play a role in facilitating scrapie pathogenesis. If, for example, the scrapie agent infects the peyer's patches in the submucosa, it will be in very close contact with the neuronal processes of the enteric nervous system, thus facilitating neuronal infection.

Another possible pathogenetic route that could exist in natural scrapie is hematogenous spread of infectivity. In this study, we found PrP<sup>Sc</sup> in the form of amyloid in the endothelial cells of capillaries within the thalamus in a 14 months-old animal at which time PrP<sup>Sc</sup> accumulation in neurons and glia cells was restricted to the DMNV in the medulla oblongata. Hematogenous spread of the scrapie agent could explain the infection of endothelial cells which seems to be independent of neural spread of the scrapie agent. Once endothelial cells are infected, the scrapie agent could spread within the central nervous tissue to infect neurons and glia cells surrounding the capillaries and bloodvessels. However, we did not find any indications suggesting that in PrP<sup>VRQ</sup>/PrP<sup>VRQ</sup> sheep hematogenous spread of the scrapie agent forms an important alternative pathway next to the neural spread to the CNS. Whether hematogenous spread of scrapie is important in sheep carrying other PrP genotype or in sheep infected with other strains of scrapie, remains to be established.

### Acknowledgements

We would like to thank A. Bossers and R. de Vries for the sheep genotyping and A. Korevaar for his help in the necropsy of the sheep.

### References

1. Balaban CD, Beryozkin G (1994) Vestibular nucleus projections to nucleus tractus solitarius and the dorsal motor nucleus of the vagus nerve: potential substrates for vestibulo-autonomic interactions. *Exp Brain Res* 98: 200–212
2. Baldauf E, Beekes M, Diringer H (1997) Evidence for an alternative direct route of access for the scrapie agent to the brain bypassing the spinal cord. *J Gen Virol* 78: 1187–1197
3. Beekes M, Baldauf E, Diringer H (1996) Sequential appearance and accumulation of pathognomonic markers in the central nervous system of hamsters orally infected with scrapie. *J Gen Virol* 77: 1925–1934
4. Beekes M, McBride PA, Baldauf E (1998) Cerebral targeting indicates vagal spread of infection in hamsters fed with scrapie. *J Gen Virol* 79: 601–607
5. Belt PBGM, Muileman IH, Schreuder BEC, Bos-de Ruijter J, Gielkens ALJ, Smits MA (1995) Identification of five allelic variants of the sheep PrP gene and their association with natural scrapie. *J Gen Virol* 76: 509–517
6. Bossers A, Schreuder BEC, Muileman IH, Belt PBGM, Smits MA (1996) PrP genotype contributes to determining survival times of sheep with natural scrapie. *J Gen Virol* 77: 2669–2673
7. Farquhar CF, Somerville RA, Dornan J, Armstrong D, Birkett CR, Hope J (1993) A review of the detection of PrP<sup>Sc</sup>. In: *Transmissible Spongiform Encephalopathies. A consultation on BSE with the Scientific Veterinary Committee of the Commission of the European Communities held in Brussels, 14–15 September 1993, Brussels*, pp 301–313
8. Farquhar CF, Somerville RA, Ritchie LA (1989) Post-mortem immunodiagnosis of scrapie and bovine spongiform encephalopathy. *J Virol Methods* 24: 215–222
9. Foster JD, Wilson MI, Hunter N (1996) Immunolocalisation of the prion protein (PrP) in the brains of sheep with scrapie. *Vet Rec* 139: 512–515
10. Hadlow WJ (1990) To a better understanding of scrapie. In: Bradley R, Savey M, Marchant B (eds) *Current topics in veterinary medicine and animal science*, vol. 55: Sub- Acute Spongiform Encephalopathies, proceedings of a seminar in the CEC Agricultural Research programme held in Brussels, 12–14 November 1990. Kluwer Academic Publishers, Dordrecht, pp 117–130
11. Hadlow WJ, Kennedy RC, Race RE (1982) Natural infection of Suffolk sheep with scrapie virus. *J Infect Dis* 146: 657–664
12. Hunter N, Goldmann W, Benson G, Foster JD, Hope J (1993) Swaledale sheep affected by natural scrapie differ significantly in PrP genotype frequencies from healthy sheep and those selected for reduced incidence of scrapie. *J Gen Virol* 74: 1025–1031
13. Hunter N, Goldmann W, Smith G, Hope J (1994) The association of a codon 136 PrP gene variant with the occurrence of natural scrapie. *Arch Virol* 137: 171–177
14. Ikeda T, Horiuchi M, Ishiguro N, Muramatsu Y, Kai Uwe GD, Shinagawa M (1995) Amino acid polymorphisms of PrP with reference to onset of scrapie in Suffolk and Corriedale sheep in Japan. *J Gen Virol* 76: 2577–2581
15. Ikegami Y, Ito M, Isomura H, Momotani E, Sasaki K, Muramatsu Y, Ishiguro N, Shinagawa M (1991) Pre-clinical and clinical diagnosis of scrapie by detection of PrP protein in tissues of sheep. *Vet Rec* 128: 271–275
16. Katz JB, Pedersen JC, Jenny AL, Taylor WD (1992) Assessment of western immunoblotting for the confirmatory diagnosis of ovine scrapie and bovine spongiform encephalopathy (BSE). *J Vet Diagn Invest* 4: 447–449

17. Kimberlin RH, Walker CA (1989) Pathogenesis of scrapie in mice after intragastric infection. *Virus Res* 12: 213–220
18. Laplanche JL, Chatelain J, Westaway D, Thomas S, Dussaucy M, Brugere-Picoux J, Launay JM (1993) PrP polymorphisms associated with natural scrapie discovered by denaturing gradient gel electrophoresis. *Genomics* 15: 30–37
19. McBride PA, Beekes M (1999) Pathological PrP is abundant in sympathetic and sensory ganglia of hamsters fed with scrapie. *Neurosci Lett* 265: 135–138
20. Miller JM, Jenny AL, Taylor WD, Marsh RF, Rubenstein R, Race RE, Detwiler LA (1993) Immunohistochemical detection of prion protein in sheep with scrapie. *J Vet Diagn Invest* 5: 309–316
21. Miller JM, Jenny AL, Taylor WD, Race RE, Ernst DR, Katz JB, Rubenstein R (1994) Detection of prion protein in formalin-fixed brain by hydrated autoclaving immunohistochemistry for the diagnosis of scrapie in sheep. *J Vet Diagn Invest* 6: 366–368
22. Mohri S, Farquhar CF, Somerville RA, Jeffrey M, Foster JD, Hope J (1992) Immunodetection of a disease specific PrP fraction in scrapie-affected sheep and BSE-affected cattle. *Vet Rec* 131: 537–539
23. Muramatsu Y, Onodera A, Horiuchi M (1994) Detection of PrP<sup>Sc</sup> in sheep at the preclinical stage of scrapie and its significance for the diagnosis of insidious infection. *Arch Virol* 134: 427–432
24. Porter JD, Balaban CD (1997) Connections between the vestibular nuclei and brain stem regions that mediate autonomic function in the rat. *J Vestib Res* 7: 63–76
25. Race RE, Ernst DR, Jenny AL, Taylor WD, Sutton D, Caughey B (1992) Diagnostic implications of detection of proteinase K-resistant protein in spleen, lymph nodes, and brain of sheep. *Am J Vet Res* 53: 883–889
26. Schreuder BEC, van Keulen LJM, Vromans MEW, Langeveld JPM, Smits MA (1996) Preclinical test for prion diseases [letter]. *Nature* 381: 563
27. Schreuder BEC, van Keulen LJM, Vromans MEW, Langeveld JPM, Smits MA (1998) Tonsillar biopsy and PrP<sup>Sc</sup> detection in the preclinical diagnosis of scrapie. *Vet Rec* 142: 564–568
28. Somerville RA, Birkett CR, Farquhar CF, Hunter N, Goldmann W, Dornan J, Grover D, Hennion RM, Percy C, Foster JD, Jeffrey M (1997) Immunodetection of PrP<sup>Sc</sup> in spleens of some scrapie-infected sheep but not BSE-infected cows. *J Gen Virol* 78: 2389–2396
29. van Keulen LJM, Schreuder BEC, Meloen RH, Mooij-Harkes G, Poelen-van den Berg M, Vromans MEW, Langeveld JPM (1995) Immunohistochemical detection and localization of prion protein in brain tissue of sheep with natural scrapie. *Vet Pathol* 32: 299–308
30. van Keulen LJM, Schreuder BEC, Meloen RH, Mooij-Harkes G, Vromans MEW, Langeveld JPM (1996) Immunohistochemical detection of prion protein in lymphoid tissues of sheep with natural scrapie. *J Clin Microbiol* 34: 1228–1231
31. van Keulen LJM, Schreuder BEC, Vromans MEW, Langeveld JPM, Smits MA (1999) Scrapie-associated prion protein in the gastro-intestinal tract of sheep with natural scrapie. *J Comp Pathol* 121: 55–63
32. Wild JM, Johnston BM, Gluckman PD (1991) Central projections of the nodose ganglion and the origin of vagal efferents in the lamb. *J Anat* 175: 105–129

33. Yates BJ, Grelot L, Kerman IA, Balaban CD, Jakus J, Miller AD (1994) Organization of vestibular inputs to nucleus tractus solitarius and adjacent structures in cat brain stem. *Am J Physiol* 267: 974–983

Authors' address: Dr. L. J. M. van Keulen, Institute for Animal Science and Health (ID-Lelystad), Edelhertweg 15, PO Box 65, NL-8200 AB Lelystad, The Netherlands.

## **Animal Models for Prion Diseases**

## Detection of cattle-derived BSE prions using transgenic mice overexpressing bovine PrP<sup>C</sup>

A. Buschmann<sup>1</sup>, E. Pfaff<sup>1</sup>, K. Reifenberg<sup>2</sup>, H. M. Müller<sup>1,3</sup>, and M. H. Groschup<sup>1</sup>

<sup>1</sup>Federal Research Centre for Virus Diseases of Animals,  
Institute of Immunology, Tübingen, Germany

<sup>2</sup>Central Animal Facility, Ulm University, Germany

<sup>3</sup>Connex GmbH, Martinsried, Germany

**Summary.** In interspecies transmissions of transmissible spongiform encephalopathies, the agent has to overcome a species barrier that is largely influenced by the rate of homology between the prion proteins (PrP<sup>C</sup>) of the two involved species. Generating transgenic mice expressing PrP<sup>C</sup> of a foreign species is an approach to develop TSE models that are at least partly devoid of a species barrier. The availability of such animals would enable the detection of low doses of infectivity in tissues or bodily fluids derived from other species. We generated transgenic mice that overexpress bovine PrP<sup>C</sup> (Tgbov XV mice) for the development of an improved detection assay for cattle derived BSE prions. These mice succumbed to the disease 250 days after inoculation with a brain homogenate from BSE diseased cattle. Diagnosis of BSE in transgenic mice was confirmed using Western blot, as well as histological and immunohistochemical methods. In contrast, transgenic mice overexpressing murine PrP<sup>C</sup> (tga20 mice) did not display shorter incubation times than nontransgenic RIII mice infected with the same inoculum. The expression of a chimaeric PrP of murine and bovine sequences rendered such mice partly, if not entirely resistant to an infection with the BSE agent.

### The species barrier in TSE transmissions

Transmissible spongiform encephalopathies (TSE) are fatal neurodegenerative diseases whose natural hosts are sheep and goats (scrapie), cervidae (chronic wasting disease; CWD), and humans (Creutzfeldt–Jakob disease, CJD; Gerstmann–Sträussler–Scheinker syndrome, GSS; fatal familial insomnia, FFI; Kuru). During the last decade, a new epidemic in the United Kingdom and elsewhere has been caused by the accidental transmission of TSE agents to domestic and exotic bovidae (bovine spongiform encephalopathy; BSE) as well as to domestic and wild cats (feline spongiform

encephalopathy; FSE). Other TSE agents have been passed on to mink (transmissible mink encephalopathy; TME). Thus, under certain conditions, TSE agents are able to cross species barriers and cause neurodegenerative diseases of similar characteristics in the new host. Although this only rarely occurs under natural conditions, a much wider range of species can be infected by experimental inoculation when applied directly into the central nervous system using high doses of infectivity. Such species include cattle, sheep, goats, rodents (mice, hamsters, guinea pigs, rats), mink, primates (New World and Old World monkeys), cats, and pigs [1]. However, in such transmissions an elevated threshold exposure dose is necessary to overcome the corresponding species barrier.

The species barrier effect is responsible for comparably long incubation times in the first transmission experiments. In contrast, upon subsequent passages in the new host species, incubation times are markedly reduced [3] and distinct strain features, such as the location of pathological changes in the brains of infected animals and strain-specific glycosylation patterns of PrP<sup>Sc</sup>, become apparent [4, 5, 11, 14].

In infectivity studies using tissues from BSE incubating or diseased cattle, conventional RIII mice have been utilized as sentinel animals. However, due to the existence of a remarkable species barrier between cattle and mice, low doses of infectivity may be missed using this assay. In contrast, transgenic mice expressing PrP<sup>C</sup> of a foreign species are expected to lack such a barrier and may therefore represent useful tools for the detection of prions derived from foreign species. The species barrier seems to be primarily determined by the rate of homology between the prion proteins of the two involved species. Sequence homology is assumed to be important for both the binding of the pathological isoform of the protein (PrP<sup>Sc</sup>) to the cellular prion protein (PrP<sup>C</sup>) and for the conversion of PrP<sup>C</sup> into PrP<sup>Sc</sup> [12]. Studies with transgenic mice indicate that minor exchanges in amino acids or even single mutations at specific sites of the protein may have an impact on the species barrier [11, 14].

### **Circumventing the species barrier by generating transgenic mice**

TSE species barriers can be circumvented by the generation of transgenic mice expressing a prion protein (PrP) of a foreign species. This effect was first reported in transgenic mice overexpressing hamster PrP<sup>C</sup>. Such mice were susceptible to an infection with the hamster scrapie strain Sc237, to which conventional mice are resistant [13]. Later, transmission experiments with other transgenic mice revealed that this is not the case for the expression of PrP<sup>C</sup> of all species: the inoculation of transgenic mice overexpressing human PrP<sup>C</sup> with an isolate of Creutzfeldt–Jakob–disease (CJD) did not result in markedly reduced incubation times as long as these mice coexpressed endogenous murine PrP<sup>C</sup>. However, when these animals were bred on a PrP-ablated background, they exhibited an elevated susceptibility to an

infection with CJD prions [16]. It was therefore assumed that endogenous murine PrP<sup>C</sup> may interfere with the incoming PrP<sup>Sc</sup> of a foreign species directly or via a chaperon-like protein, and so inhibit the formation of transgene-encoded PrP<sup>Sc</sup> by a yet unknown molecular mechanism. The carboxyterminus of PrP<sup>C</sup> has been proposed to be involved in this inhibition as this wild-type murine PrP<sup>C</sup> expression dependent inhibitory effect was not observed in transgenic mice expressing chimaeric PrP<sup>C</sup> of murine and human sequences (with human sequences from codons 97 to 168) [15, 16].

As a conclusion of these results, distinct locations within the prion protein were postulated to have an impact on the conversion process by either mediating the binding of PrP<sup>C</sup> to PrP<sup>Sc</sup>, by assuring the convertibility of the protein into its pathological isoform, or by binding a host-encoded factor (designated protein X) that may act as a chaperone during PrP<sup>Sc</sup> formation (see below).

### **Need for a detection assay for BSE infectivity**

Mouse inoculation tests using nontransgenic RIII mice were performed in the past to detect BSE infection in cattle derived tissue. Using this assay, BSE infectivity was solely detected in the central nervous system, retina, spinal cord [2], and distal ileum (of experimentally infected calves) [17], while all other tissues were not found to contain BSE infectivity [2, 7]. However, as an effect of the species barrier, RIII mice exhibit only a limited susceptibility to an infection with the BSE agent so that a negative result in such transmission experiments does not necessarily exclude the presence of low doses of infectivity.

Therefore, transgenic mice expressing bovine PrP<sup>C</sup> should be useful tools for the detection of even low amounts of cattle derived BSE infection. It has recently been reported that such transgenic mice succumbed to the disease 230 to 340 days upon inoculation, depending on the inoculum and on the infected transgenic mouse line. These transgenic mice harbor a transgene construct based on the cosShaTet vector [13] carrying the entire hamster PrP gene.

We intended to generate transgenic mice overexpressing bovine PrP<sup>C</sup> or a chimaeric PrP<sup>C</sup> of murine and bovine sequences on the basis of a transgene construct that harbors important regions of the murine PrP gene.

### **Generation and characterization of transgenic mice overexpressing bovine PrP<sup>C</sup>**

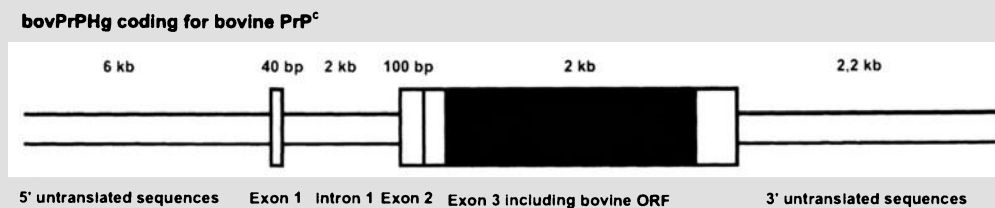
#### *Preparation and microinjection of transgene constructs*

The bovine PrP coding sequence was amplified by PCR from bovine genomic DNA with six octarepetitive sequences and subsequently cloned into the halfgenomic vector pPrPHg, harbouring the complete murine PrP gene but lacking intron 2, which was kindly provided by C. Weissmann, Zurich, and which was in his group for the generation of tga20 mice that

overexpress the murine PrP<sup>C</sup> by a factor of 6-7 [6]. For this purpose, a Sma I digestion site was introduced into codon 125 of the bovine sequence by PCR-mutagenesis using the primer phg1seq 5' GAGCCGATACCCCGGGCAGGGCAGTC 3'. At the 3' end of the ORF, four mutations towards murine sequences were introduced (position 787 A to C; position 790 A to G; position 795 A to G and position 796 G to A), using primer phg2rev 5' TCATCCCACGATGAGAAAATGAGG 3'. All the introduced mutations had no effect on the amino acid sequence of the protein. A second PCR step amplified the murine 3' noncoding sequence between the 3' end of the ORF and the Nar I digestion site 408 bp downstream the ORF. For this PCR, primers phg3seq which is complementary to phg2rev and primer phg4rev 5' GGCTGTTTTTCGACGGCGCCATCCCC 3' were used. A third PCR step using the primers phg1seq and phg4rev with the products of the first two amplifications as templates produced a fragment containing the bovine ORF together with murine 3' end noncoding sequences. This PCR product was analyzed for sequence homology with the bovine sequence and then cloned into pPrPHg using the Sma I and Nar I digestion sites resulting in vector bovPrPHg (Fig. 1).

In parallel, a chimaeric construct of murine and bovine sequences was prepared in the halfgenomic murine transgene cassette. This construct carries bovine sequences between residues 94 and 188 of murine PrP. A similar 'triple-step PCR' as for the preparation of bovPrPHg was per-

A



B

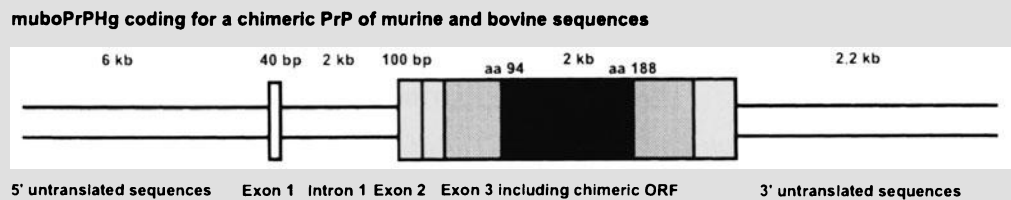


**Fig. 1.** Halfgenomic transgene cassettes on the basis of pPrPHg (kindly provided by C. Weissmann, Zurich). The coding sequence was replaced with sequences encoding authentic bovine or a murine/bovine chimaeric prion protein. Bovine coding sequences are indicated with black bars, murine coding sequences with grey bars

formed: a first PCR step amplified the bovine ORF between codon 125 (using primer phg1seq) and position 597 introducing a Bst EII digestion site at position 588 using the primer phg5rev 5' CCCTTGGTGGTGGTGG-TGACCGTGTG 3'. A second PCR step amplified the sequences between position 588 and the 3' end of the bovine ORF using the primers phg6seq which is complementary to phg5rev and primer bv3rev 5' CCCGCATG-CCTATCCTACTATGAGAAAAAT 3'. A final PCR using primers phg1seq and bv3rev amplified the bovine ORF with a Bst EII digestion site inserted by PCR mutagenesis. This fragment was digested with Kpn I and Bst EII and the 288 basepair (bp) fragment was ligated into the murine ORF digested with the same enzymes and religated into pPrPHg resulting in the vector muboPrPHg (Fig. 1).

These two transgene constructs were microinjected into oocytes of (C57BL/6 × CBA/Ca) F<sub>2</sub> hybrid mice.

#### *Characterization of transgenic mouse lines*

Expression levels of the transgene-encoded PrP were determined by Western blot analysis using mAb L42, which specifically detects ruminant PrP [9]. Signals obtained from serial dilutions of a 10% brain homogenate of transgenic mice were compared to those of a 10% normal bovine brain homogenate. Five mouse lines harboring the construct bovPrPHg (Tgbov I, XII, XIV, XV, XVI) expressed bovine PrP<sup>C</sup> at levels reaching 8-fold the cattle brain expression level. Two PrP<sup>C</sup>-overexpressing mouse lines were lost after breeding problems (Tgbov XIV and XVI). For the chimaeric construct muboPrPHg, six transgenic mouse lines (Tgmubo I, II, IV, XII, XIII, XV) were established with an up to 16-fold overexpression in the brain. Selected transgenic mouse lines were subsequently bred to a wild-type mouse PrP-ablated background.

#### *Challenge studies using four different BSE homogenates*

Four BSE inocula were used for challenge experiments with transgenic and nontransgenic mice. One was derived from the fourth BSE case detected in Germany ('Cindy'), two originated from Swiss BSE cases (kindly provided by A. Pospischil, Zurich ('BSE Zurich') and M. Vandervelde, Bern ('BSE Bern')). Finally, a British inoculum was used that has been used for cattle and mouse challenge experiments in the United Kingdom before ('BBP92', kindly provided by M. Dawson, CVL Weybridge). 10% brain homogenates were prepared and only the Swiss inoculum was gently centrifuged and heated to 70°C for 10 minutes. Mice were inoculated intracerebrally with 30 µl homogenate. Inoculum BBP92 was injected in parallel intracerebrally (20 µl) and intraperitoneally (100 µl). However, it must be concluded from the incubation times observed in RIII mice that the German and Swiss

inocula ‘Cindy’, ‘Zurich’ and ‘Bern’ contained rather low doses of infectivity, whereas the inoculum ‘BBP92’ displayed a higher infectivity titer.

Challenge experiments were performed at the same time in nontransgenic RIII mice, in murine PrP<sup>C</sup>-overexpressing transgenic mice (tga20 mice, kindly provided by C. Weissmann, London), in transgenic mice overexpressing a murine/bovine chimaeric PrP<sup>C</sup> and in transgenic mice overexpressing bovine PrP<sup>C</sup>. While transgenic mice on a PrP wild-type or on a half PrP ablated background were used for the first transmission experiments, subsequent experiments were performed with transgenic mice on a PrP ablated background.

*Expression of a chimaeric PrP of murine and bovine sequences renders transgenic mice almost or entirely resistant to an infection with BSE prions*

Expression of a chimaeric protein of murine and bovine sequences rendered such transgenic mice almost resistant to an infection with the BSE agent (Table 1). More than 700 days after the inoculation of Tgmubo XIII mice bred on a wild-type murine PrP<sup>C</sup> expressing background, none of the animals showed clear clinical symptoms of BSE. However, by using a polyclonal rabbit serum, which preferentially binds to murine PrP, Western blot as well as histological examination revealed a mild accumulation of murine PrP<sup>Sc</sup> in the brains of some of these animals. In two other experiments,

**Table 1.** Incubation times (in days) after transmission of 10% BSE homogenates to nontransgenic RIII mice, murine PrP overexpressing transgenic mice (tga20 mice), transgenic mice overexpressing a murine/bovine chimaeric PrP (Tgmubo XIII mice) and transgenic mice expressing bovine PrP (Tgbov XV mice)

Mouse line	Bern	Cindy	Zurich	BBP92
RIII	465 (15,9) <sup>a</sup>	459 (29,9)	436 (60,7)	398/374 <sup>b</sup>
tga 20	449 (13,2) <sup>a</sup>	458 (9,4)	550 (24,3)	>325
Tgmubo XIII/WT	748 (56,3)	nd	nd	nd
Tgmubo XIII/KO	nd	>710	>790	>630
Tgbov XV/WT	456 (9,0)	nd	nd	nd
Tgbov XV/KO	nd	360 (8,5)	394 (13,2)	234/251 <sup>b</sup> (7,5/11,5)

Standard errors of the mean (SEM) are indicated in brackets

nd Not done

<sup>a</sup> 1% homogenate

<sup>b</sup> In two independent experiments

Tgmubo XIII mice on a murine PrP ablated background were inoculated with BSE homogenates, but none of these animals developed clinical symptoms for more than 710 and 790 days *post inoculationem* (Table 2). All brain samples of animals that had been sacrificed more than 600 days after inoculation were negative in Western blot investigation for PrP<sup>Sc</sup> accumulation. Hence, this chimaeric PrP<sup>C</sup> is hardly, if ever convertible to PrP<sup>Sc</sup>. Similar results were reported for transgenic mice expressing a similar murine/bovine chimaeric PrP [13]. Moreover, it seems to be able to partly block the conversion of murine PrP<sup>C</sup> into its pathological isoform by a yet unknown mechanism, as incubation times in mice coexpressing the chimaeric PrP were distinctly longer (748 days) than in nontransgenic mice on the same genetic background (595 days) (Table 2). Whether the poor convertibility of this chimaeric PrP is influenced by mutations at the following positions modulating the chaperone binding site or the species barrier still needs further evaluation (Fig. 2): four mutations at positions 167, 171, 214 and 218 of the mouse sequence have been postulated to act as possible chaperone binding sites. Out of these, only position 214 differs between bovine and murine sequences, but as it is occupied with the murine sequence in chimaeric PrP, it is not expected to influence the binding efficiency of the chaperone to chimaeric PrP [10]. Four additional mutations at positions 184, 186, 203 and 205 of the mouse PrP gene were postulated to contribute to the species barrier, out of which the first three positions differ

**Table 2.** BSE incubation times in transgenic mice expressing a chimaeric PrP<sup>C</sup> or bovine PrP<sup>C</sup> either alone or in combination with murine PrP<sup>C</sup>

Mouse line	Mouse Prn-status	Transgene expression rate	Bern	Cindy	Zurich	BBP92
Tgmubo XIII	WT/WT	8x	748 (56,3) <sup>a</sup>	nd	nd	nd
		non-Tg	595 (25,1) <sup>a</sup>	nd	nd	nd
	KO/KO	8x	nd	>710	>790	>630
Tgbov XV	WT/WT	8x	456 (9,0) <sup>a</sup>	nd	nd	nd
		non-Tg	589 (32,8) <sup>a</sup>	nd	nd	nd
	KO/KO	8x	nd	360 (8,5) <sup>a</sup>	394 (13,2) <sup>a</sup>	234/251 (7,5/11,5) <sup>a,b</sup>
Tgbov XII	KO/KO	2x	4	451 (11,1) <sup>a</sup>	498 (16,4) <sup>a</sup>	nd

<sup>a</sup>Standard error of the mean (SEM)

<sup>b</sup>Results from two independent challenge experiments

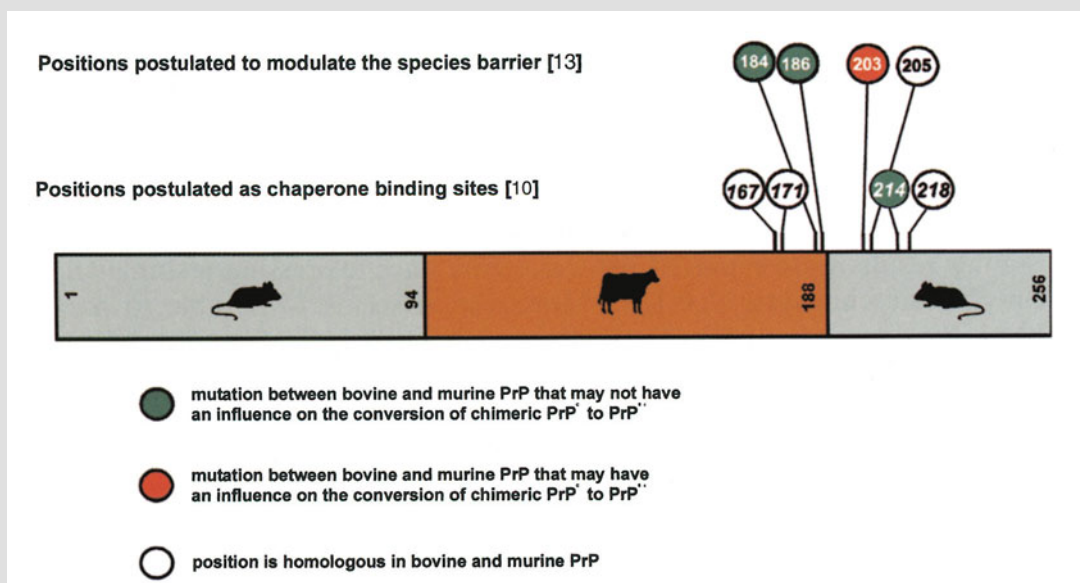


**Fig. 2.** Mutations within the PrP that have been proposed to influence the species barrier or to act as chaperone binding sites for the conversion of PrP<sup>C</sup> to PrP<sup>Sc</sup>

between cattle and mouse PrP [13]. Whether position 203, which is occupied by the murine sequence, influences the convertibility of chimaeric PrP needs to be further investigated.

*Expression of bovine PrP<sup>C</sup> renders transgenic mice highly susceptible to an infection with BSE prions*

Transgenic mice overexpressing bovine PrP<sup>C</sup> (Tgbov XV mice) were highly susceptible to an infection with the BSE agent. Upon inoculation of the high-titer BSE inoculum 'BBP92', incubation times in Tgbov XV mice were as short as 251 and 234 days in two independent experiments (Table 1) compared to more than 370 days in RIII mice. These results are in line with previously published results on transgenic mice expressing bovine PrP<sup>C</sup> [13]. BSE infection of Tgbov XV mice was confirmed by Western blot technique (Fig. 3). Diseased transgenic mice showed an accumulation of bovine PrP<sup>Sc</sup> in their brains, as detected by mAb L42. A mild vacuolation, as well as an astrocytosis (predominantly in the midbrain and the hippocampus and weakly in the cerebellum) was observed by histopathological examination of diseased animals. In addition, fine-granular, as well as plaque-like depositions of bovine PrP<sup>Sc</sup> were detected (Fig. 4).

After inoculation of the two low-titer inocula 'Cindy' and 'Zurich', the incubation times in Tgbov XV mice were 360 and 394 days (Table 2), in comparison to 459 and 436 days in RIII mice, respectively. On the contrary, animals on a wild-type mouse PrP background succumbed to the

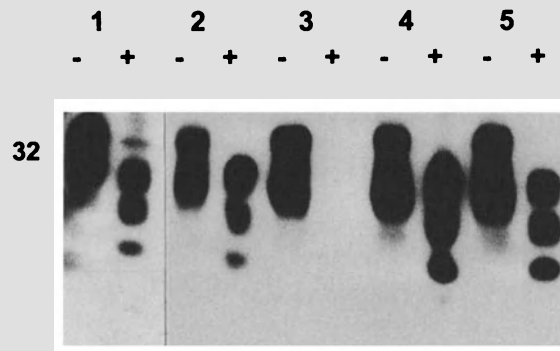


**Fig. 3.** Western blot detection of PrP<sup>Sc</sup> in preparations of scrapie-associated fibrils of 1 BSE diseased RIII mouse, 2 BSE diseased cattle, 3 uninfected Tgbov XV mouse, 4 BSE diseased Tgbov XV mouse, 5 scrapie diseased Tgbov XV mouse

disease 456 days after inoculation with the BSE inoculum 'Bern', compared to 465 days in RIII mice. This observation adds further evidence to the assumption that the coexpression of endogenous murine PrP inhibits the conversion of transgene-encoded PrP<sup>C</sup>. Animals on a wild-type background accumulated murine PrP<sup>Sc</sup> together with bovine PrP<sup>Sc</sup>, as demonstrated by Western blot technique using the polyclonal rabbit serum Ra5/7 that preferentially detects rodent PrP [8]. By immunohistochemical investigation using Ra5/7, additional PrP<sup>Sc</sup> signals became visible in the cerebellum of some animals that coexpressed murine PrP, indicating that these animals simultaneously accumulated bovine and murine PrP<sup>Sc</sup>.

Tgbov XV mice were also susceptible to an infection with the scrapie agent: mice inoculated with a scrapie sheep brain homogenate derived from an animal that carried the VRQ-PrP allele in homozygous form (valine at position 136, alanine at position 154 and glutamine at position 171), which is linked to a high scrapie susceptibility of sheep (kindly provided by T. Baron, Lyon), succumbed to the disease after 400 days.

*No increased susceptibility of mouse PrP<sup>C</sup> overexpressing tga20 mice to cattle derived BSE prions*

It has been described that the dose of PrP<sup>C</sup> overexpression and the length of incubation time were inversely correlated in transmission experiments with the mouse adapted scrapie strain 'Chandler' [6]. Surprisingly, a similar effect was not observed in transmission experiments with cattle derived BSE agent to nontransgenic RIII and transgenic tga20 mice overexpressing murine PrP<sup>C</sup>. Incubation times observed in tga20 mice were not shorter than those seen in RIII mice, even though both mouse lines express PrP<sup>C</sup> of the same amino acid sequence at substantially different ratios (Table 1).

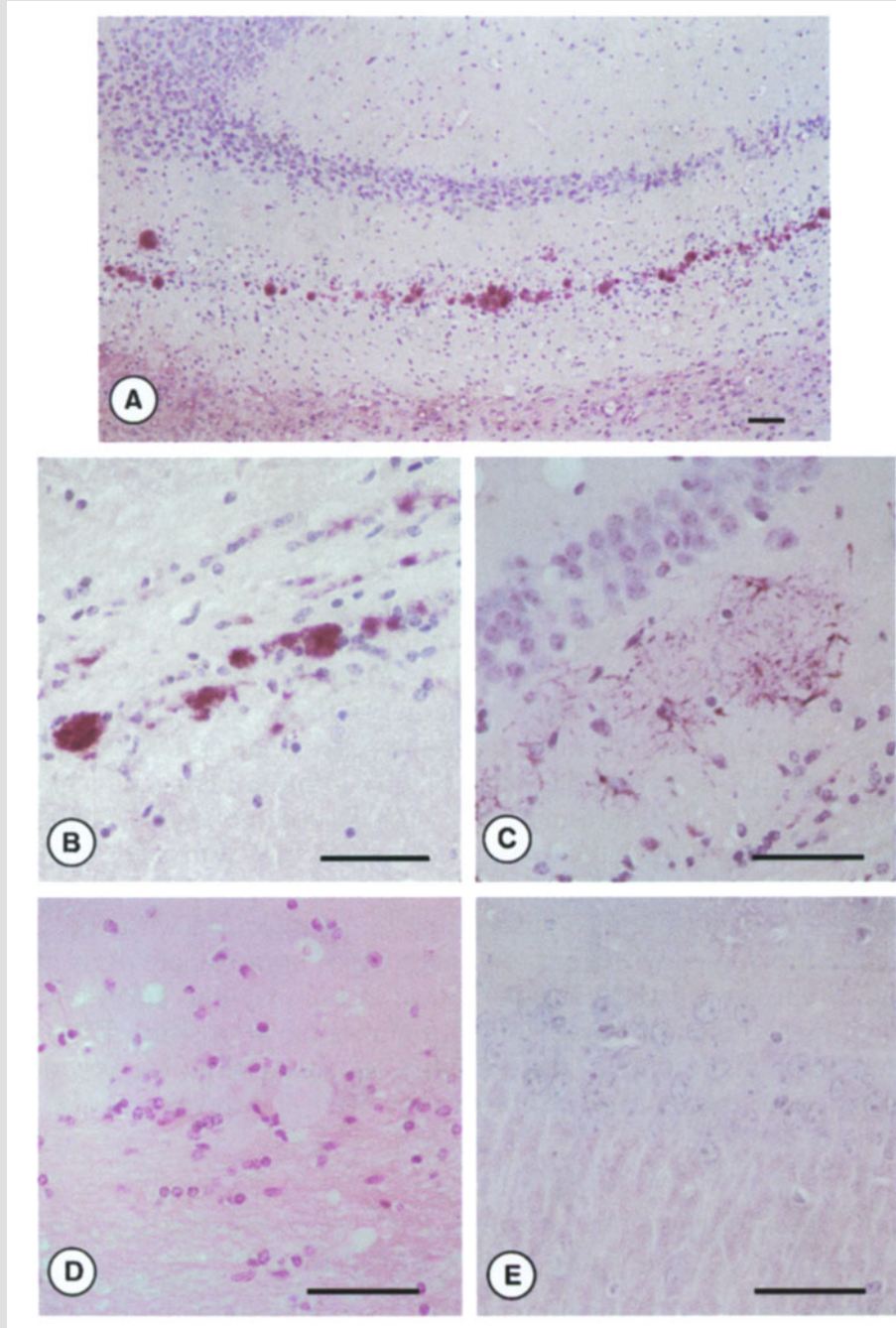


**Fig. 4.** Immunohistochemical investigation of the hippocampus of Tgbov XV mouse brains. Bars indicate 50  $\mu\text{m}$ . **A** Plaque-like  $\text{PrP}^{\text{Sc}}$  deposition in a BSE diseased Tgbov XV mouse after staining with mab L42, overview. **B**  $\text{PrP}^{\text{Sc}}$  plaques in a BSE diseased Tgbov XV mouse, staining with mab L42. **C** Astrogliosis in BSE diseased Tgbov XV mouse as shown by immunohistochemical staining for glial fibrillary acidic protein (GFAP). **D** H.E. staining of a BSE diseased Tgbov XV mouse. Note plaque-like amyloid depositions. **E** No  $\text{PrP}^{\text{Sc}}$  staining in an uninfected Tgbov XV mouse incubated with mab L42

### Acknowledgements

We are indebted to Moira Bruce (Edinburgh) and Charles Weissmann (London) for supplying us with the inbred and transgenic mouse lines. We thank Roswitha Fischer, Maria Möller and Annett Bünten for their excellent technical assistance. This work was supported in part by grants from the German 'Bundesministerium für Ernährung, Landwirtschaft und Forsten', the German 'Bundesministerium für Bildung, Wissenschaft und Technologie', as well as by grants from the EU commission.

### References

1. Buschmann A, Groschup MH (1998) Übertragbarkeit der spongiformen Enzephalopathien unter natürlichen und experimentellen Bedingungen. In: Braun U (ed) BSE und andere spongiforme Enzephalopathien. Parey Verlag, Berlin, pp 51–76
2. Bradley R (1996) Experimental transmission of bovine spongiform encephalopathy. In: Court L, Dodet B (eds) Transmissible subacute spongiform encephalopathies: Prion Diseases. Elsevier, Paris, pp 51–56
3. Bruce M, Chree A, McConnell I, Foster J, Pearson G, Fraser H (1994) Transmission of bovine spongiform encephalopathy and scrapie to mice: strain variation and the species barrier. *Phil Trans R S London B* 343: 405–411
4. Bruce ME (1996) Strain Typing Studies of Scrapie and BSE. In: Baker HF, Ridley RM (eds) Prion diseases. Humana Press Inc, Totowa, New Jersey, pp 223–236
5. Bruce ME, McBride PA, Jeffrey M, Scott JR (1994) PrP in pathology and pathogenesis in scrapie-infected mice. *Mol Neurobiol* 8: 105–112
6. Fischer M, Rulicke T, Raeber A, Sailer A, Moser M, Oesch B, Brandner S, Aguzzi A, Weissmann C (1996) Prion protein (PrP) with amino-proximal deletions restoring susceptibility of PrP knockout mice to scrapie. *EMBO* 15: 1255–1264
7. Fraser H, Foster JD (1993) Transmission to mice, sheep and goats and bioassay of bovine tissues. In: Bradley R, Marchant B (eds) Transmissible spongiform encephalopathies. Brussels, European Commission Agriculture, pp 145–160
8. Groschup MH, Pfaff E (1993) Studies on a species-specific epitope in murine, ovine and bovine prion protein. *J Gen Virol* 74: 1451–1456
9. Harmeyer S, Pfaff E, Groschup MH (1998) Synthetic peptide vaccines yield monoclonal antibodies to cellular and pathological prion proteins of ruminants. *J Gen Virol* 79: 937–945
10. Kaneko K, Zulianello L, Scott M, Cooper CM, Wallace AC, James TL, Cohen FE, Prusiner SB (1997) Evidence for protein X binding to a discontinuous epitope on the cellular prion protein during scrapie prion propagation. *Proc Natl Acad Sci USA* 94: 10069–10074
11. Kuczius T, Haist I, Groschup MH (1998) Molecular analysis of bovine spongiform encephalopathy and scrapie strain variation. *J Infect Dis* 178: 693–699
12. Prusiner SB, Scott M, Foster D, Pan KM, Groth D, Mirenda C, Torchia M, Yang SL, Serban D, Carlson GA, Hoppe PC, Westaway D, DeArmond SJ (1990) Transgenic studies implicate interactions between homologous PrP isoforms in scrapie prion replication. *Cell* 63: 673–686
13. Scott MR, Safar J, Telling G, Nguyen O, Groth D, Torchia M, Koehler R, Tremblay P, Walther D, Cohen FE, DeArmond SJ, Prusiner SB (1997) Identification of a prion protein epitope modulating transmission of bovine spongiform encephalopathy prions to transgenic mice. *Proc Natl Acad Sci USA* 94: 14279–14284

14. Somerville RA, Chong A, Mulqueen OU, Birkett CR, Wood SC, Hope J (1997) Biochemical typing of scrapie strains. *Nature* 386: 564–564
15. Telling GC, Scott M, Hsiao KK, Foster D, Yang SL, Torchia M, Sidle KC, Collinge J, DeArmond SJ, Prusiner SB (1994) Transmission of Creutzfeldt–Jakob disease from humans to transgenic mice expressing chimeric human-mouse prion protein. *Proc Natl Acad Sci USA* 91: 9936–9940
16. Telling GC, Scott M, Mastrianni J, Gabizon R, Torchia M, Cohen FE, DeArmond SJ, Prusiner SB (1995) Prion propagation in mice expressing human and chimeric PrP transgenes implicates the interaction of cellular PrP with another protein. *Cell* 83: 79–90
17. Wells GA, Dawson M, Hawkins SA, Green RB, Dexter I, Francis ME, Simmons MM, Austin AR, Horigan MW (1994) Infectivity in the ileum of cattle challenged orally with bovine spongiform encephalopathy. *Vet Rec* 135: 40–41

Authors' address: Dr. M.H. Groschup, Federal Research Centre for Virus Diseases of Animals, Institute of Immunology, Paul-Ehrlich-Str. 28, D-72076 Tübingen, Germany.

## **Analyzing the influence of PrP primary structure on prion pathogenesis in transgenic mice**

**S. Campbell<sup>2</sup>, U. Dennehy<sup>2</sup>, and G. Telling<sup>1</sup>**

<sup>1</sup>Department of Microbiology and Immunology, Department of Neurology and the Sanders-Brown Center on Aging, University of Kentucky, Lexington, Kentucky, U.S.A.

<sup>2</sup>Neurogenetics Unit, Imperial College School of Medicine at St. Mary's, London, U.K.

**Summary.** Expression of prion protein (PrP) genes in transgenic (Tg) mice has been an extremely effective means of studying human and animal prion diseases. Indeed, much of what we currently understand about the molecular basis of prion pathogenesis derives from such studies. Despite these advances, the emergence of a new variant of Creutzfeldt–Jakob disease (vCJD), apparently the human manifestation of bovine spongiform encephalopathy (BSE), demonstrates that our understanding of the factors controlling prion transmission is far from complete. We review studies in Tg mice that have addressed issues of prion strains and species barriers and have provided insights into mechanisms of prion propagation. The goal of future investigation will be to determine the interplay between PrP primary structure and conformation in determining prion transmission barriers and we discuss some ongoing transgenic studies designed to address these issues.

### **Transgenic studies of the species barrier**

The seminal transgenic studies of prion species barriers indicated that the primary structure of PrP<sup>Sc</sup> in the inoculum and PrP<sup>C</sup> in the host should be identical for optimal progression of disease [13, 16]. Based on studies with Tg mice expressing Syrian hamster PrP<sup>C</sup>, we expected that the species barrier to human prions would be abrogated in Tg FVB mice expressing human PrP. However, we found that transmission of CJD prions was generally no more efficient in these mice, referred to as Tg(HuPrP)FVB mice, than in non-Tg FVB mice, even though Tg(HuPrP)FVB mice expressed high levels of HuPrP<sup>C</sup>. In contrast, propagation of human prions was highly efficient in Tg(MHu2M)FVB mice expressing a chimeric transgene in which the region of the mouse coding sequence between

codons 94 and 188 were replaced with the corresponding human PrP sequences [21].

The barrier to CJD transmission in Tg(HuPrP) mice was abolished by expressing human PrP<sup>C</sup> in knockout mice which express no endogenous mouse PrP<sup>C</sup> (referred to as *Prnp*<sup>0/0</sup>) demonstrating that mouse PrP<sup>C</sup> inhibits the propagation of CJD prions in Tg(HuPrP)FVB mice but not Tg(MHu2M)FVB mice [22]. We proposed that an auxiliary molecule was the most likely mediator of this inhibition and provisionally designated this molecule 'protein X' and proposed that protein X facilitates the conversion of PrP<sup>C</sup> to PrP<sup>Sc</sup> [22]. These studies indicated that two regions of MHu2M PrP participated in prion propagation and PrP<sup>Sc</sup> formation: the central domain of PrP<sup>C</sup> in which 9 or fewer amino acids between residues 94 and 188 are involved in interactions with PrP<sup>Sc</sup>, and a C-terminal segment that binds protein X.

In agreement with these experimental observations the 3-dimensional structure of recombinant PrP derived from nuclear magnetic resonance (NMR) spectroscopy indicates two potential species-dependent recognition sites for protein-protein interactions on opposite molecular surfaces in the structured carboxy-terminal region of PrP [8, 14, 15]. A refinement of this model classified amino acid residues that differ between species according to their locations in the 3-dimensional structure of PrP and the chemical properties of the amino acid residues [3]. The region containing so-called 'class A' residues was suggested as the binding site for protein X, while the variable 'class C' residues were predicted to be involved in interactions between PrP<sup>C</sup> and PrP<sup>Sc</sup>. A third region, consisting of 'class B' residues constitutes an internal hydrophobic core that may affect structural transformations following PrP<sup>Sc</sup>-PrP<sup>C</sup> interactions.

While Tg mice expressing bovine PrP, referred to as Tg(BoPrP), developed disease after inoculation with BSE, albeit with long incubation times between 250 and 300 days, Tg mice expressing a chimeric mouse-bovine PrP construct referred to as MBo2M, did not develop disease after challenge with BSE [17]. Both Tg(BoPrP) and Tg(MBo2M) mice were generated on the *Prnp*<sup>0/0</sup> background. The MHu2M and MBo2M chimeras were constructed by exchanging homologous regions between codons 94 and 188 of human and mouse PrP and bovine and mouse PrP coding sequences using common restriction enzyme sites. However, while the 9 amino acids from the human PrP coding sequence in this region of MHu2M are sufficient to confer susceptibility to CJD prions in Tg mice, the 8 amino acids from bovine PrP in this region of MBo2M are not sufficient to confer susceptibility to BSE prions. Because of species-specific differences between mouse and bovine PrP at residues 183 and 185 that are not present in MHu2M,  $\alpha$ -helix 2 of MBo2M has the bovine PrP sequence while the  $\alpha$ -helix 2 of MHu2M has the mouse sequence (Fig. 1). The mouse and bovine PrP sequences also differ at position 202 in  $\alpha$ -helix 3 while the mouse and human sequences are equivalent in this region. Interestingly, all

	$\beta$ 1	$\alpha$ 1	$\beta$ 2	$\alpha$ 2	$\alpha$ 3
Mo	GLGGYMLGSAMSRPMIHFGNDWEDRYRENMYRYPNQVYYRVPVDQYSNQNNFVHDCVNIITIKQHTVTTTTKGENFTETDVKMMERVVEQMCVTQYQKESQAY				
Human		I S Y	H	M E	
Bovine		L Y	H		V E
Kudu		L S Y			V
Nyala		L Y H			V
Oryx		L Y			V
MBo2M		L Y	H		V E

**Fig. 1.** Alignment of mouse, human and ungulate PrP coding sequences. Amino acid residues differing from the mouse PrP coding sequence between residues 123 and 224 are indicated. Also shown are the secondary structural elements predicted from NMR spectroscopy studies of recombinant mouse PrP

ungulate species that have succumbed to BSE infection for which the PrP coding sequence has been determined encode valine at 183 and isoleucine at 202 raising the possibility that these residues might account for the differences in susceptibility of Tg(MHu2M) and Tg(MBo2M) mice to prion infection. We have generated additional Tg lines that express new mouse-bovine PrP chimeras to test the effect of these species-specific substitutions on the transmission of BSE prions in Tg mice (Fig. 2).

### Transgenic studies of prion strain diversity

While the degree of homology between PrP molecules in the host and inoculum is an important determinant of the species barrier, an equally important component affecting prion transmission barriers is the strain of prion. The importance of strain effects is highlighted in the case of BSE. Strain-typing studies in mice suggest that BSE-affected cattle propagate a single strain of prions that is different from over 20 historical or contemporary isolates from sheep or goats with natural scrapie. Moreover, the host-range of the BSE strain is unusually broad. BSE contaminated food-stuffs have caused disease in several other species in the United Kingdom including feline spongiform encephalopathy (FSE) in domestic cats [24] and captive wild cats in zoos from 5 different species ([9], A. Cunningham, pers. comm.). Bovidae in zoos from 8 other species have also been affected ([9], A. Cunningham, pers. comm.).

Prion incubation times, profiles of neuropathological lesions in the CNS and patterns of PrP<sup>Sc</sup> deposition in the brain are features that have been used to characterize prion strains passaged in inbred mice, hamsters and Tg mice [4, 6, 10, 20]. The passage of vCJD and BSE prions to inbred strains of mice has been used to contend that prions causing BSE and vCJD are the same prion strain [4]. These experiments are complicated by the transmission of prions across species barriers that prolong incubation times. The predominance of diglycosylated PrP<sup>Sc</sup> in both BSE and vCJD brains has also been used as an argument that the two diseases are caused by the same prion strain [5, 7]. Transmission of vCJD to Tg mice expressing bovine PrP produced incubation periods, neuropathology, PrP<sup>Sc</sup> distribution and PrP<sup>Sc</sup>

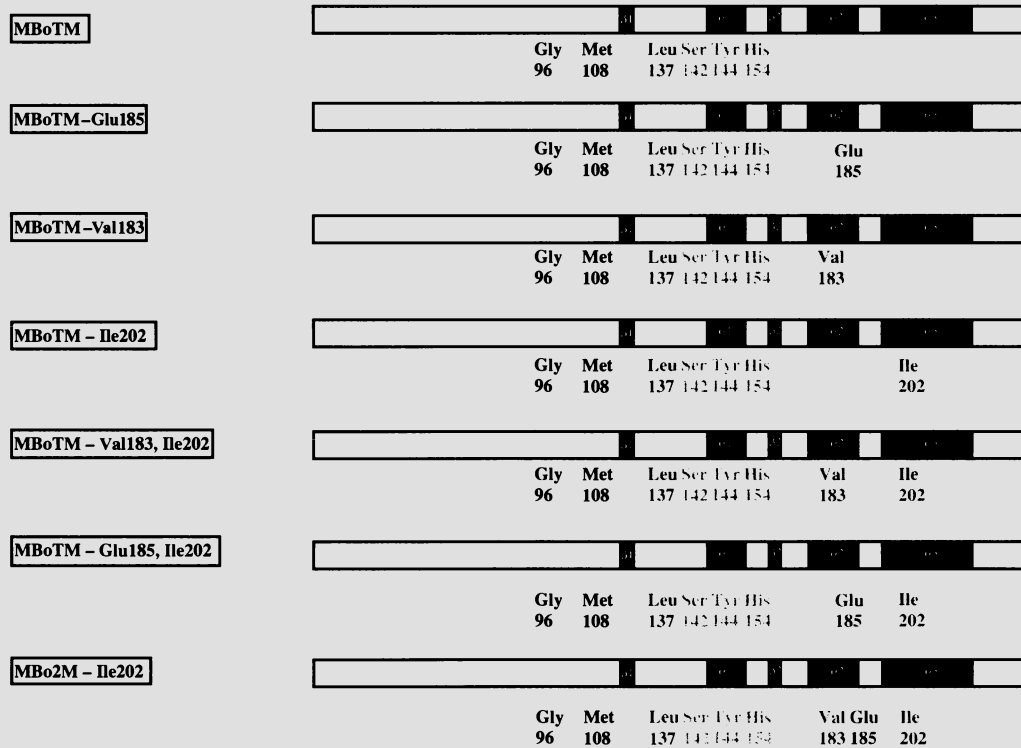


**Fig. 2.** Chimeric PrP coding sequences to test the effects of species-specific amino acid substitutions in  $\alpha$ -helices 2 and 3 on susceptibility to BSE in Tg mice. The coding sequence of the MBo2M PrP chimera [17] differs from mouse PrP at Gly96, Met108, Leu137, Ser142, Tyr144, His154, Val183 and Glu185. The new mouse-bovine chimeras are designed to test the influence of amino acid residues at positions 183, 185 and 202 on susceptibility to BSE in Tg mice. Regions of secondary structure that have been identified from NMR spectroscopic studies of recombinant PrP are shown as black boxes. MBoTM is a derivative of MBo2M [17] in which amino acid residues at 183 and 185 are changed from valine and glutamate (found in the bovine PrP sequence) to isoleucine and glutamine (found in the mouse PrP sequence). MBoTM-Glu185, MBoTM-Val183, MBoTM-Ile202, MBoTM-Val183, Ile202 and MBoTM-Glu185, Ile202 are derivatives of MBoTM in which mouse PrP amino acid residues are changed to the corresponding bovine PrP residues at specific locations. MBo2M-Ile202 differs from MBo2M in that valine at residue 202 of the mouse PrP sequence is changed to isoleucine which is found at the same location in bovine PrP

conformations that were identical to those produced by inoculation of BSE prions [18], providing the most convincing evidence to date that vCJD is human BSE.

Studies of different strains of transmissible mink encephalopathy (TME), a prion disease of captive mink, suggested that different strains might be represented by different conformational states of PrP<sup>Sc</sup> [2]. Evidence supporting this concept emerged from transmission studies of inherited human prion diseases [20]. Expression of mutant prion proteins in patients with fatal familial insomnia (FFI) and familial CJD caused by

mutation at codon 200 [fCJD(E200K)] result in variations in PrP conformation reflected in altered proteinase K cleavage sites that generate PrP<sup>Sc</sup> molecules with molecular weights of 19 kDa in FFI and 21 kDa in fCJD(E200K) [12]. Extracts from the brains of FFI and fCJD(E200K) patients transmitted disease to Tg(MHu2M) mice after about 200 days on first passage and induced formation of 19 kDa PrP<sup>Sc</sup> and 21 kDa PrP<sup>Sc</sup>, respectively [20]. Upon second passage in Tg(MHu2M) mice these characteristic molecular sizes remain constant but the incubation times for FFI and fCJD(E200K) prions diverge (Mastrianni and Telling et al., in preparation). These results indicate that PrP<sup>Sc</sup> conformers function as templates in directing the formation of nascent PrP<sup>Sc</sup> and provide a mechanism to explain strains of prions where diversity is enciphered in the tertiary structure of PrP<sup>Sc</sup>.

A sporadic form of fatal insomnia, referred to as sFI, has recently been described [11]. While patients with sFI have symptoms and neuropathological profiles indistinguishable from patients with FFI they do not express the D178N mutant form of human PrP<sup>C</sup> ions from sFI arients transmitted to Tg(MHu2M) mice were found to produce an identical pattern of neuropathology to that in Tg mice infected with FFI prions, arguing that PrP<sup>Sc</sup> isoforms associated with sporadic fatal insomnia and fatal familial insomnia have the same conformation. These findings argue that the conformation of PrP<sup>Sc</sup>, not the amino acid sequence, determines the strain-specified disease phenotype.

We have extended our initial transmission studies of human CJD cases in Tg mice to include 37 additional sporadic (sCJD) cases. Transmission of these cases to Tg(MHu2M) and Tg(HuPrP) mice reveal that the methionine/valine polymorphism at codon 129 and the strain-specified conformation of PrP<sup>Sc</sup> profoundly influence the length of the incubation time and patterns of PrP<sup>Sc</sup> deposition in recipient mice (Mastrianni and Telling et al., in preparation). Also, the size of the protease-resistant PrP<sup>Sc</sup> fragment in human brains, was reproduced on primary and secondary passages of vCJD, sCJD, fCJD(E200K), and FFI prions in Tg(MHu2M) mice. The constancy of the strain specified tertiary structure on serial passage through Tg(MHu2M) mice contrasts with other parameters used to characterize prion strains, such as incubation periods and neuropathology profiles.

### Unresolved issues and future prospects

In addition to providing insights into mechanisms of prion propagation, the ability to manipulate PrP genes by transgenesis in mice has also provided rapid and sensitive infectivity assays for human and animal prions. The continued study of intermammalian species barriers in Tg mice will allow more accurate risk assessments with respect to the risks posed to

humans from exposure to animal prions and facilitate management decisions designed to minimize interspecies prion transmission. Transgenic models of other naturally-occurring prion diseases such as chronic wasting disease (CWD) of deer and elk are urgently required to better understand modes of transmission and the pathogenesis of disease, as well as to improve diagnosis and control of CWD. Transmission of natural scrapie has recently been reported to transgenic mice expressing bovine PrP [18] and to transgenic mice expressing the sheep-VRQ PRP allele [23]. The complex genetics of susceptibility to natural sheep scrapie presents many interesting opportunities for future transgenic investigations.

In the light of BSE transmission to humans, understanding the risk of prion infections from other sources is clearly of paramount importance. Surveillance studies within the endemic Northern Colorado region indicate that 5–15% of free-ranging mule deer are affected with CWD (Mike Miller, Colorado Division of Wildlife, pers. comm.). Infected deer are hunted and presumably consumed by people, although the Department of Public Health recommends disposal of CWD carcasses. The abundant deposition of PrP<sup>Sc</sup> in lymph nodes of clinically affected animals [19] make it highly likely that meat from CWD-affected animals contains CWD prion infectivity, although this remains to be determined in experimental bioassay studies. Since CWD is transmitted in nature at a rate that appears unparalleled in other prion diseases, the need to develop a Tg model to study the biology of CWD prions and CWD pathogenesis would seem to be substantial.

Positive transmission of CWD to Tg(HuPrP) mice would have serious implications for the safety of humans exposed to CWD prions. In this regard it will be particularly informative to inoculate Tg mice with prions derived from patients suspected to have contracted disease from exposure to CWD-infected material. There have been several cases of CJD in young adults (under 40 years) in the USA in recent years (P. Gambetti, pers. comm.) and exposure to CWD has been suggested as a possible cause of disease in at least 2 cases. Similar incubation periods, neuropathology patterns and PrP<sup>Sc</sup> profiles of Tg mice inoculated with CWD and these human prion isolates would offer compelling evidence that such CJD cases were indeed acquired by exposure to CWD prions.

Of equal concern to human health is the possibility that CWD could cause a novel prion disease in livestock or other species. The remarkably high rate of CWD prion transmission brings into question the risk posed to livestock from developing a CWD-related prion disease via shared grazing of CWD contaminated rangeland. Should sheep be at risk from CWD, this would complicate scrapie eradication and constitute an additional disease threat to humans. Given the estimated one million infected cattle and >170,000 BSE-related deaths in Great Britain [1] and the evidence that BSE causes vCJD in humans, the potentially devastating health impacts of a CWD prion infection in domestic cattle are only too clear.

### References

1. Anderson RM, Donnelly CA, Ferguson NM, Woolhouse MEJ, Watt CJ, Udy HJ, MaWhinney S, Dunstan SP, Southwood TRE, Wilesmith JW, Ryan JBM, Hoinville LJ, Hillerton JE, Austin AR, Wells GAH (1996) Transmission dynamics and epidemiology of BSE in British cattle. *Nature* 382: 779–788
2. Bessen RA, Marsh RF (1992) Biochemical and physical properties of the prion protein from two strains of the transmissible mink encephalopathy agent. *J Virol* 66: 2096–2101
3. Billeter M, Riek R, Wider G, Hornemann S, Glockshuber R, Wüthrich K (1997) Prion protein NMR structure and species barrier for prion diseases. *Proc Natl Acad Sci USA* 94: 7281–7285
4. Bruce ME, Will RG, Ironside JW, McConnell I, Drummond D, Suttie A, McCardle L, Chree A, Hope J, Birkett C, Sousens S, Fraser H, Bostock CJ (1997) Transmissions to mice indicate that ‘new variant’ CJD is caused by the BSE agent. *Nature* 389: 498–501
5. Collinge J, Sidle KCL, Meads J, Ironside J, Hill AF (1996) Molecular analysis of prion strain variation and the aetiology of ‘new variant’ CJD. *Nature* 383: 685–690
6. Hecker R, Taraboulos A, et al. (1992) Replication of distinct prion isolates is region specific in brains of transgenic mice and hamsters. *Genes Dev* 6: 1213–1228
7. Hill AF, Desbruslais M, Joiner S, Sidle KCL, Gowland I, Collinge J (1997) The same prion strain causes vCJD and BSE. *Nature* 389: 448–450
8. James TL, Liu H, Ulyanov NB, Farr-Jones S, Zhang H, Donne DG, Kaneko K, Groth D, Mehlhorn I, Prusiner SB, Cohen FE (1997) Solution structure of a 142-residue recombinant prion protein corresponding to the infectious fragment of the scrapie isoform. *Proc Natl Acad Sci USA* 94: 10086–10091
9. Kirkwood JK, Cunningham AA (1994) Epidemiological observations on spongiform encephalopathies in captive wild animals in the British Isles. *Vet Rec* 135: 296–303
10. Mastrianni JA, Nixon R, Layzer R, Telling GC, Han D, DeArmond SJ, Prusiner SB (1999) Prion protein conformation in a patient with sporadic fatal insomnia. *New Eng J Med* 340: 1630–1638
11. Mastrianni JA, Telling GC, Parchi P, Torchia M, Tremblay P, Bosque P, Groth D, Will R, Ironside J, Gabizon R, Gambetti P, Prusiner SB, DeArmond SJ (2000) Fidelity of PrP<sup>Sc</sup> folding during serial transmission of prion strains from humans with new variant, familial or sporadic prion disease to transgenic mice (in preparation)
12. Monari L, Chen SG, Brown P, Parchi P, Petersen RB, Mikol J, Gray F, Cortelli P, Montagna P, Ghetti B, Goldfarb LG, Gajdusek DC, Lugaresi E, Gambetti P, Autilio-Gambetti L (1994) Fatal familial insomnia and familial Creutzfeldt–Jakob disease: Different prion proteins determined by a DNA polymorphism. *Proc Natl Acad Sci USA* 91: 2839–2842
13. Prusiner SB, Scott M, Foster D, Pan KM, Groth D, Mirenda C, Torchia M, Yang SL, Serban D, Carlson GA, Raeber AJ (1990) Transgenic studies implicate interactions between homologous PrP isoforms in scrapie prion replication. *Cell* 63: 673–686
14. Riek R, Hornemann S, Wider G, Billeter M, Glockshuber R, Wüthrich K (1996) NMR structure of the mouse prion protein domain PrP (121–231). *Nature* 382: 180–182

15. Riek R, Hornemann S, Wider G, Glockshuber R, Wüthrich K (1997) NMR characterization of the full-length recombinant murine prion protein, mPrP<sup>C</sup> (23–231). *FEBS Lett* 413: 282–288
16. Scott M, Foster D, Mirenda C, Serban D, Coufal F, Wälchli M, Torchia M, Groth D, Carlson G, DeArmond SJ, Westaway D, Prusiner SB (1989) Transgenic mice expressing hamster prion protein produce species-specific scrapie infectivity and amyloid plaques. *Cell* 59: 847–857
17. Scott MR, Safar J, Telling G, Nguyen O, Groth D, Torchia M, Koehler R, Tremblay P, Walther D, Cohen FE, DeArmond SJ, Prusiner SB (1997) Identification of a prion protein epitope modulating transmission of bovine spongiform encephalopathy prions to transgenic mice. *Proc Natl Acad Sci USA* 94: 14279–14284
18. Scott MR, Will R, Ironside J, Nguyen H-OB, Tremblay P, DeArmond SJ, Prusiner SB (1999) Compelling transgenetic evidence for transmission of bovine spongiform encephalopathy prions to humans. *Proc Natl Acad Sci USA* 26: 15137–15142
19. Sigurdson CJ, Williams ES, Miller MW, Spraker TR, O'Rourke KI, Hoover EA (1999) Oral transmission and early lymphoid tropism of chronic wasting disease PrP<sup>res</sup> in mule deer fawns. *J Gen Virol* 80: 2757–2764
20. Telling GC, Parchi P, DeArmond SJ, Cortelli P, Montagna P, Gabizon R, Mastrianni J, Lugaresi E, Gambetti P, Prusiner SB (1996) Evidence for the conformation of the pathologic isoform of the prion protein enciphering and propagating prion diversity. *Science* 274: 2079–2082
21. Telling GC, Scott M, Hsiao KK, Foster D, Yang S-L, Torchia M, Sidle KCL, Collinge J, DeArmond SJ, Prusiner SB (1994) Transmission of Creutzfeldt–Jakob disease from humans to transgenic mice expressing chimeric human-mouse prion protein. *Proc Natl Acad Sci USA* 91: 9936–9940
22. Telling GC, Scott M, Mastrianni J, Gabizon R, Torchia M, Cohen FE, DeArmond SJ, Prusiner SB (1995) Prion propagation in mice expressing human and chimeric PrP transgenes implicates the interaction of cellular PrP with another protein. *Cell* 83: 79–90
23. Vilotte JL, Soulier S, Stinnakre MG, Vaiman D, Lepourry L, Costa da Silva J, Besnard N, Essalmani R, Dawson M, Buschmann A, Groschup MH, Petit S, Madelaine MF, Vilette D, Laude H (1999) Transgenic mice expressing ovine PrP are highly susceptible to scrapie. Abstract contributed to the Prion Symposium in Tübingen, Germany, September 23–25, 1999, p 70
24. Wyatt JM, Pearson GR, Smerdon TN, Gruffydd-Jones TJ, Wells GAH, Wilesmith JW (1991) Naturally occurring scrapie-like spongiform encephalopathy in five domestic cats. *Vet Rec* 129: 233–236

Authors' address: Dr. G. Telling, Sanders-Brown Center on Aging, University of Kentucky, Lexington, KY 40536-0230, U.S.A.

## A single amino acid alteration in murine PrP dramatically alters TSE incubation time

J. C. Manson<sup>1</sup>, R. Barron<sup>1</sup>, E. Jamieson<sup>1</sup>, H. Baybutt<sup>1</sup>, N. Tuzi<sup>1</sup>,  
I. McConnell<sup>1</sup>, D. Melton<sup>2</sup>, J. Hope<sup>3</sup>, and C. Bostock<sup>3</sup>

<sup>1</sup>BBSRC Neuropathogenesis Unit, Institute for Animal Health,  
Edinburgh, Scotland, U.K.

<sup>2</sup>Institute of Cell and Molecular Biology, Edinburgh University,  
Edinburgh, Scotland, U.K.

<sup>3</sup>Institute for Animal Health, Compton Laboratory,  
Newbury, Berkshire, U.K.

**Summary.** In order to investigate mutations linked to human TSEs, we have used the technique of gene targeting to introduce specific mutations into the endogenous murine PrP gene which resulted in a P101L substitution (*Prnp*<sup>a101L</sup>) in the murine PrP gene. This mutation is equivalent to the 102L mutation in the human PrP gene which is associated with Gerstmann-Sträussler syndrome. Since the mutated gene is in the correct chromosomal location and control of the mutant gene expression is identical to that of the wild type murine PrP gene, the precise effect of the 101L mutation in the uninfected and TSE infected mouse can be investigated in this transgenic model. Mice homozygous for this mutation (101LL) while showing no spontaneous TSE disease were more susceptible to TSE disease than wild type mice following inoculation with GSS infectivity. Disease was transmitted from these mice to mice both with and without the *Prnp*<sup>a101L</sup> allele. The 101L mutation does not therefore produce spontaneous genetic disease in mice but does dramatically alter incubation periods following TSE infection. Additionally, a rapid TSE transmission was demonstrated associated with extremely low amounts of PrP<sup>Sc</sup>.

### Introduction

Polymorphisms in the PrP gene have been associated with the incubation time of TSE in a number of species. Amino acids 108 and 189 in the murine PrP gene have a major influence on incubation time of scrapie in mice [10]. Polymorphisms at amino acids 129 and 219 are associated with altered incubation time or susceptibility to human TSEs [2, 12]. Polymorphisms at amino acids 136 and 171 in the PrP gene are associated with

susceptibility to TSE disease in sheep [3]. The mechanism by which these mutations lead to altered susceptibility or incubation periods has not been defined.

While the above mutations seem to alter the susceptibility of an animal following exposure to an infectious agent, a number of point mutations and insertions in the human PrP gene apparently lead to spontaneous genetic disease [13, 14]. It has been suggested that inherited human TSEs result from mutations in the PrP gene leading to amino acid changes which destabilise the three dimensional structure of the PrP protein and that this inherent instability makes the PrP<sup>C</sup> protein more likely to convert to and accumulate as PrP<sup>Sc</sup> [1, 4, 8]. Indeed transgenic mice overexpressing a murine PrP gene with a 101L mutation (equivalent to the 102L in human PrP associated with GSS), were shown not only to develop disease spontaneously, but also to transmit this disease to mice with the same transgene [6, 7, 16]. These results suggested that the 102L mutation in humans may indeed lead to an unstable PrP protein and thus result in an inherited TSE.

We have produced a gene targeted transgenic model of the 101L mutation by the introduction of a mutation into the endogenous murine PrP gene [11]. This model allows us to investigate the precise effect of the 101L mutation without any complication from overexpression of the transgene. We have used this model to investigate the effect of the 101L mutation in both uninfected and TSE infected mice and compared the results to mice which do not carry the mutation (101PP) [9].

### 101L gene targeted mice

Gene targeting was used to alter specifically amino acid 101 from the wild type proline (101P) residue to a leucine (101L) in mouse embryonic stem (ES) cells. This generated *in situ* a modified *Prnp*<sup>a</sup> allele expressing the mutant PrP gene (*Prnp*<sup>a101L</sup>) [11]. HM-1 ES clones carrying a *Prnp*<sup>a101L</sup> mutant allele were used to produce chimaeric mice which were bred to produce progeny heterozygous (101PL) and homozygous (101LL) for the *Prnp*<sup>a101L</sup> allele. Wild type mice are referred to as 101PP. Genomic Southern and DNA sequence analysis confirmed that the *Prnp*<sup>a101L</sup> allele has undergone no detectable deletions, insertions or rearrangements during the gene targeting process or during the production of the mice [9].

Whereas the 101LL mice had identical levels of PrP mRNA to the wild type mice, the steady state level of the PrP protein was apparently lower than that in wild type mice [9], suggesting that the 101L mutation itself affected the level of PrP protein. This reduction in PrP may result from altered processing or stability of the mutant protein or alternatively altered conformation may lead to differences in the ability of the antibodies to bind to the mutant PrP protein.

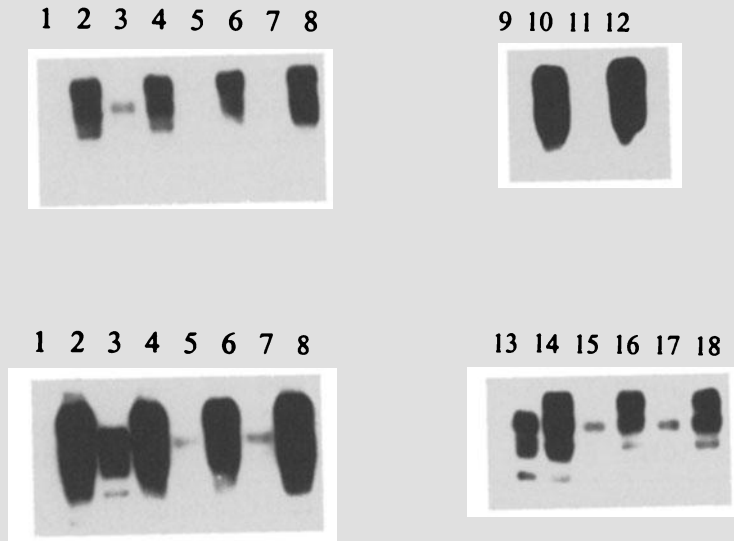


**Fig. 1.** Western analysis of uninfected and infected brain homogenates of 101PP, 101PL 101LL mice. 1–8 Brains of 101PL and 101LL mice infected with human GSS; 1, 2 and 101PL without clinical TSE disease; 3, 4 101PL at terminal stage of disease; 5–8 101LL mice at the terminal stage of disease. 9–12 brain homogenate of uninfected 101LL mice. 13–18 mice of each genotype infected with brain material from a 101LL mouse primarily infected with GSS at the terminal stage of disease (GSSLL). 13, 14 101PP; 15, 16 101PL and 17, 18 101LL. 1, 3, 5, 7, 9, 11, 13, 15, 17 with proteinase K (20 µg/ml) treatment. (+) and 2, 4, 6, 8, 10, 12, 14, 16, 18 without proteinase K (-). Samples were separated by SDS-PAGE, transferred onto PVDF membrane by electroblotting and incubated with monoclonal antibody 8H4 [18]. Proteins were visualised with horseradish peroxidase-conjugated rabbit anti-mouse and a chemiluminescence detection kit. Membranes were exposed to X-ray film for 10s (1–8 upper and 13–18) or 10 min (1–8 lower and 9–12)

### No spontaneous TSE disease in 101LL or 101PL mice

Mice (>200 animals) carrying one or two copies of the *Prnp*<sup>a101L</sup> allele showed no clinical signs of TSE disease up to 899 days of age. The brains of all the mice were examined for pathological signs of sub-clinical TSE. No sign of TSE vacuolation or PrP accumulation was detected in these brains and no PrP<sup>Sc</sup> was detected by Western blot analysis (Fig. 1).

Brains from mice homozygous for the *Prnp*<sup>a101L</sup> allele were used as an inoculum to assess whether, despite the absence of clinical or pathological signs of TSE, they carried spontaneously and endogenously generated TSE infectivity. A pool of three brains from mice (101LL) over 700 days old was inoculated intracerebrally into homozygous (101LL), heterozygous (101PL) and wild type 129Ola (101PP) mice. At the time of writing these mice have shown no clinical signs of TSE disease (650 days after inoculation).

**Table 1.** Incubation time of disease following inoculation with TSE infectivity

Inoculum	Mouse strain	No. with clinical TSE	No. without clinical TSE	Incubation time + sem
<b>GSS(10<sup>-2</sup>)</b>	101PP	1	6	456
	101PL	10	8	450±12
	101LL	15	0	288±4
<b>GSSLL(10<sup>-2</sup>)</b>	101PP	16	0	226±3
	101PL	20	0	201±3
	101LL	18	0	148±2
<b>ME7(10<sup>-2</sup>)</b>	101PP	10	0	161+2
	101PL	29	0	353±4
	101LL	18	0	338±8

Mice with no (101PP), one (101PL) and two (101LL) copies of the *Prnp<sup>a101L</sup>* allele were inoculated with primary GSS (GSS), GSS passed through a 101LL mouse (GSSLL) and ME7. The inoculum was injected intracerebrally at 10<sup>-2</sup> dilution

#### Altered susceptibility to GSS infection in 101LL mice

Mice carrying no (101PP), one (101PL) or two (101LL) copies of the *Prnp<sup>a101L</sup>* allele were inoculated with brain homogenate from a patient who died of GSS. This patient was heterozygous for the 102L mutation, homozygous for 129M and carried no other mutation in the PrP gene. Following inoculation (at 10<sup>-2</sup> dilution) only one wild type (101PP) mouse was scored as clinically positive and showed only limited vacuolar pathology. Six wild type mice showed no clinical signs of disease and no significant vacuolar pathology up to 701 days post infection (Table 1). No PrP accumulation was detected by immunocytochemical analysis and no PrP<sup>Sc</sup> was detected by Western analysis in the brains of these mice.

101LL mice were more susceptible to GSS than the wild type mice. All developed clinical signs of disease and were culled between 254 and 317 days after infection (Table 1). Despite extensive vacuolar pathology in the brains of these mice, abnormal accumulation of PrP could not be detected in five of the brains and only extremely low levels were detected in the others. The extremely low level of disease associated PrP was confirmed by Western analysis, PrP<sup>Sc</sup> only being detected following long exposure times of the immunoblot to X-ray film (Fig. 1).

Although all the 101LL mice were susceptible to disease, some of the 101PL mice showed no clinical or pathological signs of TSE disease, others showed no clinical signs of disease in their lifetimes (up to 646 days) but had significant grey and white matter vacuolar pathology, and a third group developed TSE disease between 411 and 540 days and had severe vacuolar pathology in grey and white matter regions (Table 1). Variable amounts of PrP were detected by immunocytochemical analysis in brains of the 101PL mice but the amount of PrP deposited did not appear to cor-

relate to the clinical status of the animals. PrP<sup>Sc</sup> was detected by Western analysis in TSE positive 101PL mice but not in the TSE negative animals examined (Fig. 1).

**Disease can be transmitted from a GSS-affected 101LL mouse to mice both with and without the *Prnp*<sup>a101L</sup> allele**

A brain homogenate was prepared from a 101LL mouse infected with GSS which had been culled at the terminal stage of disease (254 days). The inoculum (GSSLL) was injected intracerebrally into mice of the three genotypes (101PP, 101PL and 101LL). Despite the extremely low levels of PrP<sup>Sc</sup> in the brain used as an inoculum (equivalent to Fig. 1, lanes 5 and 7), disease was transmitted rapidly to all three groups of animals. The homozygous 101LL mice had the shortest incubation period (148 days) but significantly, even the wild type (101PP) mice developed TSE disease within 226 days (Table 1). In contrast to the primary GSS infection of 101LL mice, PrP accumulation in the brain was detected by immunocytochemistry in all three genotypes of animals, although there was marked variation in the amount of PrP detected. PrP<sup>Sc</sup> was also detected by Western analysis in extracts from all three groups of animals (Fig. 1).

**101LL mice have long incubation times with ME7**

Inoculation with a murine strain of scrapie, ME7, produced long incubation periods in mice with one (101PL) and two (101LL) copies of the *Prnp*<sup>a101L</sup> gene compared with the wild type mice (Table 1). The prolonged incubation periods in the mutant mice may in part be due to the reduced level of PrP in these mice but this is unlikely to account for such long incubation periods, thus the mutation must also be having a direct effect on the length of incubation time. PrP accumulation was detected by immunocytochemical analysis in all three genotypes of mice although there was a marked difference in the localisation of the deposits between the 101PP and 101LL mice. PrP<sup>Sc</sup> was detected by Western analysis in all three genotypes, with 101PP showing quantitatively more PrP<sup>Sc</sup> than 101PL and 101LL mice [9].

**Discussion**

GSS, linked to the 102L mutation in human PrP, has been described as a genetic disease with an autosomal dominant mode of inheritance and high penetrance [5, 15]. Introduction of this mutation *in situ* into one or both of the endogenous murine PrP genes has not resulted in spontaneous TSE in mice. The introduction of the 101L mutation into the murine PrP gene has however dramatically altered the incubation period of TSEs in the mice that carry the mutant gene. Challenge with an inoculum from a GSS102L patient has led to disease developing in all the mice carrying two copies of

this mutation in only 288 days. Despite the human to mouse “species barrier” the presence of the 101L mutation in the murine gene is sufficient to render animals highly susceptible to disease when challenged with brain homogenate from a GSS case. Moreover having passaged GSS infectivity through the 101LL mice, the infectivity from these mice was then rapidly transmitted to mice both with and without the *Prnp*<sup>101L</sup> allele.

In contrast to these results, transgenic mice expressing multiple copies of a murine PrP transgene with the 101L mutation were shown to develop a spontaneous neurological disease between 57 and 272 days [7, 16]. However transgenic mice over expressing a human PrP transgene with the 102L mutation did not develop a spontaneous neurological disease in 700 days [17]. Spontaneous disease is therefore only seen in some transgenic lines expressing high levels of the mutant gene. At low levels of expression there is no evidence for spontaneous disease. It may be that the life-time of a mouse is too short for a stochastic event that results in TSE disease in humans to occur in mice and high levels of expression of some mutant genes in mice may make this event more likely.

However, in the gene targeted 101LL mice, despite the absence of spontaneous TSE in the mice, we have demonstrated a dramatic change in incubation time of TSE infection in mice carrying the mutation. In addition, the spontaneous TSE disease in overexpressing 101L transgenic mice was not transmissible to wild type mice [6], whereas infectivity from the 101LL mice infected with GSS described here was readily transmissible to mice of all three genotypes. The infectivity replicating during spontaneous disease [7] is clearly not equivalent to the infectivity replicating in the GSS infection of the 101LL mice described here. The results presented here may suggest an alternative hypothesis for the association between the 102L mutation in human PrP and TSE disease. The 102L mutation rather than leading directly to genetic disease through an unstable PrP protein, may instead alter the susceptibility of the individual carrying the mutant gene to infection by a ubiquitous infectious agent.

In addition, we have produced a model of TSE disease in which infectivity was transmissible with rapid incubation times from a TSE infected brain with extremely low levels of disease associated PrP. Titration experiments will establish the titre of infectivity associated with these low levels of PrP, but the rapid transmission of disease from these brains suggests that relatively high titres of infectivity may equate with extremely low amounts of disease associated PrP. Thus the precise role of PrP in these diseases still remains to be established.

### Acknowledgements

The authors would like to thank V. Thomson, D. Drummond, K. Wales and J. Beaton for care and scoring of the animals, A. Suttie for tissue processing, A. Chree for lesion profile data, L. Aitchison for technical assistance, G. Miele for RNA analysis and

B. Easter for photography. Human tissues were kindly supplied by R. Will and J. Ironside and antibodies by C. Farquhar (1B3 and 1A8), M-S. Sy and P. Gambetti (8H4). This work was supported by a Grant (BS204512) from the Bovine Spongiform Encephalopathy Programme of the BBSRC to DM, JH and JM and a MRC Programme Grant (G9721848) to JM, JH, MB and CB.

### References

1. Cohen FE, Pan K, Huang Z, Baldwin M, Fletterick RJ, Prusiner SB (1994) Structural clues to prion replication. *Science* 264: 530–531
2. Goldfarb LG, Petersen RB, Tabaton M, Brown P, Leblanc AVC, Montagna P, Cortelli P, Julien J, Vital C, Pendelbury WW, Haltia M, Wills PR, Hauw JJ, McKeever PE, Monari L, Schrank B, Swergold GD, Autilio-Gambetti L, Gajdusek DC, Lugaresi E, Gambetti P (1992) Fatal familial insomnia and familial Creutzfeldt–Jakob disease phenotype determined by DNA polymorphism. *Science* 258: 806–808
3. Goldmann W, Hunter N, Smith G, Foster J, Hope J (1994) PrP genotype and agent effects in scrapie: Change of allelic interaction with different isolates of agent in sheep, a natural host of scrapie. *J Gen Virol* 75: 989–995
4. Harrison PM, Bamborough P, Daggett V, Prusiner SB, Cohen FE (1997) The protein folding problem. *Curr Opin Struct Biol* 7: 53–59
5. Hsiao K, Baker H, Crow T, Poulter M, Owen F, Terwillinger J, Westaway D, Ott J, Prusiner SB (1989) Linkage of a prion protein missense variant to Gerstmann–Straussler syndrome. *Nature* 338: 342–345
6. Hsiao K, Groth D, Scott M, Yang S-L, Serban H, Rapp D, Foster M, Torchia M, DeArmond S, Prusiner SB (1994) Serial transmission in rodents of neurodegeneration from transgenic mice expressing mutant prion protein. *Proc Natl Acad Sci USA* 91: 9126–9130
7. Hsiao K, Scott M, Foster M, Groth D, DeArmond S, Prusiner SB (1990) Spontaneous neurodegeneration in transgenic mice expressing mutant prion protein. *Science* 250: 1587–1590
8. Huang Z, Gabriel J, Baldwin MA, Fletterick RJ, Prusiner SB, Cohen FE (1994) Proposed three-dimensional structure for the cellular prion protein. *Proc Natl Acad Sci USA* 91: 7139–7143
9. Manson J, Jamieson E, Baybutt H, Tuzi N, Barron R, McConnell I, Somerville R, Ironside J, Will R, Sy M-S, Melton D, Hope J, Bostock C (1999) A single amino acid alteration (101L) introduced into murine PrP dramatically alters incubation time of transmissible spongiform encephalopathies. *EMBO J* 18: 6855–6864
10. Moore R, Hope J, McBride P, McConnell I, Selfridge J, Melton D, Manson J (1998) Mice with gene targeted prion protein alterations show that *Prnp*, *Sinc* and *Prni* are congruent. *Nat Genet* 18: 118–125
11. Moore R, Redhead N, Selfridge J, Hope J, Manson J, Melton D (1995) Double replacement gene targeting for the production of a series of mouse strains with different prion protein gene alterations. *Biotechnology* 13: 999–1004
12. Palmer M, Dryden A, Hughes J, Collinge J (1991) Homozygous prion protein genotype predisposes to sporadic Creutzfeldt–Jakob disease. *Nature* 352: 340–342
13. Parchi P, Gambetti P, Picardo P, Ghetti B (1998) Human prion diseases. In: Kirkman N, Lemoine N (eds) *Progress in pathology*. Churchill Livingstone, Edinburgh, pp 39–77
14. Prusiner SB (1997) Prion diseases and the BSE crisis. *Science* 278: 245–251

15. Speer M, Goldgaber D, Roses L, Pericak-Vance M (1991) Support of linkage of Gerstmann-Sträussler-Scheinker syndrome to the prion protein gene on chromosome 20p12-pter. *Genomics* 9: 366–368
16. Telling G, Haga T, Torchia M, Tremblay PO, DeArmond S, Prusiner SB (1996) Interactions between wild-type and mutant prion proteins modulate neurodegeneration in transgenic mice. *Genes Dev* 10: 1736–1750
17. Telling G, Scott M, Mastrianni J, Gabizon R, Torchia M, Cohen F, DeArmond S, Prusiner S (1995) Prion propagation in mice expressing human and chimaeric PrP transgenes implicates the interaction of cellular PrP with another protein. *Cell* 83: 79–90
18. Zanusso G, Lui D, Ferrari S, Hegyi I, Yin X, Aguzzi A, Hornemann S, Liemann S, Glockshuber R, Manson J, Brown P, Peteresen R, Gambetti P, Sy M-S (1998) Prion protein expression in different species: Analysis with a panel of new mAbs. *Proc Natl Acad Sci USA* 95: 8812–8816

Authors' address: Dr. J. C. Manson, BBSRC Neuropathogenesis Unit, Institute for Animal Health, Ogston Building, West Mains Road, Edinburgh EH9 3JF, Scotland, U.K.

## A transgenic model of a familial prion disease

D. A. Harris<sup>1</sup>, R. Chiesa<sup>1</sup>, B. Drisaldi<sup>1</sup>, E. Quaglio<sup>1</sup>, A. Migheli<sup>2</sup>,  
P. Piccardo<sup>3</sup>, and B. Ghetti<sup>3</sup>

<sup>1</sup>Department of Cell Biology and Physiology, Washington University School  
of Medicine, St. Louis, Missouri, U.S.A.

<sup>2</sup>Laboratory of Neuropathology, Department of Neuroscience,  
University of Turin, Turin, Italy

<sup>3</sup>Division of Neuropathology, Indiana University School of Medicine,  
Indianapolis, Indiana, U.S.A.

**Summary.** We have generated lines of transgenic mice that express a mutant prion protein containing 14 octapeptide repeats whose human homologue is associated with an inherited prion dementia. These mice develop an ataxic illness that begins at 65 days of age when the transgene array is homozygous, and results in death by 115–138 days. Starting from birth, mutant PrP is converted into a protease-resistant and detergent-insoluble form that resembles PrP<sup>Sc</sup>, and this form accumulates dramatically in many brain regions throughout the lifetime of the mice. As PrP accumulates, there is massive apoptosis of cerebellar granule cells, as well as astrogliosis and deposition of PrP in a punctate pattern. These results establish a new transgenic animal model of an inherited human prion disease, and provide important insights into the molecular pathogenesis of these disorders.

### Introduction

Prion diseases are fatal neurodegenerative disorders of humans and animals that result from the conformational conversion of a normal, cell surface glycoprotein (PrP<sup>C</sup>) into a pathogenic isoform (PrP<sup>Sc</sup>) that is the main component of infectious prions [16]. Hereditary prion diseases, which include 10% of the cases of Creutzfeldt–Jakob disease and all cases of Gerstmann-Sträussler syndrome and fatal familial insomnia, are linked in an autosomal dominant fashion to point and insertional mutations in the PrP gene on chromosome 20 [8, 20]. These mutations are presumed to favor spontaneous conversion of PrP to the PrP<sup>Sc</sup> state.

We describe here the construction and analysis of mice bearing a mouse PrP (moPrP) transgene containing a nine-octapeptide insertional mutation [5, 6]. The human homologue of this mutation, which is the largest insertion

thus far described in the PrP gene, has been found in two patients (one British and one German) who were afflicted with an illness characterized by progressive dementia and ataxia, and in the one autopsied case by the presence of PrP-containing amyloid plaques in the cerebellum and basal ganglia [7, 11, 14]. The transgenic mice model key clinical and neuropathological features of human familial prion diseases, and unlike other mice harboring PrP transgenes [9, 10, 13, 17, 19], they spontaneously accumulate PrP<sup>Sc</sup> in their brains. Analysis of these mice has provided important insights into the natural history and pathogenesis of familial prion diseases.

### Generation of Tg mice

Mammalian PrP normally contains a series of 5 octapeptide repeats in its N-terminal half. We have engineered mice that express a moPrP transgene that contains a nine-octapeptide insertional mutation homologous to the one seen in human patients. We refer to this mutant as PG14, since it contains a total of 14 peptide repeats that are rich in proline and glycine. For control purposes, we have also produced mice that carry a wild-type moPrP transgene. Both wild-type and PG14 molecules carry an epitope tag for the monoclonal antibody 3F4 [2], which makes it possible to distinguish transgene-encoded PrP from endogenous PrP. Wild-type and PG14 PrP cDNAs were cloned in the transgenic vector MoPrP.Xho, which contains the promoter and intron 1 of the moPrP gene. This vector has been shown to drive expression of foreign genes in a tissue pattern similar to that of endogenous PrP, with the exception that expression is absent in cerebellar Purkinje cells [3]. Transgenic founders produced on a C57BL/6J × CBA/J background were bred back to the parental line, and were also crossed into a *Prn-p*<sup>0/0</sup> line [4] in which both copies of the endogenous PrP gene have been disrupted. A summary of the transgenic lines is given in Table 1.

### Neurological symptoms of Tg(PG14) mice

Tg(PG14) mice from the A2 and A3 lines (both of which express mutant PrP at levels similar to that of endogenous PrP) develop a progressive and ultimately fatal neurological disorder characterized by ataxia, kyphosis, foot-clasp reflex, waddling gait, difficulty righting, and weight loss (Fig. 1) [5, 6]. Similar symptoms were also observed in the A1 founder that did not breed, and that expressed PG14 PrP at 4 times the level of endogenous PrP. In contrast, Tg(WT) mice that express wild-type PrP at even higher levels (3–4 times endogenous PrP) remain healthy. We observed that breeding the transgene array to homozygosity dramatically accelerated the onset of disease (from 235 ± 10 to 68 ± 9 days of age), and shortened its duration (from 154 ± 14 to 49 ± 11 days). This effect is most likely attributable to the two-fold higher expression of PG14 PrP in homozygous compared to heterozygous mice. This explanation is consistent with our finding that the

**Table 1.** Characteristics of Tg lines. Modified with permission from [6]

Transgene	Line	Transgene copy no. <sup>a</sup>	Tg PrP protein <sup>b</sup>	Clinical symptoms/ Neuropathology
PG14 PrP (3F4-tagged)	Tg(PG14-A1) <sup>c</sup>	28	4.0	Yes
	Tg(PG14A2)	5	1.0	Yes
	Tg(PG14-A3)	33	1.0	Yes
	Tg(PG14-B)	2	0.15	No
	Tg(PG14-C)	4	0.15	No
Wild-type PrP (3F4-tagged)	Tg(WT-D) <sup>d</sup>	92	N.D. <sup>e</sup>	No
	Tg(WT-E1)	9	1.8	No
	Tg(WT-E2)	1	0.25	No
	Tg(WT-E3)	59	3.6	No
	Tg(WT-E4)	15	3.0	No

<sup>a</sup>Determined by quantitative Southern blotting of tail DNA. Data are for mice that are hemizygous for the transgene array

<sup>b</sup>Determined relative to endogenous hamster PrP by quantitative Western blotting of brain homogenates using 3F4 antibody. Data are for mice that are hemizygous for the transgene array

<sup>c</sup>The founder did not breed, and was sacrificed when terminally ill at 319 days of age

<sup>d</sup>The founder did not breed, and died without prior neurological symptoms at 617 days of age

<sup>e</sup>Not determined

Tg(PG14) B and C lines, which express low levels of the mutant protein (15% of the endogenous PrP level), do not develop a neurological disorder within the life span of the animals. Taken together, our results indicate that overexpression of wild-type PrP does not produce neurological dysfunction, and that development of the disease in Tg(PG14) mice is related to the expression level of the mutant protein. We observed relatively little effect of co-expression of endogenous wild-type PrP on the characteristics of the illness.

### Neuropathological abnormalities in Tg(PG14) mice

Several pathological changes were observed in the A2 and A3 lines of Tg(PG14) mice, and in the A1 founder [5, 6]. The most obvious was a massive degeneration of cerebellar granule cells, which begins by 30 days of age in Tg(PG14<sup>+/+</sup>) mice, and eventually results in severe atrophy of the cerebellum (Fig. 2A, C). Granule cell loss is also seen in a number of cases of human prion diseases [15]. Several features indicate that, in Tg(PG14) mice, degeneration of granule cells occurs by an apoptotic mechanism. These include the presence of numerous pyknotic and fragmented granule cell nuclei, positive staining of degenerating neurons both by in situ

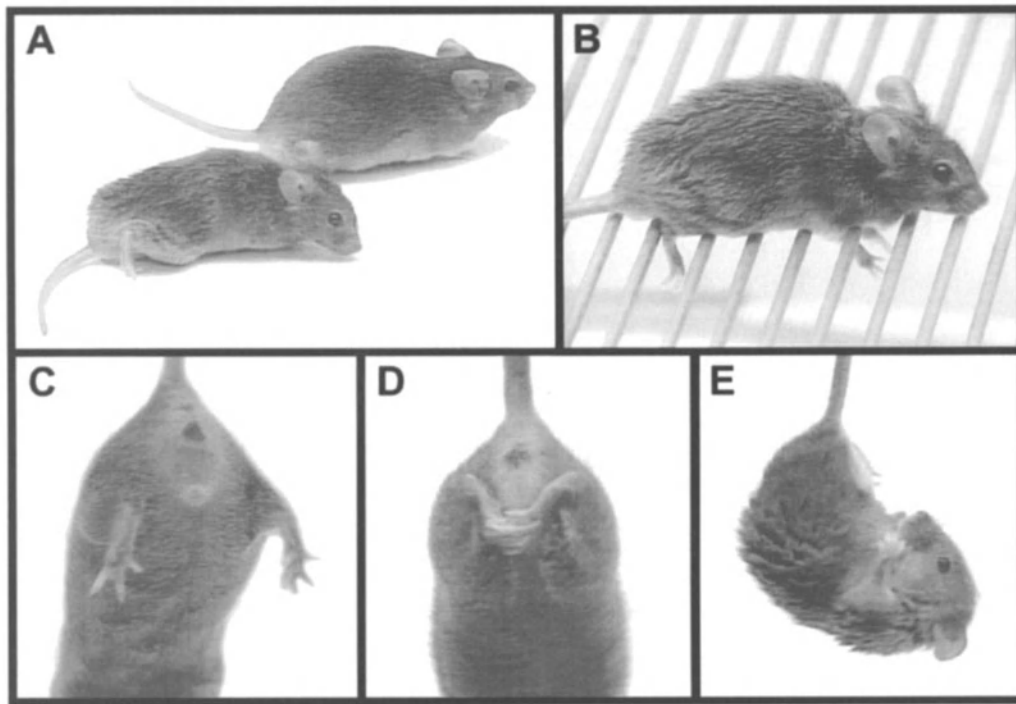


**Fig. 1.** Neurological symptoms in Tg(PG14) mice. **A** Tg(PG14-A3)/*Prn-p*<sup>0/0</sup> mouse at 84 days of age (left), and Tg(WT-E1)/*Prn-p*<sup>0/0</sup> mouse at 89 days of age. Note the ataxic posture of the PG14 mouse with hind limbs extended, the hunchback orientation of the body, and the ruffled appearance of the coat. **B** The Tg(PG14-A1) founder at 319 days of age is completely incapable of ambulating on a metal grill. Normal mice walk easily on the grill and rarely let their feet slip through the bars. **C** When suspended by its tail, a Tg(WT) mouse, like a non-transgenic mouse, splays its hind limbs apart. **D** In contrast, the Tg(PG14-A3) founder at 324 days of age tightly clasps its hind limbs together. **E** At 84 days of age, a Tg(PG14-A3)/*Prn-p*<sup>0/0</sup> mouse suspended by its tail assumes a flexed posture, attempting to clasp all four limbs together. Reproduced with permission from [6]

end-labeling of DNA (ISEL) and by an antibody to activated caspase-3, and the presence in cerebellar DNA preparations of a 200 bp ladder indicative of inter-nucleosomal cleavage. Tg(PG14) mice thus provide a particularly clear-cut demonstration of the role of apoptosis in a prion disease.

A second abnormal feature in Tg(PG14) mice was the presence of punctate, “synaptic-like” deposits of PrP that labeled with antibody 3F4 following treatment of brain sections with guanidine thiocyanate and hydrolytic autoclaving (Fig. 2B, D, F). These deposits were most prominent in the cerebellum, hippocampal formation, and olfactory bulb, and were present to a lesser extent in the neocortex and inferior colliculus. A third finding was astrocytic gliosis, which was observed in the cerebellar cortex (particularly the molecular layer, which displayed markedly hypertrophied Bergmann glial fibers; Fig. 2E), the hippocampus and the neocortex. PrP

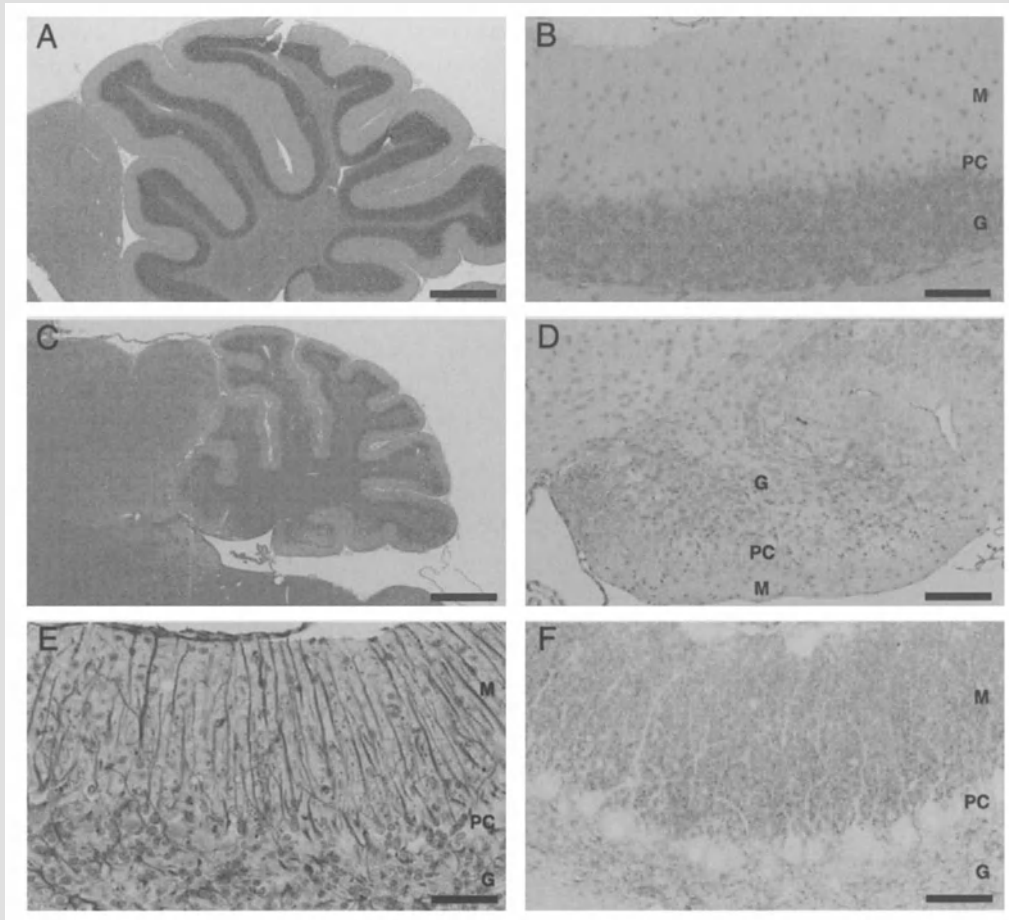


**Fig. 2.** Neuropathological findings in the cerebella of Tg(PG14) mice. **A** Cerebellum of a healthy Tg(WT-E1)/*Prn-p*<sup>0/0</sup> mouse at 184 days of age appears normal after staining with hematoxylin and eosin. **B** Cerebellar cortex of the same mouse shown in panel A, stained with antibody 3F4, shows no deposits of PrP, and normal appearance of the molecular (*M*), Purkinje cell (*PC*) and granule cell (*G*) layers. **C** Cerebellum of a terminally ill Tg(PG14-A3<sup>+/+</sup>)/*Prn-p*<sup>0/0</sup> mouse at 183 days of age after staining with hematoxylin and eosin. There is marked atrophy of cerebellum, with reduction in the thickness of the granule cell and molecular layers. **D** Cerebellar cortex of the same mouse shown in **C**, stained with antibody 3F4. There is a dramatic reduction in the density of granule cells, and relatively weak staining for PrP. **E** Cerebellar cortex of the symptomatic Tg(PG14-A1) founder at 319 days of age, stained for GFAP. There is marked hypertrophy of Bergmann glial fibers in the molecular layer, and increased numbers of astrocytes in the granule cell layer. **F** Cerebellar cortex of a moderately symptomatic Tg(PG14-A3<sup>+/+</sup>)/*Prn-p*<sup>0/0</sup> mouse at 71 days of age, stained with antibody 3F4. There is heavy PrP deposition in a synaptic-like pattern in the molecular layer, and less prominent staining in the granule cell layer. Purkinje cells are unstained, since the transgenic vector does not drive expression in this cell type. PrP staining is more intense in this mouse compared to the older animal shown in **D**, since the granule cell layer is more intact in this animal, and granule cells are an important source of PrP. Scale bars are 556  $\mu$ m (**A**, **C**), 97  $\mu$ m (**B**, **D**), 44  $\mu$ m (**E**), and 62  $\mu$ m (**F**).

Reproduced with permission from [6]

deposition and gliosis began at 30–40 days of age in Tg(PG14<sup>+/+</sup>) mice, and increased as the illness progressed. Neither thioflavin-positive plaques, nor obvious spongiosis were observed at any time. No pathological changes were seen in Tg(WT) or non-transgenic mice.

### **PrP from Tg(PG14) mice displays biochemical properties of PrP<sup>Sc</sup>**

PrP<sup>Sc</sup> can be recognized by several distinctive biochemical properties, including detergent-insolubility, protease-resistance, and resistance of the glycosyl-phosphatidylinositol (GPI) anchor to cleavage by phosphatidylinositol-specific phospholipase C (PIPLC). We have found that mutant PrP from the brains of Tg(PG14) mice displays each of these characteristics [5, 6].

We determined the amount of PrP that is detergent-insoluble by subjecting Triton-deoxycholate extracts of brain to ultracentrifugation under conditions that sediment PrP<sup>Sc</sup> but leave PrP<sup>C</sup> in the supernatant. PG14 PrP from all Tg(PG14) lines was partially detergent-insoluble, while wild-type PrP from Tg(WT) mice was completely soluble.

To assess protease-resistance, we digested detergent extracts of brain with 1–5 µg/ml of proteinase K (PK) for 30 min at 37 °C. We found that, under these conditions, PG14 PrP from all Tg lines yielded a protease-resistant core fragment of 27–30 kDa (PrP 27–30) (Fig. 3B, C). In contrast, moPrP from all four Tg(WT) lines was completely degraded at PK concentrations as low as 0.5 µg/ml (Fig. 3A). Mapping of the immunoreactive epitopes present in PrP 27–30 from Tg(PG14) mice suggested that this fragment is produced by cleavage between the end of the octapeptide repeats and amino acid 94, the same region where authentic PrP<sup>Sc</sup> is cut.

To assay PIPLC-resistance, suspensions of brain microsomal membranes were treated with phospholipase, and the amount of PrP released into the medium was determined by immunoblotting pellet and supernatant fractions obtained after sedimenting the membranes by centrifugation. While ~50% of the wild-type PrP from Tg(WT) mice was releasable by PIPLC, none of the PG14 PrP from Tg(PG14) mice was releasable. PG14 PrP was also found to be relatively PIPLC-resistant in a second assay in which removal of the GPI anchor was measured by Triton X-114 phase partitioning.

Mutant PrP in the brains of Tg(PG14) mice differs from authentic PrP<sup>Sc</sup> in an important respect, namely its considerably lower level of protease resistance. PrP<sup>Sc</sup> found in the brains of humans and animals with familial, infectious, or sporadic prion diseases will typically yield a PrP 27–30 fragment after treatment with 20–100 µg/ml of PK for 0.5–2 h at 37 °C [16]. The PK concentration we have used to digest PG14 PrP from our Tg mice is 10–100 times lower. This biochemical difference raises the question of whether PG14 PrP is authentic PrP<sup>Sc</sup>. One possibility is that PG14 PrP is

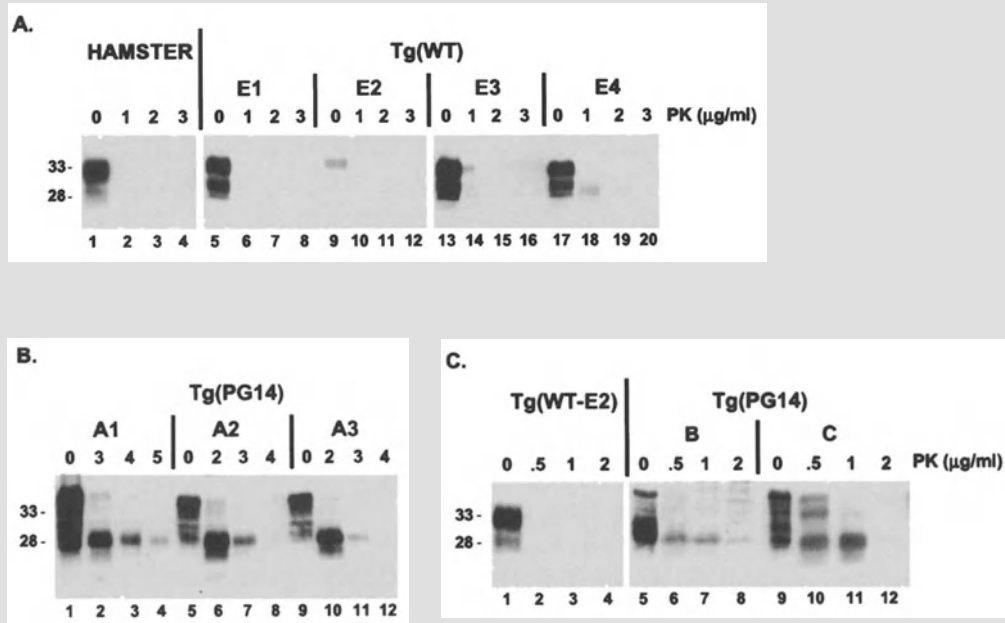


**Fig. 3.** PG14 PrP in the brains of transgenic mice is protease-resistant. Detergent lysates of brain from transgenic mice and Syrian hamster were incubated with the indicated amounts of PK for 30 min at 37 °C. Digestion was terminated by addition of PMSF, and methanol-precipitated proteins were separated by SDS-PAGE and immunoblotted using antibody 3F4. 200 µg (A, B) or 800 µg (C) of initial protein was subjected to digestion. The lanes containing undigested samples (0 µg/ml PK) represent 50 µg (A, B) or 200 µg (C) of protein. Mice were of the following ages and clinical status at the time of sacrifice: E1-E4, 203 days old (all healthy); A1, 319 days old (severely symptomatic); A2, 71 days old (healthy); A3, 205 days old (mildly symptomatic); B, 169 days old (healthy); C, 226 days old (healthy). Reproduced with permission from [6]

true PrP<sup>Sc</sup>, but that it represents a prion strain whose level of protease-resistance is low. It is well known that PrP<sup>Sc</sup> preparations can vary considerably in their protease-resistance, depending on the prion strains from which they are derived [1]. An alternative hypothesis is that PG14 PrP represents a biochemical intermediate along the pathway from PrP<sup>C</sup> to PrP<sup>Sc</sup>. In this scenario, the mutant protein has acquired some of the biochemical features of PrP<sup>Sc</sup>, but is structurally distinct, perhaps because it has only partial  $\beta$ -sheet character or is less aggregated or polymerized. An important test will be to determine whether PG14 PrP from Tg(PG14) mice is infectious after inoculation into other mice, an experiment which is currently underway. Even if the mutant protein should not turn out to be infectious however, the fact that it possesses other PrP<sup>Sc</sup>-like properties in addition to protease-resistance, and the fact that it is associated with a neurological illness make it likely that at least some aspects of PrP<sup>Sc</sup> formation are being modeled in Tg(PG14) mice.

### **PG14 PrP and its PrP<sup>Sc</sup>-like isoform accumulate throughout life**

Detergent-insoluble and protease-resistant PG14 PrP is already synthesized in the brains of transgenic mice during the first week of life, well before the animals develop clinical symptoms or neuropathological changes [5, 6]. Moreover, the amount of detergent-insoluble and protease-resistant PrP increased dramatically with age, with levels in the oldest, terminally ill animals that were up to 80-fold and 20-fold higher, respectively, than in newborn mice. PrP<sup>Sc</sup>-like protein accumulated more rapidly and to higher levels in Tg(PG14<sup>+/+</sup>) mice than in Tg(PG14<sup>+/-</sup>) mice, correlating with the accelerated disease progression in the homozygous animals. These results indicate that mutant PrP is converted continuously to a PrP<sup>Sc</sup>-like state throughout life, but that clinical symptoms and neuropathological lesions do not ensue until the amount of this form reaches a critical threshold level. If the same is true in human patients, this would explain why familial prion diseases do not manifest themselves clinically until adulthood, even though mutant PrP is probably synthesized beginning before birth [12].

Accumulation of the PrP<sup>Sc</sup>-like isoform paralleled an increase in the total amount of PG14 PrP in Tg(PG14) mice [5]. As Tg(PG14) mice aged, there was a nearly 10-fold increase in the total amount of mutant PrP in their brains. This phenomenon was specific for the mutant form of the protein, since the amount of wild-type PrP in the brains of Tg(WT) and non-transgenic CD1 mice varied by <2-fold over the lifetime of the animals. To address the possibility that accumulation of PG14 PrP was due to increased gene transcription, we performed Northern blots to assay PrP mRNA. We found that there was no significant change in the amount of transgenically encoded PrP mRNA during postnatal development of either Tg(PG14) or Tg(WT) mice. These results imply that PG14 PrP is degraded or cleared more slowly than wild-type PrP.

### **PrP<sup>Sc</sup>-like molecules are widely distributed in the brains and peripheral organs of Tg(PG14) mice**

To assess the neuroanatomical distribution of the PrP<sup>Sc</sup>-like form of PG14 PrP, we carried out histoblots of cryostat sections of brain [18]. Protease-resistant PrP was found throughout the brains of both pre-clinical and terminally ill Tg(PG14) mice, with particular concentrations in the medial caudate-putamen, septum, corpus callosum, anterior commissure, ventral thalamus, globus pallidus, and hippocampus [5]. Protease-resistant and detergent-insoluble PrP was also detected by Western blot analysis of individually dissected brain regions [5]. The widespread anatomical distribution of the PrP<sup>Sc</sup>-like isoform revealed by these methods contrasts with the more restricted distribution of punctate PrP deposits seen by immunohistochemistry (see above), raising the possibility that the protein may be

more aggregated in certain regions such as the cerebellum. Surprisingly, we have also found a detergent-insoluble and protease-resistant form of PG14 PrP in a number of the peripheral tissues in which PrP is normally expressed (although at lower levels than in brain), including skeletal muscle, heart, kidney, and testis.

### Conclusions

We have produced a mouse model of a familial prion disorder by introduction of a transgene that encodes the moPrP homologue of a nine-octapeptide insertional mutant associated with an inherited dementia in humans. These mice develop progressive neurological symptoms, display neuropathological changes, and accumulate a PrP<sup>Sc</sup>-like isoform that is recognizable by four different biochemical criteria. Since these abnormalities are not observed in mice expressing a wild-type PrP transgene, the phenotype in Tg(PG14) mice results specifically from the presence of the octapeptide insertion. These mice have been extremely valuable for analyzing the cellular and biochemical and mechanisms involved in inherited prion disorders, and correlating the appearance of the PrP<sup>Sc</sup>-like form with clinical and neuropathological findings. We expect that these mice will also be useful for testing new therapeutic agents.

### Acknowledgements

This work was supported by grants to D.A.H. from the American Health Assistance Foundation and the Alzheimer's Association, and to B.G. from the NIH (R01 NS14426 and P30 AG10133). R.C. was the recipient of fellowships from the Comitato Telethon Fondazione Onlus, and the McDonnell Center for Cellular and Molecular Neurobiology at Washington University.

### References

1. Bessen RA, Marsh RF (1992) Biochemical and physical properties of the prion protein from two strains of the transmissible mink encephalopathy agent. *J Virol* 66: 2096–2101
2. Bolton DC, Seligman SJ, Bablanian G, Windsor D, Scala LJ, Kim KS, Chen CM, Kacsak RJ, Bendheim PE (1991) Molecular location of a species-specific epitope on the hamster scrapie agent protein. *J Virol* 65: 3667–3675
3. Borchelt DR, Davis J, Fischer M, Lee MK, Slunt HH, Ratovitsky T, Regard J, Copeland NG, Jenkins NA, Sisodia SS, Price DL (1996) A vector for expressing foreign genes in the brains and hearts of transgenic mice. *Genet Anal Biomol Eng* 13: 159–163
4. Büeler H, Fischer M, Lang Y, Fluethmann H, Lipp H-P, DeArmond SJ, Prusiner SB, Aguet M, Weissmann C (1992) Normal development and behavior of mice lacking the neuronal cell-surface PrP protein. *Nature* 356: 577–582
5. Chiesa R, Drisaldi B, Quaglio E, Migheli A, Piccardo P, Ghetti B, Harris DA (2000) Accumulation of protease-resistant prion protein (PrP) and apoptosis of cerebellar granule cells in transgenic mice expressing a PrP insertional mutation. *Proc Natl Acad Sci USA* 97: 5574–5579

6. Chiesa R, Piccardo P, Ghetti B, Harris DA (1998) Neurological illness in transgenic mice expressing a prion protein with an insertional mutation. *Neuron* 21: 1339–1351
7. Duchen LW, Poulter M, Harding AE (1993) Dementia associated with a 216 base pair insertion in the prion protein gene: clinical and neuropathological features. *Brain* 116: 555–567
8. Gambetti P, Petersen RB, Parchi P, Chen SG, Capellari S, Goldfarb L, Gabizon R, Montagna P, Lugaresi E, Piccardo P, Ghetti B (1999) Inherited prion diseases. In: Prusiner SB (ed) *Prion biology and diseases*. Cold Spring Harbor Laboratory Press, Cold Spring Harbor, pp 509–583
9. Hegde RS, Mastrianni JA, Scott MR, Defea KA, Tremblay P, Torchia M, DeArmond SJ, Prusiner SB, Lingappa VR (1998) A transmembrane form of the prion protein in neurodegenerative disease. *Science* 279: 827–834
10. Hsiao KK, Scott M, Foster D, Groth DF, DeArmond SJ, Prusiner SB (1990) Spontaneous neurodegeneration in transgenic mice with mutant prion protein. *Science* 250: 1587–1590
11. Krasemann S, Zerr I, Weber T, Poser S, Kretzschmar H, Hunsmann G, Bodemer W (1995) Prion disease associated with a novel nine octapeptide repeat insertion in the PRNP gene. *Mol Brain Res* 34: 173–176
12. Manson J, West JD, Thomson V, McBride P, Kaufman MH, Hope J (1992) The prion protein gene: a role in mouse embryogenesis? *Development* 115: 117–122
13. Muramoto T, DeArmond SJ, Scott M, Telling GC, Cohen FE, Prusiner SB (1997) Heritable disorder resembling neuronal storage disease in mice expressing prion protein with deletion of an  $\alpha$ -helix. *Nature Med* 3: 750–755
14. Owen F, Poulter M, Collinge J, Leach M, Lofthouse R, Crow TJ, Harding AE (1992) A dementing illness associated with a novel insertion in the prion protein gene. *Mol Brain Res* 13: 155–157
15. Parchi P, Gambetti P, Piccardo P, Ghetti B (1998) Human prion diseases. In: Kirkham N, Lemoine NR (eds) *Progress in pathology* 4. Churchill Livingstone, Edinburgh, pp 39–77
16. Prusiner SB (1998) Prions. *Proc Natl Acad Sci USA* 95: 13363–13383
17. Shmerling D, Hegyi I, Fischer M, Blättler T, Brandner S, Götz J, Rüllicke T, Flechsig E, Cozzio A, von Mering C, Hangartner C, Aguzzi A, Weissmann C (1998) Expression of amino-terminally truncated PrP in the mouse leading to ataxia and specific cerebellar lesions. *Cell* 93: 203–214
18. Taraboulos A, Jendroska K, Serban D, Yang S-L, DeArmond SJ, Prusiner SB (1992) Regional mapping of prion proteins in brain. *Proc Natl Acad Sci USA* 89: 7620–7624
19. Westaway D, DeArmond SJ, Cayetano-Canlas J, Groth D, Foster D, Yang S-L, Torchia M, Carlson GA, Prusiner SB (1994) Degeneration of skeletal muscle, peripheral nerves, and the central nervous system in transgenic mice overexpressing wild-type prion proteins. *Cell* 76: 117–129
20. Young K, Piccardo P, Dlouhy S, Bugiani O, Tagliavini F, Ghetti B (1999) The human genetic prion diseases. In: Harris DA (ed) *Prions: molecular and cellular biology*. Horizon Scientific Press, Wymondham, pp 139–175

Authors' address: Dr. D. A. Harris, Department of Cell Biology and Physiology, Washington University School of Medicine, 660 So. Euclid Ave., St. Louis, MO 63110, U.S.A.

## Transgenic models of prion disease

M. R. Scott<sup>1,2</sup>, S. Supattapone<sup>1,2</sup>, H.-O. B. Nguyen<sup>1,2</sup>, S. J. DeArmond<sup>1,4</sup>,  
and S. B. Prusiner<sup>1,2,3</sup>

<sup>1</sup>Institute for Neurodegenerative Diseases, Departments of <sup>2</sup>Neurology, <sup>3</sup>Biochemistry and Biophysics, and <sup>4</sup>Pathology, University of California, San Francisco, California, U.S.A

**Summary.** There is growing concern that bovine spongiform encephalopathy (BSE) may have passed from cattle to humans, resulting in ~70 cases of an atypical, variant CJD (vCJD) in teenagers and young adults. We report here that transgenic (Tg) mice expressing full-length bovine (Bo) PrP serially propagate BSE prions and that there is no species barrier for transmission from cattle to Tg(BoPrP) mice. Surprisingly, these same mice were also highly susceptible to vCJD and natural sheep scrapie. The incubation times (~250 d), neuropathology, and PrP<sup>Sc</sup> isoforms in Tg(BoPrP) mice inoculated with vCJD and BSE brain extracts were indistinguishable and differed dramatically from those seen in these mice injected with natural scrapie. In efforts to identify PrP sequences required for prion formation, we found that a redacted prion protein of only 106 amino acids (PrP106) containing two large deletions supported prion propagation. In Tg(PrP106) mice, an artificial transmission barrier for the passage of full-length mouse prions was diminished by the coexpression of full-length wt MoPrP<sup>C</sup>, suggesting that wt MoPrP acts in trans to accelerate the replication of “miniprions” containing PrP<sup>Sc</sup>106. Following a single passage (~300 d) in Tg(PrP106) mice, the miniprions efficiently transmitted disease to Tg(PrP106) mice after only ~66 days. Our findings with Tg(BoPrP) mice provide compelling evidence that prions from cattle with BSE have infected humans and caused fatal neurodegeneration, the unique features of miniprions offer new insights into the mechanism of prion replication, and the trans-acting effects of full-length PrP coexpression suggest a new approach to the development of even more efficient animal models for prion diseases.

### Prion transmission barriers

A major objective in prion research is to decipher the factors that govern susceptibility of animals to prions derived from a foreign species. Without such information, it may not be possible to evaluate the impact of the BSE

epidemic on human health, where more than 175,000 cattle have died of BSE in Britain over the past decade [1]. Since epidemiological findings [38, 39], gel electrophoresis of the prion protein (PrP) [10], and transmissions to inbred mice [4, 12] and primates [15] have each raised the possibility of a link between BSE and vCJD, the immense size of the affected cattle population in the UK has mandated the need for a means of assessing risk to the human population [1]. The death rate from vCJD per year had remained approximately constant until recently when a disturbingly high number of deaths from the disease, a total of nine new cases, was reported in the last quarter of 1998 [38] leading to increased concern that a large section of the population is at high risk. In assessing this potential risk, it is generally assumed that humans would benefit from some degree of protection from exposure to BSE prions because of the “species barrier”. This term refers to the relative lack of susceptibility of one species to prions derived from another species [17].

The observation has frequently been made that the species barrier is characterized by a prolongation of the incubation time on the initial interspecies transfer of prions, followed by a pronounced shortening on subsequent passage [17]. Furthermore, the interspecies passage of prions is often inefficient, with only a minority of those inoculated developing prion disease. However, animals that do develop prion disease readily transmit their prions on subsequent intraspecies transfer.

Much of our current understanding of the factors that determine susceptibility to prions is attributable to studies using transgenic (Tg) and PrP gene knockout mice. The development of Tg mice for prion studies led to the discovery that the species barrier is attributable largely to differences between the amino acid sequence of PrP<sup>Sc</sup> in the inoculum and PrP<sup>C</sup> expressed in the recipient animal [25, 27]. At first, expression of a Syrian hamster (SHa) PrP transgene in mice was shown to render the animals highly susceptible to SHa prions, which demonstrated that expression of a foreign PrP gene could abrogate the species barrier [25]. Later, PrP-deficient (*Prnp*<sup>0/0</sup>) mice were created and found to be resistant to prion infection [5, 19]. The results of these studies and many others over the last decade [13, 14, 21, 26, 33, 35, 36] established that PrP has a central role in the transmission and pathogenesis of prion disease.

### **Artificial “miniprions”: a 106 residue prion protein supports prion propagation**

The successful propagation of prion infectivity in *Prnp*<sup>0/0</sup> mice expressing a PrP transgene encoding a protein of 106 residues may have profound implications for both structural and molecular genetic studies of prions [32]. By systematic deletion mutagenesis, the number of amino acids in murine PrP<sup>Sc</sup> was reduced from 209 to 106, representing a decrease in the size of the PrP polypeptide of almost 50% [32]. Following a “prion

transmission barrier” analogous to a classical species barrier, 106-residue miniprions were created after inoculation of Tg(PrP106) Prnp<sup>0/0</sup> mice with the RML strain of mouse prions. These miniprions comprising PrP<sup>Sc</sup>106 molecules were found to recapitulate all the properties of prions containing full-length PrP<sup>Sc</sup> proteins [32]. The RML106 miniprions efficiently transmitted to Tg(PrP106) mice, causing disease at ~60 days. The neuropathology was highly characteristic of prion disease, with both spongiform degeneration and a profound reactive astrocytic gliosis. Like full-length PrP<sup>Sc</sup>, the PrP<sup>Sc</sup>106 of the miniprion was found to possess a high  $\beta$ -sheet content, and was insoluble in an array of non-denaturing detergents. Furthermore, PrP<sup>Sc</sup>106 polymerized into rod-shaped structures morphologically similar to the infectious prion rods composed of PrP 27–30 [32].

#### **An intermediate in prion propagation: evidence for PrP\*106**

Although PrP<sup>Sc</sup>106-containing miniprions exhibited many similarities to naturally occurring prions, several key differences in the properties of the redacted protein have provided insight into the mechanism of prion propagation. Significantly, recombinant PrP106 was found to refold into a  $\beta$ -sheet conformation under conditions where SHaPrP lacking the internal deletion of residues 141–176, SHaPrP(90–231) or SHaPrP(29–231), did not [32]. While  $\alpha$ -helical SHaPrP(90–231) and SHaPrP(29–231) were predominantly monomeric, PrP106 in a  $\beta$ -sheet conformation formed spherical aggregates of ~9 nm in diameter [32].

The biophysical properties of recombinant PrP106 were intriguingly consistent with the findings of studies on the formation of protease-resistant PrP106 expressed in cultured neuroblastoma-2a (N2a) cells. In an empirical study, we determined that treatment of cells with mild proteinase K digestion conditions (7  $\mu$ g/ml of proteinase K for 30 min at 37 °C) was sufficient to completely hydrolyse PrP<sup>C</sup>wt expressed in N2a or ScN2a cells, but that this procedure left PrP106 largely undegraded. In contrast, more stringent proteinase K digestion conditions (>20  $\mu$ g/ml of proteinase K for 60 min at 37 °C) completely degraded PrP106 yet did not significantly hydrolyse PrP<sup>Sc</sup> in either ScN2a cells or infected Tg(PrP106) mice [32]. The partial resistance of PrP106 expressed in N2a cells to limited digestion with protease as well as its insolubility in 0.5% NP40 and 0.5% deoxycholate argues that a subset of PrP106 molecules possesses some of the characteristics of PrP<sup>Sc</sup> [32]. Whether these characteristics arise because this subset of PrP106 lies further along the pathway toward formation of PrP<sup>Sc</sup> than wt PrP<sup>C</sup> is not yet known. The term PrP\* has been used to describe metastable intermediates of PrP<sup>C</sup> that lie along the pathway of PrP<sup>Sc</sup> formation [8, 22]; hence, one possible interpretation is that the partially protease-resistant form of PrP106 represents PrP\*106 (Fig. 1). However, the lack of physical tools to assess the structure of PrP\* makes it difficult to

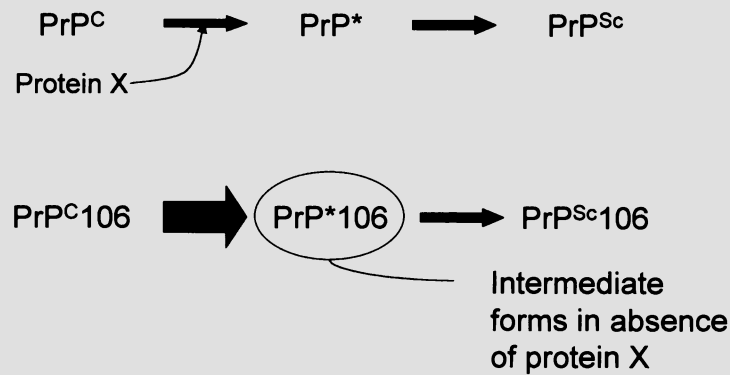


**Fig. 1.** Accumulation of PrP\*106 in the absence of protein X. Upper schematic: the rate-limiting step in propagation of wild type prions (depicted by a narrow arrow) is formation of PrP\* and requires protein X. Conversion of PrP\* to PrP<sup>Sc</sup> follows independently of protein X. Lower panel: PrP106 does not require protein X for conversion, hence formation of PrP\*106 is no longer rate-limiting (depicted by wide arrow), resulting in accumulation of the partially protease-resistant PrP\*106 form

judge whether recombinant PrP106 or that expressed in N2a cells is more poised to adopt the structure of PrP<sup>Sc</sup> than is wt PrP<sup>C</sup>. The propensity of recombinant PrP106 to form  $\beta$ -sheet rich structures suggests that unlike wt PrP, it may not be kinetically trapped in an  $\alpha$ -helix rich state like the PrP<sup>C</sup> isoform [9, 32].

### Deletion mutations reveal *trans*-acting effects on prion propagation

PrP106 contains two deletions,  $\Delta 23-88$  and  $\Delta 141-155$ . We initially deleted the N-terminal residues 23 to 88 because limited proteolysis removes these amino acids from PrP<sup>Sc</sup> without altering prion infectivity [20]. Although MHM2( $\Delta 23-88$ ) was readily converted into a protease-resistant isoform in ScN2a but not N2a cells [24], it was not converted into PrP<sup>Sc</sup> in Tg(MHM2, $\Delta 23-88$ )Prnp<sup>0/0</sup> mice inoculated with RML prions [32]. In contrast, Tg(MoPrP, $\Delta 32-80$ )Prnp<sup>0/0</sup> and Tg(MoPrP, $\Delta 32-92$ )Prnp<sup>0/0</sup> mice, both of which preserved the 10 N-terminal amino acids, readily produced PrP<sup>Sc</sup> after inoculation with RML prions [11, 30].

The extreme prion transmission barrier that was observed when RML prions were inoculated into Tg(PrP106)Prnp<sup>0/0</sup> and Tg(MHM2, $\Delta 23-88$ )Prnp<sup>0/0</sup> mice led to the discovery that wt PrP could act in *trans* to accelerate prion propagation [32]. When Tg(PrP106)Prnp<sup>0/0</sup> and Tg(MHM2, $\Delta 23-88$ )Prnp<sup>0/0</sup> mice were crossed with FVB mice carrying two copies of the Prnp gene, the susceptibilities of the resulting Tg(PrP106)Prnp<sup>+/0</sup> and Tg(MHM2, $\Delta 23-88$ )Prnp<sup>+/0</sup> mice to RML prions carrying full-length wt MoPrP<sup>Sc</sup> were greatly enhanced [32]. Notably, Prnp<sup>+/0</sup> mice that are hemizygous for ablation of the PrP gene have very prolonged incubation times exceeding 400 days [6, 7, 19].

### **Transgenic mice expressing bovine PrP**

Transgenic mice expressing foreign PrP genes have conclusively established that the PrP gene is the primary determinant controlling susceptibility to foreign prions [21, 23, 25, 26, 28, 35]. Transgenic mice expressing human (Hu) PrP with the V<sub>129</sub> polymorphism have been reported to be somewhat susceptible to human vCJD prions [12], but these same mice were not susceptible to BSE. In contrast, Prnp<sup>0/0</sup> mice expressing bovine PrP transgenes (BoPrP) are highly susceptible to BSE prions; 100% of the mice became ill at ~250 d after inoculation with BSE prions [28]. Significantly, the properties of BSE prions were not altered following serial transmission in Tg(BoPrP) mice [29]. Although nontransgenic mice seem moderately susceptible to BSE prions, a considerable change in incubation period from first to second passage is always observed [4, 15]. This change is indicative of a species barrier [17] and is clear evidence that the properties, and especially the pathogenicity of the prion, have changed during passage. In contrast, virtually identical incubation periods of ~250 d in Tg(BoPrP) mice were obtained upon serial transmission of BSE (Fig. 3) [29]. It is clear from a comparison of the data that expression of BoPrP in mice eliminates the species barrier for transmission of BSE.

### **Efficient transmission of variant CJD from humans to Tg(BoPrP) mice**

Prion strain “typing” experiments have been cited as evidence in favor of the hypothesis that vCJD is caused by the transmission of BSE to humans [4, 10, 12]. To test this hypothesis, we inoculated Tg(BoPrP) mice with vCJD prions. We reasoned that the reintroduction of BSE from humans, i.e., vCJD, into transgenic mice expressing BoPrP might restore the original strain properties of the BSE prions. If this transmission were negotiated successfully, the newly formed vCJD prions, which would be comprised of BoPrP<sup>Sc</sup>, would be indistinguishable from native BSE prions. To our surprise, we found that vCJD prions readily transmitted to Tg(BoPrP) mice [29]. Three separate cases of vCJD produced an incubation period of 250–270 d on first passage (Fig. 2), which was comparable to that obtained with BSE prions from cattle tissue, as well as serially passaged BSE prions obtained from Tg(BoPrP) mice (Fig. 3). Furthermore, clinical signs observed in affected animals were indistinguishable from those in Tg(BoPrP) mice inoculated with serially-passaged BSE [29]. In addition to being highly susceptible to human vCJD prions, the Tg(BoPrP)Prnp<sup>0/0</sup> mice were also highly susceptible to natural scrapie arising in the USA in Suffolk sheep [29].

### **Neuropathology of vCJD in Tg(BoPrP) mice is indistinguishable from serially-passaged BSE but distinct from scrapie**

The neuropathological changes of Tg(BoPrP) mice infected with BSE [28] are strikingly similar to those previously reported in cattle affected with

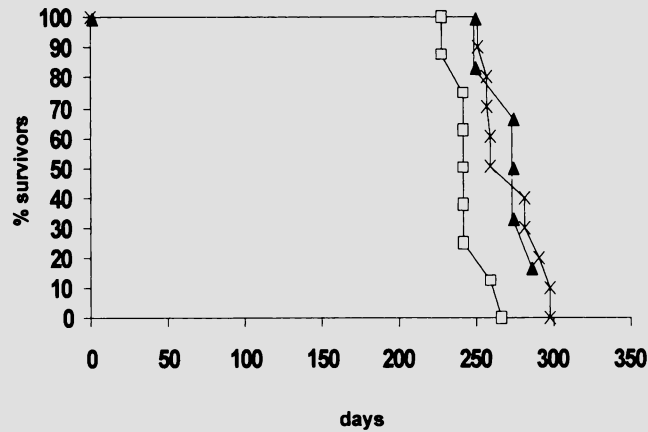


**Fig. 2.** Transmission of vCJD to Tg(BoPrP) mice. Tg(BoPrP)Prnp<sup>0/0</sup> E4125 mice were inoculated intracerebrally with 30  $\mu$ l of a 10% brain homogenate derived from vCJD patients RU96/02 ( $\blacktriangle$ ), RU96/07 ( $\times$ ), and RU 96/110 ( $\square$ ). The well-being of the mice was monitored daily, while the neurologic status was assessed semi-weekly. Mice were scored positive for prion disease when at least two signs of neurologic dysfunction were present and progressive deterioration of the animals was apparent

BSE [37]. Following a second transmission in Tg(BoPrP) mice, the neuro-anatomic distribution of vacuolation was unchanged [29]. Of particular note was the presence of PrP immunopositive amyloid plaques, which bound to Congo red dye and displayed apple green birefringence in polarized light [29]. The first passage of vCJD in Tg(BoPrP)Prnp<sup>0/0</sup> mice resulted in a neuropathological phenotype that was essentially identical to that caused by BSE prions [29]. Concerned that the highly characteristic and essentially identical pattern of neuropathology found in Tg(BoPrP) mice infected with BSE and vCJD could be attributable to an unusual property of the host Tg(BoPrP) mice, we evaluated the neuropathological lesions of Tg(BoPrP) mice that developed neurologic dysfunction following inoculation with sheep scrapie. In these mice, the pattern of neuropathology differed markedly; inocula derived from sheep scrapie resulted in a mild degree of vacuolation in virtually all brain regions and no amyloid plaques [29]. When the neuroanatomic distribution of PrP<sup>Sc</sup> deposition was determined by histoblot analysis, the distribution of PrP<sup>Sc</sup> was virtually identical in Tg(BoPrP) mice inoculated with either serially-passaged BSE or vCJD prions, and dramatically different following inoculation with scrapie prions. Together, these data establish that vCJD and BSE produce an identical disease in Tg(BoPrP) mice, and that vCJD prions appear to have retained the potential to regenerate authentic BSE prions upon retransmission to animals expressing bovine PrP [29].

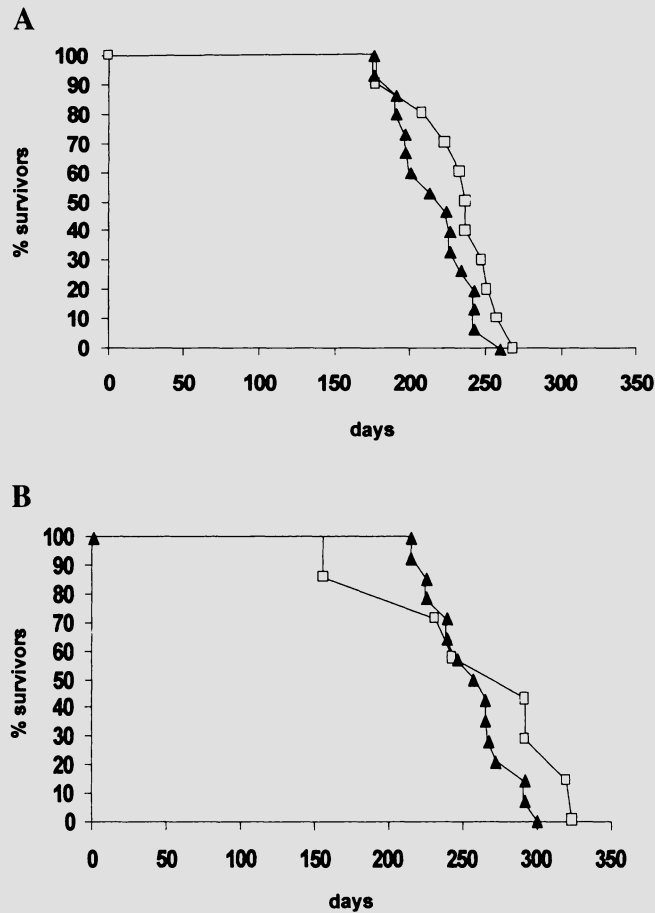


**Fig. 3.** Serial transmission of BSE in Tg(BoPrP) mice. Tg(BoPrP)Prnp<sup>0/0</sup> E4125 mice were inoculated intracerebrally with 30  $\mu$ l of a 10% brain homogenate. **A** Inoculum for primary transmission prepared with the medulla from BSE isolate PG31/90 (□) 18. Following the primary transmission, 30  $\mu$ l of a 10% brain homogenate prepared from an affected Tg(BoPrP)Prnp<sup>0/0</sup> E4125 mouse was re-transmitted to Tg(BoPrP)Prnp<sup>0/0</sup> E4125 mice (▲). **B** Inoculum for primary transmission was prepared with the medulla from BSE isolate GJ248/85 (□) 18. Following the primary transmission, 30  $\mu$ l of a 10% brain homogenate prepared from an affected Tg(BoPrP)Prnp<sup>0/0</sup> E4125 mouse was re-transmitted to Tg(BoPrP)Prnp<sup>0/0</sup> E4125 mice (▲). Mice were scored for prion disease as described in the legend to Fig. 2

### Convergent molecular properties of vCJD and BSE prions in Tg(BoPrP) mice

Assessment of the size of deglycosylated, protease-resistant fragment of PrP<sup>Sc</sup> [2, 34] or the relative amounts of di- and mono-glycosylated PrP<sup>Sc</sup> have both been used to characterize prion strains [10, 31]. The size of the unglycosylated PrP<sup>Sc</sup> after limited proteolysis and the relative amount

of diglycosylated PrP<sup>Sc</sup> were similar in vCJD and BSE samples before and after passage to Tg(BoPrP)Prnp<sup>0/0</sup> mice. In all cases, the size of the unglycosylated PrP<sup>Sc</sup> was of ~19 kDa, strikingly smaller than the ~21 kDa fragment found in human sCJD [29]. Furthermore, the amount of diglycosylated PrP<sup>Sc</sup> was substantially less in sCJD compared to BSE and vCJD as previously reported [10]. From these data, it seems clear that a single passage of vCJD prions from humans to Tg(BoPrP) mice was sufficient to produce a disease that is in all respects indistinguishable from that produced by BSE prions, and the conservation of the 19 kDa protease-resistant fragment size upon passage of vCJD to Tg(BoPrP) mice argues that the conformation of the prion may be maintained during propagation from the HuPrP to BoPrP background [2, 34].

### **The advantages of Tg(BoPrP)Prnp<sup>0/0</sup> mice**

One of the major obstacles to assessing the possible risk of exposure of humans to BSE prions through contaminated animal products has been the lack of an efficient bioassay system. The logistical and economic problems arising from the use of cattle or other ungulates are extreme, and have led to the search for viable alternatives for bioassay experiments. The demonstration that there is no significant difference in incubation period when Tg(BoPrP) mice are inoculated with either bovine brain or Tg(BoPrP) mouse-passaged BSE prions confirms that these animals seamlessly and precisely transmit BSE prions, with no detectable alteration of strain or species-specific properties attributable to the host animal [29]. This result supports our assertion that Tg(BoPrP) mice represent the best available rodent model for detecting BSE prions [28]. In contrast, studies with nontransgenic mice demonstrate differences in incubation period between first and second passage and between strains of inbred mice [3, 4, 16]. Whereas it is apparent from the extreme change in incubation period between first and second passage that mouse-passaged BSE prions are significantly more pathogenic in inbred mice than BSE prions of bovine origin, the same critique cannot be made of BSE prions passaged in Tg(BoPrP) mice; these retain their original pathogenicity. By obviating the species barrier, expression of BoPrP allows detection of BSE prions from cattle with maximum possible efficiency. In contrast, it is probable that only relatively high titers of BSE prions can be detected in normal mice. In the future, it may prove possible to create transgenic mice that express modified BoPrP, eliminate the species barrier, and provide even shorter incubation periods. However, until such mice are available, Tg(BoPrP) mice represent the best rodent model for BSE.

### The origin of vCJD

We have demonstrated that vCJD prions assume an identity indistinguishable from that of BSE prions following a single passage in Tg(BoPrP) mice. Incubation periods obtained after inoculation of human vCJD brain tissues into Tg(BoPrP) mice were remarkably similar to those obtained after inoculation with BSE prions obtained from either bovine brain or Tg(BoPrP) mice, and clinical signs of disease were indistinguishable. Neuropathological analysis revealed the same distribution of spongiform degeneration, and both the appearance and localization of amyloid plaques, as well as the regional distribution of PrP<sup>Sc</sup>, were identical when Tg(BoPrP) were inoculated with vCJD and serially-passaged BSE. In addition, the size of unglycosylated, protease-resistant PrP<sup>Sc</sup> remained 19 kDa through multiple passaging of BSE prions. Moreover, the predominance of the diglycosylated fragments also remained unchanged on passage of either BSE or vCJD prions. Thus, by all available criteria, vCJD and BSE are the same when passaged in Tg(BoPrP) mice.

That human vCJD prions so precisely duplicate the properties of native bovine BSE prions in their behavior on transmission to Tg(BoPrP)Prnp<sup>0/0</sup> mice creates a compelling argument for an etiologic link between BSE and vCJD. Although earlier proposals of an etiological link between BSE and vCJD were disquieting [4, 10, 12, 15, 38, 39], they did not seem overwhelmingly persuasive. The investigations reviewed here with Tg(BoPrP)Prnp<sup>0/0</sup> mice inoculated with either BSE prions from cattle or vCJD prions from humans provide the first compelling, etiologic link between the two diseases. Moreover, these findings raise increased concern that a large section of the UK population may be at considerable risk.

### Acknowledgements

We thank Drs. Gerald Wells, John Wilesmith, and Ray Bradley for the BSE brain tissue; Drs. Robert Will, James Ironside, and Jeanne Bell for the vCJD brain tissue; Vincenza Itri and Dr. Jiri Safar for BSE brain extracts; Dr. David Westaway and Dr. Pat Blanchard for natural sheep scrapie samples; and Juliana Cayetano, Ignatius Arellano, and Thomas Lisse for excellent technical assistance. This work was supported by grants from the National Institutes of Health (NS14069, AG08967, AG02132, and NS22786) and the American Health Assistance Foundation, as well as by gifts from the G. Harold and Leila Y. Mathers Foundation, the Sherman Fairchild Foundation, the Bernard Osher Foundation, and Centeon, Inc.

### References

1. Anderson RM, Donnelly CA, Ferguson NM, Woolhouse MEJ, Watt CJ, Udy HJ, MaWhinney S, Dunstan SP, Southwood TRE, Wilesmith JW, Ryan JBM, Hoinville LJ, Hillerton JE, Austin AR, Wells GAH (1996) Transmission dynamics and epidemiology of BSE in British cattle. *Nature* 382: 779–788

2. Bessen RA, Marsh RF (1994) Distinct PrP properties suggest the molecular basis of strain variation in transmissible mink encephalopathy. *J Virol* 68: 7859–7868
3. Bruce M, Chree A, McConnell I, Foster J, Pearson G, Fraser H (1994) Transmission of bovine spongiform encephalopathy and scrapie to mice: strain variation and the species barrier. *Phil Trans R Soc London Ser B* 343: 405–411
4. Bruce ME, Will RG, Ironside JW, McConnell I, Drummond D, Suttie A, McCardle L, Chree A, Hope J, Birkett C, Cousens S, Fraser H, Bostock CJ (1997) Transmissions to mice indicate that ‘new variant’ CJD is caused by the BSE agent. *Nature* 389: 498–501
5. Büeler H, Aguzzi A, Sailer A, Greiner R-A, Autenried P, Aguet M, Weissmann C (1993) Mice devoid of PrP are resistant to scrapie. *Cell* 73: 1339–1347
6. Büeler H, Raeber A, Sailer A, Fischer M, Aguzzi A, Weissmann C (1994) High prion and PrP<sup>Sc</sup> levels but delayed onset of disease in scrapie-inoculated mice heterozygous for a disrupted PrP gene. *Mol Med* 1: 19–30
7. Carlson GA, Ebeling C, Yang S-L, Telling G, Torchia M, Groth D, Westaway D, DeArmond SJ, Prusiner SB (1994) Prion isolate specified allotypic interactions between the cellular and scrapie prion proteins in congenic and transgenic mice. *Proc Natl Acad Sci USA* 91: 5690–5694
8. Cohen FE, Pan K-M, Huang Z, Baldwin M, Fletterick RJ, Prusiner SB (1994) Structural clues to prion replication. *Science* 264: 530–531
9. Cohen FE, Prusiner SB (1998) Pathologic conformations of prion proteins. *Annu Rev Biochem* 67: 793–819
10. Collinge J, Sidle KCL, Meads J, Ironside J, Hill AF (1996) Molecular analysis of prion strain variation and the aetiology of “new variant” CJD. *Nature* 383: 685–690
11. Fischer M, Rüllicke T, Raeber A, Sailer A, Moser M, Oesch B, Brandner S, Aguzzi A, Weissmann C (1996) Prion protein (PrP) with amino-proximal deletions restoring susceptibility of PrP knockout mice to scrapie. *EMBO J* 15: 1255–1264
12. Hill AF, Desbruslais M, Joiner S, Sidle KCL, Gowland I, Collinge J, Doey LJ, Lantos P (1997) The same prion strain causes vCJD and BSE. *Nature* 389: 448–450
13. Hsiao K, Scott M, Foster D, DeArmond SJ, Groth D, Serban H, Prusiner SB (1991) Spontaneous neurodegeneration in transgenic mice with prion protein codon 101 proline → leucine substitution. *Ann NY Acad Sci* 640: 166–170
14. Hsiao KK, Groth D, Scott M, Yang S-L, Serban H, Rapp D, Foster D, Torchia M, DeArmond SJ, Prusiner SB (1994) Serial transmission in rodents of neurodegeneration from transgenic mice expressing mutant prion protein. *Proc Natl Acad Sci USA* 91: 9126–9130
15. Lasmézas CI, Deslys J-P, Demaimay R, Adjou KT, Lamoury F, Dormont D, Robain O, Ironside J, Hauw J-J (1996) BSE transmission to macaques. *Nature* 381: 743–744
16. Lasmézas CI, Deslys J-P, Robain O, Jaegly A, Beringue V, Peyrin J-M, Fournier J-G, Hauw J-J, Rossier J, Dormont D (1997) Transmission of the BSE agent to mice in the absence of detectable abnormal prion protein. *Science* 275: 402–405
17. Pattison IH (1965) Experiments with scrapie with special reference to the nature of the agent and the pathology of the disease. In: Gajdusek DC, Gibbs CJ Jr, Alpers MP (eds) *Slow, latent and temperate virus infections*. NINDB Monograph 2, U.S. Government Printing, Washington, pp 249–257
18. Prusiner SB, Fuzi M, Scott M, Serban D, Serban H, Taraboulos A, Gabriel J-M, Wells G, Wilesmith J, Bradley R, DeArmond SJ, Kristensson K (1993)

- Immunologic and molecular biological studies of prion proteins in bovine spongiform encephalopathy. *J Infect Dis* 167: 602–613
19. Prusiner SB, Groth D, Serban A, Koehler R, Foster D, Torchia M, Burton D, Yang S-L, DeArmond SJ (1993) Ablation of the prion protein (PrP) gene in mice prevents scrapie and facilitates production of anti-PrP antibodies. *Proc Natl Acad Sci USA* 90: 10608–10612
  20. Prusiner SB, Groth DF, Bolton DC, Kent SB, Hood LE (1984) Purification and structural studies of a major scrapie prion protein. *Cell* 38: 127–134
  21. Prusiner SB, Scott M, Foster D, Pan K-M, Groth D, Mirenda C, Torchia M, Yang S-L, Serban D, Carlson GA, Hoppe PC, Westaway D, DeArmond SJ (1990) Transgenic studies implicate interactions between homologous PrP isoforms in scrapie prion replication. *Cell* 63: 673–686
  22. Prusiner SB, Scott MR, DeArmond SJ, Cohen FE (1998) Prion protein biology. *Cell* 93: 337–348
  23. Race RE, Priola SA, Bessen RA, Ernst D, Dockter J, Rall GF, Mucke L, Chesebro B, Oldstone MBA (1995) Neuron-specific expression of a hamster prion protein minigene in transgenic mice induces susceptibility to hamster scrapie agent. *Neuron* 15: 1183–1191
  24. Rogers M, Yehiely F, Scott M, Prusiner SB (1993) Conversion of truncated and elongated prion proteins into the scrapie isoform in cultured cells. *Proc Natl Acad Sci USA* 90: 3182–3186
  25. Scott M, Foster D, Mirenda C, Serban D, Coufal F, Wälchli M, Torchia M, Groth D, Carlson G, DeArmond SJ, Westaway D, Prusiner SB (1989) Transgenic mice expressing hamster prion protein produce species-specific scrapie infectivity and amyloid plaques. *Cell* 59: 847–857
  26. Scott M, Groth D, Foster D, Torchia M, Yang S-L, DeArmond SJ, Prusiner SB (1993) Propagation of prions with artificial properties in transgenic mice expressing chimeric PrP genes. *Cell* 73: 979–988
  27. Scott MR, Groth D, Tatzelt J, Torchia M, Tremblay P, DeArmond SJ, Prusiner SB (1997) Propagation of prion strains through specific conformers of the prion protein. *J Virol* 71: 9032–9044
  28. Scott MR, Safar J, Telling G, Nguyen O, Groth D, Torchia M, Koehler R, Tremblay P, Walther D, Cohen FE, DeArmond SJ, Prusiner SB (1997) Identification of a prion protein epitope modulating transmission of bovine spongiform encephalopathy prions to transgenic mice. *Proc Natl Acad Sci USA* 94: 14279–14284
  29. Scott MR, Will R, Ironside J, Nguyen H-OB, Tremblay P, DeArmond SJ, Prusiner SB (1999) Compelling transgenic evidence for transmission of bovine spongiform encephalopathy prions to humans. *Proc Natl Acad Sci USA* 96: 15137–15142
  30. Shmerling D, Fischer M, Blättler TT, Hegy I, Brandner S, Aguzzi A, Weissmann C (1997) Expression in mice of amino-proximally truncated but not of full-length PrP causes a cerebellar syndrome (Abstr.). 29th Annual Meeting of the Union of the Swiss Societies for Experimental Biology in Geneva, March 20–21 A46
  31. Somerville RA, Chong A, Mulqueen OU, Birkett CR, Wood SCER, Hope J (1997) Biochemical typing of scrapie strains. *Nature* 386: 564
  32. Supattapone S, Bosque P, Muramoto T, Wille H, Aagaard C, Peretz D, Nguyen H-OB, Heinrich C, Torchia M, Safar J, Cohen FE, DeArmond SJ, Prusiner SB, Scott M (1999) Prion protein of 106 residues creates an artificial transmission barrier for prion replication in transgenic mice. *Cell* 96: 869–878

33. Telling GC, Haga T, Torchia M, Tremblay P, DeArmond SJ, Prusiner SB (1996) Interactions between wild-type and mutant prion proteins modulate neurodegeneration in transgenic mice. *Genes Dev* 10: 1736–1750
34. Telling GC, Parchi P, DeArmond SJ, Cortelli P, Montagna P, Gabizon R, Mastrianni J, Lugaresi E, Gambetti P, Prusiner SB (1996) Evidence for the conformation of the pathologic isoform of the prion protein enciphering and propagating prion diversity. *Science* 274: 2079–2082
35. Telling GC, Scott M, Mastrianni J, Gabizon R, Torchia M, Cohen FE, DeArmond SJ, Prusiner SB (1995) Prion propagation in mice expressing human and chimeric PrP transgenes implicates the interaction of cellular PrP with another protein. *Cell* 83: 79–90
36. Telling GC, Tremblay P, Torchia M, DeArmond SJ, Cohen FE, Prusiner SB (1997) N-terminally tagged prion protein supports prion propagation in transgenic mice. *Protein Sci* 6: 825–833
37. Wells GAH, Wilesmith JW (1995) The neuropathology and epidemiology of bovine spongiform encephalopathy. *Brain Pathol* 5: 91–103
38. Will RG, Cousens SN, Farrington CP, Smith PG, Knight RSG, Ironside JW (1999) Deaths from variant Creutzfeldt–Jakob disease. *Lancet* 353: 979
39. Will RG, Ironside JW, Zeidler M, Cousens SN, Estibeiro K, Alperovitch A, Poser S, Pocchiari M, Hofman A, Smith PG (1996) A new variant of Creutzfeldt–Jakob disease in the UK. *Lancet* 347: 921–925

Authors' address: Dr. S. B. Prusiner, Institute for Neurodegenerative Diseases, Department of Neurology, Box 0518, University of California, San Francisco, CA 94143-0518, U.S.A.

## **Epidemiology and Diagnosis of Prion Diseases**

## Surveillance of BSE

D. Heim<sup>1</sup> and J. W. Wilesmith<sup>2</sup>

<sup>1</sup>Swiss Federal Veterinary Office, Liebefeld, Switzerland

<sup>2</sup>Veterinary Laboratories Agency, Central Veterinary Laboratory, Epidemiology Department, New Haw/Addlestone, U.K.

**Summary.** The current method used to identify suspect BSE cases is based on reporting cattle displaying clinical signs compatible with BSE. The reporting of such cases is dependent on the ability of farmers and veterinarians to recognise the disease symptoms and on the willingness to report such cases. Furthermore, it depends on the stage of the disease, because early clinical signs of BSE are not always typical.

Histology and immunohistochemistry are established and reliable to confirm BSE in cattle, but the procedure is cumbersome, time consuming and therefore not suited for mass testing of animals.

A targeted surveillance system using the Prionics-Western-Blot Test was initiated in Switzerland in 1999. Prionics-positive results are confirmed by histology or immunohistochemistry by the BSE-reference laboratory. This surveillance scheme has confirmed fallen stock and cows subjected to emergency slaughter as the major risk groups. Currently all cattle from these two categories are tested. As a further measure a random sample of cows from regular slaughtering is tested. This enables to determine the BSE status independent of the inaccuracies of a clinical case reporting system. This approach may be helpful to reliably assess the BSE situation in countries with low incidence in order to verify their BSE status and in countries which want to prove their BSE-free status.

### BSE cases in the world

Bovine spongiform encephalopathy (BSE) was first described in the United Kingdom in 1986 [6]. The first BSE cases outside of the UK were diagnosed in the Falkland Islands and Oman in 1989, in animals imported from the UK. The first cases in cattle that were born and raised in countries outside the UK were reported in the Republic of Ireland in 1989, in Switzerland in 1990 and in France in 1991. In 1997, the first cases were diagnosed in Belgium, the Netherlands and Luxembourg. Other countries with native BSE cases were Portugal and Liechtenstein. Imported cases have been diagnosed in Canada, Denmark, Falkland Islands, Oman, Germany and Italy [4].

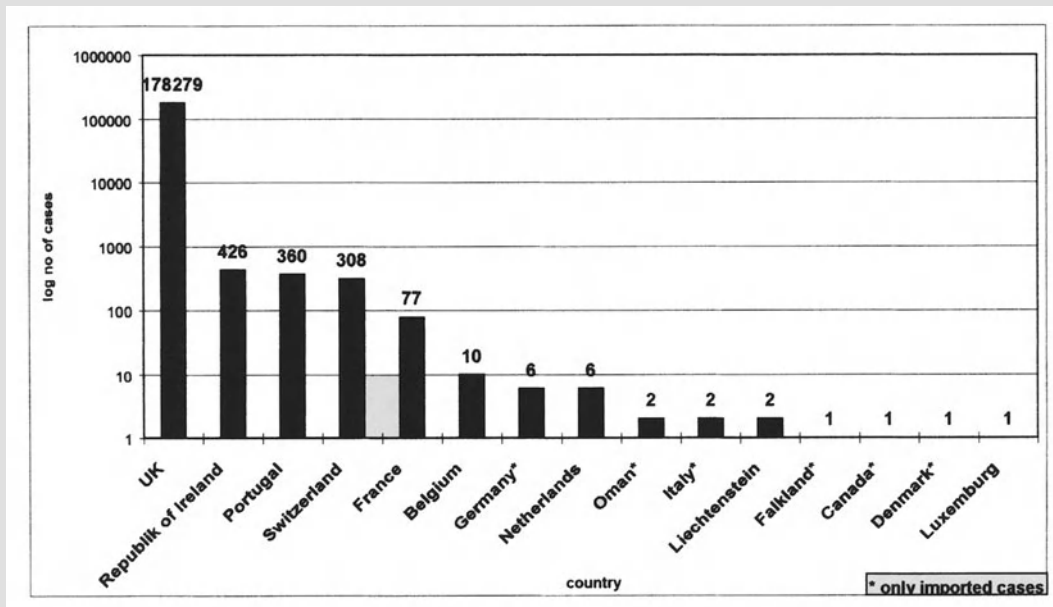


**Fig. 1.** Number of clinical BSE cases in the world (as of December 1999)

Indigenous cases have been diagnosed in nine countries and imported cases in six countries (Fig. 1).

The epidemic is declining in some countries and rising in others. The number of clinical cases in the United Kingdom is steadily declining; in Switzerland there is, after a steady decline in the incidence of reported clinical cases, an apparent increase in the observed incidence of infected animals in 1999, because of a new targeted surveillance system. The trend in other countries is not that obvious and the true course of the epidemic is often uncertain (Fig. 2). The reported number of cases, in a number of countries including those with no cases in indigenous cattle need to be considered in the light of the quality of the surveillance system and the measures taken.

Reporting is usually based on the observation of clinical signs which must be notified by the owner and/or the veterinarian. In all countries surveillance is targeted at animals showing clinical signs compatible with BSE; the most important of these are hypersensitivity to manipulation of the head and neck, and disturbances in behaviour and locomotion. Reduced milk yields and loss of weight are also frequently seen [1, 3, 7]. Usually the clinical signs are very mild and non-specific at the beginning of the clinical course.

### **Influences on the number of cases**

Mandatory notification of suspect clinical cases of BSE is the basic means of surveillance. For this surveillance to be effective, the level of disease awareness and the willingness of keepers of cattle to notify suspected cases are of greatest importance. Therefore, the number of cases alone cannot

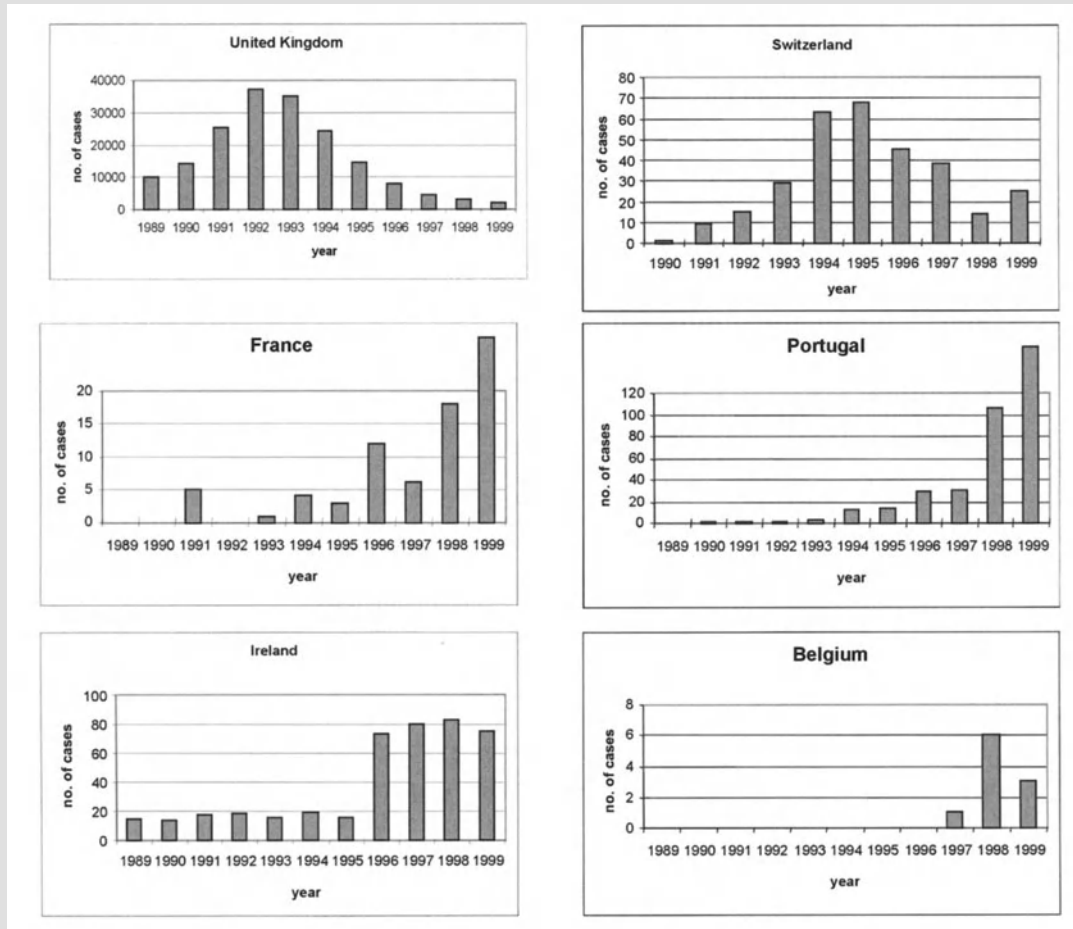


**Fig. 2.** Number of clinical BSE cases in several countries (as of December 1999)

necessarily provide a true picture of the BSE situation in a given country and must be interpreted with caution. The reliability of the reported number of cases can be evaluated, using a risk assessment approach, but this, in turn depends on the availability and quality of the necessary data and information.

A crucial part of a surveillance system are the herdsmen, veterinarians, personnel at the slaughterhouses and others handling cattle who must be fully aware of the clinical signs of the disease. A laboratory with suitably trained pathologists and which is therefore capable of diagnosing BSE is also of paramount importance.

It is essential to familiarize veterinarians, farmers and other professionals continuously with the typical clinical signs of BSE. Veterinarians must be stimulated to notify the veterinary authorities of all cattle with neurological disorders for specialized pathological examination and to make the procedure for notifying, and what to do with a suspect case, clear and easy.

An efficient notification system of all suspect cases can only be guaranteed if the farmers and veterinarians are willing to notify the cases. Full

compensation of the animal's value and of all the costs related with the management of the case, such as the diagnosis, the veterinarian's visit, the incineration and any other cost are essential. Merely making the disease statutorily notifiable is not sufficient.

With respect to diagnostic laboratories, training in the pathological diagnosis has been facilitated by the OIE diagnostic reference laboratories. Also, more recently a number of laboratories are providing a commercial service to market newly developed immunodiagnostic methods.

### **The Swiss experience**

The surveillance system in every country until 1999 was based on disease awareness and the willingness of the veterinarians and farmers to report suspected cases. Based on the findings that what may be considered as typical signs are not consistently expressed in animals reaching the clinical phase of the disease and can be confused with those of other diseases, it was considered that in Switzerland approximately 50% of all clinical cases are detected through mandatory reporting.

With the availability of the Prionics Western Blot, studies were initiated in Switzerland in 1998.

During 1998, a total of 1719 cattle brains were examined by histology and immunohistochemistry and tested with the Prionics-Check-Test – a Western blot test. Five brains were found to be test-positive. Two of them were found to be histologically negative. One of the animals was subjected to a detailed clinical examination and no signs of any disease were found.

The objective of this study was to estimate the risk of herdmates of BSE-cases and to validate the Prionics-Check-Test. The test results showed a good agreement with those obtained by immunohistochemistry.

It was therefore decided to use the test on 3000 routinely slaughtered cattle so as to evaluate its performance under practical conditions, which result in time-pressures and the need to provide a rapid result via high throughput rates of samples. 3022 cattle, 90% over two years of age, were sampled at slaughter, tested for PrP accumulation in the brain, using the Prionics-Check-Test, and confirmed by histology and/or immunohistochemistry. One 4-year-old animal was found to be positive to the test and confirmed for BSE by means of immunohistochemistry and histology.

This study indicated that the Prionics-Check-Test performs satisfactorily under field conditions; i.e., with large numbers of samples being processed and independent of the tissue quality. The results were available within 6–8 h. Furthermore, it was evident that sampling the brainstem through the foramen magnum with a special spoon is easy to perform and provides a practical method to achieve samples of a high quality.

Results from these studies initiated a reconsideration of the current surveillance and optimising surveillance of BSE. This is simply because surveillance based only on reporting of subjective impressions by pro-

ducers and veterinarians has limitations. A preferred approach would be targeted surveillance based on active case detection among defined risk cohorts. Thus, it was decided to use such a test for screening risk populations.

Encouraged by the results of the studies in 1998, the Swiss authorities initiated a targeted surveillance programme in January 1999 to enhance detection of BSE cases in all segments of the adult cattle population and to complement detection through mandatory reporting of clinically suspect animals [2]. Because the youngest animal diagnosed with BSE in Switzerland was 32 months old, the target population was cattle with at least four permanent incisor teeth; i.e., over 24 months of age. In studies of experimentally infected cattle, detectable PrP accumulations were not reached earlier than 28 months after inoculation and the time between detectable levels of PrP in the brain and occurrence of first clinical signs was less than or equal to 6 months [5].

It was assumed that the population most likely to contain BSE cases would be fallen adult cattle. These are animals that are too ill to be slaughtered, wasting or dead animals, and animals that do not recover after treatment. Carcasses from such animals and all specified bovine offal are collected and processed at one particular Swiss rendering plant. Thus, samples were taken in this rendering plant by two veterinarians. To make certain that an infected animal could be traced back, all collection points and transporters of culled animals use special ear tags to identify these animals in addition to issuing an accompanying document.

The cohort of emergency slaughtered animals was expected to be the second most likely population to yield BSE cases, since these animals were ill or had an accident prior to slaughter.

Thus since January 1999, in addition to the mandatory reporting of all suspect cases (based on clinical neurological signs) all fallen adult cattle showing at least 4 permanent teeth, i.e., more than 24 months of age, that are brought to the single rendering plant designated for fallen stock, and since March 1999 all adult cattle subject to emergency slaughter have been examined. In addition, a random sample of routinely slaughtered cattle for human consumption have been examined. Samples are taken by veterinarians responsible for meat inspection. A total of 17892 animals have been examined in this study. This enables further data about the BSE epidemic in Switzerland to be obtained, together with the clinical examinations of veterinarians and ante mortem inspections in slaughterhouses.

All brain samples are being tested for the presence of PrP(Sc) using the Prionics-Check-Test; test-positive samples are examined at the Swiss reference laboratory for animal TSE by means of histology and/or immunohistochemistry.

As of 31st December 1999, 25 clinical cases of BSE had been reported to the Swiss authorities under the original passive surveillance system. Two of these animals were born before the official feed ban in December 1990, the

others were born between December 1990 and June 1995. None of these animals was less than 49 months old. During the same time period a total of 7176 fallen animals, 3578 emergency-slaughtered animals, and 7138 routinely slaughtered cows have been examined. Sixteen of the fallen animals, six of the emergency slaughtered cows and three of the routinely slaughtered cows were found to be BSE-positive. All of these animals were born after the feed ban of December 1990, and the youngest animal was born in December 1995. All affected cattle were older than 43 months of age. Retrospective investigations of these cases demonstrated that only some of them showed signs typical for BSE. Most of them had displayed some signs of distress, non-specific disease or loss of productivity.

In summary, the greater number of BSE cases in Switzerland in 1999, when compared to the 1998 figures, is the result of a strongly improved surveillance, resulting in a better case ascertainment, and a result of more convincing control measures involving a change from herd slaughtering to cohort slaughtering. All available evidence points towards an ongoing decrease in the epidemic in line with all model predictions.

### Conclusions

Because active detection of preclinical cases of BSE infection in the population at risk has not been implemented until recently, the true prevalence of the disease and past incidence of infection in the different countries is not known. Under these circumstances new surveillance methods must be developed in order to assess the likely prevalence, before a country can be considered free from disease or infection. To this effect, surveillance in Great Britain was enhanced by a slaughterhouse survey, from January to March 1999, of 4000 animals, 5 years and older, slaughtered in the Over Thirty Months Scheme. This represents the first of a series of such surveys to provide independent evidence for a true decline in the incidence of BSE in Great Britain (J. W. Wilesmith, unpubl. findings).

The results obtained so far clearly show that mandatory reporting of clinically suspect animals alone is not sufficient to derive a true picture of the BSE status in a country, because such reporting is too dependent on subjective factors. It is obvious that by using a targeted surveillance scheme – such as the one outlined here – it is expected to detect more BSE cases than through mandatory reporting alone (Fig. 3). This scheme, in concert with the mandatory reporting of clinically suspect animals, is considered to be a very good approach to further evaluate the status and monitor the evolution of the BSE epidemic in the cattle population.

Logistical problems can and have been solved. The costs for this surveillance in Switzerland amounts to approximately 1 million Euro per year to examine 17892 samples.

In 1999, 50% of the detectable cases of infection or disease, in Switzerland, were identified by targeted surveillance.

<b><u>Mandatory reporting of clinically suspect cases</u></b> 25 BSE positive		
<b><u>Fallen stock</u></b> 16/7176 samples tested BSE positive <b>80 x the incidence of passive surveillance</b>	<b><u>Emergency slaughter</u></b> 6/3578 samples tested BSE positive <b>60 x the incidence of passive surveillance</b>	<b><u>Regular slaughter</u></b> 3/7138 samples tested BSE positive <b>15 x the incidence of passive surveillance</b>

**Fig. 3.** Factors by which the incidence was increased in the tested groups when compared to the general population prevalence derived through mandatory reporting

Most BSE positive cases detected in the targeted surveillance have weak or atypical clinical signs. The targeted surveillance is independent of the efficiency of the passive surveillance system. The risk groups identified, fallen stock and emergency slaughter, are suitable for targeted surveillance.

We conclude that a targeted surveillance scheme, applied particularly to all fallen stock and emergency-slaughtered animals, is the most effective approach to detect a rare disease such as BSE on a country-wide scale.

### References

1. Braun U, Schicker E, Pusterla N, Schönmann M (1998) Klinische Befunde bei 50 Kühen mit boviner spongiformer Enzephalopathie (BSE) [Clinical findings in 50 cows with bovine spongiform encephalopathy]. Berl Münch tierärztl Wochenschr 111: 27–32
2. Doherr MG, Oesch B, Moser M, Vandeveld M, Heim D (1999) Targeted surveillance for bovine spongiform encephalopathy (BSE). Vet Rec 145: 672
3. Hörnlimann B, Braun U (1994) Bovine spongiform encephalopathy (BSE): clinical signs in Swiss BSE cases. Proc Consultation on BSE with the Scientific Committee of the European Communities (CEC), 14–15 September 1993, Brussels. CEC, Brussels, pp 289–299
4. Office International des Epizooties (OIE) (1998) Final Report of the 66th General Session 25–29 May, Paris. OIE, Paris, p 24
5. Wells GAH, Hawkins SAC, Green RB, Austin AR, Dexter I, Spencer YI, Chaplin MJ, Stack MJ, Dawson M (1998) Preliminary observations on the pathogenesis of experimental bovine spongiform encephalopathy (BSE): an update. Vet Rec 142: 103–106
6. Wells GAH, Scott AC, Johnson CT, Gunning RF, Hancock RD, Jeffrey M, Dawson M, Bradley R (1987) A novel progressive spongiform encephalopathy in cattle. Vet Rec 121: 419–420
7. Wilesmith JW, Hoinville LJ, Ryan JBM, Sayers AR (1992) Bovine spongiform encephalopathy: aspects of the clinical picture and analyses of possible changes 1986–1990. Vet Rec 130: 197–201

Authors' address: Dr. D. Heim, Swiss Federal Veterinary Office, CH-3097 Liebefeld, Switzerland.

# **Histopathology and immunohistochemistry of human transmissible spongiform encephalopathies (TSEs)**

**H. Budka**

Austrian Reference Centre for Human Prion Diseases (ÖRPE) and Institute of Neurology, University of Vienna, Austria

**Summary.** Neuropathological examination has remained the most important tool to give a definite diagnosis of human transmissible spongiform encephalopathies (TSEs). In recent years, immunohistochemistry (IHC) for the disease-associated prion protein (PrP) has emerged as an indispensable adjunct to the neuropathological confirmation of TSEs, especially in cases with equivocal histopathological changes. The clinico-pathological phenotype including histopathology and IHC for PrP depends upon PrP<sup>res</sup> fragment size and codon 129 genotype in the PrP gene, *PRNP*. However, some TSEs have little or no spongiform change or detectable PrP, such as fatal familial insomnia (FFI). IHC for PrP requires appropriate technique, has some pitfalls and thus should be interpreted by experienced observers. The amount and distribution of PrP deposits do not always correlate with type and severity of local tissue damage. PrP deposition occurs only where neuronal parenchyma is present; in pre-existing tissue lesions such as scarred infarctions with prominent gliosis, PrP does not accumulate. Most recently, new patterns of granular ganglionic and tiny adaxonal PrP deposits were described in the peripheral nervous system in rare human TSE cases and experimental scrapie. There is early, severe and selective loss of a peculiar parvalbumin-expressing subset of inhibitory GABAergic neurons both in human and experimental TSEs.

## **Introduction**

Neuropathological examination has remained the most important tool to give a definite diagnosis of human transmissible spongiform encephalopathies (TSEs) [6]. In recent years, immunohistochemistry (IHC) for the disease-associated prion protein (PrP) has emerged as an indispensable adjunct to the neuropathological confirmation of TSEs, especially in cases with equivocal histopathological changes [6, 20]. This brief review focuses on recently emerging points to consider and newly recognised features in the histopathology and IHC of human TSEs (Table 1).

**Table 1.** Important points to consider and newly recognised features in the histopathology and immunocytochemistry of human TSEs

---

1. Histopathology of human TSEs	<ul style="list-style-type: none"> <li>• classical triad: spongiform change, neuronal loss, and gliosis (astro- and microglia)</li> <li>• correlation with disease (sub)type: sporadic CJD, FFI</li> </ul>
2. Immunohistochemistry for PrP	<ul style="list-style-type: none"> <li>• use and significance</li> <li>• technique and pitfalls</li> <li>• patterns, development and distribution of PrP deposition</li> <li>• correlation of PrP deposition with disease (sub)type</li> <li>• correlation of PrP deposition with histopathology</li> <li>• new patterns of PrP deposition in the PNS</li> </ul>

---

### Histopathology of human TSEs

The classical histopathological features of human TSEs have been extensively described (e.g., [5]) and will not be fully elaborated here. The *triad* of spongiform change, neuronal loss, and gliosis (astro- and microglia) is the neuropathological hallmark of TSEs. Since neuronal loss and gliosis accompany many other conditions of the CNS, it is the *spongiform change* that is mostly specific to TSEs. This spongiform change is characterised by diffuse or focally clustered small round or oval vacuoles in the neuropil of the deep cortical layers, cerebellar cortex or subcortical grey matter, which might become confluent. Spongiform change should not be confused with non-specific spongiosis. This includes status spongiosus (“spongiform state”), comprising irregular cavities in gliotic neuropil following extensive neuronal loss (including also lesions of “burnt-out” CJD), “spongy” changes in brain oedema and metabolic encephalopathies, and artefacts such as superficial cortical, perineuronal, or perivascular vacuolation. Focal changes indistinguishable from spongiform change may occur in some cases of Alzheimer’s and diffuse Lewy body diseases [6].

Presence and distribution of spongiform change vary greatly between cases and disease subtypes. In sporadic Creutzfeldt–Jakob disease (CJD), the regional distribution of spongiform change in distinct patterns was shown to depend upon PrP<sup>res</sup> fragment size and codon 129 genotype in the PrP gene, *PRNP* [21]. However, some TSEs, in fact, have equivocal, little or no spongiform change, such as fatal familial insomnia (FFI) [1] which is specifically characterised by prominent thalamic atrophy with profound astrogliosis (Fig. 1D). Then IHC for PrP and *PRNP* genotyping have a decisive diagnostic role [16]. Current neuropathological criteria for human TSEs [24], including the specific diagnostic features of variant CJD (vCJD), are listed in Table 2.

Neuronal loss appears to follow an apoptotic pathway that is apparently independent from local deposition of PrP<sup>res</sup> but correlates with

astrogliosis and microglial activation [7]. Specific vulnerability of a peculiar, parvalbumin-expressing subset of inhibitory GABAergic neurons was found both in human [2, 11] and experimental TSEs [10]. In fact, this vulnerability was detectable already early in the incubation period and thus represents the earliest changes ever described after experimental inoculation [10]. However, FFI differs in such vulnerability [12] from all other human TSEs.

### **Immunohistochemistry for PrP**

#### *Use and significance*

IHC for the disease-associated PrP (PrP<sup>res</sup>) is feasible on routinely formol-fixed and paraffin-embedded tissues and has become indispensable for the diagnostic confirmation of TSEs [6, 20]. Unfortunately, routine PrP IHC might yield a negative result in exceptional cases, especially in FFI [1]. Most recently developed techniques such as the paraffin-embedded tissue (PET) blot [22] or the use of Carnoy's fixative [8] are promising alternatives to increase sensitivity for the detection of disease-associated PrP in tissues. However, in our European neuropathological surveillance study of human TSEs [4] that encompasses now tissues from more than 700 patients, we have seen only 2 FFI brains negative with IHC for PrP among tissue specimens fulfilling criteria for a human TSE.

Given the long incubation periods that make experimental transmission impractical, IHC for PrP has also been used as surrogate marker for infectivity in peripheral tissues which are important for considerations of infectivity risks, such as the lymphoid system [18] or the peripheral nervous system [9, 15]. Moreover, PrP is also an important marker for development, spread and distribution of pathology. However, the amount and distribution of PrP deposits do not always correlate with type and severity of local tissue damage [14]. In a sequential experimental study on the time course and intensity of tissue lesioning and IHC for PrP in mice inoculated with a human CJD agent, PrP accumulation does not precede, but follow spongiform change [19]. Local PrP deposition requires the presence of neuronal but not glial elements: in pre-existing brain lesions such as infarctions in which neuronal elements had been focally destroyed (Fig. 1F, G) and replaced by a gliotic scar (Fig. 1H), PrP deposition is absent (Fig. 1E).

#### *Technique and pitfalls*

It is important to realise that the antibodies used for IHC do not distinguish between the normal PrP<sup>C</sup> and PrP<sup>res</sup>, including the widely used 3F4 antibody. Thus it is crucial to abolish immunoreactivity of PrP<sup>C</sup> by specific pre-treatment of formol-fixed, paraffin-embedded sections. In our hand

as well as that of others, a protocol using formic acid, guanidine thiocyanate, and hydrated autoclaving [3] gave strongest and most consistent signals. Minor modifications were recently recommended [23]. It must be noted that the possibility of pitfalls requires extensive experience in technique and interpretation. Sometimes unspecific labelling of diffuse neuronal somata, dystrophic neurites,  $\beta$ /A4 amyloid, and neurofibrillary tangles may be seen [17], probably representing incomplete abolishment of PrP<sup>C</sup> immunoreactivity. Thus interpretation of positive labelling has to be made by experienced observers and must consider the morphology of obtained signals.

#### *Patterns and distribution of PrP deposition*

Characteristic patterns of PrP deposition are synaptic (Fig. 1E), patchy/perivacuolar, and plaque types, which may overlap in the individual brain [6, 14]. Frequencies of these patterns differ between cerebral and cerebellar cortex (Table 3). Synaptic-type deposits and unicentric PrP plaques occur both in CJD and Gerstmann–Sträussler–Scheinker disease (GSS), while abundant multicentric plaques are peculiar to GSS [13]. Plaque-like deposits are the only type of PrP deposits extending to the subcortical white matter [14] and are more frequent than true kongophilic Kuru-type plaques that are well visible already without IHC. While very rarely “florid” or “daisy-like” plaques may be observed in other TSEs [14], their prominence is restricted to vCJD. Again, type and distribution of PrP deposition in sporadic CJD were shown to depend upon PrP<sup>res</sup> fragment size and *PRNP* codon 129 genotype [21]. Large bihemispheric sections are most useful to study the distribution of accumulated PrP (Fig. 1A–C) and demonstrate that abundant PrP deposits occur irrespective of the absence (Fig. 1A, C) or the presence (Fig. 1B) of profound brain atrophy.

---

**Fig. 1.** A–C Large bihemispheric sections immunostained for PrP. Sporadic CJD with prominent diffuse PrP deposition in cerebral (A) and cerebellar (C) cortex but without brain atrophy and hippocampal involvement. B Gerstmann–Sträussler–Scheinker disease, CJD-like phenotype [13], with prominent diffuse cortical PrP deposition and massive brain atrophy. D Fatal familial insomnia with prominent atrophy and massive gliosis of the thalamus (*Th*). Immunostain for the astrocytic marker protein GFAP. E–H Sporadic CJD with pre-existing cerebellar infarctions. Adjacent cerebellar sections immunostained for PrP (E), the neuronal marker proteins synaptophysin (F) and neurofilament protein (G), and GFAP (H). In the centre, some cerebellar gyri are still preserved and express PrP (synaptic pattern) as well as neuronal markers but not GFAP, whereas surrounding gyri are scarred with gliosis, and lack PrP and neuronal marker proteins

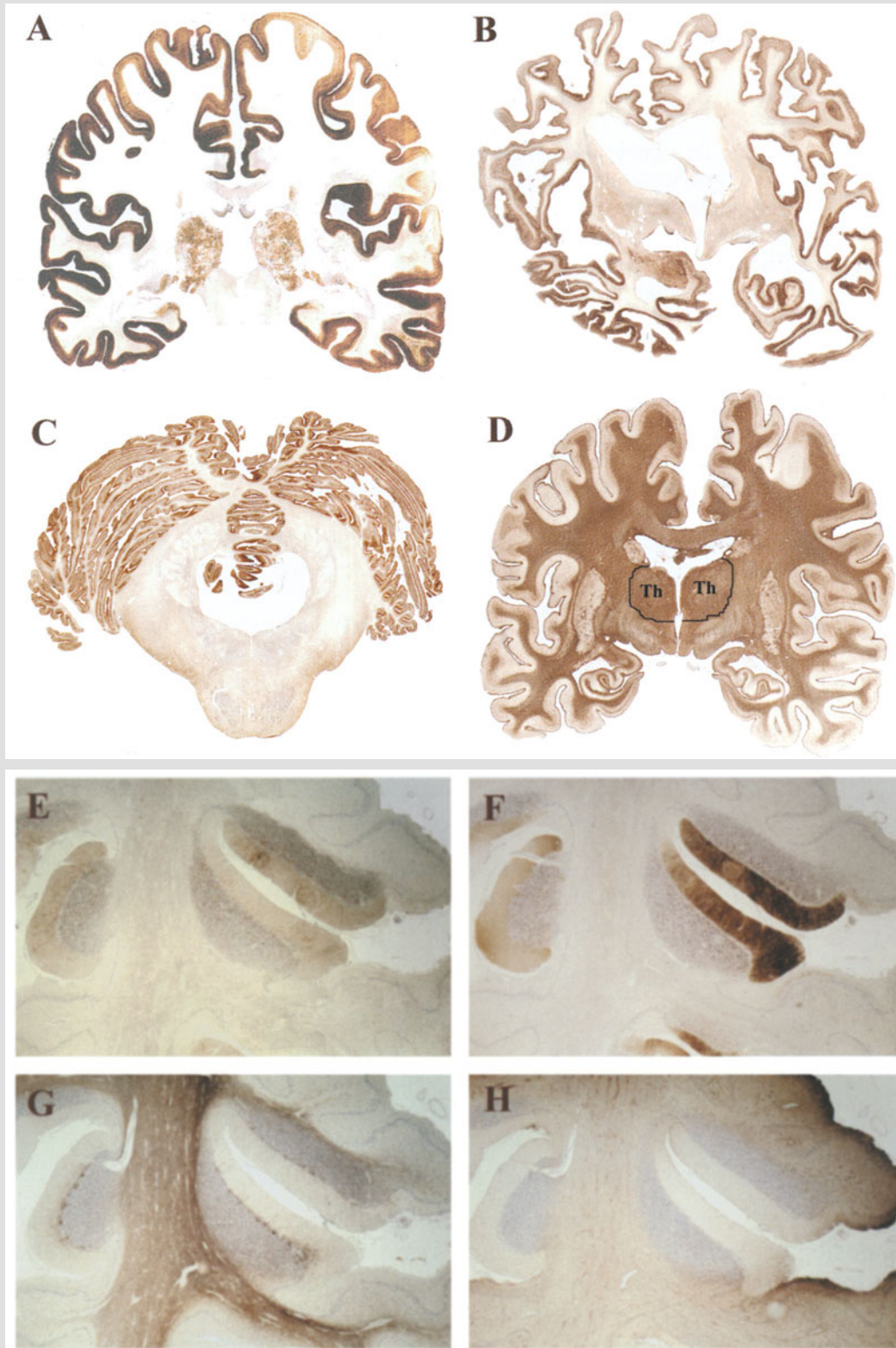


**Table 2.** Neuropathological criteria for CJD and other human TSEs (updated and modified from [6], as currently used by the WHO [24])

- 
1. Creutzfeldt–Jakob disease (CJD)
    - 1.1. sporadic, iatrogenic (recognised risk) or familial (same disease in 1st degree relative or disease-associated PrP gene mutation):  
Spongiform encephalopathy in cerebral and/or cerebellar cortex and/or subcortical grey matter; and/or  
Encephalopathy with prion protein (PrP) immunoreactivity (plaque and/or diffuse synaptic and/or patchy/perivacuolar types).
    - 1.2. variant CJD (vCJD)  
Spongiform encephalopathy with abundant PrP deposition, in particular multiple fibrillary PrP plaques surrounded by a halo of spongiform vacuoles (“florid” plaques, “daisy-like” plaques) and other PrP plaques, and amorphous pericellular and perivascular PrP deposits especially prominent in the cerebellar molecular layer.
  2. Gerstmann–Sträussler–Scheinker disease (GSS) (in family with dominantly inherited progressive ataxia and/or dementia and one of a variety of PrP gene mutations):  
Encephalo(myelo)pathy with multicentric PrP plaques.
  3. Familial fatal insomnia (FFI) (in family with *PRNP*<sup>178</sup> mutation):  
Thalamic degeneration, variably spongiform change in cerebrum.
  4. Kuru: Spongiform encephalopathy in the Fore population of Papua-New Guinea.
- 

**Table 3.** Frequency of synaptic (syn), patchy/perivacuolar (pp) and plaque (pl) type PrP deposition patterns in cerebral and cerebellar cortex of sporadic CJD cases [14]

	Cerebral cortex	Cerebellar cortex
syn	91%	94%
pp	38%	6%
pl	10%	19%

#### *New patterns of PrP deposition in the PNS*

Most recently, new patterns of granular ganglionic and tiny adaxonal PrP deposits were described in spinal and vegetative ganglia, spinal roots and peripheral nerves in rare human TSE cases [15] and experimental scrapie [9]. It remains to be established by sequential studies whether this involvement of the peripheral nervous system reflects centripetal or centrifugal spread of PrP deposition and follows the pathways of travel by the infectious agent.

### Acknowledgements

The Austrian Federal Ministry for Labour, Health and Social Affairs funds the Austrian Reference Centre for Human Prion Diseases (ÖRPE). The author gratefully acknowledges the collaboration by numerous European neuropathologists in the EU BIOMED-2 Concerted Action "Human TSEs: neuropathology and phenotypic variation" and the skilled technical assistance by Ms. Helga Flicker.

### References

1. Almer G, Hainfellner JA, Brücke T, Jellinger K, Kleinert R, Bayer G, Windl O, Kretzschmar HA, Hill A, Sidle K, Collinge J, Budka H (1999) Fatal familial insomnia: a new Austrian family. *Brain* 122: 5–16
2. Belichenko PV, Miklossy J, Belser B, Budka H, Celio MR (1999) Early destruction of the extracellular matrix around parvalbumin-immunoreactive interneurons in Creutzfeldt–Jakob disease. *Neurobiol Dis* 6: 269–279
3. Bell JE, Gentleman SM, Ironside JW, McCardle L, Lantos PL, Doey L, Lowe J, Fergusson J, Luthert P, McQuaid S, Allen IV (1997) Prion protein immunocytochemistry–UK five centre consensus report. *Neuropathol Appl Neurobiol* 23: 26–35
4. Budka H (1997) The human prion diseases: from neuropathology to pathobiology and molecular genetics. Final report of an EU Concerted Action. *Neuropathol Appl Neurobiol* 23: 416–422
5. Budka H (1997) Transmissible spongiform encephalopathies (prion diseases). In: Garcia JH (ed) *Neuropathology. The diagnostic approach*. Mosby, St. Louis, pp 449–474
6. Budka H, Aguzzi A, Brown P, Brucher J-M, Bugiani O, Gullotta F, Haltia M, Hauw J-J, Ironside JW, Jellinger K, Kretzschmar HA, Lantos PL, Masullo C, Schlote W, Tateishi J, Weller RO (1995) Neuropathological diagnostic criteria for Creutzfeldt–Jakob disease (CJD) and other human spongiform encephalopathies (prion diseases). *Brain Pathol* 5: 459–466
7. Dorandeu A, Wingertsmann L, Chrétien F, Delisle M-B, Vital C, Parchi P, Montagna P, Lugaresi E, Ironside JW, Budka H, Gambetti P, Gray F (1998) Neuronal apoptosis in fatal familial insomnia. *Brain Pathol* 8: 531–537
8. Giaccone G, Canciani B, Puoti G, Rossi G, Goffredo D, Iussich S, Fociani P, Tagliavini F, Bugiani O (2000) Creutzfeldt–Jakob disease: Carnoy's fixative improves the immunohistochemistry of the proteinase K-resistant prion protein. *Brain Pathol* 10: 31–37
9. Groschup MH, Beekes M, McBride PA, Hardt M, Hainfellner JA, Budka H (1999) Deposition of disease-associated prion protein involves the peripheral nervous system in experimental scrapie. *Acta Neuropathol* 98: 453–457
10. Guentchev M, Groschup MH, Kordek R, Liberski PP, Budka H (1998) Severe, early and selective loss of a subpopulation of GABAergic inhibitory neurons in experimental transmissible spongiform encephalopathies. *Brain Pathol* 8: 615–623
11. Guentchev M, Hainfellner J-A, Trabattoni GR, Budka H (1997) Distribution of parvalbumin positive neurons in brain correlates with hippocampal and temporal cortical pathology in Creutzfeldt–Jakob disease. *J Neuropathol Exp Neurol* 56: 1119–1124
12. Guentchev M, Wanschitz J, Voigtlaender T, Flicker H, Budka H (1999) Selective neuronal vulnerability in human prion diseases. Fatal familial insomnia differs from other types of prion diseases. *Am J Pathol* 155: 1453–1457

13. Hainfellner JA, Brantner-Inthaler S, Cervenakova L, Brown P, Kitamoto T, Tateishi J, Diringer H, Liberski PP, Regele H, Feucht M, Mayr N, Wessely P, Summer K, Seitelberger F, Budka H (1995) The original Gerstmann-Sträussler-Scheinker family of Austria: divergent clinicopathological phenotypes but constant PrP genotype. *Brain Pathol* 5: 201–211
14. Hainfellner JA, Budka H (1996) Immunomorphology of human prion diseases. In: Court L, Dodet B (eds) *Transmissible spongiform encephalopathies: prion diseases*. Elsevier, Paris, pp 75–80
15. Hainfellner JA, Budka H (1999) Disease associated prion protein may deposit in the peripheral nervous system in human transmissible spongiform encephalopathies. *Acta Neuropathol* 98: 458–460
16. Hainfellner JA, Jellinger K, Diringer H, Guentchev M, Kleinert R, Pilz P, Maier H, Budka H (1996) Creutzfeldt–Jakob disease in Austria. *J Neurol Neurosurg Psychiatry* 61: 139–142
17. Hegyi I, Hainfellner JA, Flicker H, Ironside JW, Hauw JJ, Tateishi J, Haltia M, Bugiani O, Aguzzi A, Budka H (1997) Prion protein immunocytochemistry: reliable staining protocol, immunomorphology, and diagnostic pitfalls. *Clin Neuropathol* 16: 262–263
18. Hill AF, Butterworth RJ, Joiner S, Jackson G, Rossor MN, Thomas DJ, Frosh A, Tolley N, Bell JE, Spencer M, King A, Al-Sarraj S, Ironside JW, Lantos PL, Collinge J (1999) Investigation of variant Creutzfeldt–Jakob disease and other human prion diseases with tonsil biopsy samples. *Lancet* 353: 183–189
19. Kordek R, Hainfellner JA, Liberski PP, Budka H (1999) Deposition of the prion protein (PrP) during the evolution of experimental Creutzfeldt–Jakob disease. *Acta Neuropathol* 98: 597–602
20. Kretzschmar HA, Ironside JW, DeArmond SJ, Tateishi J (1996) Diagnostic criteria for sporadic Creutzfeldt–Jakob-disease. *Arch Neurol* 53: 913–920
21. Parchi P, Giese A, Capellari S, Brown P, Schulz-Schaeffer W, Windl O, Zerr I, Budka H, Kopp N, Piccardo P, Poser S, Rojiani A, Streichemberger N, Julien J, Vital C, Ghetti B, Gambetti P, Kretzschmar H (1999) Classification of sporadic Creutzfeldt–Jakob disease based on molecular and phenotypic analysis of 300 subjects. *Ann Neurol* 46: 224–233
22. Schulz-Schaeffer WJ, Tschoke S, Kranefuss N, Drose W, Hause-Reitner D, Giese A, Groschup MH, Kretzschmar HA (2000) The paraffin-embedded tissue blot detects PrP(Sc) early in the incubation time in prion diseases. *Am J Pathol* 156: 51–56
23. Van Everbroeck B, Palsa P, Martina J-J, Cras P (1999) Antigen retrieval in prion protein immunohistochemistry. *J Histochem Cytochem* 47: 1465–1470
24. WHO (1998) Global surveillance, diagnosis and therapy of human transmissible spongiform encephalopathies: report of a WHO consultation. Geneva, Switzerland, 9–11 February 1998. WHO, Geneva

Authors' address: Prof. H. Budka, Institute of Neurology, University of Vienna, AKH 4J, Währinger Gürtel 18-20, A-1097 Wien, Austria.

## **Pathology of variant Creutzfeldt–Jakob disease**

**J. W. Ironside**

CJD Surveillance Unit, University of Edinburgh, Edinburgh, Scotland, U.K.

**Summary.** Variant Creutzfeldt–Jakob disease (vCJD) is a novel prion disease in man which was first described in 1996 in the UK. There is substantial evidence to indicate that vCJD represents the effects of the bovine spongiform encephalopathy (BSE) agent in man. The neuropathology of vCJD is characterised by the florid plaque, composed of a central amyloid core with a fibrillary periphery, surrounded by a rim of spongiform change in an intact neuropil. Unique patterns of PrP accumulation in vCJD are revealed by immunocytochemistry in the cerebral and cerebellar cortices, the basal ganglia, thalamus and brainstem. The neuropathology of the thalamus and midbrain is also characterised by severe neuronal loss and gliosis. vCJD is distinct from other human prion diseases in that disease-associated PrP accumulates within follicular dendritic cells in lymphoid tissue, and consistently in peripheral sensory ganglia. All vCJD patients so far have been methionine homozygotes at codon 129 in the PrP gene. There is no evidence to indicate that cases of BSE infection have occurred in individuals in the UK who are MV or VV at codon 129 in the PrP gene. It is conceivable that BSE incubation periods in these groups may be longer than in methionine homozygotes, hence the precise numbers of future cases of vCJD are difficult to estimate at present.

### **Introduction**

Human transmissible spongiform encephalopathies or prion diseases are a group of rare fatal neurological disorders which occur in sporadic, familial and acquired forms [15] (see Table 1). The commonest of these is the sporadic form of Creutzfeldt–Jakob disease, which occurs in a world-wide distribution with an incidence of around one case per million of the population per annum. The pathological hallmarks of human prion diseases occur in the central nervous system, with no consistent abnormalities occurring in other organs. Characteristic neuropathological features comprise spongiform change (the presence of vacuoles in the gray matter), neuronal loss, astrocytic and microglial proliferation, and the accumulation of disease-associated prion protein (PrP) [12]. These pathological features are

**Table 1.** Human prion diseases

Sporadic		Sporadic Creutzfeldt–Jakob disease Sporadic fatal insomnia
Acquired	Human source	Iatrogenic Creutzfeldt–Jakob disease Kuru
	Bovine source	Variant Creutzfeldt–Jakob disease
Familial		Gerstmann-Sträussler-Scheinker syndrome and variants Familial Creutzfeldt–Jakob disease Fatal familial insomnia

markedly variable from case to case, even within the individual disease entities; sporadic Creutzfeldt-Jakob disease (sCJD) shows a wide range of clinical and neuropathological phenotypic variation which is substantially influenced by the naturally occurring polymorphism at codon 129 in the PrP gene on chromosome 20, and the PrP isotype identified on Western blot analysis following protease K digestion of brain homogenates [14]. Phenotypic variation also occurs within acquired and inherited human prion diseases, but the underlying determinants of this variability are uncertain. It is conceivable that other genes may influence disease phenotype in human prion diseases, but no consistent information is yet available on this important point.

Surveillance of CJD in the UK was reinstated in 1990 in light of the bovine spongiform encephalopathy (BSE) epidemic in the cattle population. BSE was first reported in 1987 [20], and early epidemiological studies identified that meat and bone-meal animal feed was the source of the epidemic. Characterisation of the transmissible agent in BSE by strain typing studies have revealed only one strain of the BSE agent, unlike scrapie, where numerous different strains of the transmissible agent have been detected by this technique [3]. The BSE agent has also caused novel prion diseases in a range of other species who were exposed to BSE in meat and bone-meal animal feed (including antelopes in zoos) and BSE-contaminated meat (domestic and large wild cats). The consumption of cattle brain, spinal cord and other organs was banned for human consumption in the late 1980s in the UK, but it is clear that the population in the UK could have been exposed to the BSE agent in meat products in the early 1980s. In order to investigate the possibility that BSE could cause disease in humans, the National CJD Surveillance Unit was established in Edinburgh, where cases of suspected CJD were referred by healthcare professionals across the UK, principally neurologists, general physicians and neuropathologists. The surveillance project aims to identify clinical and neuropathological parameters in each case with a detailed epidemiological study to identify risk factors for CJD, and PrP genetic analysis is performed with informed consent from relatives. The referral of suspected CJD cases to the Sur-

veillance Unit is entirely voluntary and there has been a remarkable co-operation with this project from clinicians and pathologists across the UK.

### Variant CJD

In 1996, the CJD Surveillance Unit published details of ten patients with an apparently new form of human prion disease which had not been previously encountered in the UK or in other European countries in which surveillance studies for CJD using comparable methodology had been established [21]. The clinical features of these cases were distinct from those of sporadic CJD and were characterised by an unusually young age at onset (the first two cases had occurred in teenagers and were initially reported as separate cases). The clinical features were relatively uniform and featured psychiatric symptoms at onset followed by sensory abnormalities, ataxia, myoclonus and other movement disorders and eventually dementia and akinetic mutism. All patients showed a similar PrP genotype with and methionine homozygosity at the polymorphic locus at codon 129 and no mutations present [22].

### Pathology of vCJD

The neuropathology of these cases showed all the classical features of human prion diseases with spongiform change, neuronal loss, astrocytic and microglial proliferation and accumulation of disease-associated PrP in the central nervous system [21]. However, the detailed features of the brain lesions were strikingly different from those of sporadic CJD [11] (see Table 2).

**Table 2.** Comparison of pathological features in variant Creutzfeldt–Jakob disease (vCJD) and sporadic Creutzfeldt–Jakob disease (sCJD)

vCJD	sCJD
Numerous florid plaques in all cases	No florid plaques; kuru-type plaques in MV type 2 cases
Spongiform change most marked in lentiform nuclei	Spongiform change widespread and usually most marked in cerebral cortex
Severe neuronal loss and gliosis in pulvinar and periaqueductal grey matter	Severe thalamic gliosis is rare and usually present in anterior and medial nuclei
PrP accumulation in large plaques, small cluster plaques, amorphous “feathery” deposits and neuronal/axonal patterns	PrP accumulation mainly in reticular/synaptic, perivacuolar, plaque-like and kuru plaque deposits
Western blots show a single PrP isotype in brain and lymphoid tissue	Western blots show variable PrP isotypes in brain; lymphoid tissues are negative
All cases are MM at codon 129 in the PrP gene	78% are MM, 12% are MV and 10% are VV at codon 129 in the PrP gene

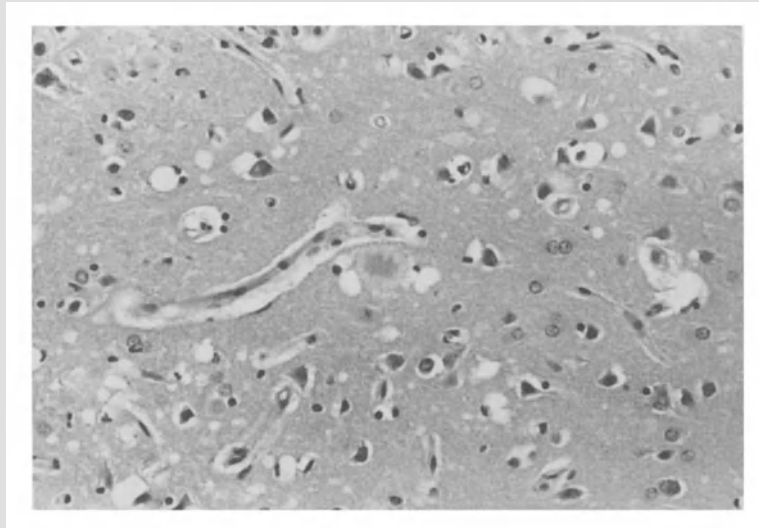


**Fig. 1.** The florid plaque in vCJD (centre) comprises a dense central amyloid core and a paler peripheral zone, with spongiform change in the surrounding neuropil. Haematoxylin and eosin,  $\times 240$

In the cerebral and cerebellar cortex, the most striking abnormality was the presence of large rounded amyloid plaques surrounded by a rim or halo of spongiform change (Fig. 1). This occurred in a widespread distribution but in the cerebrum was usually most conspicuous in the occipital cortex. These plaques resembled the florid plaques first identified on transmission of Icelandic scrapie into mice [6], and had not been previously identified in cases of sporadic CJD [12]. Other consistent neuropathological features included spongiform change most conspicuous in the lentiform nuclei (particularly the caudate nucleus and putamen), marked neuronal loss and astrocytic gliosis in the gray matter in the posterior and medial thalamus (particularly the pulvinar) and in the periaqueductal gray matter in the midbrain [11]. The brain areas exhibit a characteristic high signal in T2-weighted magnetic resonance images of the brain in vCJD [23]; this neuroradiological feature is of considerable clinical diagnostic value [22].

Immunocytochemistry for prion protein showed strong staining of the large amyloid plaques but in addition revealed numerous smaller plaque-like aggregates which were not detectable on routine stains and usually occurred as small clusters in the cerebral and cerebellar cortex. In addition, amorphous “feathery” deposits of PrP also occurred in a widespread distribution in the cerebral and cerebellar cortex particularly around neurones and blood vessels (Fig. 2). These patterns of PrP accumulation appear specific for vCJD. No evidence of a true amyloid angiopathy has been identified in this condition. PrP immunocytochemistry in the lentiform nuclei showed a different pattern of accumulation with perineuronal and axonal decoration and fewer amyloid plaques. In the thalamus and

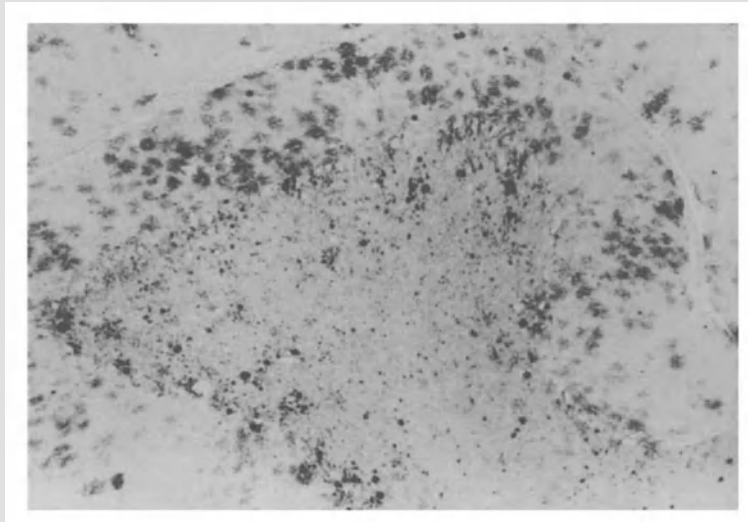


**Fig. 2.** Extensive PrP accumulation in the cerebellar cortex in vCJD occurs predominantly in the molecular layer, with numerous plaques and amorphous deposits. KG9 monoclonal antibody with haematoxylin counterstain,  $\times 100$

hypothalamus, a reticular or synaptic pattern of PrP accumulation predominated with only occasional small plaques. In the brainstem, there was neuronal and perineuronal staining in the pontine nuclei and in the colliculi, whilst in the medulla strong staining around the dorsal nucleus of the vagus was observed with intense reticular/synaptic staining of the inferior olivary nuclei and the dentate nuclei in the cerebellum. PrP accumulation was also identified within the gray matter of the spinal cord, particularly in and around the posterior horns and the substantia gelatinosa.

Western blotting studies in vCJD identified a consistent PrP isotype, with a predominance of the diglycosylated form of the protein and an unglycosylated band with a mobility of around 19 kD, distinct from other forms of human prion disease [11]. The predominance of the diglycosylated form of the protein resembled that seen in Western blotting in BSE, and in other BSE-related illnesses in other species [4]. Subsequent strain typing studies and transmission studies using human and bovine transgenic mice have revealed that the transmissible agent in vCJD is identical to that in BSE [2, 9, 17]. These studies helped confirm the hypothesis (based on pathological, clinical and epidemiological data) that vCJD is a novel acquired human disease, which represents the first example of transmission of a prion disease to humans from another species (all other currently identified acquired human prion diseases represent examples of human to human transmission). In contrast, numerous epidemiological studies have failed to demonstrate that scrapie (the widespread naturally occurring prion disease in sheep and goats) is responsible for any cases of human prion disease.

### **Peripheral pathogenesis of vCJD**

Current epidemiological studies have not identified any consistent risk factors for the development of vCJD other than dietary exposure to the BSE agent in the 1980s. Although it is not possible to formally exclude other possible routes of exposure to the BSE agent, it therefore seems likely that currently identified cases of vCJD arise from oral exposure to the BSE agent. This in turn raises questions concerning the peripheral pathogenesis of this disorder, and in particular the mechanisms and routes by which the transmissible agent reaches the central nervous system from the gut. There is a large body of information from experimental murine and hamster prion disease models following peripheral exposure to indicate that the transmissible agent can involve lymphoreticular tissues and the peripheral nervous system during the incubation period prior to the onset of clinical symptoms [1, 13]. In view of this, examination of a wide range of lymphoid tissues in vCJD has been undertaken, initially in autopsy tissues and more recently in biopsies from a small series of patients clinically suspected to have this disorder. These studies have revealed the presence of disease-associated isoform of prion protein in a wide range of lymphoid tissues including the tonsil, spleen, gut-associated lymphoid tissue and a wide range of lymph nodes from many sites in the body [8]. Comparable studies in other forms of human prion disease have not revealed the presence of disease-associated PrP, but studies in natural scrapie have shown a comparable distribution of disease-associated PrP in sheep [19]. In one patient who died from vCJD, examination of an appendix removed eight months prior to the onset of neurological disease revealed the presence of PrP by immunocytochemistry within the lymphoid tissues in the wall of the appendix [10]. Immunocytochemical studies have revealed that PrP positivity occurs primarily in follicular dendritic cells, as identified in co-labelling studies with the CD21 and CD35 antigens [9]. More recent studies indicate that other cell types, including tingible body macrophages, may also be involved, as appears to be the case in scrapie and experimental murine prion infections. The presence of disease-associated PrP in lymphoid tissues has led to the study of tonsil biopsy as a diagnostic tool for vCJD; this may well prove to be a useful investigation in patients in whom other characteristic abnormalities (e.g. MRI changes in the posterior thalamus) are not present.

The presence of disease-associated PrP in lymphoid tissues has led to questions concerning the presence of infectivity in these tissues and in blood during the incubation period of the disease. Studies to investigate infectivity in these tissues have been established, but no data are yet available. However, this concern has led to the implementation of leucodepletion of blood units for transfusion in the UK, and the sourcing of plasma products outwith the UK for the time being. Detailed consideration is also being given to the possibility of iatrogenic transmission of vCJD by contaminated surgical instruments used on lymphoid tissues. The presence of disease

associated-PrP in the tonsil and appendix has also allowed a large retrospective anonymous study of tonsillectomy and appendicectomy specimens to detect disease-associated PrP in order to help estimate the population exposure to the BSE agent in the UK.

Recent pathological studies in vCJD have focussed on the detection of disease-associated PrP by immunocytochemistry in other organs, particularly the peripheral nervous system. Preliminary results indicate that, in contrast to other forms of human prion diseases, there is consistent and extensive involvement of sensory ganglia including dorsal root ganglia and trigeminal ganglia. Positive staining has also been observed in autonomic ganglia within the gut, in the sympathetic chain and in parasympathetic ganglia, however these results need to be interpreted with caution at present since current immunocytochemical detection methods may also detect normal PrP from uninfected individuals at these sites. Additional studies including Western blotting to detect disease-associated PrP may help resolve these difficulties. However, the overall findings in vCJD are consistent with a peripheral pathogenesis that corresponds to that following oral exposure to a prion agent in animal models [13].

#### **Future studies in vCJD**

Considerable uncertainties remain as to the likely numbers of future cases of this disease both in the UK [5] and in other countries in which BSE exists. In particular, we have no information relating to the incubation period of the disease in humans although it seems likely that this will be lengthy and will therefore have a major influence on future disease numbers. Although at present only methionine homozygotes have developed this disease, the possibility that other PrP genotypes may become infected cannot be excluded; comparison with kuru and with iatrogenic CJD in growth hormone recipients has indicated that heterozygotes at codon 129 may have a longer disease incubation period than homozygotes. Particular vigilance is being given to cases of prion disease in humans who are valine homozygotes or heterozygotes at this important genetic locus. The possibility that BSE in a human with a PrP genotype other than methionine homozygotes at codon 129 in the PrP gene might lead to a different clinical and neuropathological phenotype has to be acknowledged, and particular attention will be required to identify examples of BSE-related disorders in these genetic subgroups using the widest possible range of clinical and laboratory-based techniques [11].

The presence of detectable PrP in lymphoid tissues in vCJD has led to the possibility that infectivity may be detectable in blood and a range of studies are currently underway to detect disease-associated PrP at low levels in blood, using the DELFIA technique or a recently described capillary electrophoresis technique [16]. The development of a blood-based screening test would represent a major step forward in our understanding of vCJD, as

it would allow large-scale anonymous screening of the population to determine the potential scale of future cases, and could also help resolve current difficulties concerning blood and organ donation. Furthermore, should any prophylactic or therapeutic agents become available for clinical use [7, 18], the development of a blood-based detection system would allow the implementation of any potential therapy at a pre-clinical stage of the illness before established brain dysfunction has occurred. The occurrence of vCJD outside the UK also reinforces the need for continued disease surveillance, not only in the UK but in other European countries where cases of BSE have occurred, in order that any future disease trends can be adequately monitored and identified. This surveillance needs to be backed up by adequate laboratory methods for the diagnosis and investigation of human prion diseases, in which neuropathological studies are of paramount importance.

### Acknowledgements

I thank my colleagues Prof. R.G. Will and Dr. M.W. Head for helpful discussion, Mrs. L. McCardle for technical assistance and Ms. B.A. Mackenzie and Ms. A. Penman for assistance in the preparation of the manuscript. Dr C Birkett, Institute for Animal Health, Compton, kindly supplied the KG9 monoclonal antibody. The National CJD Surveillance Unit is supported by the Department of Health and the Scottish Executive, and by the Medical Research Council (Grant number G9627376). The contributions of all Neurologists and Neuropathologists in the UK are gratefully acknowledged.

### References

1. Brown KL, Stewart K, Ritchie DL, Mabbott NA, Williams A, Fraser H, Morrison WI, Bruce ME (1999) Scrapie replication in lymphoid tissues depends on prion protein-expressing follicular dendritic cells. *Nature Med* 5: 1308–1312
2. Bruce ME, Will RG, Ironside JW, McConnell I, Drummond D, Suttie A, McCardle L, Chree A, Hope J, Birkett C, Cousens S, Fraser H, Bostock CJ (1997) Transmissions to mice indicate that “new variant” CJD is caused by the BSE agent. *Nature* 389: 498–501
3. Bruce ME, Chree A, McConnell I, Foster J, Pearson G, Fraser H (1994) Transmission of bovine spongiform encephalopathy and scrapie to mice: strain and variation and the species barrier. *Phil Trans R Soc London Ser B Biol Sci* 343: 405–411
4. Collinge J, Sidle KC, Meads J, Ironside J, Hill AF (1996) Molecular analysis of prion strain variation and the aetiology of “new variant” CJD. *Nature* 383: 666–667
5. Cousens SN, Vynnycky E, Zeidler M, Will RG, Smith PG (1997) Predicting the CJD epidemic in humans. *Nature* 385: 197–198
6. Fraser H (1979) The pathogenesis and pathology of scrapie. In: Tyrrel DAJ (ed) *Aspects of slow and persistent viral infection*. Martinus Nijhoff, The Hague, pp 30–58
7. Head MW, Ironside JW (2000) Inhibition of prion-protein conversion: a therapeutic tool? *Trends Microbiol* 8: 6–8

8. Hill AF, Butterworth RJ, Joiner S, Jackson G, Rossor MN, Thomas DJ, Frosh A, Tolley N, Bell JE, Spencer M, King A, Al-Sarraj S, Ironside JW, Lantos PL, Collinge J (1999) Investigation of variant Creutzfeldt–Jakob disease and other human prion diseases with tonsil biopsy samples. *Lancet* 353: 183–189
9. Hill AF, Desbruslais M, Joiner S, Sidle KC, Gowland I, Collinge J, Doey LJ, Lantos P (1997) The same prion strain causes vCJD and BSE. *Nature* 389: 448–450
10. Hilton DA, Fathers E, Edwards P, Ironside J, Zajicek J (1998) Prion immunoreactivity in appendix before clinical onset of variant Creutzfeldt–Jakob disease. *Lancet* 352: 703–704
11. Ironside JW, Head MW, Bell JE, McCardle L, Will RG (2000) Laboratory diagnosis of variant Creutzfeldt–Jakob disease. *Histopathology* (in press)
12. Ironside JW (1996) Review: Creutzfeldt–Jakob disease. *Brain Pathol* 6: 379–388
13. McBride PA, Beekes M (1999) Pathological PrP is abundant in sympathetic and sensory ganglia of hamsters fed with scrapie. *Neurosci Lett* 265: 135–138
14. Parchi P, Giese A, Capellari S, Brown P, Schulz-Schaeffer W, Windl O, Zerr I, Budka H, Kopp N, Piccardo P, Poser S, Rojiani A, Streichemberger N, Julien J, Vital C, Ghetti B, Gambetti P, Kretzschmar H (1999) Classification of sporadic Creutzfeldt–Jakob disease based on molecular and phenotypic analysis of 300 subjects. *Ann Neurol* 46: 224–233
15. Prusiner SB (1998) Prions. *Proc Natl Acad Sci USA* 95: 13363–13383
16. Schmerr MJ, Jenny AL, Bulgin MS, Miller KM, Hamir AN, Cutlip RC, Goodwin KR (1999) Use of capillary electrophoresis and fluorescent labelled peptides to detect abnormal prion protein in the blood of animals that are infected with transmissible spongiform encephalopathy. *J Chromatogr A* 853: 207–214
17. Scott MR, Will R, Ironside J, Nguyen HO, Tremblay P, DeArmond SJ, Prusiner S (1999) Compelling transgenic evidence for transmission of bovine spongiform encephalopathy prions to humans. *Proc Natl Acad Sci USA* 96: 15137–15142
18. Soto C, Kasczak RJ, Saborio GP, Aucouturier P, Wisniewski T, Prelli F, Kasczak R, Mendez E, Harris DA, Ironside J, Tagliavini F, Carp R, Frangione B (2000) Reversion of prion protein conformational changes by synthetic  $\beta$ -sheet breaker peptides. *Lancet* 355: 192–197
19. Van Keulen LF, Schreuder BE, Meloen RH, Mooij-Harkess G, Vromans ME, Langveld JP (1996) Immunohistochemical detection of prion protein in lymphoid tissues of sheep with natural scrapie. *J Clin Microbiol* 34: 1228–1231
20. Wells GA, Scott AC, Johnson CT, Gunning RF, Hancock RD, Jeffrey M, Dawson M, Bradley R (1987) A novel progressive spongiform encephalopathy in cattle. *Vet Rec* 121: 419–420
21. Will RG, Ironside JW, Zeidler M, Cousens S, Estibeiro K, Alperovitch A, Poser S, Pocchiari M, Hofman A, Smith PG (1996) A new variant of Creutzfeldt–Jakob disease in the UK. *Lancet* 347: 921–925
22. Will RG, Zeidler M, Stewart G, Macleod M-A, Ironside JW, Cousens S, Mackenzie J, Estibeiro K, Green AJE, Knight RSG (2000) The diagnosis of new variant Creutzfeldt–Jakob disease. *Ann Neurol* 47: 575–582
23. Zeidler M, Sellar R, Collie DA, Knight R, Stewart G, Macleod M-A, Ironside JW, Cousens S, Hadley DM, Will RG (2000) The pulvinar sign on magnetic resonance imaging in variant Creutzfeldt–Jakob disease. *Lancet* 355: 1412–1418

Author's address: Dr. J. W. Ironside, CJD Surveillance Unit, University of Edinburgh, Western General Hospital, Crewe Road, Edinburgh EH4 2XU, U.K.

## Clinical and differential diagnosis of Creutzfeldt–Jakob disease

S. Poser<sup>1</sup>, I. Zerr<sup>1</sup>, A. Schroeter<sup>1</sup>, M. Otto<sup>1</sup>, A. Giese<sup>3</sup>, B. J. Steinhoff<sup>2</sup>,  
and H. A. Kretzschmar<sup>3</sup>

<sup>1</sup>Departments of Neurology, <sup>2</sup>Neurophysiology and <sup>3</sup>Neuropathology,  
University of Goettingen, Goettingen, Germany

**Summary.** Until recently, the clinical diagnosis of CJD relied mainly on three criteria. These include patient history (rapidly progressive dementia), neurological findings (ataxia, pyramidal/extrapyramidal signs, myoclonus, akinetic mutism) and typical electroencephalographic (EEG) findings. These criteria are fulfilled in typical cases. The occurrence or increase of certain proteins in cerebrospinal fluid (CSF; 14-3-3, neuron-specific enolase) now provide important adjuncts in recognizing variant forms. Although these proteins can be detected in other neurological diseases accompanied with substantial brain damage such as encephalitis, they are also characterized by their high sensitivity and specificity with regard to other dementing processes (Alzheimer and vascular dementia). The increase in the number of positive cases during the last years in Germany reflects an improved case ascertainment rather than the appearance of the variant CJD (vCJD). Although several recent cases with a long duration of the disease were actually recognized, they did not reveal the typical florid plaques at autopsy. They were revealed as a rare variant of sporadic CJD, which is characterized by homocystosity for valine at codon 129 and PrP<sup>Sc</sup> type 1. This variant is positive for the 14-3-3 protein in CSF. Further subtypes described by Parchi et al. [5] can also be characterized by a certain pattern of clinical symptomatology, EEG- and 14-3-3-findings. In addition, differential diagnosis revealed some treatable dementias among the most common diseases (Alzheimer and vascular dementia) such as herpes encephalitis, multiple sclerosis and Hashimoto encephalitis, particularly in the younger age group.

### Introduction

Sporadic Creutzfeldt–Jakob disease (CJD) is the most important human prion disease occurring with a frequency of about 1 per million inhabitants throughout the world. The fear that the BSE epidemic could lead to an increase of CJD cases initiated a research program sponsored by the

German Ministry of Health. The epidemiological, diagnostical and neuropathological features of CJD were investigated by the BIOMED I and BIOMED II projects of the European Community. At present, a definite diagnosis can only be ascertained by autopsy. The wide spectrum of non-CJD-disorders shows that the clinical diagnosis of CJD is difficult during the lifetime of a person. Although CJD is still a fatal disease that cannot be treated, the correct diagnosis must be taken as early as possible for two reasons: (1) to ensure that rare but treatable dementias such as Hashimoto encephalitis are not missed, and (2) to support clinicians and relatives in their decisions regarding further therapeutic measures. Up to the present, the electroencephalogram (EEG) has been the only well-established method that allowed the differential diagnosis of CJD. The detection of a cerebrospinal fluid (CSF) marker (p130 and p131) that indicates rapid brain destruction and is useful in the diagnosis of CJD was first described by Harrington et al. [2]. A modification (14-3-3 protein), published by Hsich et al. [3], was introduced into the BIOMED program by our group [10] and accepted as a new diagnostic criterion at the beginning of 1999.

The 14-3-3 proteins are a group of highly conserved proteins involved in the regulation of protein phosphorylation and the mitogen-activated protein kinase pathway. The  $\gamma$ -isoform is thought to be specific for nervous tissue. It cannot be detected in CSF of normal controls. Neuron-specific enolase (NSE) is another biochemical CSF marker that occurs in a high concentration in a number of neurological diseases that are characterized by rapid neuronal loss [11]. NSE is localized in neurons and neuroendocrine cells and is virtually completely synthesized in the central nervous system. In addition to the well-established electroencephalogram (EEG), techniques involving the analysis of CSF and magnetic resonance imaging (MRI) thus turned out to contribute to an improved diagnosis of the disease in living individuals.

#### *Epidemiology of sporadic CJD*

During the last six years, 977 patients with suspected CJD were notified to the German CJD Surveillance Unit, located in Goettingen. They were referred from treating physicians in neurological and psychiatric hospitals throughout Germany. The patients were examined by a physician of the Surveillance Unit in the referring hospital. Clinical findings, data from the patients' case history, EEG and MRI findings were discussed among the group in Goettingen. CSF and blood could be obtained from most patients and used for the determination of neuron-specific enolase (NSE), 14-3-3 protein, S-100 protein and tau protein. All cases were initially grouped into three classes, namely "probable CJD", "possible CJD" and "other disease". A definite CJD diagnosis could indeed only be made if the findings were confirmed by autopsy. The 977 suspected CJD cases, notified between May 1993 and August 1999, were classified into 324 "definite", 246

“probable”, 76 “possible” and 286 “other” cases. Three iatrogenic and 42 hereditary cases were not included in the epidemiologic survey. Criteria published by Masters and colleagues were used for the classification [4]. “Probable CJD” was diagnosed in patients who revealed rapidly progressive dementia, periodic sharp waves in the EEG and at least two of the following four findings: myoclonus, visual and/or cerebellar symptoms, pyramidal and/or extrapyramidal signs, and akinetic mutism. Cases that met the above criteria but did not have a typical EEG were originally classified as “possible” CJD. The recent extension of these criteria, which involves the presence of 14-3-3 proteins in CSF, allowed the reclassification of a number of “possible CJD cases” into the “probable” category. Thus, a patient who presented with a typical clinical picture, but without periodic sharp wave complexes in the EEG, was taken as a “probable case” if 14-3-3 proteins were observed in the CSF. This extended set of criteria was applied to the cases described in this paper. The classification “other disease” was made if (1) either dementia was insufficiently documented or had been present for more than two years; (2) there was a lack of the typical neurological symptoms and signs; (3) there was CSF evidence of an inflammatory process of the disease. The incidence figures of CJD only take the definite and probable categories into account. The observed increase (from 0.9 to 1.5; Table 1) in the number of positive cases detected in Germany during 1994 and 1998 reflects the improved procedure of case identification and ascertainment. The mortality figures for sporadic CJD in Germany are comparable with those in other European countries (BIOMED program) using the same protocol of case finding (Table 2). In Great Britain, the cases of vCJD (56 until April 2000) are not included. vCJD was first described in 1996 [8] and is characterized by a younger age at the time of disease onset, a longer duration of the disease, some atypical clinical features and a normal EEG pattern. The neuropathological hallmark is the observation of so-called florid plaques. In all other European countries involved, no cases of vCJD were noticed except for France (2 cases) and Ireland (1 case). In Germany, a few cases with a young age at onset and longer survival were identified, but no florid plaques were observed at autopsy. These cases turned out to belong to the phenotype that is characterized by valin/valin homocystosity at codon 129 and the PrP<sup>Sc</sup> type 1.

**Table 1.** Incidence of CJD in Germany from 1994–98

Year	Incidence
1994	0.9
1995	1.1
1996	1.1
1997	1.3
1998	1.5

**Table 2.** Mortality rates of sporadic CJD in European countries (BIOMED) in 1998

Country	Mortality rate
Austria	1.03
France	1.12
Germany	1.27
Italy	0.85
Netherlands	1.15
Spain	0.71
Switzerland	1.27
UK	0.87

### *Subtypes of sporadic CJD*

Parchi et al. [5] differentiated six variants of sporadic CJD depending on their genetic background (codon 129 VV, MM, MV) and PrP<sup>Sc</sup> type 1 or 2. These two PrP<sup>Sc</sup> types differ in their size and glycosylation pattern. The most frequent phenotypes are the following: MM and PrP<sup>Sc</sup> type 1 (67%) correspond to the classic pattern of CJD. They present with early cognitive disturbances, ataxia, myoclonus and a typical EEG pattern and can easily be diagnosed. VV and PrP<sup>Sc</sup> type 2 (16%) are characterized by initial ataxia and only occasionally by a typical EEG pattern. MV and PrP<sup>Sc</sup> type 2 (9%) have a longer duration and only occasionally a typical EEG pattern. Inga Zerr analyzed the 14-3-3 and NSE pattern of these subtypes. Both proteins were usually positive in MM1 and VV2 cases, whereas only one-third to one-half of the MV2 cases were positive (see Table 3 and Fig. 1). The reason why these proteins appear with different frequencies in CSF is not well understood. In view of an atypical clinical symptomatology (younger age at the time of onset, longer duration of the disease, late dementia) some of these subtypes can easily be overlooked, especially the VV1 variant mentioned before. Although tested only in a limited number of cases, 14-3-3 was indeed positive in these patients.

**Table 3.** CJD phenotype and 14-3-3 protein in CSF

PrP type	14-3-3 in CSF
MM1	67/70
MM2	3/3
MV1	8/8
MV2	3/10
VV1	1/1
VV2	15/15

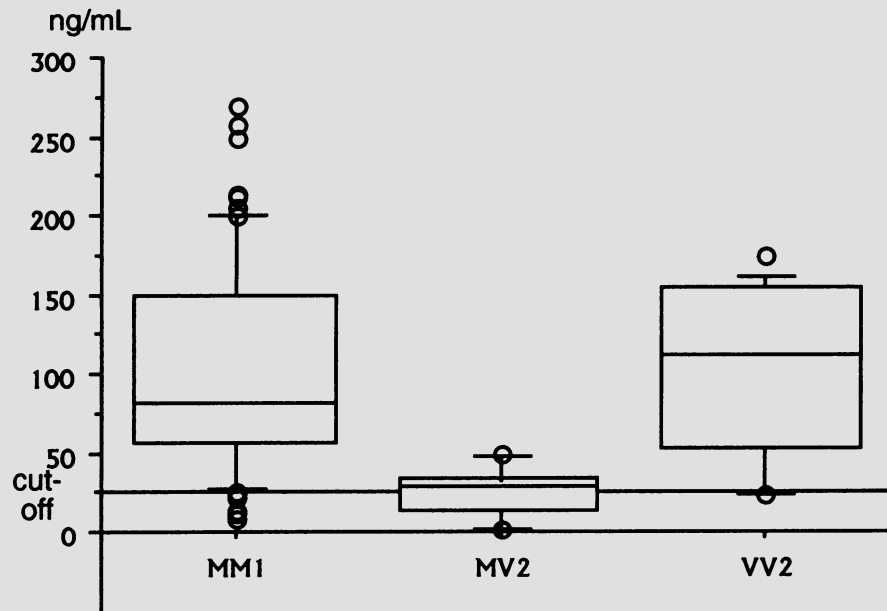


Fig. 1. Box plots for cerebrospinal fluid levels of neuron-specific enolase in CJD

#### *Differential diagnoses*

The pattern of the 14-3-3 proteins and other parameters of cell destruction in CSF cannot only help to differentiate subtypes of sporadic CJD, but also exclude other dementing processes, Alzheimer's disease (AD) in particular. Table 4 shows the comparison of the sensitivity and specificity of the presence of 14-3-3 proteins in CSF, the typical EEG recording and MRI in the patients undergoing these tests. The presence of the 14-3-3 proteins in CSF [3, 10] turned out to be a better marker in the differential diagnosis of CJD than EEG or MRI (Table 4). Although 14-3-3 is found in other neurological diseases with substantial brain damage such as herpes encephalitis, ischemia, shortly after the occurrence of epileptic fits and malignant brain tumors (Table 5), these acute disorders are easily recognized by other diagnostic procedures and 14-3-3 does not persist. In agreement with the literature [1, 9], AD used to be frequently diagnosed in cases that were classified as "other disease" [1, 6, 9], followed by unclassified dementia,

**Table 4.** Frequency of abnormal additional findings in CJD

Findings	Sensitivity	Specificity
14-3-3 in CSF (N = 289)	95%	93%
MRI typical (N = 213)	67%	93%
EEG typical (N = 256)	65%	86%

**Table 5.** 14-3-3 detectable in other neurological diseases (data from the European CJD Surveillance study)

Diseases	Detection of 14-3-3
Inflammatory	21/72
Ischemia	5/27
Grand mal	4/9
Glioblastoma	2/3

**Table 6.** Differential diagnoses of CJD

Disease	Own series N = 124	Series of Brown et al. [1] N = 673
Alzheimer's disease	27%	16%
Unclassified dementia	16%	17%
Vascular dementia	9%	?
Chronic encephalitis of unknown cause	8%	4%

vascular disease and chronic encephalitis (Table 6). Patients with confirmed AD were older compared to the group suffering from chronic inflammatory diseases (61 vs. 46 years). Although the clinical symptomatology overlaps with a number of other diseases, particularly with rapidly progressive AD, some differences could be observed. Visual symptoms discriminated best between CJD and other diseases at the beginning of the illness. In later stages, myoclonus, gait ataxia, visual disturbances and particularly akinetic mutism all occurred more frequently in CJD. Epilepsy, however, occurred more frequently in other diseases. The CSF findings were most helpful in excluding inflammatory processes. Twelve of the 18 patients with inflammatory diseases revealed either pleocytosis and/or an oligoclonal appearance of the CSF  $\gamma$ -globulin region. Herpes encephalitis was the most frequent diagnosis (N = 10), followed by multiple sclerosis (N = 3), paraneoplastic syndromes (N = 2) and Hashimoto encephalitis (N = 2). Among these potentially treatable diseases, Hashimoto encephalitis was not mentioned as differential diagnosis in other series of CJD. We became aware of this treatable dementia through a patient with a known history of Hashimoto thyroiditis. Since then, six further patients without thyroiditis were diagnosed and subsequently treated [7]. Some of these were not included in our study because the notifying hospitals were asked to test the patients on anti-thyroid autoantibodies prior to including them in our survey. In our research program, certain features of CJD could be identified that help to distinguish it from other diseases and, in particular, the value of the 14-3-3 protein as a marker of CJD could be assessed.

### References

1. Brown P, Gibbs CJ Jr, Rodgers-Johnson P, Asher DM, Sulima MP, Bacote A, Goldfarb LG, Gajdusek DC (1994) Human spongiform encephalopathy: the National Institutes of Health series of 300 cases of experimentally transmitted disease. *Ann Neurol* 35: 513–529
2. Harrington MG, Merrill CR, Asher DM, Gajdusek DC (1986) Abnormal proteins in the cerebrospinal fluid of patients with Creutzfeldt-Jakob disease. *N Engl J Med* 315: 279–283
3. Hsich G, Kenney K, Gibbs CJ, Lee KH, Harrington MG (1996) The 14-3-3 brain protein in cerebrospinal fluid as a marker for transmissible spongiform encephalopathies. *N Engl J Med* 335: 924–930
4. Masters CL, Harris JO, Gajdusek DC, Gibbs CJJ, Bernoulli C, Asher DM (1979) Creutzfeldt-Jakob disease: patterns of worldwide occurrence and the significance of familial and sporadic clustering. *Ann Neurol* 5: 177–188
5. Parchi P, Giese A, Capellari S, Brown P, Schulz-Schaeffer W, Windl O, Zerr I, Budka H, Kopp N, Piccardo P, Poser S, Rojiani A, Streichemberger N, Julien J, Vital C, Ghetti B, Gambetti P, Kretzschmar HA (1999) Classification of sporadic Creutzfeldt-Jakob disease based on molecular and phenotypic analysis of 300 subjects. *Ann Neurol* 46: 224–233
6. Poser S, Mollenhauer B, Krauss A, Zerr I, Steinhoff BJ, Schroeter A, Finkenstaedt M, Schulz-Schaeffer W, Kretzschmar HA, Felgenhauer K (1999) How to improve the clinical diagnosis of Creutzfeldt–Jakob disease. *Brain* 122: 2345–2351
7. Seipelt M, Zerr I, Nau R, Mollenhauer B, Kropp S, Steinhoff BJ, Wilhelm-Goessling C, Bamberg C, Janzen RWC, Berlit P, Manz F, Felgenhauer K, Poser S (1999) Hashimoto encephalitis as a differential diagnosis of Creutzfeldt–Jakob disease. *J Neurol Neurosurg Psychiatr* 66: 172–176
8. Will RG, Ironside JW, Zeidler M, Cousens SN, Estibeiro K, Alperovitch A, Poser S, Pocchiari M, Hofman A, Smith PG (1996) A new variant of Creutzfeldt–Jakob disease in the UK. *Lancet* 347: 921–925
9. Will RG, Matthews WB (1984) A retrospective study of Creutzfeldt–Jakob disease in England and Wales 1970–79. I: Clinical features. *J Neurol Neurosurg Psychiatr* 47: 134–140
10. Zerr I, Bodemer M, Gefeller O, Otto M, Poser S, Wiltfang J, Windl O, Kretzschmar HA, Weber T (1998) Detection of 14-3-3 protein in the cerebrospinal fluid supports the diagnosis of Creutzfeldt–Jakob disease. *Ann Neurol* 43: 32–40
11. Zerr I, Bodemer M, Raecker S, Grosche S, Poser S, Kretzschmar HA, Weber T (1995) Cerebrospinal fluid concentration of neuron-specific enolase in diagnosis of Creutzfeldt–Jakob disease. *Lancet* 345: 1609–1610

Authors' address: Dr. S. Poser, Department of Neurology, Georg-August-University, Robert-Koch-Str. 40, D-37075 Goettingen, Germany.

## Putting prions into focus: application of single molecule detection to the diagnosis of prion diseases

A. Giese<sup>1,\*</sup>, J. Bieschke<sup>2,\*</sup>, M. Eigen<sup>2</sup>, and H. A. Kretzschmar<sup>1</sup>

<sup>1</sup>Department of Neuropathology, University of Göttingen, Göttingen, Germany

<sup>2</sup>Max-Planck-Institute for Biophysical Chemistry, Göttingen, Germany

**Summary.** Prion diseases are characterized by the cerebral deposition of an aggregated pathological isoform of the prion protein (PrP<sup>Sc</sup>) which constitutes the principal component of the transmissible agent termed prion. In order to develop a highly sensitive method for the detection of PrP<sup>Sc</sup> aggregates in biological samples such as cerebrospinal fluid (CSF), we used a method based on Fluorescence Correlation Spectroscopy (FCS), a technique which allows detection of single fluorescently labeled molecules in solution. Within the FCS setup, fluorescent photons emitted by molecules passing an open volume element defined by the beam of an excitation laser focussed into a diffraction-limited spot are imaged confocally onto a single photon counting detector. Aggregates of PrP<sup>Sc</sup> could be labeled by co-aggregation of probe molecules such as monomeric recombinant PrP or PrP-specific antibodies tagged with a fluorescent dye. In addition to slow diffusion, labeled aggregates are characterized by high fluorescence intensity, which allows detection and quantification by analysis of fluorescence intensity distribution. To improve detection of rare target particles, the accessible volume element was increased by scanning for intensely fluorescent targets (SIFT). To further improve sensitivity and specificity, two different probes were used simultaneously in a two-color setup. In a diagnostic model system of CSF spiked with purified prion rods, dual-color SIFT was more sensitive than Western blot analysis. In addition, a PrP<sup>Sc</sup>-specific signal was also detected in a number of CSF samples derived from CJD patients but not in controls.

\*Both authors contributed equally to this work.

### Introduction

Prion diseases such as Creutzfeldt–Jakob disease (CJD) in humans and scrapie and bovine spongiform encephalopathy (BSE) in animals are invariably fatal neurodegenerative diseases caused by an unusual transmissible agent termed prion [18]. Prion diseases have caused a major concern in regard to public health due to the emergence of BSE. It appears that the BSE agent can be transmitted to humans causing a new variant of Creutzfeldt–Jakob disease (nvCJD) characterized by distinctive neuropathological and biochemical features [4, 22]. At present, the available epidemiological data on nvCJD does not exclude the possibility of an impending large epidemic, mainly because of the long asymptomatic incubation times that are characteristic of prion diseases [9]. For epidemiological surveillance, for prevention of secondary transmission, and for early diagnosis as a prerequisite for any potential treatment of infected persons, there is a need for a specific and highly sensitive diagnostic test for prion disease that can be used on diagnostic specimens available for routine analysis such as cerebrospinal fluid (CSF).

Prions seem to be devoid of a nucleic acid genome and consist mainly, if not exclusively, of a conformationally altered pathological isoform of the host-encoded prion protein (PrP) that has been termed PrP<sup>Sc</sup> [18]. Therefore, a specific diagnosis of prion diseases relies on the detection of PrP<sup>Sc</sup>. However, the diagnostic methods currently used such as immunohistochemistry, Western blot, and ELISA techniques apparently lack sufficient sensitivity to detect PrP<sup>Sc</sup> in cerebrospinal fluid, although transmission studies indicate the presence of some infectivity [3]. PrP<sup>Sc</sup> can be distinguished from the physiological cellular prion protein (PrP<sup>C</sup>) by its high content in beta-sheet structure [15], its partial resistance to protease digestion [14], and its tendency to form large aggregates both in vivo and in vitro [17]. The formation of multimeric aggregates can be assumed to be closely related to the infectious process [5, 8]. Since the ultimate detection limit for prion particles should be one PrP<sup>Sc</sup> aggregate within a given sample volume, we aimed at establishing a diagnostic test system capable of detecting single aggregates of PrP<sup>Sc</sup>. To achieve this goal, we used a novel approach based on Fluorescence Correlation Spectroscopy, a method that allows single molecule detection.

### Fluorescence correlation spectroscopy (FCS)

FCS in its current confocal form is applied widely as an analytical tool for the study of freely diffusing fluorescent molecules in solution [7, 19, 20]. Molecules are excited by a laser beam focussed into a focal volume of approximately 1 fl, i.e. the size of an *E. coli*, and the trail of emitted fluorescent photons is imaged confocally through a high aperture microscope objective onto a single photon-counting detector. The diffusion of fluorescent molecules through the open volume element defined by this mea-

surement setup causes fluctuations in fluorescence. Mathematical analysis of these fluctuations by auto-correlation analysis can be used to calculate the lateral diffusion coefficient and thus the size of the molecule. This analysis works best when the relative signal fluctuation is unity or greater, i.e. at an average of less than one molecule present in the measurement volume of  $10^{-15}$  l, which is equivalent to nano- to picomolar concentrations.

### **Fluorescent labeling of PrP<sup>Sc</sup> aggregates and detection by analysis of fluorescence intensity distribution**

Detection of single aggregates of PrP<sup>Sc</sup> within an FCS setup requires fluorescent labeling of the target aggregates. This can be achieved by labeling with suitable probe molecules tagged with a fluorescent dye. Fluorescent labeling of pathological aggregates of A $\beta$ -peptide in the CSF of Alzheimer's patients by incorporating fluorescently labeled monomeric A $\beta$ -peptide and subsequent detection by FCS has been reported recently [16]. Therefore, we applied the principle of seeded aggregation to CSF samples derived from CJD patients and to control CSF samples spiked with aggregates of PrP<sup>Sc</sup> purified from scrapie-infected Syrian hamster brain, so-called prion rods. In addition to fluorescently labeled recombinant Syrian hamster prion protein, we tested PrP-specific antibodies for their ability to serve as probe molecules in our assay. Whereas in heterogeneous assays (such as Western blot) detection of labeled target molecules relies on the physical separation of bound and unbound probe molecules, the FCS setup allows the signal derived from bound and unbound probe molecules to be separated in homogeneous assay conditions. Conventionally, this is done by analysis of changes in diffusion time of bound probe molecules, which cause a shift in the auto-correlation curve. However, this approach is limited when measuring very rare targets in the presence of an excess of unbound probe molecules. Therefore, we used cross-correlation analysis in a two-color FCS setup [21] and an approach based on the analysis of fluorescence intensity distribution. The basic principle of target detection by intensity distribution analysis is illustrated in Fig. 1. If the target molecules are large multimeric aggregates, they can become heavily labeled due to the binding of a large number of probe molecules. Thus, when passing the confocal detection volume, the target molecules emit a fluorescent burst up to 50 times stronger than the signal of free fluorescent probe molecules. If the concentration of free probe molecules is kept sufficiently low (i.e. in the nanomolar range, which means that only very few free probe molecules are present within the focal volume at any time), this burst can be easily seen as a peak in the fluorescence recorded from the confocal detection volume. In order to quantify the target-derived peak signal, we used a simple cumulative on-line intensity analysis of the fluorescent signal. Detected photons were summed over time intervals of constant length (bins) and the number of bins in which a specific number of photons was counted

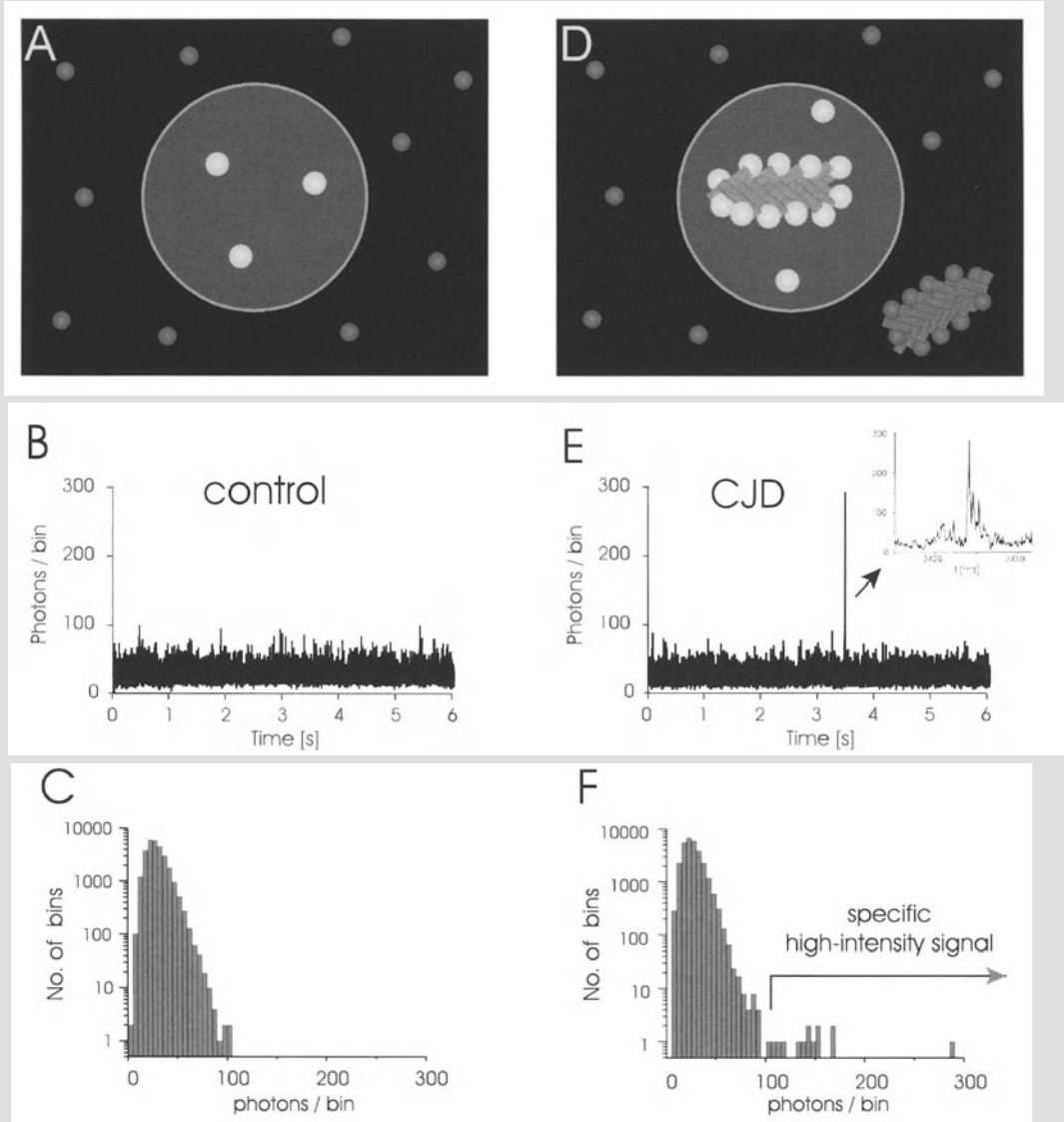


**Fig. 1.** Detection of highly labeled aggregates by analysis of fluorescence intensity distribution. **A, B** Diffusion of probe molecules causes stochastic variations in the number of fluorescent molecules present in the confocal detection volume of the FCS setup, which leads to fluctuations in the recorded fluorescence intensity. **C** The intensity distribution histogram of a sample containing only free probe molecules is well-defined and contains no signal above a certain threshold value. **D, E** Large targets such as aggregates of PrP<sup>Sc</sup> can become heavily labeled by binding a large number of probe molecules. Thus, when passing the focus, the targets emit a fluorescent burst, which can be seen as a peak in the fluorescence trace. **F** Therefore, with intensely fluorescent targets present, a specific high-intensity component can be seen in the intensity distribution histogram. The target-derived signal can be quantified by counting the number of bins above a threshold value. Methods: A fluorescently labeled PrP probe was added to CSF samples obtained from a control patient (**B, C**) and from a CJD patient (**E, F**). Recordings were done using a single-color ConfoCor FCS instrument (C. Zeiss, Jena, Germany) and a multi-channel scaler-timer-card. Shown are representative traces of fluorescence intensity (**B, E**) and the corresponding intensity distribution histograms (**C, F**; bin size = 250  $\mu$ s)

was plotted in an intensity distribution histogram. The intensity distribution histogram of a sample containing only free probe molecules contains no signal above a certain threshold value [6]. In contrast, with intensely fluorescent targets present, a high-intensity component can be seen. The target-derived signal can be quantified by counting the number of bins above a threshold value.

### **Scanning for intensely fluorescent targets (SIFT)**

Intensity distribution analysis allows an easy quantification of the target-derived signal. However, for large molecules at sub-picomolar concentrations, diffusion becomes a limiting factor for detection, as longer and longer measurement times are needed until a slowly diffusing molecule happens to pass the focus. In contrast to conventional FCS, target recognition by intensity analysis does not require analysis of changes in diffusion times. Therefore, detection sensitivity can be increased considerably by scanning the sample. Within our measurement setup, scanning was achieved by moving the sample relative to the focus. Samples were enclosed in a glass capillary, sealed onto a glass support, placed on a positioning table (Märzhäuser, Wetzlar, Germany), and moved in a meander-like fashion at a speed of 1 mm/s. The measurement volume is thus shifted by the length of one focus diameter within 500  $\mu\text{s}$ . In this setup, the time a large, slowly diffusing target aggregate stays in the measurement volume is effectively determined by the displacement time of the focal volume analogous to the situation observed in flow capillaries. For fluorescently labeled prion rods, we found a decrease of the average passage time from 10–100 ms to about 0.5–1 ms. Thus, scanning increased the number of target particles passing the measurement volume within a given time by about 100-fold when compared with static measurements. To quantitatively detect target-derived fluorescent peaks, the temporal resolution of detection should be at least equal to the average passage time of the target aggregates through the focal volume. For practical purposes a bin size of 500  $\mu\text{s}$  was found to be sufficient. Since the passage time is now determined only by the scanning speed and the excitation profile of the laser beam, the number of high-intensity bins can be assumed to be proportional to the number of target aggregates, even if only a small number of events is detected.

### **Dual-color SIFT analysis**

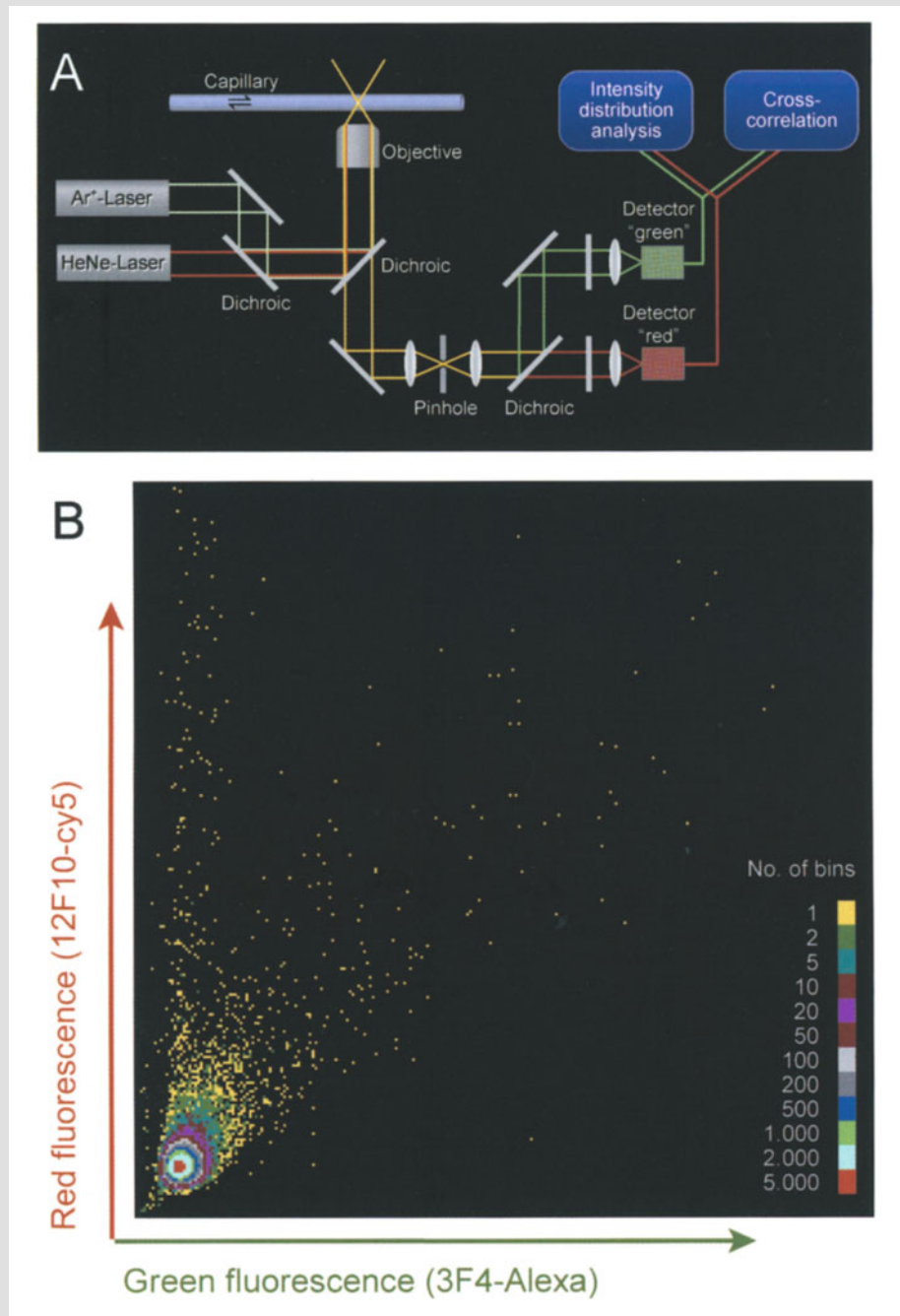
With increased sensitivity, it became apparent that our recombinant PrP probes already contained a significant intrinsic amount of intensely fluorescent particles, most likely due to self-aggregation of rPrP molecules during purification and labeling procedures. In contrast, use of PrP-specific antibody probes resulted in a specific labeling of prion rods with virtually no endogenous background, which significantly improved the detection limit by almost two orders of magnitude [2].

To further improve specificity, we simultaneously used two independent antibody probes tagged with different fluorescent dyes (Alexa488 (Molecular Probes, “green”) and Cy5 (Amersham, “red”). Measurements were performed in a dual-color FCS setup as shown in Fig. 2A originally developed by Schwille [21], now built into a commercial prototype by C. Zeiss (Dual Color ConfoCor, Carl Zeiss, Jena, Germany). Within this setup, the target-derived signal can be identified as peaks of high fluorescence intensity occurring simultaneously in both detection channels. For dual-color intensity distribution analysis, the red and green photocounts were recorded onto a multi-channel-scaler card for consecutive bins of 500  $\mu\text{s}$ . The pairs of red and green photocounts could then be analyzed in a two-dimensional histogram (Fig. 2B). Target molecules which simultaneously yield a high-intensity signal in both detection channels can thus be separated from the low-intensity fluorescent signal of the free probe molecules and from the single-color high-intensity signal derived from aggregates of the probe molecules themselves or from particles which unspecifically bind only one of the two probes.

Sensitivity and specificity of dual-color SIFT analysis were evaluated by using pooled cerebrospinal fluid spiked with purified prion rods as a diagnostic model system. The theoretical detection limit of this method is proportional to the measurement time. For 10-minute measurements with a bin size of 500  $\mu\text{s}$  and a scanning speed of 1 mm/s, recording of one high-intensity bin corresponds to one particle in a volume of about  $1.2 \times 10^6$  times the focal volume of the FCS setup, i.e. to a particle concentration of approximately 2 fM. In a series of control CSF samples the maximum number of bins containing a two-color high-intensity signal was one (mean =  $0.2 \pm 0.4$  SD). The low background signal allowed the concentration of added prion rods to be measured over more than four orders of magnitude with a detection limit of 2 pM PrP<sup>Sc</sup>, which was more than one order of magnitude more sensitive than Western blot analysis of the same samples (Fig. 3A and [2]). Comparison of this value with the aggregate concentration calculated from the SIFT measurements yielded an average of approximately 1000 PrP molecules/aggregate, which is in line with theoretical considerations [13].

---

**Fig. 2. A** Schematic representation of the dual-color measurement setup. The confocal detection volume is formed by the superimposed focal spots of a He-Ne-laser (633 nm) and an Ar<sup>+</sup>-laser (488 nm). The sample is enclosed in a glass capillary placed on a positioning table, thus permitting scanning of the sample. The fluorescent signal of the “red” and “green” detection channel is split for simultaneous cross-correlation analysis and dual-color intensity distribution analysis. **B** Typical intensity distribution histogram obtained from a 10-minute dual-color SIFT measurement with a bin size of 500  $\mu\text{s}$  and a scanning speed of 1mm/s. Monoclonal antibodies 3F4 [10] labeled with



Alexa488 (Molecular Probes) and 12F10 [11] (IBA, Heiligenstadt) labeled with Cy5 (Amersham) were added to pooled control CSF spiked with prion rods. The pairs of "red" and "green" photocounts are displayed as a two-dimensional intensity distribution histogram. The target-specific dual-color high-intensity signal can be seen in the upper right quadrant. Most of the bins contain only a low-intensity signal derived from free probe molecules (lower left). In addition, some unspecific single-color high-intensity background signal can be seen (upper left and lower right), which is clearly separated from the specific signal

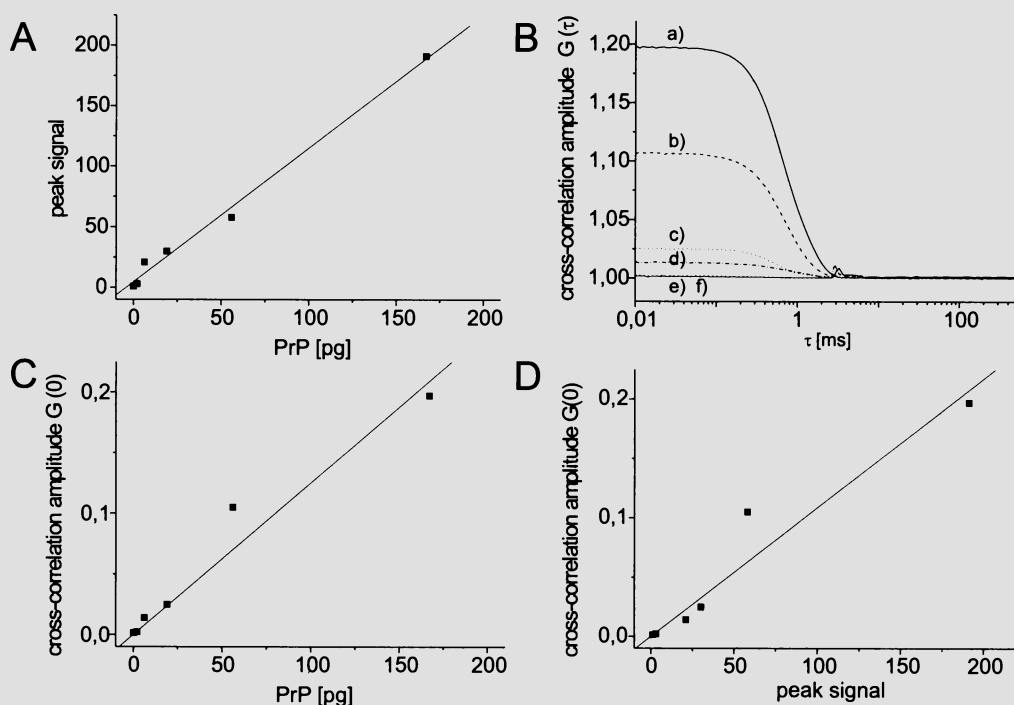


**Fig. 3.** PrP-specific antibodies 3F4-Alexa488 and 12F10-Cy5 were added to pooled CSF of control patients spiked with prion rods (2 – 167 pg in 20  $\mu$ l CSF) derived from scrapie-infected hamster brain. Measurements were performed for a measurement time of 600 s with a scanning speed of 1 mm/s and a bin size of 500  $\mu$ s. SIFT analysis was performed as described in Fig. 2 and the number of bins containing a dual-color high-intensity signal (“peak signal”) was plotted against PrP<sup>Sc</sup> concentration (A). In parallel, the fluorescence signal was evaluated by cross-correlation analysis (B: a = 167 pg PrP<sup>Sc</sup>, b = 56 pg, c = 19 pg, d = 6 pg, e = 2 pg, f = control). The cross-correlation amplitude at  $\tau = 0$  was plotted against PrP<sup>Sc</sup> concentration (C) and SIFT peak signal (D)

### Cross-correlation analysis

In parallel to dual-color SIFT, the fluorescent signal was also evaluated by cross-correlation analysis. The theoretical background of cross-correlation analysis has been described thoroughly by Schwille et al. [21]. In contrast to conventional FCS auto-correlation analysis, where the fluorescent signal is compared with itself at different lag times  $\tau$ , dual-color cross-correlation analysis is performed by comparing two different emission signals observed from the same volume. Under the assumption of uniformly labeled particles, the amplitude of the cross-correlation curve at  $\tau = 0$  is proportional to the concentration of doubly labeled particles. As shown in Fig. 3, the cross-correlation amplitude is in fact proportional to the target concentration and to the number of bins containing peak signal found by simultaneous SIFT analysis. However, the small number of events recorded at low target

concentrations introduces a significant statistical error into the cross-correlation signal, as it does not evaluate the number of coincidence events but the number of photons emitted in these events, which also depends on the size of the target molecules and their path through the detection volume. Furthermore, the signal-to-noise ratio of the cross-correlation signal, and thus sensitivity, increases only by the square root of measurement time, whereas the number of high-intensity bins detected by SIFT analysis increases linearly with time. At low target concentrations, dual-color SIFT thus proved to be more reliable than cross-correlation analysis for the detection of large aggregates.

### Diagnostic application

To evaluate the diagnostic potential of dual-color SIFT, we applied this technique to CSF samples collected within the framework of the German National CJD Surveillance Study. CSF samples were obtained from probable or definite CJD patients and from non-CJD cases reported to the Surveillance Unit because of suspected CJD. In a series of 24 CJD samples and 13 non-CJD control samples, a CJD-specific high-intensity signal could be detected after addition of antibody probes to otherwise untreated CSF with a sensitivity of 21% and a specificity of 100% [2]. To our knowledge, this represents the first direct detection of PrP<sup>Sc</sup> in CSF samples. It may be that pathological aggregates of PrP<sup>Sc</sup> can only be found in a subset of CJD patients, since transmission studies using primates only had a sensitivity of approximately 15% [3]. However, we have no indication so far that the subset of SIFT-positive patients represents a specific molecular subtype of CJD. Therefore, we believe that further improvement of our assay such as faster scanning speed will also improve diagnostic sensitivity. In addition, improved sample preparation should increase the sensitivity of target detection.

Most established methods for the detection of PrP<sup>Sc</sup> are based on its partial protease K resistance. However, different pathological isoforms of PrP<sup>Sc</sup> exist which exhibit considerable differences in susceptibility to protease digestion [1, 12]. In contrast, detection of PrP<sup>Sc</sup> by the SIFT technique is based on its aggregated state which is closely related to the infectious mechanism [5, 8]. Therefore, SIFT analysis does not require any protease treatment and can be performed under near-native conditions. In addition, direct detection of PrP<sup>Sc</sup> in a homogeneous assay allows fast measurement of a large number of samples, providing the basis for a rapid and highly sensitive diagnostic test. Furthermore, this method could be adapted to the sensitive detection of other disease-associated pathological aggregates such as in Alzheimer's disease. Within a two-color setup, the analysis of differences in the labeling ratio obtained with different pairs of probes may also provide a parameter for further characterization of target aggregates, which may permit direct prion strain typing.

### Acknowledgements

We thank M. Pitschke, O. Schäfer, D. Riesner (Institut für Physikalische Biologie, Düsseldorf), I. Zerr, S. Poser (Neurologische Universitätsklinik, Göttingen), T. Winkler, U. Kettling, A. Koltermann and P. Schwille (Max-Planck-Institut für Biophysikalische Chemie, Göttingen) for helpful discussions and cooperation. Prion rods were a gift from the groups of D. Riesner (Düsseldorf) and S.B. Prusiner (San Francisco), 3F4 antibody was provided by H. Diringer/M. Beekes (RKI, Berlin). We thank Carl Zeiss Jena for technical cooperation. This work was supported by the German Ministry for Education, Science, Research and Technology (Grant No. 01 KI 9454/0), by the German Ministry of Health (Grant No. 325-4471-02/15), and by the European Union (BMH4-CT98-7024, FAIR5-CT97-3314).

### References

1. Bessen RA, Marsh RF (1994) Distinct PrP properties suggest the molecular basis of strain variation in transmissible mink encephalopathy. *J Virol* 68: 7859–7868
2. Bieschke J, Giese A, Schulz-Schaeffer W, Zerr I, Poser S, Eigen M, Kretzschmar HA (2000) Ultra-sensitive detection of pathological prion protein aggregates by dual-color scanning for intensely fluorescent targets. *Proc Natl Acad Sci USA* 97: 5468–5473
3. Brown P, Gibbs CJ Jr, Rodgers-Johnson P, Asher DM, Sulima MP, Bacote A, Goldfarb LG, Gajdusek DC (1994) Human spongiform encephalopathy: the National Institutes of Health series of 300 cases of experimentally transmitted disease. *Ann Neurol* 35: 513–529
4. Bruce ME, Will RG, Ironside JW, McConnell I, Drummond D, Suttie A, McCardle L, Chree A, Hope J, Birkett C, Cousens S, Fraser H, Bostock CJ (1997) Transmissions to mice indicate that new variant CJD is caused by the BSE agent. *Nature* 389: 498–501
5. Caughey B, Kocisko DA, Raymond GJ, Lansbury PT Jr (1995) Aggregates of scrapie-associated prion protein induce the cell-free conversion of protease-sensitive prion protein to the protease-resistant state. *Chem Biol* 2: 807–817
6. Chen Y, Muller JD, So PT, Gratton E (1999) The photon counting histogram in fluorescence fluctuation spectroscopy. *Biophys J* 77: 553–567
7. Eigen M, Rigler R (1994) Sorting single molecules: application to diagnostics and evolutionary biotechnology. *Proc Natl Acad Sci USA* 91: 5740–5747
8. Eigen M (1996) Prionics or the kinetic basis of prion diseases. *Biophys Chem* 63: A1–18
9. Ghani AC, Ferguson NM, Donnelly CA, Hagenaars TJ, Anderson RM (1998) Estimation of the number of people incubating variant CJD. *Lancet* 352: 1353–1354
10. Kascsak RJ, Rubenstein R, Merz PA, Tonna-DeMasi M, Fersko R, Carp RI, Wisniewski HM, Diringer H (1987) Mouse polyclonal and monoclonal antibody to scrapie-associated fibril proteins. *J Virol* 61: 3688–3693
11. Krasemann S, Groschup MH, Harmeyer S, Hunsmann G, Bodemer W (1996) Generation of monoclonal antibodies against human prion proteins in PrP<sup>0/0</sup> mice. *Mol Med* 2: 725–734
12. Kuczius T, Groschup MH (1999) Differences in proteinase K resistance and neuronal deposition of abnormal prion proteins characterize bovine spongiform encephalopathy (BSE) and scrapie strains. *Mol Med* 5: 406–418

13. Masel J, Jansen VA, Nowak MA (1999) Quantifying the kinetic parameters of prion replication. *Biophys Chem* 77: 139–152
14. Meyer RK, McKinley MP, Bowman KA, Braunfeld MB, Barry RA, Prusiner SB (1986) Separation and properties of cellular and scrapie prion proteins. *Proc Natl Acad Sci USA* 83: 2310–2314
15. Pan K-M, Baldwin M, Nguyen J, Gasset M, Serban A, Groth D, Mehlhorn I, Huang Z, Fletterick RJ, Cohen FE, Prusiner SB (1993) Conversion of  $\alpha$ -helices into  $\beta$ -sheets features in the formation of the scrapie prion proteins. *Proc Natl Acad Sci USA* 90: 10962–10966
16. Pitschke M, Prior R, Haupt M, Riesner D (1998) Detection of single amyloid beta-protein aggregates in the cerebrospinal fluid of Alzheimer's patients by fluorescence correlation spectroscopy. *Nature Med* 4: 832–834
17. Prusiner SB, McKinley MP, Bowman KA, Bolton DC, Bendheim PE, Groth DF, Glenner GG (1983) Scrapie prions aggregate to form amyloid-like birefringent rods. *Cell* 35: 349–358
18. Prusiner SB (1998) Prions. *Proc Natl Acad Sci USA* 95: 13363–13383
19. Rigler R, Mets Ü, Widengren J, Kask P (1993) Fluorescence correlation spectroscopy with high count rate and low background: analysis of translational diffusion. *Eur Biophys J* 22: 169–173
20. Schwille P, Bieschke J, Oehlenschläger F (1997) Kinetic investigations by fluorescence correlation spectroscopy: the analytical and diagnostic potential of diffusion studies. *Biophys Chem* 66: 211–228
21. Schwille P, Meyer-Almes FJ, Rigler R (1997) Dual-color fluorescence cross-correlation spectroscopy for multicomponent diffusional analysis in solution. *Biophys J* 72: 1878–1886
22. Will RG, Ironside JW, Zeidler M, Cousens SN, Estibeiro K, Alperovitch A, Poser S, Pocchiari M, Hofman A, Smith PG (1996) A new variant of Creutzfeldt–Jakob disease in the UK. *Lancet* 347: 921–925

Authors' address: Prof. Dr. H.-A. Kretzschmar, Department of Neuropathology, University of Munich, Marchioninstr. 17, D-81377 München, Germany.

## **Detection of PrP<sup>Sc</sup> in subclinical BSE with the paraffin-embedded tissue (PET) blot**

**W. J. Schulz-Schaeffer<sup>1</sup>, R. Fatzer<sup>2</sup>, M. Vandeveld<sup>2</sup>, and H. A. Kretzschmar<sup>1</sup>**

<sup>1</sup>Institute of Neuropathology, Georg-August University, Göttingen, Germany

<sup>2</sup>Institute of Animal Neurology, Bern, Switzerland

**Summary.** The appearance of a new variant of CJD (vCJD) in young patients has caused considerable public concern and there is evidence that this novel disease is caused by the same agent as BSE. BSE is a prion disease that became epidemic in the UK, with a peak incidence in January 1993. New test systems should aim to identify BSE-infected cattle early in the incubation period. We compared the established histological and immunohistochemical methods and the Western blot method used by Prionics with the PET blot method that detects prion PrP<sup>Sc</sup> deposits in formalin-fixed and paraffin-embedded tissue. Investigating the obex region with the PET blot, all BSE cases were detectable and no false positive cases occurred. From the Swiss culling program, five clinically healthy cattle out of 1761 were identified as incubating BSE. With the PET blot method four of them showed the same PrP<sup>Sc</sup> deposition pattern that was seen in clinical BSE, though less conspicuous. In one of the five cases, PrP<sup>Sc</sup> was restricted to two brain stem nuclei, a pattern that was reported to be the first manifestation of PrP<sup>Sc</sup> deposits in the brain after peripheral infection and one that occurs after half of the incubation time. In this case, histology and Western blot were negative.

### **Introduction**

Bovine spongiform encephalopathy (BSE) is a prion disease like scrapie in sheep and Creutzfeldt–Jakob disease (CJD) in humans. It was first reported in the UK in November 1986. Ten cases were seen from four herds in southern England [18], and the histopathological findings in these cattle were similar to scrapie and CJD. In the following years, BSE developed into an epidemic in the UK, reaching its highest level in 1992, with more than 37,000 cases [2]. Until 1992, four-to six-year-old cattle had the highest incidence, with up to nearly seven percent in 1992. During the following years, the incidence decreased markedly and the highest incidence was seen

in older animals [20]. Epidemiological studies revealed that the source of exposure to the BSE agent in feeding ruminants was ruminant-derived contaminated meat and bone meal [22].

A relatively small number of BSE cases was identified in other countries in Europe. Cases were registered in Switzerland, Ireland, Portugal and France [6]. In some other countries, BSE was found in animals imported from the UK.

The recent appearance of a new variant of CJD in young patients [23] has caused considerable public concern since it has been suspected to be caused by consumption of food derived from BSE-infected cattle. There is evidence that the BSE agent causes vCJD in humans: (1) the cases of vCJD occur in the geographical region in which BSE was epidemic; (2) after experimental BSE-infection, macaques developed the same typical neuropathological lesion pattern as was seen in vCJD [13]; (3) BSE, vCJD as well as the BSE agent after transmission to other animals revealed the same strain pattern. This was different from sporadic CJD and scrapie [5]. (4) Mice transgenic for the bovine prion protein gene show identical infection kinetics and lesion patterns after inoculation with brain tissue from BSE cases or vCJD patients [17].

It was estimated that in the years from 1985 to 1995, tissue from more than 700,000 animals incubating BSE entered the human food chain, while at the same time, BSE was identified in 150,000 carcasses which were destroyed [1]. This shows the necessity of sensitive test methods that are able to identify BSE early in the incubation time. Here we compare the established histological and immunohistochemical methods and the Western blot method used by Prionics with the new, sensitive PET blot method that detects prion PrP<sup>Sc</sup> deposits in formalin-fixed and paraffin-embedded tissue after blotting on a nitrocellulose membrane.

### Materials and methods

We investigated formalin-fixed and paraffin-embedded tissue from 40 cattle compiled from two series of samples that were collected in the BSE reference center in Bern, Switzerland. Samples were taken from the medulla oblongata caudal to the caudal tip of the IV ventricle (obex region). All samples were coded and investigated blindly. The first series contained 10 histologically and immunohistochemically confirmed BSE cases and 10 cases in which BSE was histologically and immunohistochemically excluded. Of these cases, one suffered from Listeriosis and three were diagnosed as encephalitis. Five animals without BSE were from the culling program in which all animals born before 1 December, 1990, were killed in herds with one or more BSE cases. In the second series, all 20 animals were from the Swiss culling program. In the program, a total of 1761 cases were investigated histologically, by immunohistochemistry or Western blot with the Prionics test. Our series contained all cases in which one of the diagnostic procedures showed a positive result and all suspect cases from this culling program.

### *Histology*

Brains were fixed in 4% buffered formalin and processed for paraffin embedding. Four micrometer sections were made at the caudal level of the fourth ventricle (obex) for microscopic examinations and placed onto glass slides which were coated with araldite. The histological examinations were made on hematoxylin- and eosin-stained sections.

### *Immunohistochemistry*

Immunohistochemical staining for PrP deposits was performed after deparaffinization and pretreatment of the mounted slides with proteinase K followed by hydrated autoclaving for 20 min to enhance immunoreactivity [10]. The slides were washed with TBS and immersed in 5% normal bovine serum in TBS for 30 min. Rabbit antisera against bovine PrP was used as primary antibody at a dilution of 1:500 and incubated for 48 h at 4 °C. Bovine anti-rabbit immunoglobulin (1:20) was added for 30 min followed by repeated washing with TBS and incubation with rabbit peroxidase antiperoxidase (PAP) complex (1:100) for 30 min at room temperature. After washing with TBS, diaminobenzidine tetrahydrochloride (DAB) and hydrogen peroxidase were used to visualize immunoreactivity.

### *Western blot*

Western blots were performed with the Prionics test system as described elsewhere [14]. In brief, a 10% brain tissue homogenate was used in a SDS-PAGE system after proteinase K treatment. Proteins were transferred to a polyvinylidene difluoride (PVDF) membrane and proteinase-resistant PrP was detected using the monoclonal antibody 6H4 [11].

### *PET blot*

The PET blot was carried out as described elsewhere [15]. Five µm sections were cut on a microtome, placed on prewetted 0.45 µm pore size nitrocellulose membranes (Bio-Rad, Richmond, CA) and dried for at least 30 min at 55 °C. The nitrocellulose membranes were deparaffinized, rehydrated and dried. After this step they were stored at room temperature for months without loss of quality of subsequent PrP<sup>Sc</sup> staining. After prewetting, digestion was performed using 250 µg/ml proteinase K (Boehringer) in PK-buffer (10 mM TrisHCl pH 7.8; 100 mM NaCl; 0.1% Brij 35) for 8 h at 55 °C. With this step the membrane-attached proteins were fixed to the membrane. After washing in TBST, the proteins on the membranes were denatured with 4 M guanidine isothiocyanate in 10 mM TrisHCl pH 7.8 for 10 min. Guanidine was washed out with TBST. Immunodetection was performed after preincubation in blocking solution (0.2% casein in TBST) for 30 min. The monoclonal antibody 12F10 (1:50) [12] was used as primary antibody in the blocking solution and incubated at least 1 h. After washing in TBST, incubation for at least 1 h was performed with an alkaline phosphatase-coupled rabbit anti-mouse antibody (Dako, Hamburg) at a dilution of 1:500. After intensive washing in TBST, the membranes were adjusted to alkaline pH by incubating two times for 5 min in NTM (100 mM TrisHCl pH 9.5; 100 mM NaCl; 50 mM MgCl<sub>2</sub>). The visualization of the antibody reaction was provided by formazan reaction using NBT/BCIP. Blots were evaluated using a dissecting microscope.

### Results

In the first blinded series, the ten BSE cases that were diagnosed histologically and immunohistochemically could easily be identified using the PET blot method. In contrast, none of the other ten cases showed any PrP<sup>Sc</sup> deposition in the PET blot. In positive cases, reticular and sometimes granular deposits were found predominantly in the solitary tract nucleus, the dorsal motor nucleus of vagus, the spinal tract nucleus of the trigeminal nerve and the inferior olivary nucleus. Marked reticular deposits were found in the reticular formation of the medulla oblongata (Fig. 1A).

Twenty-five of the 1761 cases from the Swiss culling program were investigated with the PET blot. Five were found positive, including one 4-year-old animal, in which sparse PrP<sup>Sc</sup> deposits were found limited to two brain stem nuclei (Fig. 1C). In this case, neither the histological hallmarks were found nor was PrP<sup>Sc</sup> detection with the Western blot possible, but PrP<sup>Sc</sup> deposits were seen immunohistochemically.

Three out of five PET blot-positive cases showed histopathological hallmarks of BSE. In all five cases, pathological PrP deposits were identifiable immunohistochemically. The Western blot was positive in four cases. A sixth case was positive immunohistochemically, but that could not be

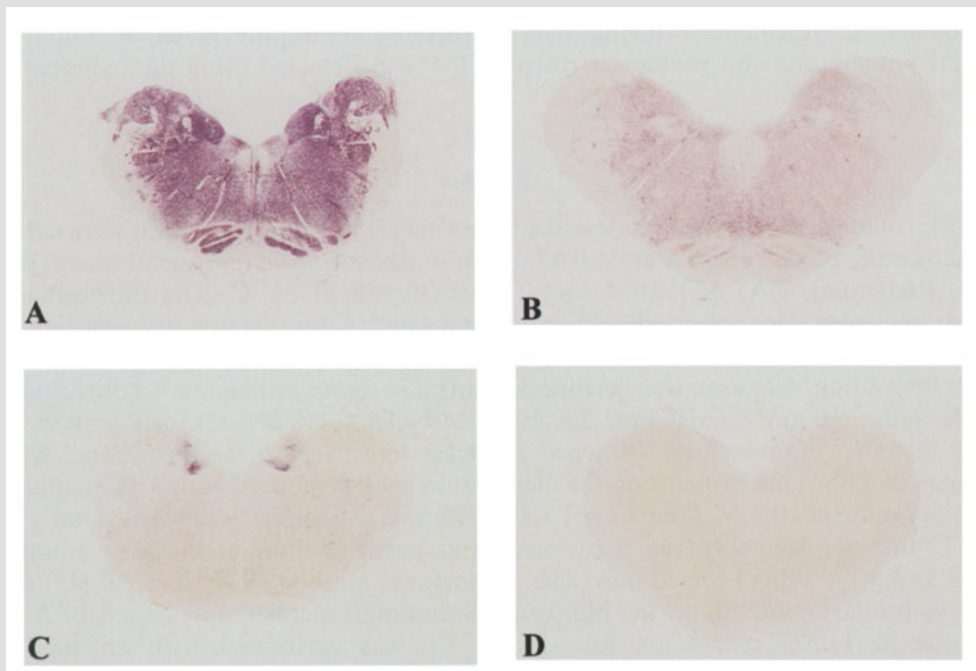


**Fig. 1.** PET blot from the medulla oblongata caudal to the posterior tip of the IV ventricle (obex region); **A** BSE case discovered clinically; **B** subclinical BSE case from the Swiss culling program; picture as was seen in four out of the five cases identified incubating BSE; **C** early pathological onset of BSE showing only PrP<sup>Sc</sup> deposits in the dorsal motor nucleus of vagus and the solitary tract nucleus; **D** negative control case

**Table 1.** Comparison of different methods in detection of subclinical BSE

No.	Histology	IHC	Western blot	PET blot
1	vacuolar changes	positive	positive	whole medulla positive
2	vacuolar changes	positive	positive	whole medulla positive
3	vacuolar changes	positive	positive	whole medulla positive
4	inconspicuous	positive	positive	whole medulla positive
5	inconspicuous	n. vagus only	negative	n. tr. solitarii/vagus pos.
6	inconspicuous	for. retic. pos	negative	negative
7	inconspicuous	negative	positive	negative
8	inconspicuous	negative	positive	negative

confirmed with any of the other techniques. Using Western blot, a seventh and an eighth case were positive which could not be confirmed with other techniques (Table 1).

In principle, with the PET blot method the same PrP<sup>Sc</sup> deposition pattern was detectable in subclinical BSE cases seen in the Swiss culling program as in clinical BSE. In all five cases, the intensity of deposits was less as compared to clinical BSE cases (Fig. 1B). One case showed PrP<sup>Sc</sup> deposits only in the solitary tract nucleus and the dorsal motor nucleus of vagus (Fig. 1C).

### Discussion

It cannot be predicted at present how widespread vCJD may become, but public awareness is high and further entry of BSE-contaminated food into the human food-chain must be prevented. For this reason, discussion concentrates on diagnostic tests for identifying BSE cases early in the incubation, which averages from 4 to 6 years. Routinely, BSE is identified by its characteristic neuropathological lesions. There are no gross pathological changes, but in the central nervous system spongiform changes in the neuropil of the gray matter and single or multiple vacuoles in the cytoplasm of neurons are characteristic. Astrocytic gliosis is common [20, 21]. Neuronal degeneration may be evident. The main localisations for vacuolar changes are the dorsal vagal nucleus, the solitary tract nucleus, the spinal tract nucleus of the trigeminal nerve, the vestibular nuclei, the reticular formation in the medulla oblongata and the central gray matter in the midbrain [21].

Immunohistological methods for detection of pathognomonic PrP<sup>Sc</sup> deposits are well established [19] and part of the routine diagnostic process. Preparation and electron microscopic detection of scrapie-associated fibrils (SAF) provide proof of the diagnosis, but this diagnostic process is labor-intensive and its sensitivity depends on the region investigated [16]. Western blot for PrP<sup>Sc</sup> is a sensitive technique and new applications such as the Prionics test offer a rapid method of testing even large numbers [14].

It has been shown that the PET blot method is a most sensitive and specific technique for PrP<sup>Sc</sup> detection even early in the incubation time.

Investigation of sequentially intracerebrally infected mice demonstrated that PrP<sup>Sc</sup> deposits were detectable 30 days after infection, identifying the first replication sites more than 140 days before the clinical terminal stage [15].

Identifying BSE-infected cattle early in the incubation time is the main aim of new test systems. In the experimental scrapie model, infectivity in the brain after intraperitoneal or intragastric infection was detectable after 37–55% of the incubation time [7–9]. With the Western blot, PrP<sup>Sc</sup> was detectable in the brain of hamsters after intraperitoneal or oral infection after 48–58% of the incubation time [3, 4]. Topographically, infectivity in the brain was found in the medulla oblongata first [7, 9] and PrP<sup>Sc</sup> was first detectable in the dorsal motor nucleus of the vagus [4]. In the Swiss culling program, five animals were found incubating BSE with the PET blot method. In one animal, only the dorsal motor nucleus of the vagus and the solitary tract nucleus showed PrP<sup>Sc</sup> deposits indicating that this case may still be at half of the incubation time. That the Western blot failed to detect this case may be due to a dilution effect of adjacent, non-PrP<sup>Sc</sup>-accumulating tissue.

The PET blot method is not a rapid test tool for screening large numbers of animals, for example in the slaughterhouse. This is the domain of Western blot or Elisa-based test systems. The PET blot, with superior sensitivity and excellent specificity, provides verification of the test results of other methods and gives good results for experimental procedures and pathological investigations.

### Acknowledgements

The authors thank Wolfgang Dröse for excellent technical assistance and Dr. Bruno Oesch (Prionics) for the gift of data. This work was supported by a grant from the European Community (BMH4-CT-98 7024 (DG 12 SSMI)).

### References

1. Anderson RM, Donnelly CA, Ferguson NM, Woolhouse MEJ, Watt CJ, Udy HJ, MaWhinney S, Dunstan SP, Southwood TRE, Wilesmith JW, Ryan JBM, Hoinville LJ, Hillerton JE, Austin AR, Wells GAH (1996) Transmission dynamics and epidemiology of BSE in British cattle. *Nature* 382: 779–788
2. Anonymous (1999) BSE Enforcement Bulletin. See website: <http://www.maff.gov.uk/maffhome.htm>, 33: 1–22
3. Baldauf E, Beekes M, Diring H (1997) Evidence for an alternative direct route of access for the scrapie agent to the brain bypassing the spinal cord. *J Gen Virol* 78: 1187–1197
4. Beekes M, McBride PA, Baldauf E (1998) Cerebral targeting indicates vagal spread of infection in hamsters fed with scrapie. *J Gen Virol* 79: 601–607
5. Bruce ME, Will RG, Ironside JW, McConnell I, Drummond D, Suttie A, McCardie L, Chree A, Hope J, Birkett C, Cousens S, Fraser H, Bostock CJ (1997) Transmissions to mice indicate that ‘new variant’ CJD is caused by the BSE agent. *Nature* 398: 489–501

6. Butler D (1996) Statistics suggest BSE now 'Europa-wide'. *Nature* 382: 4
7. Kimberlin RH, Walker CA (1982) Pathogenesis of mouse scrapie: patterns of agent replication in different parts of the CNS following intraperitoneal infection. *J R Soc Med* 75: 618–624
8. Kimberlin RH, Walker CA (1988) Incubation periods in six models of intraperitoneally injected scrapie depend mainly on the dynamics of agent replication within the nervous system and not the lymphoreticular system. *J Gen Virol* 69: 2953–2960
9. Kimberlin RH, Walker CA (1989) Pathogenesis of scrapie in mice after intragastric infection. *Virus Res* 12: 213–220
10. Kitamoto T, Shin R-W, Doh-ura K, Tomokane N, Miyazono M, Muramoto T, Tateishi J (1992) Abnormal isoform of prion proteins accumulates in the synaptic structures of the central nervous system in patients with Creutzfeldt–Jakob disease. *Am J Pathol* 140: 1285–1294
11. Korth C, Stierli B, Streit P, Moser M, Schaller O, Fischer R, Schulz-Schaeffer W, Kretzschmar H, Raeber A, Braun U, Ehrensperger F, Hornemann S, Glockshuber R, Riek R, Billeter M, Wüthrich K, Oesch B (1997) Prion (PrP<sup>Sc</sup>)-specific epitope defined by a monoclonal antibody. *Nature* 390: 74–77
12. Krasemann S, Groschup MH, Harmeyer S, Hunsmann G, Bodemer W (1996) Generation of monoclonal antibodies against human prion proteins in PrP<sup>0/0</sup> mice. *Mol Med* 2: 725–734
13. Lasmézas CI, Deslys J-P, Demalmay R, Adjou KT, Lamoury F, Dormont D, Robain O, Ironside J, Hauw J-J (1996) BSE transmission to macaques. *Nature* 381: 743–744
14. Schaller O, Fatzer R, Stack M, Clark J, Cooley W, Biffiger K, Egli S, Doherr M, Vandevelde M, Heim D, Oesch B, Moser M (1999) Validation of a Western immunoblotting procedure for bovine PrP<sup>Sc</sup> detection and its use as a rapid surveillance method for the diagnosis of bovine spongiform encephalopathy (BSE). *Acta Neuropathol* 98: 437–443
15. Schulz-Schaeffer WJ, Tschöke S, Kranefuss N, Dröse W, Hause-Reitner D, Giese A, Groschup MH, Kretzschmar HA (2000) The paraffin-embedded tissue blot detects PrP(Sc) early in the incubation time in prion diseases. *Am J Pathol* 156: 51–56
16. Scott AC, Wells GAH, Stack MJ, White H, Dawson M (1990) Bovine spongiform encephalopathy: detection and quantitation of fibrils, fibril protein (PrP) and vacuolation in brain. *Vet Microbiol* 23: 295–304
17. Scott MR, Will R, Ironside J, Nguyen HO, Tremblay P, DeArmond SJ, Prusiner SB (1999) Compelling transgenetic evidence for transmission of bovine spongiform encephalopathy prions to humans. *Proc Natl Acad Sci USA* 96: 15137–15142
18. Wells GAH, Scott AC, Johnson CT, Gunning RF, Hancock RD, Jeffrey M, Dawson M, Bradley R (1987) A novel progressive spongiform encephalopathy. *Vet Rec* 121: 419–420
19. Wells GAH, Spencer YI, Haritani M (1994) Configurations and topographic distribution of PrP in the central nervous system in bovine spongiform encephalopathy: an immunohistochemical study. *Ann NY Acad Sci* 724: 350–352
20. Wells GAH, Wilesmith JW (1995) The neuropathology and epidemiology of bovine spongiform encephalopathy. *Brain Pathol* 5: 91–103
21. Wells GAH, Wilesmith JW, McGill IS (1991) Bovine spongiform encephalopathy: a neuropathological perspective. *Brain Pathol* 1: 69–78

22. Wilesmith JW, Wells GAH, Cranwell MP, Ryan JBM (1988) Bovine spongiform encephalopathy: epidemiologic studies. *Vet Rec* 123: 638–644
23. Will RG, Ironside JW, Zeidler M, Cousens SN, Estibeiro K, Alperovitch A, Poser S, Pocchiari M, Hofman A, Smith PG (1996) A new variant of Creutzfeldt–Jakob disease in the UK. *Lancet* 347: 921–925

Authors' address: Prof. Dr. H. Kretzschmar, Institute of Neurology, Ludwig-Maximilians-University Munich, Marchioninstr. 17, D-81377 Munich, Germany.

## **Sheep and goats: natural and experimental TSEs and factors influencing incidence of disease**

**N. Hunter, W. Goldmann, E. Marshall, and G. O'Neill**

Institute for Animal Health, Neuropathogenesis Unit, Edinburgh, Scotland, U.K.

**Summary.** The major factor influencing incidence of disease following challenge with transmissible spongiform encephalopathies (TSEs) in sheep is the allotype at amino acid numbers 136, 154 and 171 of the PrP protein. There are at least two groups of TSEs, one which targets the amino acid encoded at position 136 and the other which is more influenced by the amino acid at codon 171. Within these groups of TSE types, there may additionally be sub-types, as resistance to some, but not all, "136-type" TSEs can also be affected by the amino acid at codon 154. In goats, there are also PrP polymorphisms which apparently influence incubation period of TSE disease, however, this has not found to be true for cattle and BSE incidence. Sheep PrP amino acid codons 136, 154 and 171 do not explain everything about, for example, natural scrapie occurrence in sheep flocks, and attention is now turning to the flanking regions of the PrP gene looking for sequence differences in gene expression control motifs which may also have an influence on disease development. The sheep PrP gene produces two mRNAs in peripheral tissues [17], the result of alternative polyadenylation in the 3' untranslated region of the gene. Results from transfection assays of murine neuroblastoma cells with constructs expressing different regions of ovine PrP mRNA have revealed the presence of sequences in the 3' untranslated region that modulate protein synthesis and have therefore the potential to affect disease progression.

### **Introduction**

Since the first discovery, in 1989, that restriction fragment length polymorphisms in the sheep PrP gene untranslated regions were associated with differences in incidence of scrapie [15], it has become apparent that in sheep, the PrP gene is highly polymorphic. DNA base changes which result in amino acid differences in the resulting protein have been of most interest to those studying natural scrapie in many countries throughout Europe and in USA and Japan. Table 1 shows the published amino acid variants at the time of writing. Of particular importance are those amino acids at codons

**Table 1.** Amino acid polymorphisms in the sheep PrP gene, with date published

Codon	AA change (3 letter code)	Breed/ country	Reference example
112	Met/Thr	Romanov Ile de France	Laplanche et al. (1993) <i>Genomics</i> 15: 30–37
136	Ala/Val	Several	Goldmann et al. (1991) <i>J Gen Virol</i> 72: 2411–2417
137	Met/Thr	Flemish Texel	Bossers et al. (1996) <i>J Gen Virol</i> 77: 2669–2673
138	Ser/Asn	Iceland  Norway	Thorgeirsdottir et al. (1999) <i>J Gen Virol</i> 80: 2527–2534 Tranulis (1999) <i>J Gen Virol</i> 80: 1073–1077
141	Leu/Phe	Swifter UK breeds	Bossers et al. (1996) <i>J Gen Virol</i> 77: 2669–2673
151	Arg/Cys	Iceland  Norway	Thorgeirsdottir et al. (1999) <i>J Gen Virol</i> 80: 2527–2534 Tranulis (1999) <i>J Gen Virol</i> 80: 1073–1077
154	Arg/His	Several	Goldmann et al. (1991) <i>J Gen Virol</i> 72: 2411–2417
171	Gln/Arg	All so far	Goldmann et al. (1990) <i>PNAS</i> 87: 2476–2480
	His	Several	Belt et al. (1995) <i>J Gen Virol</i> 76: 509–517
211	Arg/Gln	Flemish Swifter Texel	Bossers et al. (1996) <i>J Gen Virol</i> 77: 2669–2673

136, 154 and 171 which give rise to the protein allotypes of VRQ, ARQ, ARR, and AHQ (for review see [11]). The vast majority of sheep which succumb to natural scrapie are homozygous for Q at codon 171 (i.e. are VRQ/VRQ, VRQ/ARQ or ARQ/ARQ). The VRQ allele represents a very high risk of disease, especially in the VRQ/VRQ and VRQ/ARQ genotypes. For those who thought that scrapie was a genetic disease in sheep, VRQ was the best candidate for such a lethal allele. However, as it has been shown that animals of VRQ/VRQ and VRQ/ARQ genotype can live to old age in the scrapie free countries of Australia and New Zealand [2, 12, 13], it is now believed that these genotypes influence susceptibility to an infection rather than that the mutations themselves directly produce a genetic disease. ARQ/ARQ animals in breeds which encode the VRQ allele are usually resistant to disease and in some, but not all, outbreaks, the presence of the AHQ allele in the genotype VRQ/AHQ will also protect the sheep from scrapie. In other breeds, for example Suffolks in the UK, VRQ is generally absent in pedigree animals and it is the ARQ/ARQ sheep which are the most susceptible. The breed difference in the susceptibility of the ARQ/

ARQ genotype is not understood. However, the sheep PrP allele disease linkage results are solid, convincing and becoming even more so as increasing numbers of studies of sheep of different breed, flock and country are published [3].

Sheep PrP genetics is therefore providing indirect information about the interaction of scrapie with PrP protein allotypes and may mean that there are a number of distinct scrapie strains affecting various flocks or breeds, or present in different countries. However, the natural scrapie strains may be limited in number judging by the overall similarity in PrP genetics in scrapie outbreaks in Europe and elsewhere [1, 4, 14, 18, 20–22]. There is experimental evidence for sources of TSE targeting sheep of particular PrP genotypes. Injection with SSBP/1 affects animals encoding at least one copy of VRQ and does not affect ARQ/ARQ, ARR/ARQ or ARR/ARR animals. On the other hand injection with CH1641 scrapie or BSE affects ARQ/ARQ animals with shorter incubation periods than ARQ/ARR homozygotes and the VRQ allele apparently lengthening the incubation period with BSE [7].

Sheep PrP genetics does not explain everything about the incidence of natural scrapie. For example the occasional occurrence of scrapie in animals which have one ARR allele (in the genotype ARQ/ARR or VRQ/ARR) [16] or the survival to old age of animals of susceptible genotypes in flocks with endemic scrapie.

There may be genes other than PrP which influence incidence of disease and this is under investigation in a number of labs (e.g. Prnd, described in other papers in this volume) however we have chosen to investigate the control of expression of sheep PrP mRNA in order to establish whether variation in the amount of PrP protein present in different tissues of the sheep may help explain the more unusual instances of scrapie incidence which have been observed in natural scrapie flocks. PrP expression is crucial to the development of scrapie following artificial challenge in transgenic mice and there is an inverse link between levels of PrP protein produced by multi-copy transgenes and the length of scrapie incubation period. It is possible, therefore, that some individual sheep have sequence variation in gene expression control which would result in low levels of protein expression in tissues important in the spread of scrapie from the site of initial infection resulting in the alteration of an apparently susceptible genotype to a resistant phenotype.

### **Expression patterns of PrP mRNA in sheep**

Our results highlight three properties of PrP gene regulation which might influence TSE susceptibility and pathogenesis in sheep [8]. Firstly, PrP gene transcripts were found in the sheep fetus and throughout development to the adult animal, in brain and many other tissues. Secondly, two PrP gene transcripts of 4.6 kb and 2.1 kb in length, encoding the same PrP ORF, are

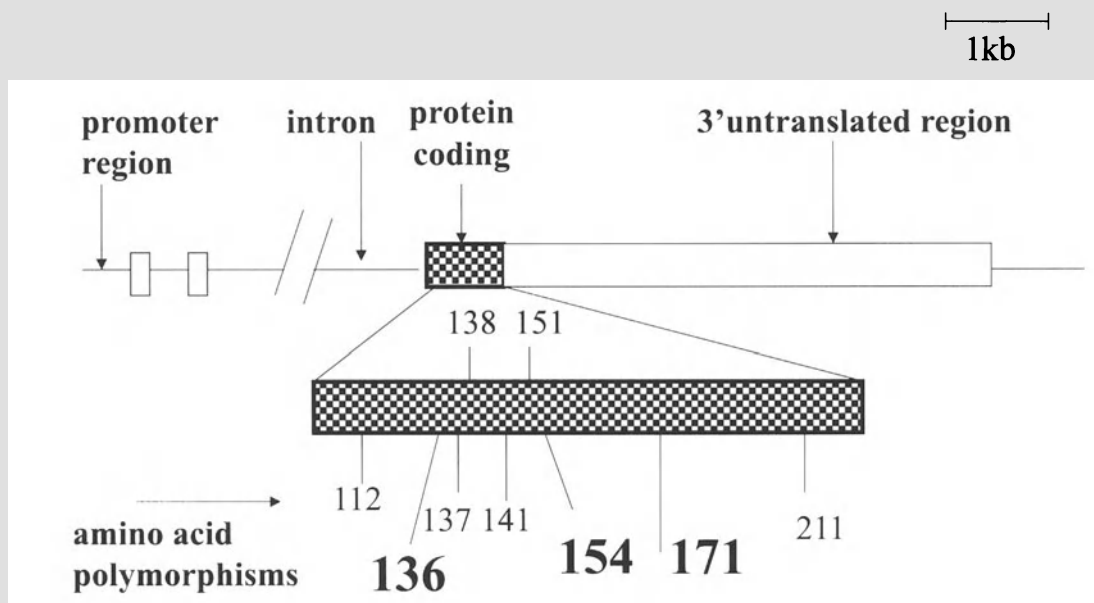


**Fig. 1.** Sheep PrP gene structure

produced by alternative polyadenylation with tissue-specific levels, the highest level of the 4.6 kb transcript in brain tissue and the highest level of the 2.1 kb transcript in spleen. The 2.1 kb PrP transcripts were expressed significantly in sheep and goat but only marginally in bovine tissues. Alternative polyadenylation was not detected in human and murine tissues. Lastly, *in vitro* experiments showed that the level of protein expressed from RNA transcripts with different ovine PrP gene 3'UTRs is related to sequences within the UTRs. The 3'UTR of the 2.1 kb mRNA did not preclude protein expression.

Both PrP mRNAs of sheep are encoded by the same three exons (Fig. 1). The 4.6 kb mRNA has a 150 nucleotide (n) 5'UTR, a 768 n coding region and a 3220 n 3'UTR [8, 22]. A similar structure has been described for bovine PrP mRNA [10, 19], whereas rodent and human PrP transcripts have shorter 3'UTRs of about 1300 n [5]. Despite these considerable differences in length, regions of high sequence similarity in rodent, human and ruminant 3'UTRs can be identified. The 3'UTR of the sheep 4.6 kb mRNA has previously been divided into regions A to G (Fig. 2) on the basis of sequence similarity to human (encoding regions A, B, C, E and G) and mouse PrP mRNA (encoding regions A, C, E, G) [6].

From S1 protection assays with 3'UTR-specific probes, Northern blot hybridisations with single stranded probes and sequencing of 3'RACE products, we found that the sheep 2.1 kb mRNA is produced by alternative polyadenylation rather than alternative splicing. Furthermore, long range RT-PCR and 5'RACE identified the 5'UTR of the 2.1 kb and 4.6 kb mRNAs from lymph node as identical to each other and to that published

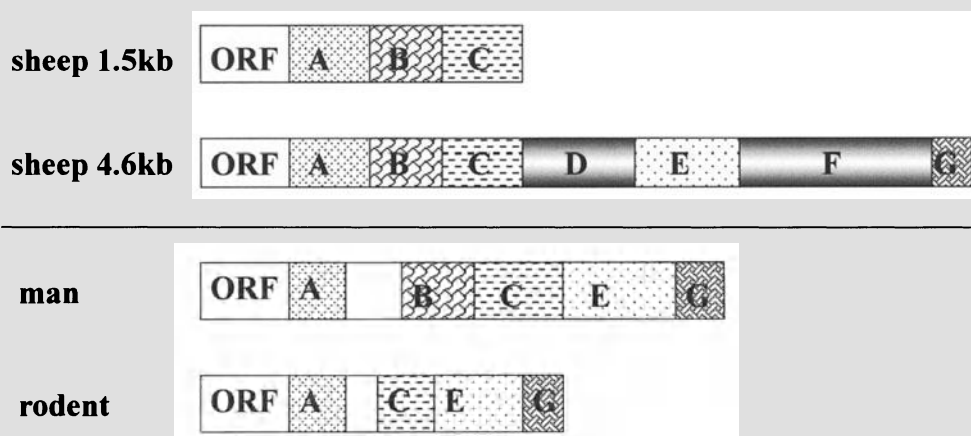


**Fig. 2.** ORF: open reading frame of PrP gene. Regions A to G inclusive: areas of sequence similarity in 3'UTRs of mRNA from sheep, man and rodent

for the 4.6 kb mRNA [22]. Although the 2.1 kb sheep mRNA is similar in length to human and mouse PrP mRNA, it is not their homologue as its 3'UTR encodes only regions A to C (Fig. 2). However, two regions of about 0.5 kb and 1.4 kb (D and F) are found only in the longer 3'UTRs of ruminant PrP [8] and could be involved in ruminant specific RNA processing and translation. We have previously pointed out that the ruminant specific regions (D, F) of PrP 3'UTR have homology to retroposons [5]. PrP gene analysis [9] confirmed that the 4.6 kb mRNA contains almost 2 kb sequence originating from LINE, SINE or transposon elements, sequences that are not present on the 2.1 kb mRNA. The gross level of expression of the ovine 4.6 kb and 2.1 kb mRNA appears to be correlated with neither sheep breed nor PrP genotypes and the 2.1 kb mRNA is present independent of whether the sheep has scrapie or not.

### **In vitro transfection studies**

The major mechanisms that link the kinetics of mRNA with protein synthesis involve the mRNA degradation rate, the rate of initiation and the rate of translation. Mouse N2a cell transfections show that 3'UTR sequences of the sheep PrP gene can significantly affect production of protein from CAT reporter gene constructs [8]. The highest protein levels were expressed from constructs with the shortest 3'UTRs processed using the polyA site in region G whereas the short 3'UTR processed using the polyA site in region C resulted in distinctly lower level of protein (Fig. 3). Taken together with the fact that the long 3'UTRs all resulted in low protein expression we speculate that the stability of these RNAs and a difference in the utilisation of the two poly-A-signal sequences could explain these observations. Surprisingly, the RNA with the full length sheep PrP 3'UTR is poorly, if at all, translated in transfected mouse N2a cells, which is in

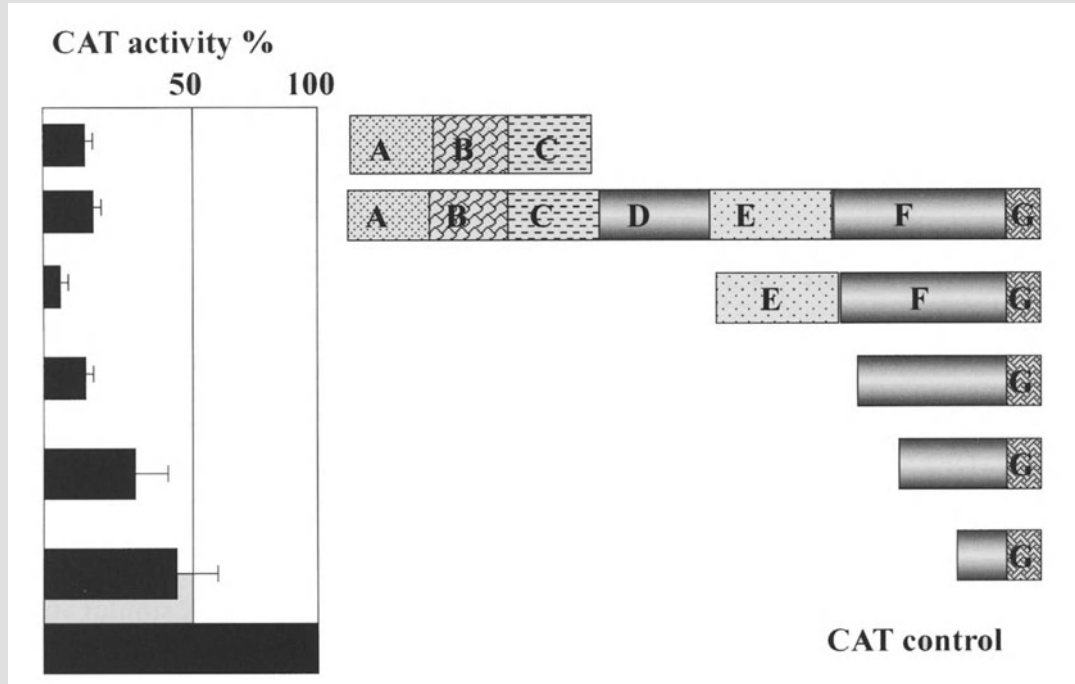


**Fig. 3.** Regions A to G, inclusive. Each block indicates the regions of sheep 3'UTR present in each CAT reporter gene construct. *CAT* Chloramphenicol acetyl transferase. CAT control: control plasmid expressing CAT at maximal levels

contrast to sheep brain *in vivo*, in which the major PrP transcript of 4.6 kb mRNA is associated with high levels of PrP protein. This suggests that the 4.6 kb RNA may be stabilised or translationally activated *in vivo* in sheep by factors that are missing in the murine neuroblastoma cells. We propose that sequence motifs encoded in regions D–F may interact with sheep specific proteins *in vivo*.

These studies of the 3'UTR of the sheep PrP gene are now being extended into sheep cell lines using constructs including the sheep PrP ORF.

### Non coding region polymorphisms

The very first scrapie incidence-linked polymorphism was detectable as an *EcoRI* restriction fragment length polymorphism (RFLP) in individual sheep susceptible and resistant to scrapie challenge [15]. The sequence difference which results in this RFLP is in the 3'UTR of the PrP gene and it was of interest to discover that this region and parts of the 5' promoter region and intronic regions are also highly polymorphic in the sheep. Finding such polymorphisms is not difficult and more are being found every month. Proving that any of them have importance in disease progression or in modes of transmission of the infection is more difficult and requires both *in vitro* cell expression and genetic linkage studies in the few sheep families available for such detailed analysis.

### Implications for the future

The modes of transmission of natural scrapie in the sheep are not understood and the development of transgenic mice expressing sheep PrP gene alleles has long been expected to provide a good model system for studying transmission characteristics of field strains of scrapie. However, in beginning to untangle the expression patterns of the sheep PrP gene and in realising the potential of the mRNA for differential control of protein synthesis, it is clear that a transgenic mouse expressing a single sheep PrP mRNA in all tissues may not after all be a realistic model for the sheep. Such information will, however, guide future attempts both to create suitable transgenes and to understand the spread of scrapie throughout the body tissues of susceptible and resistant animals.

### References

1. Belt PBGM, Muileman IH, Schreuder BEC, Bos-de Ruijter J, Gielkens ALJ, Smits MA (1995) Identification of five allelic variants of the sheep PrP gene and their association with natural scrapie. *J Gen Virol* 76: 509–517
2. Bossers A, Harders FL, Smits MA (1999) PrP genotype frequencies of the most dominant sheep breed in a country free from scrapie. *Arch Virol* 144: 829–834
3. Dawson M, Hoinville LJ, Hosie BD, Hunter N (1998) Guidance on the use of PrP genotyping as an aid to the control of clinical scrapie. *Vet Rec* 142: 623–625
4. Elsen J-M, Amigues Y, Schelcher F, Ducrocq V, Andereoletti O, Eychenne F, Tien Khang JV, Poivey J-P, Lantier F, Laplanche J-L (1999) Genetic susceptibility and transmission factors in scrapie: detailed analysis of an epidemic in a closed flock of Romanov. *Arch Virol* 144: 431–445
5. Goldmann W (1993) PrP gene and its association with spongiform encephalopathies. *Br Med Bull* 49: 839–859
6. Goldmann W, Hunter N, Foster JD, Salbaum JM, Beyreuther K, Hope J (1990) Two alleles of a neural protein gene linked to scrapie in sheep. *Proc Natl Acad Sci USA* 87: 2476–2480
7. Goldmann W, Hunter N, Smith G, Foster J, Hope J (1994) PrP genotype and agent effects in scrapie – change in allelic interaction with different isolates of agent in sheep, a natural host of scrapie. *J Gen Virol* 75: 989–995
8. Goldmann W, O'Neill G, Cheung F, Charleson F, Ford P, Hunter N (1999) PrP (prion) gene expression in sheep may be modulated by alternative polyadenylation of its messenger RNA. *J Gen Virol* 80: 2275–2283
9. Horiuchi M, Ishiguro N, Nagasawa H, Toyada Y, Shinagawa M (1997) Alternative usage of exon 1 of bovine PrP mRNA. *Biochem Biophys Res Commun* 233: 650–654
10. Horiuchi M, Ishiguro N, Nagasawa H, Toyada Y, Shinagawa M (1998) Genomic structure of the bovine PrP gene and complete nucleotide sequence of bovine PrP cDNA. *Anim Gen* 29: 37–40
11. Hunter, N (1997) Molecular biology and genetics of scrapie in sheep. In: Piper L, Ruvinsky A (eds) *The genetics of sheep*. CAB International, Wallingford, pp 225–240
12. Hunter N, Cairns D (1998) Scrapie-free Merino and Poll Dorset sheep from Australia and New Zealand have normal frequencies of scrapie-susceptible PrP genotypes. *J Gen Virol* 79: 2079–2082

13. Hunter N, Cairns D, Foster J, Smith G, Goldmann W, Donnelly K (1997) Is scrapie a genetic disease? Evidence from scrapie-free countries. *Nature* 386: 137
14. Hunter N, Foster J, Goldmann W, Stear M, Hope J, Bostock C (1996) Natural scrapie in a closed flock of Cheviot sheep occurs only in specific PrP genotypes. *Arch Virol* 141: 809–824
15. Hunter N, Foster JD, Dickinson AG, Hope J (1989) Linkage of the gene for the scrapie-associated fibril protein (PrP) to the Sip gene in Cheviot sheep. *Vet Rec* 124: 364–366
16. Hunter N, Goldmann W, Foster J, Cairns D, Smith G (1997) Natural scrapie and PrP genotype: case-control studies in British sheep. *Vet Rec* 141: 137–140
17. Hunter N, Manson JC, Charleson FC, Hope J (1994) Comparison of expression patterns of PrP mRNA in the developing sheep and mouse. *Ann New York Acad Sci* 724: 353–354
18. Ikeda T, Horiuchi M, Ishiguro N, Muramatsu Y, Kai-Uwe G, Shinagawa M (1995) Amino acid polymorphisms of PrP with reference to onset of scrapie in Suffolk and Corriedale sheep in Japan. *J Gen Virol* 76: 2577–2581
19. Inoue S, Tanaka M, Horiuchi M, Ishiguro N, Shinagawa M (1997) Characterization of the bovine prion protein gene: the expression requires interaction between the promoter and intron. *J Vet Med Sci* 59: 175–183
20. Thorgeirsdottir S, Sigurdarson S, Thorisson HM, Georgsson G, Palsdottir A (1999) PrP gene polymorphism and natural scrapie in Icelandic sheep. *J Gen Virol* 80: 2527–2534
21. Tranulis MA, Osland A, Bratberg B, Ulvund MJ (1999) Prion protein gene polymorphisms in sheep with natural scrapie and healthy controls in Norway. *J Gen Virol* 80: 1073–1077
22. Westaway D, Zuliani V, Cooper CM, Dacosta M, Neuman S, Jenny AL, Detwiler L, Prusiner SB (1994) Homozygosity for prion protein alleles encoding glutamine-171 renders sheep susceptible to natural scrapie. *Gen Dev* 8: 959–969

Authors' address: Dr. N. Hunter, Institute for Animal Health, Neuropathogenesis Unit, West Mains Road, Edinburgh EH9 3JF, Scotland, U.K.

## **Application of Prionics Western blotting procedure to screen for BSE in cattle regularly slaughtered at Swiss abattoirs**

**B. Oesch<sup>1</sup>, M. Doherr<sup>2</sup>, D. Heim<sup>3</sup>, K. Fischer<sup>1</sup>, S. Egli<sup>1</sup>, S. Bolliger<sup>1</sup>,  
K. Biffiger<sup>1</sup>, O. Schaller<sup>1</sup>, M. Vandeveld<sup>2</sup>, and M. Moser<sup>1</sup>**

<sup>1</sup>Prionics AG, University of Zürich, Zürich, Switzerland

<sup>2</sup>Institut für Tierneurologie, University of Bern, Bern, Switzerland

<sup>3</sup>Bundesamt für Veterinärwesen, Liebefeld, Switzerland

**Summary.** Disease-specific PrP (PrP<sup>Sc</sup>) is at least part of the infectious particle (prion) causing bovine spongiform encephalopathy (BSE) or scrapie in sheep. Digestion with protease allows a distinction between normal PrP (PrP<sup>C</sup>) and PrP<sup>Sc</sup> i.e. PrP<sup>C</sup> is completely digested while PrP<sup>Sc</sup> is cleaved at the N-terminus leading to a fragment of reduced molecular weight (PrP 27–30). Detection of this fragment by Western blotting has been described more than a decade ago for rodent PrP. We have now optimized the technique in order to allow rapid analysis of hundreds of samples per day. Here we report the application of this technique to the analysis of 3000 regularly slaughtered cattle from Swiss abattoirs. For comparison all the animals were subsequently examined by classical methods (i.e. histology and immunohistochemistry). All but one animal were negative for BSE by all methods. The Western blot positive animal was confirmed to be a BSE case and the carcass was removed from the food chain. We conclude that it is feasible to examine slaughtered cattle on a routine basis without causing delays to the meat processing industry.

### **Introduction**

Detection of BSE in clinically normal and diseased cattle has become a major issue in determining the size of the BSE problem in various countries. Western blot analysis of brain homogenates for the disease-specific form of the prion protein has been established as a technique for more than a decade [1]. Nevertheless, it was rarely used for cattle because cattle PrP<sup>Sc</sup> appeared to be less protease resistant than PrP<sup>Sc</sup> from rodent species like hamsters or mice [2].

Application of a Western blot technique for screening large numbers of cattle was not considered because it was assumed that it would be difficult to perform. We have developed a rapid Western blotting procedure (named

Prionics Check or PWB) which has gone through validation work carried out with the Swiss and British Veterinary Authorities as well as the European Commission. Samples of the brain stem from officially confirmed BSE or scrapie cases could be diagnosed with 100% specificity and sensitivity [3, 4]. Furthermore, autolyzed samples could still be diagnosed correctly leading to the unique surveillance program in Switzerland to test fallen stock for hidden cases of BSE. Results for the 1999 surveillance program are available on the internet [5]. The routine application of the Prionics Western blotting technique has also revealed unrecognized BSE cases which would have gone into the food chain. Transfer of the test system to other diagnostic laboratories has been accomplished which will allow for standardized surveillance of BSE in Europe.

Here we would like to review the sampling procedure and describe the experience in applying this test to BSE surveillance of 3000 regularly slaughtered cattle in Switzerland.

### **Materials and methods**

Screening of cattle from Swiss abattoirs had to be performed such that PrP<sup>Sc</sup>-positive animals could be identified and removed from the production chain before they left the abattoir. The project was performed in three steps: 1 – removal of brain samples from cattle, their immediate analysis with the PWB and notification of the abattoir of the results. 2 – histological/immunohistochemical analysis of brain section of all cattle. 3 – epidemiological analysis of findings.

The main premise for the logistics was the requirement of the sample to be taken at an abattoir, transported to Prionics and analyzed within the time that the carcass was still at the abattoir. This time varied widely from abattoir to abattoir but generally the results had to be known by 3:00 to 8:00 am the day following the slaughtering. As the PWB takes about 6–7 h the samples had to be at Prionics no later than 9:00 pm. The target population was considered to be animals older than 2.5 to 3 years. As the teeth give some indication on the age of the animals, we had decided to put the main emphasis on the sampling of animals with at least 4 permanent teeth. A brain stem sample (which included the obex) was removed after the head had been cut off using a modified spoon. The head was usually identified by an animal tag which was included with the sample in the container. As an alternative the running number of the abattoir was recorded. The obex region of the medulla was used for analysis. The medulla was cut along the midline; one side was fixed in 4% formalin/PBS while from the other side a piece of tissue (0.5–0.8 g) was cut out to be used for Western blotting. The latter piece was then processed according to the Prionics Check protocol [3]. Detection of PrP on Western blots was done with monoclonal antibody 6H4 (Prionics).

### **Results and discussion**

The different steps were evaluated according to their ease of performance in the slaughterhouse as well as the results obtained thereafter. Eleven different abattoirs spread throughout Switzerland participated in this pilot study.

*Evaluation of sampling/identification of animals in abattoirs*

The majority of samples were taken by previously untrained personnel. They were instructed at an abattoir for about 15 min which was sufficient for them to learn the procedure. It is therefore possible to instruct personnel within a short time such that good sample quality could be assured.

The time required to take the sample and place it in a container is about 30 sec for a newly trained person and thereafter shortened to about 10–20 sec. In some cases an additional bar code or abattoir serial number was placed with the sample. It is feasible that this step is done by the person handling the head in the abattoir.

*Sampling of animals*

A total of 3022 animals have been tested from the 11 different abattoirs spread throughout Switzerland (Fig. 1). More than half of the cattle were from 2 major abattoirs, a further thousand animals from 3 additional abattoirs. Despite this apparent bias to abattoirs in the German part of Switzerland, there was a fair number of animals raised in different parts of Switzerland as there is a large amount of trading of animals.

One animal was found to be positive by Western blotting. It was a 4 year old animal with a history of a severe mastitis followed by an apparent

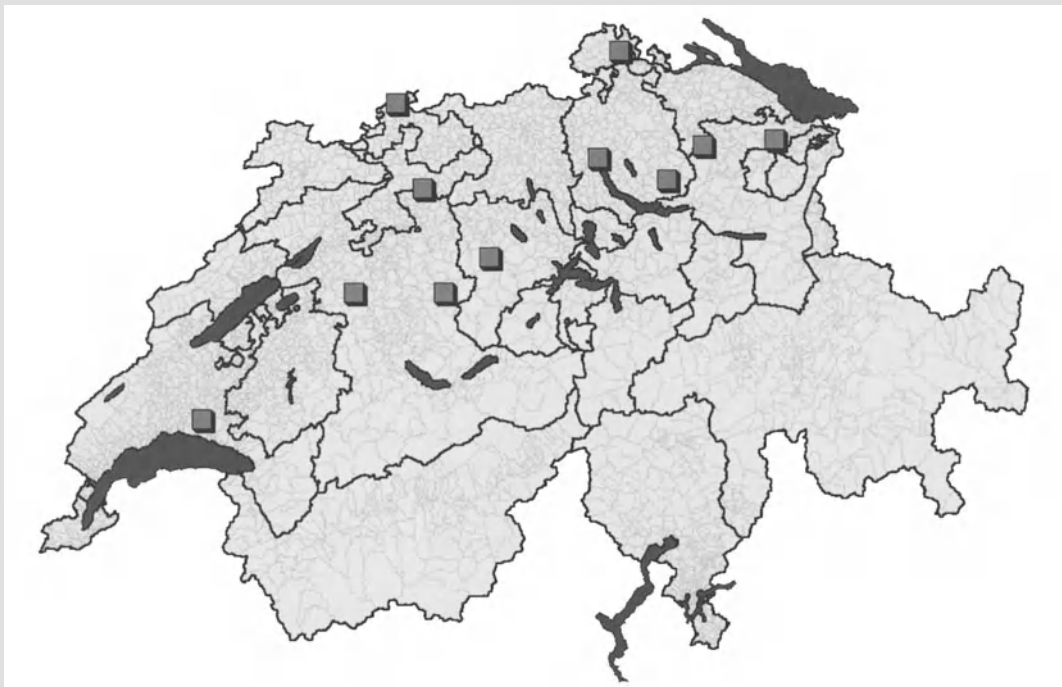


**Fig. 1.** Geographic distribution of 11 participating abattoirs (■) within Switzerland. The thicker lines represent the cantonal borders while the thinner lines are the country boundaries (Gemeinden)

unease of being milked. As the animal also showed a reduction in milk production, it was decided to slaughter this animal. This animal was subsequently confirmed by histology and immunohistochemistry to be a BSE case. Detailed results for this animal are shown elsewhere [3].

The remaining 3021 animals were test-negative both in the Prionics Western blot and in immunohistochemistry for PrP<sup>Sc</sup> (IHC). Agreement between the two tests therefore was 100%. These results confirm a very high specificity (>99.99%) of the PWB when compared to IHC. Calculating the sensitivity from the results of this study alone would not be feasible due to the very small number of positive animals detected, however, other evaluations have demonstrated that the currently used Western blot protocol also leads to a sensitivity of 100% [4]. These results indicate that the Prionics Western blot is a fast and reliable test for screening cattle brain samples for the presence of the disease-specific form of PrP.

#### *Age and geographical distribution of sampled animals*

This study was designed as a pilot survey, and did not provide a statistically representative sample of all cattle slaughtered in Switzerland. Inclusion criteria of abattoirs and cattle into the study were as follows:

- Potential abattoirs for the study were identified based on the number of cattle slaughtered in 1997, and the 30 abattoirs with highest numbers were selected and asked – on a voluntary basis – for their participation. Of these 30 abattoirs, 11 agreed to take part in the pilot study;
- Samples at the individual abattoirs were taken on between 1 and 16 working days in August and September of 1998. The dates were selected based on the cow slaughtering schedule at the individual plants and on the availability of resources at the laboratory;
- For a given slaughter day as many cattle above 24 months of age as possible were sampled. True random selection of individual animals was not attempted.

All cattle in Switzerland intended for slaughter have to be delivered to the abattoir with a cattle identification form containing at least the origin of the animal (last owners name and address), age of the animal and its identification (ear tag numbers). The abattoirs were asked to submit copies of the cattle identification forms of all sampled animals for evaluation of the age and geographical distribution of the sampled cohort. From 9 abattoirs all but a few forms were received. One abattoir returned only the forms from 1 of 6 slaughter days (29 of 312 forms), and from another abattoir forms of almost 1000 slaughtered cattle were received while only 631 cattle were actually tested from this abattoir. With additional information provided by the plant, however, it was impossible to identify the forms of sampled animals.

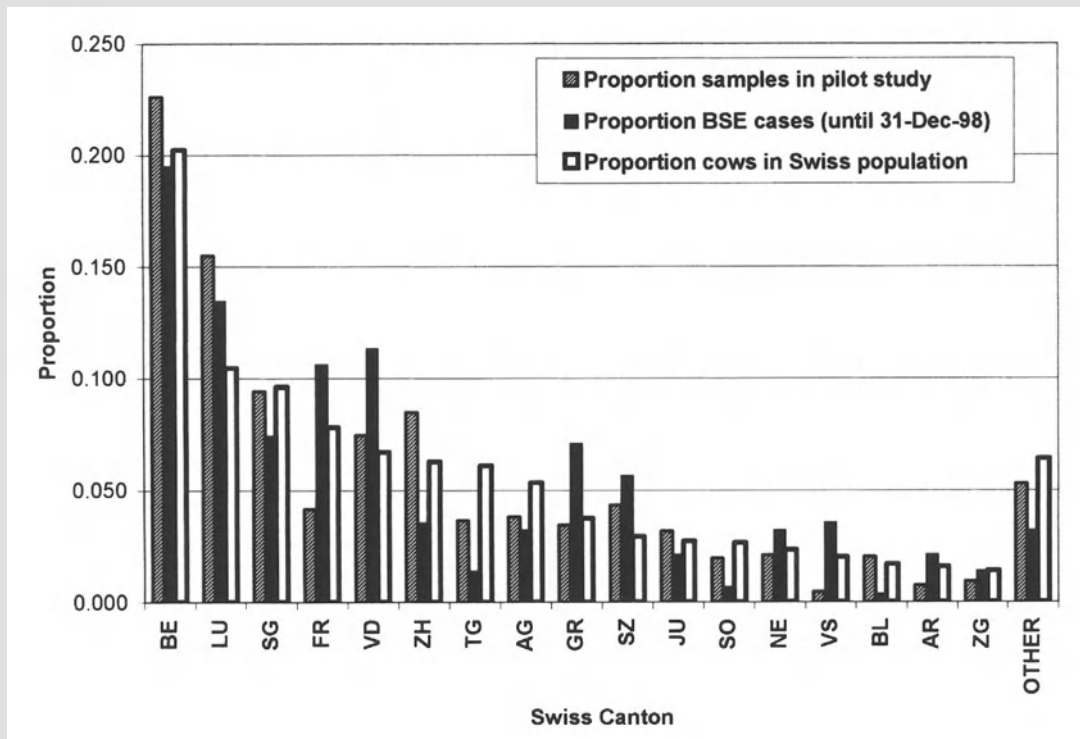
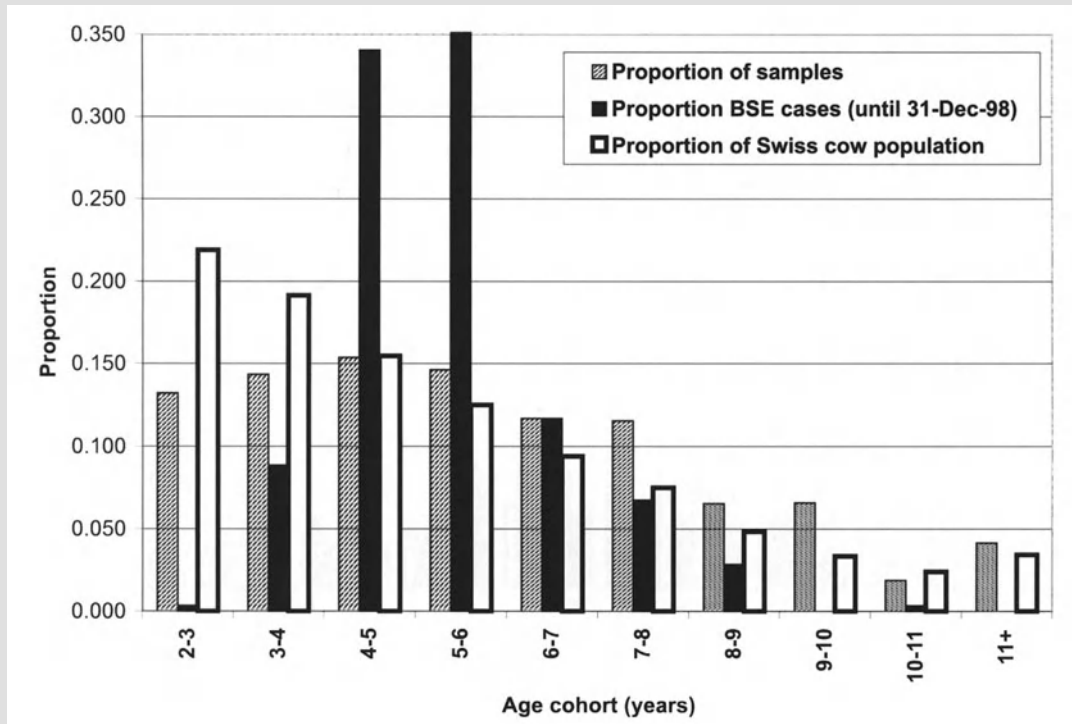


Fig. 2. Proportion of samples, BSE cases and cows within each Swiss canton. Only cantons with at least 10000 cows registered in 1996 are listed separately, all other cantons are summarized in the last category denoted "OTHER"

Geographical information at the cantonal level was available for 2644 of the 3022 sampled animals (87%), while age information (in years) was retrieved for 2423 of 3022 cattle sampled (80%). The participating abattoirs were mainly located in the central and northern regions of Switzerland (Fig. 1), which in fact are the areas with the highest cattle density.

A comparison of the proportion of the total cow population, BSE cases and sampled cattle originating from each canton is given in Fig. 2. Even though the proportion of samples was significantly different from the cow population for some of the cantons, the geographic representation was satisfactory: tested animals originated from 25 of the 26 Swiss cantons and from the "Fürstentum Lichtenstein", and a minimum of 11 animals was sampled from each of the 21 cantons that have reported one or more BSE cases to date.

During the sampling it was attempted to target older cows since these constitute a surviving "risk" population in which subclinically infected animals, should they exist in the population, would be detected. The age distribution of the sampled cohort shows that proportionally more older animals were selected than to be expected from the age distribution of the Swiss cow population. In addition, the age range covered by the sample extended further into higher age classes than the age distribution of the observed BSE cases (Fig. 3).



**Fig. 3.** Age distribution of the abattoir sample, the Swiss BSE cases and the Swiss cow population (24 months of age and older)

Our results show that we have analyzed a representative sample of the Swiss cattle population for the occurrence of BSE. In 1999, the active surveillance in Switzerland has been further extended to all fallen stock and sick slaughtered cattle as well as a random sample from normally slaughtered cattle (7200 out of about 200,000 slaughtered cattle in the age range defined above).

### Conclusions

This study describes the sampling and analysis of about 3000 cattle older than 2 years selected from different abattoirs to detect the presence of subclinical BSE. One positive case has been detected. The results suggest that for the surveillance of BSE larger numbers of animals will have to be tested in order to get a statistically meaningful answer. Nevertheless, the speed of the Prionics Western blot and its precision (no false positives in 3000 animals) will allow its use as a surveillance tool. The standardized procedure in combination with inexpensive equipment will allow a wider dissemination of the assay to other diagnostic laboratories in different countries in order to allow for unbiased active surveillance of BSE.

### Acknowledgements

We would like to thank the abattoirs and their personnel in making this study possible. This work was supported by the Bundesamt für Veterinärwesen (Swiss Veterinary Authorities).

### References

1. Oesch B, Westaway D, Walchli M (1985) A cellular gene encodes scrapie PrP 27–30 protein. *Cell* 40: 735–746
2. Pocchiari M, Xi YG, Ingrosso L (1994) Immunodiagnosis of bovine spongiform encephalopathy. *Livestock Prod Sci* 38: 41–46
3. Schaller O, Fatzer R, Stack MJ, Clark JK, Cooley WA., Biffiger K, Egli S, Doherr M, Vandevelde M, Heim D, Oesch B, Moser M (1999) Validation of a Western immunoblotting procedure for bovine PrP<sup>Sc</sup> detection and its use as a rapid surveillance method for the diagnosis of bovine spongiform encephalopathy (BSE). *Acta Neuropathol* 98: 437–443
4. Schimmel H, Moynagh J (1999) Preliminary Report concerning the evaluation of tests for the diagnosis of Transmissible Spongiform Encephalopathy in Bovines. Available at [http://europa.eu.int/comm/dg24/health/bse/bse12\\_en.html](http://europa.eu.int/comm/dg24/health/bse/bse12_en.html)
5. Surveillance program of the Swiss Veterinary Authorities (UP99): [http://www.admin.ch/bvet/focus\\_bse/d/0\\_subfr.html](http://www.admin.ch/bvet/focus_bse/d/0_subfr.html)

Authors' address: Dr. B. Oesch, Prionics AG, University of Zürich, Winterthurerstr. 190, CH-8057 Zürich, Switzerland.

## **Specific determination of the proteinase K-resistant form of the prion protein using two-site immunometric assays. Application to the post-mortem diagnosis of BSE**

**J. Grassi<sup>1</sup>, C. Créminon<sup>1</sup>, Y. Frobert<sup>1</sup>, P. Frétier<sup>1</sup>, I. Turbica<sup>1</sup>, H. Rezaei<sup>2</sup>,  
G. Hunsmann<sup>3</sup>, E. Comoy<sup>4</sup>, and J.-P. Deslys<sup>4</sup>**

<sup>1</sup>CEA, Service de Pharmacologie et d'Immunologie, CEA Saclay,  
Gif sur Yvette, France

<sup>2</sup>Institut National de la Recherche Agronomique (INRA), Muséum National  
d'Histoire Naturelle, Institut de Biologie Physicochimique, Paris, France

<sup>3</sup>Deutsches Primatenzentrum, Abteilung Virologie und Immunologie,  
Göttingen, Germany

<sup>4</sup>CEA, Service de Neurovirologie, CEA/CRSSA Fontenay aux Roses,  
Fontenay aux Roses, France

**Summary.** The aim of this work was to establish an immunological test suitable for specifically detecting PrP<sup>res</sup> in tissues from animals or humans developing TSEs. We chose to use as detection method a conventional two-site immunometric assay (sandwich immunoassay) because over the last 20 years this technique has clearly been shown to be more sensitive and specific than other tests. We have established numerous two-site immunometric assays based on the use of monoclonal antibodies and suitable for measurement of PrP<sup>sen</sup> in various mammalian species (human, bovine, ovine, mouse and hamster). A detection limit below 100 pg/ml was estimated from standard curves established using ovine recombinant PrP. PrP<sup>res</sup> was selectively detected by processing samples (currently brain homogenates) to enable specific purification and concentration of PrP<sup>res</sup>, which was finally solubilized by a strong denaturing treatment. This sample-processing procedure can be achieved within 30 minutes. The capacity of this test to detect bovine PrP<sup>res</sup> was estimated in the framework of an evaluation study organized by the Directorate-General XXIV of the European Commission during May 1999. On this occasion, a blind test on 1400 brain stem samples taken from either healthy (1000) or BSE-infected (300) cows demonstrated 100% sensitivity and specificity. In addition, dilution experiments showed that the test can significantly detect PrP<sup>res</sup> in homogenates diluted 1/300 and was at least as sensitive as a conventional bioassay performed on mice.

### Introduction

So far the diagnosis of BSE is essentially based on clinical signs and is confirmed post-mortem using histopathological, immunohistochemical or Western-blot techniques. None of these techniques are adapted to high throughput analysis and they are therefore unsuitable for either large epidemiological studies or individual testing of bovine carcasses before they enter in the food chain. The aim of our work was to establish an immunological test suitable for specifically detecting the abnormal, protease-resistant form of the prion protein ( $\text{PrP}^{\text{res}}$ ) in tissues from animals or humans developing transmissible spongiform encephalopathy (TSE) and suitable for high throughput analysis. The main difficulty of this project was to determine  $\text{PrP}^{\text{res}}$  selectively in samples which also contain significant (and usually higher) amounts of the cellular form of the protein ( $\text{PrP}^{\text{sen}}$ ). We chose to develop as detection method a conventional two-site immunometric assay (sandwich immunoassay) based on the use of two different monoclonal antibodies recognizing two distinct epitopes on the PrP molecule. In this category of immunoassay, a first antibody (capture antibody) is immobilized on a solid phase (microtitre plate, for instance) while a second antibody, covalently labelled with an enzyme (here acetylcholinesterase, AChE), is used as a tracer. PrP in a sample is detected by measuring enzyme activity bound to the solid phase through the intermediary of capture antibody-PrP-tracer antibody interactions. A two-site immunometric assay was chosen because it has clearly been demonstrated that this kind of immunoassay provides more sensitive, more specific and faster measurements than other tests (competitive immunoassay for instance [2]).

However, the immunometric assays we have developed do not specifically target  $\text{PrP}^{\text{res}}$ . Selective detection of  $\text{PrP}^{\text{res}}$  was achieved by applying to the samples a specific procedure which includes proteinase K (PK) treatment (under conditions where  $\text{PrP}^{\text{sen}}$  is entirely degraded while most of the sequence of  $\text{PrP}^{\text{res}}$  is preserved) and takes advantage of the peculiar aggregation properties of  $\text{PrP}^{\text{res}}$ . The same procedure allows  $\text{PrP}^{\text{res}}$  (as scrapie-associated fibrils, SAFs) to be concentrated by low-speed centrifugation. The corresponding pellet is resuspended by addition of an appropriate solution which leads to complete denaturation of the protein. This sample-processing procedure can be achieved within 30 minutes. PrP was finally determined using the immunometric assay, after 1/3 dilution in an appropriate buffer. This approach has the following advantages:

- PK treatment and centrifugation ensure the selectivity of the test since resistance to proteolysis and aggregation are well-established characteristics of  $\text{PrP}^{\text{res}}$ .
- The sample-treatment procedure concentrates  $\text{PrP}^{\text{res}}$ , thus increasing the sensitivity of the test. It does not significantly protract the test, since it is completed within 30 minutes.

- PK treatment and the denaturation/renaturation process yield “cleaner” samples partially or totally devoid of infectious properties and less subject to non-specific interference (non-specific adsorption, interference due to heterophilic antibodies...) possibly leading to false-positive responses.
- Final measurements are made using conventional two-site immunometric assays which do not require antibodies specifically recognizing PrP<sup>res</sup>. This allows more possibilities in selecting high-affinity antibodies for sensitive detection of PrP.
- The immunometric assay can easily be adapted to any existing automatic apparatus (currently used in this kind of test) thus allowing high throughput analysis.

The performance of our test was analysed, together with three other tests, in the framework of an evaluation study conducted by the Directorate General XXIV (DG XXIV) of the European Commission. This study took place during May 1999 and on this occasion approximately 1600 brain stem samples were analysed by our group. The results of this study were published in the form of a preliminary report (<http://europa.eu.int/comm/dg24/health/>) and as a letter in Nature [5]. We present here the main results we recorded during this exercise, including additional data and comments.

### Immunometric assays for PrP

In recent years we have produced and characterised more than 90 monoclonal antibodies (mAbs) directed against PrP by immunising mice with synthetic peptides, recombinant PrP or Scrapie-Associated Fibril (SAF) preparations obtained from infected hamster brain. These mAbs were used to establish two-site immunometric assays allowing sensitive and specific determination of human, bovine, ovine, mouse and hamster PrP<sup>sen</sup>, as observed in brain extracts for instance [1]. These assays involved a capture antibody passively adsorbed on polystyrene microtitre plates and, as tracer antibody, Fab' fragments labelled with the enzyme acetylcholinesterase (AChE, patent). The Fab' fragment was labelled as previously described for other immunometric assays [3]. As an illustration, standard curves obtained with a recombinant ovine PrP are presented in Fig. 1. In this case, a detection limit close to 50 pg/ml was determined with the best pair of mAbs (SAF-34/12F10). In addition, we observed that the detection was little influenced by the composition of the medium as exemplified by the pair 8G8 + 3B5/12F10 (see Fig. 1) since very similar standard curves were observed in buffer and in a 1% brain extract from a knock-out mouse. This illustrates the advantage of using a specific capture of PrP in contrast with ELISA methods [4, 6, 7] which involve direct adsorption of PrP on the solid phase and are thus dependent on the composition of the sample which may contain other proteins competing with PrP for solid-phase immobilisation.

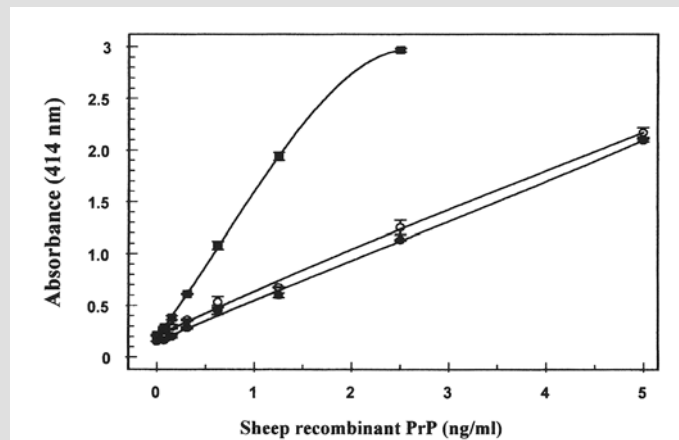


**Fig. 1.** Standard curves established with recombinant sheep PrP. ■ SAF-34/12F10; ● 3B5+8G8/12F10; ○ 3B5+8G8/12F10, standard diluted in 1% PrP<sup>0/0</sup> mouse brain extract

### The DG XXIV evaluation study

At the beginning of May 1999, we received 1605 brain stem samples divided in two series. The first series was composed of 1400 brain stem pieces (about 1 g each) taken either from 1000 healthy cows of similar age slaughtered in New Zealand (1064 samples, including 64 replicates) or from 300 BSE-positive cows showing clinical signs (confirmed by histopathological examination) slaughtered in Great Britain (336 samples, including 36 replicates). The second series was composed of 205 homogenates samples which were obtained by diluting a positive brain homogenate of known infectivity titre ( $10^{3.1}$  mouse i.c./i.p. LD<sub>50</sub>/g of tissue) in a negative brain homogenate up to  $10^{-5}$ . This second series was intended for estimation of the capacity of each test to detect low levels of PrP<sup>res</sup>. The entire study was done under blind conditions using coded samples and under the constant supervision of a DG XXIV representative. Each participant was compelled to perform the assay within 24 hours and to provide every day the results of his measurements.

In our case, samples were divided into batches of 32 which were analysed in a single microtitre plate (in duplicate) which also included 3 negative controls (brain stem from healthy cows slaughtered in France) and 3 positive controls (3 dilutions of brain stem homogenates from BSE-positive cows slaughtered in Great Britain). Nonspecific binding was estimated in separate wells by adding assay buffer instead of samples. A standard curve was also established using a synthetic peptide carrying the two epitopes recognised by capture and tracer antibodies.

The sensitivity and specificity of the assay were estimated for the first series of 1400 samples by interpreting the results with a cut-off point proposed by the participants before the beginning of the study (0.25 absorbance units (AU), in our case).

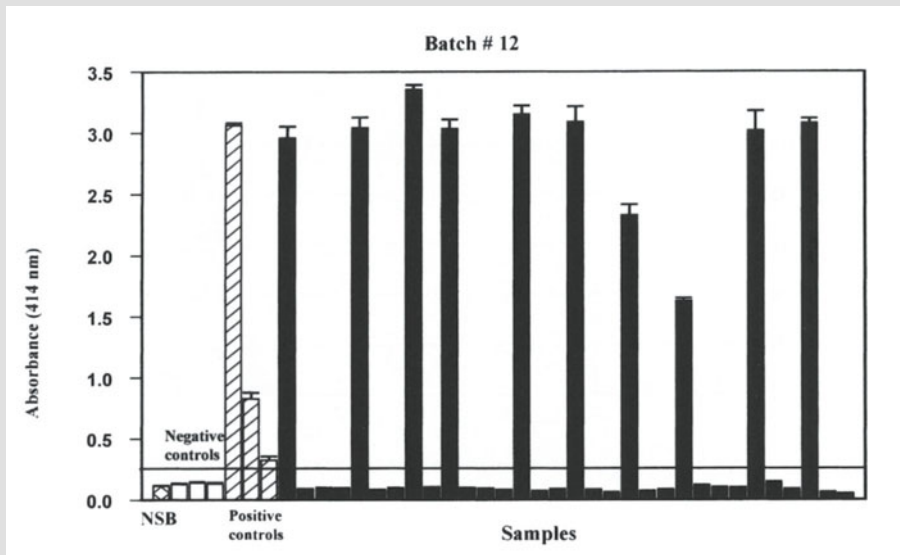


**Fig. 2.** Results obtained with batch # 12 (brain stem samples). Cross-hatched bars: nonspecific binding (NSB), open bars: negative controls, hatched bars: positive controls (3 dilutions of a positive homogenate) full bars: samples. The horizontal line represents the cut-off value (0.25 AU) chosen for categorizing negative and positive samples. It is worth noting that this batch is one of the few containing positive samples giving absorbance values below 2.5 AU (only five samples out of 336)

Our test exhibited 100% sensitivity and specificity, as did two other tests, and 336 positive samples were correctly identified, while no false-positives were observed. This very good result reflects the fact that a very important difference was observed between negative and positive samples with no overlapping of the two populations. This is illustrated in Fig. 2 which schematically represents the results obtained with one batch of 32 samples, and in Figs. 3 and 4 which respectively present the distribution of

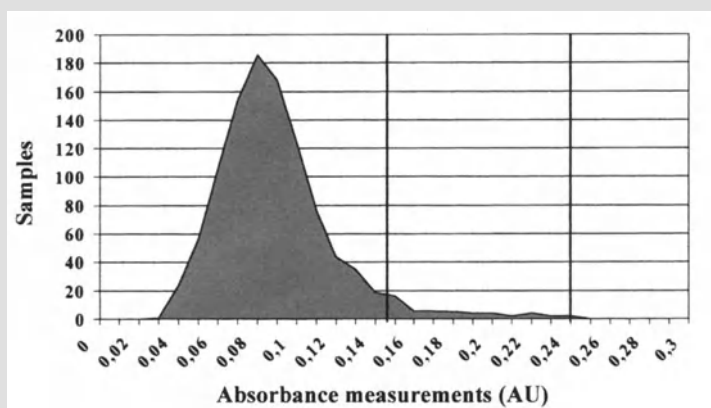


**Fig. 3.** Distribution of the 1064 negative samples (brain stem samples). The first vertical line represents the average + 3 standard deviations (0.156 AU) of the 1036 samples and the second vertical line the arbitrary cut-off value defined at the beginning of the study

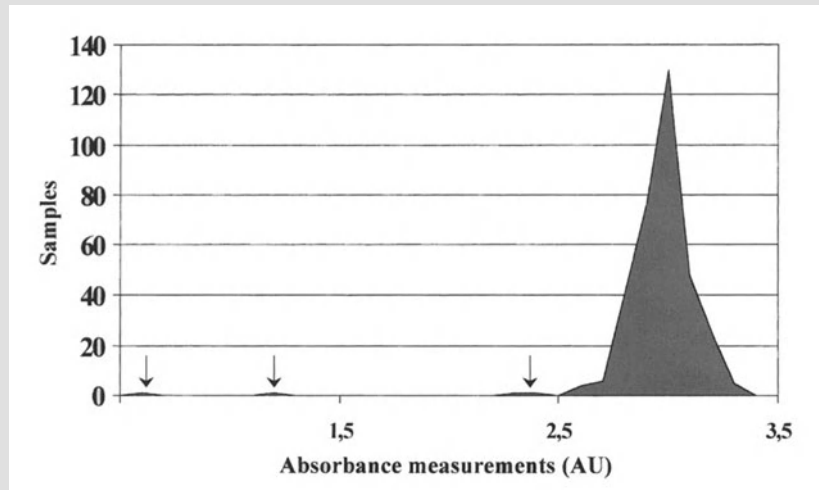


**Fig. 4.** Distribution of the 336 positive samples (brain stem samples). It is worth noting that only five samples (arrows) gave absorbance values below 2.5 AU

negative and positive samples. These data show that all negative samples (as well as negative controls) gave signals below 0.25 AU (mean  $0.093 \pm 0.021$  AU) while positive samples were generally close to 3 AU. Close examination of negative samples shows that a small proportion of them (about 1%, see Fig. 3) gave a significantly higher signal than the average population. We think that this is linked to an imperfect homogenisation of brain stem resulting in the persistence of small pieces of tissue in which PrP<sup>sen</sup> was inaccessible to proteinase K treatment. The presence of these outliers constrained us to define as an arbitrary threshold a 0.25 AU value based on our experience with the negative samples analysed before the beginning of the DG XXIV study. By contrast, few positive samples (5 out of 336) gave signals below 2.5 AU, with 1 sample below 0.5 AU.

It is worth noting that two false-positives were recorded after the whole series had been analysed once. Repeat assay of these two samples, starting with original brain stem tissues, clearly gave negative results indicating that the first positive results were very likely due to cross-contamination by a positive sample. This is not surprising taking into account the huge difference between positive and negative samples (our estimation is that positive samples usually contain 1000 to 10,000 times more immunoreactivity than negative samples) and the very high proportion of positive samples in this particular study (close to 25%). It is clear that the risk of contamination will be much lower in a real situation with the proportion of BSE-positive animals very likely being below 0.5%.

Results obtained in dilution series experiments have shown that our test can significantly detect PrP<sup>res</sup> up to a  $10^{-2.5}$  dilution (see Fig. 5), and are therefore 10 to 300 times more sensitive than the test developed by other participants [5]. It is worth noting that the corresponding brain homogenate contains low levels of PrP<sup>res</sup>, since in most other brain samples we

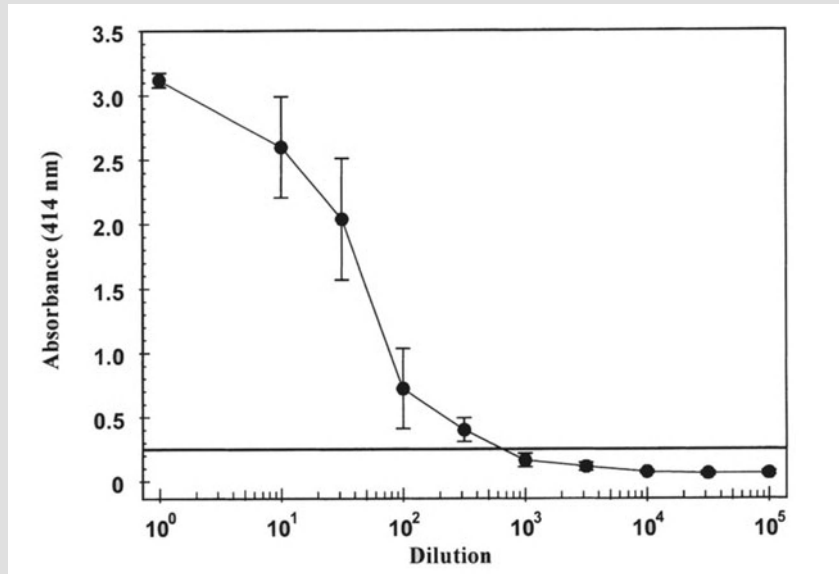


**Fig. 5.** Results obtained from dilution series. Homogenates (series of 20 replicates) were obtained by diluting a positive brain homogenate of known infectivity titre ( $10^{3.1}$  mouse i.c./i.p. LD50/g of tissue) in a negative brain homogenate up to  $10^{-5}$ . The horizontal line represents the cut-off value (0.25 AU) chosen for categorizing negative and positive samples

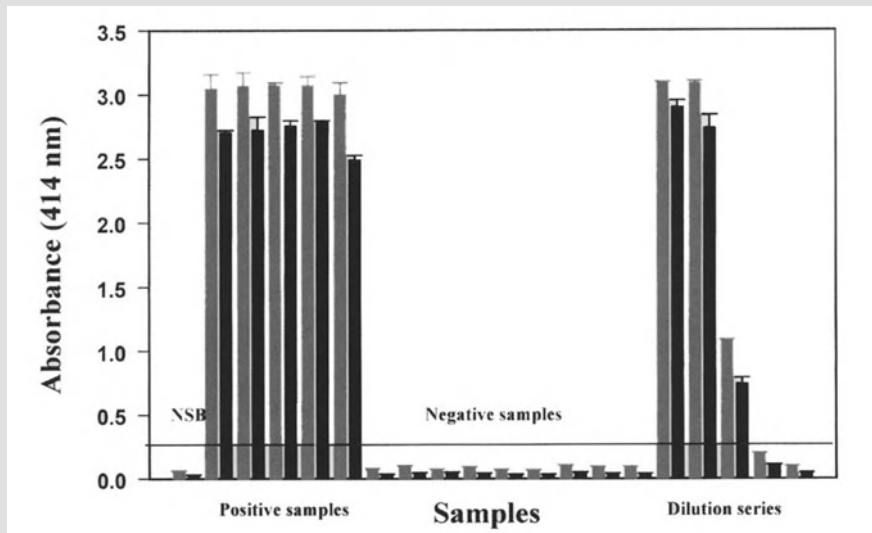


**Fig. 6.** Comparison between a long (3 h + 16 h) and a short (3 h + 3 h) immunometric assay. In these experiments, we compared the results of a long immunometric assay (grey bars, 3 h + 16 h) and a short immunometric assay (black bars, 3 h + 3 h). The comparison was made on 5 positive samples (brain stem), 9 negative samples and one dilution series. It is worth noting that the long procedure gave slightly higher signals with positive samples, which was counterbalanced by higher signals for negative samples, so that the sensitivities of the two assays were identical

could detect PrP<sup>res</sup> after a 1/1000 to 1/10,000 dilution (unpublished results). To compare the sensitivity of our test with the bioassay using mice, it is necessary to adjust the titre measured using this method ( $10^{3.1}$  mouse i.c./i.p. LD50/g of tissue) to the weight of brain actually used in our test (28 mg). This conversion leads to a titre of 35.2 mouse i.c./i.p. LD50/28 mg of tissue, thus demonstrating that our assay can detect 0.11 infectious units ( $35.2/10^{-2.5}$ ).

During the DG XXIV study, the immunometric assay was performed using a long procedure (19 h). By optimising the different steps of the assay, the duration has been reduced to 6 h without affecting the sensitivity of the test as demonstrated in Fig. 6.

### Conclusion

The DG XXIV study has clearly demonstrated that our test is perfectly suited to detection of BSE in the brains of animals presenting clinical signs of the disease. The next step is to evaluate its capacity to detect the PK-resistant form of PrP before the onset of clinical symptoms. This appears very likely since, in most cases, brain samples diluted 1/1000 still contain detectable levels of PrP<sup>res</sup>. However, the demonstration has to be made on real samples obtained from animals currently developing the disease. If this can be demonstrated, this test would be a very efficient tool for evaluating the actual extent of BSE in the framework of large epidemiological studies.

### Acknowledgement

The authors are greatly indebted to P. Lamourette, M. Plaisance, D. Marcé, F. Lamoury, H. Boe and V. Nouvel for expert technical assistance.

### References

1. Créminon C, Rodolfo K, Frobert Y, Turbica I, Fretier P, Demart S, Comoy E, Rezaei H, Hunsmann G, Deslys JP, Grassi J (1999) Production and characterization of monoclonal antibodies against PrP. Measurement of cellular PrP from various mammalian species using two-site immunometric assays. International Symposium "Characterization and diagnosis of prion diseases in animals and man", September 23–25, Tübingen, Germany
2. Ekins RP, Jackson T (1984) Non isotopic immunoassays. An overview. In: Bizollon CA (ed) *Monoclonal antibodies and new trends in immunoassay*. Elsevier, Amsterdam, pp 149–163
3. Grassi J, Frobert Y, Pradelles P, Chercuite F, Gruaz D, Dayer JM, Poubelle PE (1989) Production of monoclonal antibodies against interleukin 1 $\alpha$  and 1 $\beta$ . Development of two enzyme immunometric assays (EIA) using acetylcholinesterase and their application to biological media. *J Immunol Methods* 123: 193–210
4. Grathwohl K-U, Horiuchi M, Ishiguro N, Shiganawa M (1997) Sensitive enzyme-linked immunosorbent assay for detection of PrP<sup>sc</sup> in crude extract from scrapie-affected mice. *J Virol Methods* 64: 205–216

5. Moynagh J, Schimmel H (1999) Tests for BSE evaluated. *Nature* 400: 105
6. Safar J, Wille H, Itri V, Groth D, Serban H, Torchie M, Cohen FE, Prusiner SB (1998) Eight prion strains have PrP<sup>Sc</sup> molecules with different conformations. *Nature Med* 10: 1157–1165
7. Serban D, Taraboulos A, DeArmond SJ, Prusiner SB (1990) Rapid detection of Creutzfeldt–Jakob disease and scrapie prion protein. *Neurology* 40: 110–117

Authors' address: Dr. J. Grassi, CEA, Service de Pharmacologie et d'Immunologie, CEA Saclay, 91191 Gif sur Yvette Cedex, France.

## **Characterization of the Infectious Agent**

## **PrP<sup>Sc</sup> typing by N-terminal sequencing and mass spectrometry**

**S. G. Chen, W. Zou, P. Parchi, and P. Gambetti**

Division of Neuropathology, Institute of Pathology, Case Western Reserve University, Cleveland, Ohio, U.S.A.

**Summary.** The heterogeneity of the clinicopathological phenotype in human prion diseases is associated with the presence of the different forms of the abnormal prion protein, PrP<sup>Sc</sup>. We have previously shown that PrP<sup>Sc</sup> in FFI and a subtype of familial CJD linked to the D178N mutation can be distinguished by their difference in gel mobility following proteinase K (PK) treatment. To further characterize the structural difference of PrP<sup>Sc</sup> in familial prion diseases, N-terminal sequencing and mass spectrometry were used to identify the protease cleavage sites in PrP<sup>Sc</sup> extracted from affected brains. We found that the main PK cleavage sites of PrP<sup>Sc</sup> are located at residue 97 in FFI, and residue 82 in both CJD<sup>178</sup> and a GSS subtype linked to the P102L mutation. The differential accessibility to protease in the native PrP<sup>Sc</sup> suggests that PrP<sup>Sc</sup> exist as distinct conformers in different disease states.

### **Introduction**

Prion diseases are a group of neurodegenerative disorders characterized by the presence of abnormal protease-resistant isoform of prion protein, PrP<sup>Sc</sup> [19]. They include scrapie and bovine spongiform encephalopathy (BSE) in animals, and Creutzfeldt-Jakob disease (CJD), Gerstmann-Sträussler-Scheinker syndrome (GSS), fatal familial insomnia (FFI) and kuru in humans. CJD occurs usually as a sporadic form, but can also be inherited through mutations in the PrP gene or acquired by contamination involving medical procedures (iatrogenic CJD). A distinct CJD subtype often referred to as new variant CJD, has emerged recently and is casually linked to BSE in cattle. GSS and FFI are mostly familial whereas kuru is acquired. The phenotypic differences based on disease pathology and PrP<sup>Sc</sup> distribution in different brain regions have traditionally been used to distinguish these disease groups. Such phenotypic diversity is reminiscent of the existence of “prion strains” in animal models [2] and presents a challenge to the protein-only hypothesis, which proposes that the major component of the pathogen causing prion diseases is PrP<sup>Sc</sup> derived from the normal PrP

(PrP<sup>C</sup>) by the  $\alpha$ -helix to  $\beta$ -sheet conformational change [18]. Detailed studies on familial forms of prion diseases should provide insight into the role that conformational changes of PrP<sup>Sc</sup> caused by the mutations play in the pathogenesis of prion diseases.

Previously, we have presented the first example of PrP<sup>Sc</sup>-associated prion diversity in humans in a comparative study of FFI and a familial form of CJD (CJD<sup>178</sup>) [13]. Both diseases are linked to the same PrP mutation at codon 178 but to different polymorphism at codon 129 on the mutant allele which encodes methionine (M) in FFI and valine (V) in CJD<sup>178</sup> [9]. Western blot analysis revealed that, following treatment with proteinase K (PK) and enzymatic deglycosylation, PrP<sup>Sc</sup> migrated as a 19 kDa band in FFI and a 21 kDa band in CJD<sup>178</sup> [13]. This study has provided the rationale for the subsequent typing of PrP<sup>Sc</sup> based on gel mobility in sporadic CJD [16]. While PrP<sup>Sc</sup> typing as determined by gel migration of protein bands has been highly effective in assisting the identification of different PrP<sup>Sc</sup> subtypes in human prion diseases [6, 15, 16], the limited resolution of SDS-PAGE precludes the detailed studies of their molecular nature. Here, we will review our work on the analysis of the precise protease cleavage sites in PrP<sup>Sc</sup> by N-terminal sequencing and mass spectrometry in FFI and CJD<sup>178</sup>, as well as GSS linked to P102L mutation (GSS<sup>102</sup>). Our studies provide a strong support for the role of PrP<sup>Sc</sup> conformational variations in the phenotypic expression of prion diseases.

### PrP<sup>Sc</sup> subtypes in familial prion diseases

Three familial prion diseases were chosen for the detailed studies. They are characterized by the presence of specific mutations coupled with the 129M/V polymorphism on the mutant PrP allele: D178N-129M in CJD<sup>178</sup>, D178N-129M in FFI, and P102L-129M in GSS. Although all cases studied are heterozygous for the respective mutation, the wild-type PrP encoded by the normal allele is not part of the PK-resistant PrP<sup>Sc</sup> core fragment [3, 17, 24]. Thus, the following work can be regarded as the characterization of mutant PrP<sup>Sc</sup> in these familial cases.

PrP<sup>Sc</sup> migrated on SDS-PAGE as three bands representing unglycosylated, monoglycosylated and diglycosylated forms, as shown on immunoblots of PK-treated brain homogenates (Fig. 1, lanes 1–3). A difference in electrophoretic mobility in PrP<sup>Sc</sup> bands between three cases was seen which became more apparent after deglycosylation (lanes 4–6). The unglycosylated PrP<sup>Sc</sup> had relative molecular weight of either  $\sim$ 21 kDa or  $\sim$ 19 kDa, which corresponded to type 1 and type 2 PrP<sup>Sc</sup> as proposed by Parchi et al. [16]. It is clear that CJD<sup>178</sup> and GSS<sup>102</sup> were characterized by the presence of type 1 PrP<sup>Sc</sup>, whereas FFI was associated with type 2 PrP<sup>Sc</sup>. At variance with CJD<sup>178</sup> and FFI, GSS<sup>102</sup> also contained an additional smaller PrP<sup>Sc</sup> fragment of  $\sim$ 8 kDa (data not shown) [17]. The  $\sim$ 8 kDa fragment is a

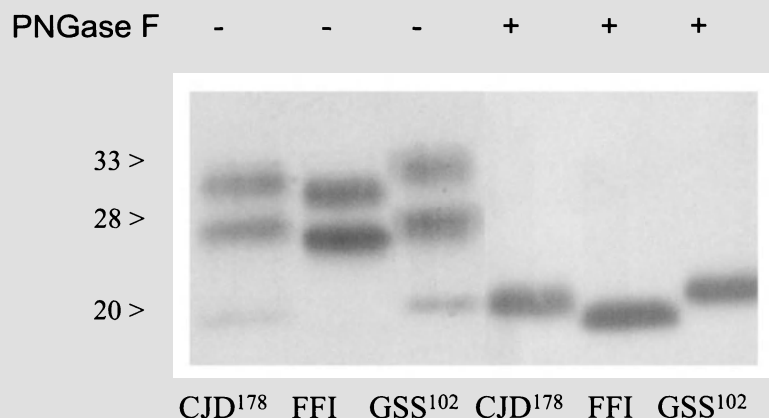


**Fig. 1.** Western blot analysis of brain homogenates from subjects affected by CJD<sup>178</sup>, FFI and GSS<sup>102</sup>. Brain homogenates from three subjects affected by CJD<sup>178</sup>, FFI and GSS<sup>102</sup>, respectively, were incubated with 50 µg/ml of PK for 1 h at 37 °C. Proteins were then either left untreated (-) or treated (+) with PNGase F prior to separation by SDS-PAGE. Molecular size markers of 20-, 28-, and 33-kDa are shown on the left

major component of PrP amyloid, which is present in relatively large quantity in the GSS brains [8].

#### Mapping of PK cleavage sites in PrP<sup>Sc</sup> by N-terminal sequencing and mass spectrometry

PK was used originally by Prusiner et al. [12] to conveniently distinguished PrP<sup>Sc</sup> from normal PrP<sup>C</sup>. The unusual resistance to PK of PrP<sup>Sc</sup> correlates with the spectroscopic data showing a drastic increase in the β-sheet content in PrP<sup>Sc</sup> [14, 22]. Interestingly, PK is also widely used in structural studies to probe protein conformation, taking advantage of differential accessibility of different folded protein domains to the protease.

The N-terminal part of the native human PrP<sup>Sc</sup> (starting at residue 23) was shown to be degraded by PK, generating a newly created C-terminal core fragment resistant to the proteolytic digestion [13]. Previous studies on scrapie PrP<sup>Sc</sup> in animal models [18] have mapped a main PK cleavage site at residue 90. However, no PK cleavage sites were mapped in a systemic way in human PrP<sup>Sc</sup>.

To obtain sufficient amount of PrP<sup>Sc</sup> for detailed structural studies, we had undertaken a relative large scale purification of PrP<sup>Sc</sup> in diseased brains using previously reported methods [1, 3] which involved differential detergent extraction and ultracentrifugation to sediment PrP<sup>Sc</sup>, followed by PK treatment to eliminate normal PrP<sup>C</sup> and other protein contaminants. The final PrP<sup>Sc</sup> preparation was further purified by the continuous elution preparative SDS-PAGE. The fractions containing PrP<sup>Sc</sup> were concentrated

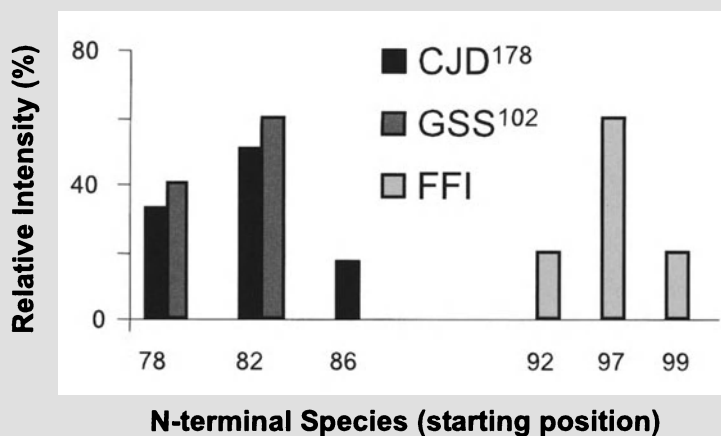


**Fig. 2.** PK cleavage sites identified by N-terminal sequencing. PK-treated PrP<sup>Sc</sup> purified from brain tissues of three subjects affected by CJD<sup>178</sup>, GSS<sup>102</sup>, and FFI, respectively, was analyzed by automated N-terminal protein sequencing. The N-terminal species detected were used to derive the PK cleavage sites which were found to be located at residues 78, 82, and 86 for CJD<sup>178</sup>, at residues 78 and 82 for GSS<sup>102</sup>, and at residues 92, 97, and 99 for FFI. The relative signal intensities of individual N-terminal species starting at specific residue positions were shown for each case. The most prevalent PK cleavage sites were residue 82 for CJD<sup>178</sup> and GSS<sup>102</sup>, and residue 97 for FFI

and were transferred to Problott membrane for protein sequence analysis. In addition, PrP<sup>Sc</sup> was also analyzed by peptide mapping using mass spectrometry.

The N-terminal sequence of purified PrP<sup>Sc</sup> was determined by automated Edman degradation. Alignment of all residues determined in each consecutive cycle with the known human PrP sequence [20] revealed several N-terminal sequences for either type 1 or type 2 PrP<sup>Sc</sup> (Fig. 2). A mixture of N-terminal variants was seen in CJD<sup>178</sup>, GSS<sup>102</sup> and FFI. However, there were marked differences between PrP<sup>Sc</sup> in the three diseases in the location of the N-termini. For CJD<sup>178</sup> and GSS<sup>102</sup>, the major N-terminal sequence started at residue G82, with ragged sequences beginning at G78 or G86. In contrast, FFI was characterized by the predominant presence of the N-terminal sequence beginning at residue S97, flanked by that starting at residues G92 and W99.

The presence of the N-terminal species was confirmed by the peptide mass mapping by matrix-assisted laser desorption/ionization mass spectrometry using a previously established strategy [17]. As shown for the 21 kDa, type 1 PrP<sup>Sc</sup> in GSS<sup>102</sup> (Fig. 3), the mass spectrum revealed signals for two prominent N-terminal species starting at residues 82 and 78. Therefore, our approach using more accurate analytical tools has provided data on the exact PK cleavage sites in human PrP<sup>Sc</sup> that are unobtainable by the previous gel-based typing studies.

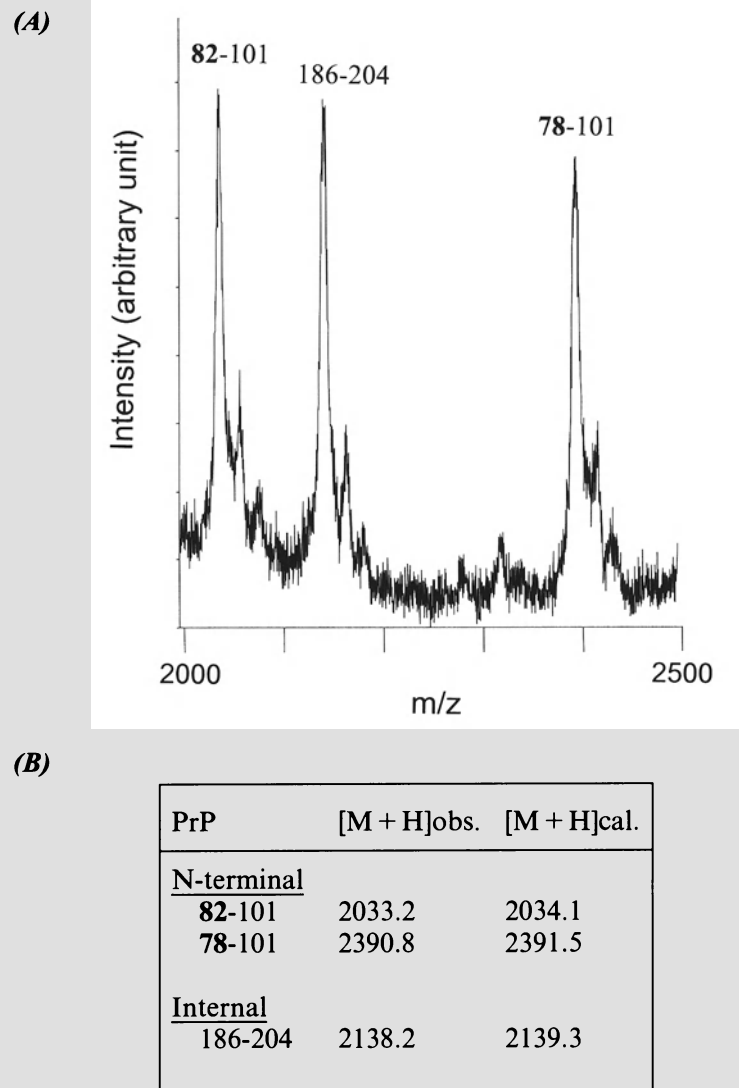


**Fig. 3.** Mass spectrometric analysis of PK cleavage sites of PrP<sup>Sc</sup> in GSS<sup>102</sup>. Purified and PK-resistant 21 kDa PrP<sup>Sc</sup> from a case of GSS linked to the P102L mutation was digested with endoprotease Lys-C. **A** Matrix-assisted laser desorption/ionization mass spectrum of the digest showed three major signals in the  $m/z$  2000–2500 range, corresponding to two N-terminal peptides of PrP82-101 and PrP78-101, and one internal peptide of PrP186-204. **B** The basis for the assignment of the PrP peptides was presented. The observed signals in *A* have the values of  $m/z$  ([M + H]obs.) that match closely with those derived from the theoretical calculation ([M + H]cal.) for the protonated PrP peptides as assigned. Therefore, the PK cleavage sites in the N-terminal region of PrP<sup>Sc</sup> in GSS<sup>102</sup> are located at residues 82 and 78, respectively

### Discussion

Recent NMR measurements of recombinant PrP have provided a structural model of PrP<sup>C</sup> which shares the dominant presence of  $\alpha$ -helices [7, 11, 21]. However, to date no 3-D structure is available for PrP<sup>Sc</sup> which is rich in  $\beta$ -sheets, insoluble and aggregated. The formation of PrP<sup>Sc</sup> involving a change from  $\alpha$ -helical to  $\beta$ -pleated conformation is believed to be essential in the pathogenesis of prion diseases [5]. Current approaches for the structural studies of PrP<sup>Sc</sup> include spectroscopic measurements [14, 22], antibody affinity assay [10, 23] and proteolysis followed by gel electrophoresis [6, 13, 16]. Currently, PK digestion followed by Western blot analysis allows for rapid and definitive diagnosis of prion diseases since PK completely degrades PrP<sup>C</sup> while it only partially hydrolyzes PrP<sup>Sc</sup> to produce a protease-resistant core. Using this simple method, we have previously detected the existence of two distinct PrP<sup>Sc</sup> subtypes in CJD<sup>178</sup> and FFI [13]. As demonstrated here, we have now successfully used accurate N-terminal microsequencing and mass spectrometry to locate the precise PK cleavage sites. The finding that a protease of a broad spectrum such as PK cleaves susceptible sites in solvent-exposed and unstructured regions may provide insights into conformations adopted by the different PrP<sup>Sc</sup> subtypes or “prion strains”.

Here we have reviewed our studies on PrP<sup>Sc</sup> typing based on the precise PK cleavage sites in three prion diseases linked to PrP gene mutations. Our data provide evidence for distinct conformational states in which PrP<sup>Sc</sup> exists in different disease phenotypes. No PK-resistant component was found in the region spanning residues 23–81, a finding consistent with the previous results [4, 13]. This indicates that the N-terminal domain between residues 23–81 region is very sensitive and susceptible to the degradation by PK regardless of the source of PrP<sup>Sc</sup>, and thus is likely to be most flexible and unstructured as in PrP<sup>C</sup>. The PrP<sup>Sc</sup> region between residues 82–97 seems to be structurally dimorphic since it is largely preserved and remains inaccessible to PK in CJD<sup>178</sup> and GSS<sup>102</sup>, whereas it is still sensitive to PK in FFI. Therefore, this region appears to be part of the N-terminal flexible region in FFI while it may become a structurally more rigid region in CJD<sup>178</sup> and GSS<sup>102</sup>. Since PrP<sup>Sc</sup> in CJD<sup>178</sup> and FFI differs only by one amino acid change at position 129 (V vs M), the codon 129 may be involved in conformational change in the PrP<sup>Sc</sup> structure. The fact that GSS<sup>102</sup> may also adopt a PrP<sup>Sc</sup> structure similar to that of CJD<sup>178</sup> suggest that the PK-resistant PrP<sup>Sc</sup> in CJD<sup>178</sup> and GSS<sup>102</sup> is in a similar conformation. Alternatively, there is a possibility that there is further heterogeneity in the PrP<sup>Sc</sup> structure between CJD<sup>178</sup> and GSS<sup>102</sup> in the C-terminal PK resistant region but this region remains inaccessible to PK in both diseases. In this case, a higher resolution method is needed to resolve the difference.

In summary, our studies have enabled us to derive important structural information of PrP<sup>Sc</sup> in three familial prion diseases using more accurate analytical tools than the current gel-based PrP<sup>Sc</sup> typing. This approach will undoubtedly be useful in characterizing the PrP<sup>Sc</sup> structure in other prion diseases, and more importantly, it will provide a basis for a more detailed understanding of the prion diversity in both humans and animals.

### References

1. Bolton DC, Bendheim PE, Marmorstein AD, Potempska A (1987) Isolation and structural studies of the intact scrapie agent protein. *Arch Biochem Biophys* 258: 579–590
2. Bruce ME, McConnell I, Fraser H, Dickinson AG (1991) The disease characteristics of different strains of scrapie in Sinc congenic mouse lines: implications for the nature of the agent and host control of pathogenesis. *J Gen Virol* 72: 595–603
3. Chen SG, Parchi P, Brown P, Capellari S, Zou W, Cochran EJ, Vnencak-Jones CL, Julien J, Vital C, Mikol J, Lugaresi E, Autilio-Gambetti L, Gambetti P (1997) Allelic origin of the abnormal prion protein isoform in familial prion diseases. *Nature Med* 3: 1009–1015
4. Chen SG, Teplow DB, Parchi P, Teller JK, Gambetti P, Autilio-Gambetti L (1995) Truncated forms of the human prion protein in normal brain and in prion diseases. *J Biol Chem* 270: 19173–19180
5. Cohen FE, Prusiner SB (1998) Pathologic conformations of prion proteins. *Annu Rev Biochem* 67: 793–819
6. Collinge J, Sidle KC, Meads J, Ironside J, Hill AF (1996) Molecular analysis of prion strain variation and the aetiology of ‘new variant’ CJD. *Nature* 383: 685–690
7. Donne DG, Viles JH, Groth D, Mehlhorn I, James TL, Cohen FE, Prusiner SB, Wright PE, Dyson HJ (1997) Structure of the recombinant full-length hamster prion protein PrP(29–231): the N terminus is highly flexible. *Proc Natl Acad Sci USA* 94: 13452–13457
8. Ghetti B, Dlouhy SR, Giaccone G, Bugiani O, Frangione B, Farlow MR, Tagliavini F (1995) Gerstmann–Sträussler–Scheinker disease and the Indiana kindred. *Brain Pathol* 5: 61–75
9. Goldfarb LG, Petersen RB, Tabaton M, Brown P, LeBlanc AC, Montagna P, Cortelli P, Julien J, Vital C, Pendelbury WW, Haltia M, Willis PR, Hauw JJ, McKeever PE, Monari L, Schrank B, Swergold GD, Autilio-Gambetti L, Gajdusek DC, Lugaresi E, Gambetti P (1992) Fatal familial insomnia and familial Creutzfeldt–Jakob disease: disease phenotype determined by a DNA polymorphism. *Science* 258: 806–808
10. Korth C, Stierli B, Streit P, Moser M, Schaller O, Fischer R, Schulz-Schaeffer W, Kretschmar H, Raeber A, Braun U, Ehrensperger F, Hornemann S, Glockshuber R, Riek R, Billeter M, Wüthrich K, Oesch B (1997) Prion (PrP<sup>Sc</sup>)-specific epitope defined by a monoclonal antibody. *Nature* 390: 74–77
11. Liu H, Farr-Jones S, Ulyanov NB, Llinas M, Marqusee S, Groth D, Cohen FE, Prusiner SB, James TL (1999) Solution structure of Syrian hamster prion protein rPrP(90–231). *Biochemistry* 38: 5362–5377

12. McKinley MP, Bolton DC, Prusiner SB (1983) A protease-resistant protein is a structural component of the scrapie prion. *Cell* 35: 57–62
13. Monari L, Chen SG, Brown P, Parchi P, Petersen RB, Mikol J, Gray F, Cortelli P, Montagna P, Ghetti B, Goldfarb LG, Gajdusek DC, Lugaresi E, Gambetti P, Autilio-Gambetti L (1994) Fatal familial insomnia and familial Creutzfeldt–Jakob disease: different prion proteins determined by a DNA polymorphism. *Proc Natl Acad Sci USA* 91: 2839–2842
14. Pan KM, Baldwin M, Nguyen J, Gasset M, Serban A, Groth D, Mehlhorn I, Huang Z, Fletterick RJ, Cohen FE, Prusiner SB (1993) Conversion of alpha-helices into beta-sheets features in the formation of the scrapie prion proteins. *Proc Natl Acad Sci USA* 90: 10962–10966
15. Parchi P, Capellari S, Chen SG, Petersen RB, Gambetti P, Kopp N, Brown P, Kitamoto T, Tateishi J, Giese A, Kretzschmar H (1997) Typing prion isoforms. *Nature* 386: 232–234
16. Parchi P, Castellani R, Capellari S, Ghetti B, Young K, Chen SG, Farlow M, Dickson DW, Sima AA, Trojanowski JQ, Petersen RB, Gambetti P (1996) Molecular basis of phenotypic variability in sporadic Creutzfeldt–Jakob disease. *Ann Neurol* 39: 767–778
17. Parchi P, Chen SG, Brown P, Zou W, Capellari S, Budka H, Hainfellner J, Reyes PF, Golden GT, Hauw JJ, Gajdusek DC, Gambetti P (1998) Different patterns of truncated prion protein fragments correlate with distinct phenotypes in P102L Gerstmann–Straussler–Scheinker disease. *Proc Natl Acad Sci USA* 95: 8322–8327
18. Prusiner SB (1991) Molecular biology of prion diseases. *Science* 252: 1515–1522
19. Prusiner SB (1998) The prion diseases. *Brain Pathol* 8: 499–513
20. Puckett C, Concannon P, Casey C, Hood L (1991) Genomic structure of the human prion protein gene. *Am J Hum Genet* 49: 320–329
21. Riek R, Hornemann S, Wider G, Billeter M, Glockshuber R, Wüthrich K (1996) NMR structure of the mouse prion protein domain PrP(121–321). *Nature* 382: 180–182
22. Safar J, Roller PP, Gajdusek DC, Gibbs CJ Jr (1993) Thermal stability and conformational transitions of scrapie amyloid (prion) protein correlate with infectivity. *Protein Sci* 2: 2206–2216
23. Safar J, Wille H, Itri V, Groth D, Serban H, Torchia M, Cohen FE, Prusiner SB (1998) Eight prion strains have PrP(Sc) molecules with different conformations. *Nature Med* 4: 1157–1165
24. Tagliavini F, Prelli F, Porro M, Rossi G, Giaccone G, Farlow MR, Dlouhy SR, Ghetti B, Bugiani O, Frangione B (1994) Amyloid fibrils in Gerstmann–Straussler–Scheinker disease (Indiana and Swedish kindreds) express only PrP peptides encoded by the mutant allele. *Cell* 79: 695–703

## Characterization of BSE and scrapie strains/isolates

M. H. Groschup<sup>1</sup>, T. Kuczius<sup>1</sup>, F. Junghans<sup>1</sup>, T. Sweeney<sup>2</sup>,  
W. Bodemer<sup>1</sup>, and A. Buschmann<sup>1</sup>

<sup>1</sup>Federal Research Centre for Virus Diseases of Animals, Tübingen, Germany

<sup>2</sup>Faculty of Veterinary Medicine, University College Dublin, Ireland

**Summary.** Following the BSE epidemic in cattle and the emergence of a variant form of Creutzfeldt–Jakob disease in humans, the question was raised whether BSE has been transmitted to small ruminants by the inadvertent feeding of infectious meat and bone meal. Such infections could easily be concealed in countries where scrapie is endemic. To address this issue by immuno-chemically analyzing the PrP<sup>Sc</sup> fragments, we have developed two lines of research. Firstly we have focused on the development of criteria for the differential characterization of experimental BSE and scrapie strains/isolates in rodents. To date, three criteria have been identified: quantification of the relative banding intensities of PrP<sup>Sc</sup> glycotypes using a photoimaging technique; the non-uniform kinetic of proteinase K degradation of PrP<sup>Sc</sup>; and differences in the molecular masses of their non-glycosylated PrP<sup>Sc</sup> fragments after PK cleavage in immunoblot. The second line of research focused on the implementation of the criteria described above to representative samples from scrapie diseased Irish sheep. Using these three criteria, no evidence was found for the presence of a BSE infection in these animals. However, the final conclusion must take into account the results of mouse incubation time and mouse lesion profile data which are currently being generated.

### Introduction

A variety of TSE strains can be discriminated by their different host ranges and by the clinical signs, incubation times and neuropathology in the brains of affected rodents [2, 8, 10, 14]. Some TSE strains differ also in their resistance to physical and chemical inactivation [22]. In the seventies and eighties, mouse incubation time and brain lesion profile scoring assays were developed by thorough standardization and analysis of mouse infection experiments [3–5, 13–15]. However, in these assays large numbers of animals (26 mice per line) from three different highly inbred mouse lines (C57Bl, VM95, RIII) plus their intercrosses needed to be infected and

subsequently analysed. Although the results obtained using this mouse inoculation procedure are very reliable, the effort and time needed for conducting these experiments are considerable.

Hence alternative criteria and techniques were sought to characterize TSE agents. Prion infections are accompanied by the accumulation of an abnormal isoform (designated PrP<sup>Sc</sup>) of normal (PrP<sup>C</sup>) host-encoded prion protein. Both isoforms have the same amino acid sequence and molecular mass, but differ dramatically in their three dimensional structure and biochemical characteristics.

### **Molecular mass determination and 'glycotyping' of proteinase K treated PrP<sup>Sc</sup>**

Glycotyping is a procedure involving the isolation, proteinase K digestion and immunoblotting of PrP<sup>Sc</sup> from infected animals. The protein normally segregates into three bands of different molecular masses on a SDS-PAGE gel. The different molecular masses are caused by the number of glycosylation chains on the protein molecule. As PrP<sup>C</sup> can be glycosylated twice at asparagines at positions 180 and 196 of the protein [11], three differently glycosylated isoforms can be found in the cell, i.e. non-, mono- and diglycosylated fractions. As early as 1985, differences in the molecular masses of nonglycosylated PrP<sup>Sc</sup> fragments of scrapie strains after proteinase K digestion had been identified. While PrP<sup>Sc</sup> of most scrapie strains had a molecular mass of 21 kDa, PrP<sup>Sc</sup> of strain 87V was slightly smaller in size, approximately 19 kDa [20]. A similar difference was later noted for the two known and well characterized transmissible mink encephalopathy (TME) strains 'hyper' and 'drowsy' using an antibody raised against amino acid residues 89 to 103 of PrP [2, 25]. Hence, PrP<sup>Sc</sup> of these two strains carry either different proteinase K cleavage sites or are derived from different posttranslationally processed PrP precursors and therefore differ in composition or conformation, or both.

In conventional human TSE cases, three different molecular masses were found for nonglycosylated PrP<sup>Sc</sup>. These are 21, 20 kDa, or 19 kDa. In contrast, vCJD cases accumulated PrP<sup>Sc</sup> of a molecular mass of 19 kDa [9]. These authors proposed four human PrP<sup>Sc</sup> types according to their fragment sizes and relative amounts of the three glycoforms (types 1–4, see below). However, others did not observe the nonglycosylated 20 kDa PrP<sup>Sc</sup> type, but only nonglycosylated PrP<sup>Sc</sup> of molecular masses 19 and 21 kDa [7, 26]. Although the reason for some differences in the results obtained in different laboratories are still unclear, it was recently identified that the presence or absence of divalent cations, such as copper, may influence the molecular mass of PrP<sup>Sc</sup> after proteinase K cleavage [30]. Addition of the metal chelator EDTA to the PK digestion results in a reduction in molecular mass from 21 kDa (type 1) or 20 kDa (type 2) to 19 kDa in types 1 and 2. Albeit not proven, copper seems to bind to the long and flexible amino terminus of

PrP<sup>Sc</sup> and thereby modulates the proteolytic stability. It was shown for PrP<sup>C</sup> that proteinase K also first processes the amino terminus before degrading the well structured carboxy terminus [6].

In addition to the different molecular masses for nonglycosylated PrP<sup>Sc</sup>, Collinge and colleagues also noted differences in the ratios of the three glycoforms of PrP<sup>Sc</sup>. While monoglycosylated PrP<sup>Sc</sup> dominates in all conventional human TSE cases analysed to date, vCJD PrP<sup>Sc</sup> is characterized by a predominance of diglycosylated PrP<sup>Sc</sup> [9]. By combining the two results of molecular mass and glycotyping analysis, it became clear that vCJD truly represented a novel type of human prion diseases. As PrP<sup>Sc</sup> derived from BSE infected mice displayed similar molecular characteristics, i.e. low molecular mass and strongly stained diglycosylated PrP<sup>Sc</sup>, a link between both diseases was proposed [9]. However, little was known at that time about the molecular characteristics of PrP<sup>Sc</sup> derived from other experimental murine and sheep scrapie strains/isolates from rodents and no data were available for the BSE and scrapie PrP<sup>Sc</sup> derived directly from ruminants.

#### **Experimental scrapie strains are distinguishable by their PrP<sup>Sc</sup> ‘glycotypes’**

Glycotypes of experimental scrapie and BSE strains were determined in two independent studies using SDS-PAGE and immunoblotting techniques [24, 27]. At the Federal Research Centre, PrP<sup>Sc</sup> glycoprofiles of scrapie strains ME7, 79A, 22A, 87V (propagated in VM95 mice), Chandler and two BSE isolates, all propagated in C57BL/6 mice, were analysed as described [24]. In brief, 10% brain homogenates were analysed by immunoblot using either the polyclonal serum Ra5/7 raised against amino acids 95–110 of murine PrP [16] or, for detection of hamster-passaged PrP<sup>Sc</sup>, the monoclonal antibody 3F4 raised against amino acids 109–112 of human PrP [21]. It was necessary to analyse each sample in at least four different gel runs as substantial artefactual differences between immunoblots of the same samples were already detectable for the naked eye. To further improve the analytical precision we recorded the photon emission of the individual bands electronically.

Four different PrP<sup>Sc</sup> glycotypes were found in the investigated experimental BSE and scrapie strains. PrP<sup>Sc</sup> derived from scrapie strains 79A and Chandler possessed a glycoprofile which was similar to that of PrP<sup>Sc</sup> derived from conventional CJD cases, i.e. the monoglycosylated form represented the main signal (>50%). In contrast, scrapie strain 87V-derived PrP<sup>Sc</sup> consisted of more than 70% of diglycosylated protein. In conventional well established scrapie strains, the diglycosylated band generally represented less than 55% of signal, while in this experiment with BSE PrP<sup>Sc</sup>, the diglycosylated PrP<sup>Sc</sup> represented 55–65%. It is important to note, however, that a clear cut distinction between scrapie 87V and BSE PrP<sup>Sc</sup> was difficult, as both had, apart from the similarity in the glycotype,

nonglycosylated bands of a low molecular mass of 19 kDa. A mouse passaged scrapie isolate from Germany gave a glycotyping pattern similar to ME7, which is believed to be the most common scrapie strain in sheep.

The mouse line used for propagation of the strains/isolate had a minor albeit not negligible influence on the PrP<sup>Sc</sup> glyco-type revealed: while the Chandler PrP<sup>Sc</sup> pattern almost remained unchanged when produced in CD1 or C57BL/6 mice, the BSE pattern revealed in C57BL/6, RIII and VM95 mice was rather non-uniform.

### **PrP<sup>Sc</sup> of different prion strains are characterized by distinct PK cleavage sites**

The observation that PrP<sup>Sc</sup> derived from different strains had different molecular masses after PK digestion lead to the assumption that PrP<sup>Sc</sup> molecules are processed by PK at different cleavage sites. One approach to determine to what extent the amino acid backbone is degraded is by microsequencing the aminotermi-nus [29]. As an alternative technique, we probed such compounds on immunoblots with a panel of different antibodies which bind in the vicinity of the amino acid stretch where the PK cleavage site in PrP<sup>Sc</sup> is assumed. Antibodies binding to the carboxyterminus of PrP (such as mab L42 for ruminant PrP and Ra5/7 for murine PrP) served as positive controls to verify the presence of the PrP<sup>Sc</sup> bands. Interestingly, when using the monoclonal antibody 3B5 which is directed to the octapeptide repeat region of PrP (stretching from amino acids 54–95) PrP<sup>Sc</sup> derived from different strains and species was not detected uniformly. Mab 3B5 did not react with PrP<sup>Sc</sup> derived from BSE infected C57BL/6 mice, while PrP<sup>Sc</sup> fragments of all investigated scrapie strains (22A, ME7, 87V, Chandler) propagated in this mouse line were easily detectable. BSE-PrP<sup>Sc</sup> propagated in RIII mice or tga20 mice also remained unstained when using mab 3B5. However, when BSE and scrapie were passaged in VM95 mice and subsequently analysed, PrP<sup>Sc</sup> of all strains was detected, including BSE (Fig. 1). This result indicates that the host-encoded PrP sequence may also have an impact on the PK cleavage site on PrP<sup>Sc</sup>, as VM95 mice carry the sinc p7p7 allele instead of the sinc s7s7 allele expressed in C57BL/6, RIII and tga20 mice.

Further experiments will now be performed using material from sheep experimentally infected with either scrapie or BSE and with cattle derived BSE or scrapie samples. If a differentiation between scrapie and BSE in sheep was possible using mab 3B5, an improved assessment of TSE cases in sheep would be feasible.

### **Long-term proteinase K resistance of PrP<sup>Sc</sup>**

As 87V and BSE PrP<sup>Sc</sup> were difficult to distinguish on basis of the above mentioned criteria, we studied the proteinase K resistance of PrP<sup>Sc</sup>, to find further molecular and physicochemical markers of strains/isolates [23].

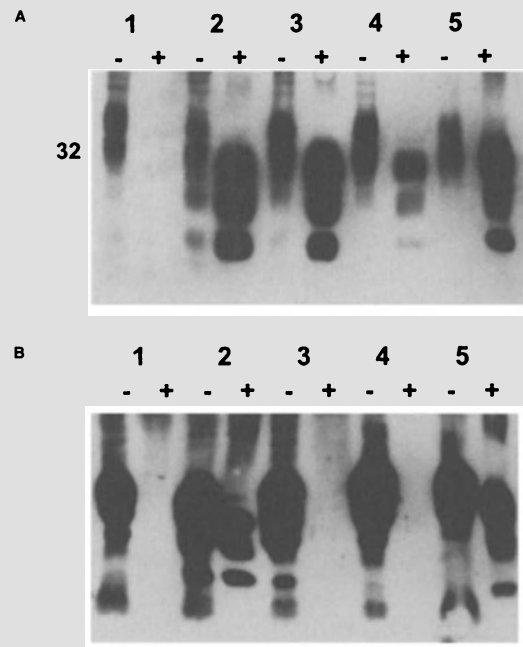


**Fig. 1.** Immunoblots illustrating differences in the proteinase K (PK) cleavage sites of BSE and scrapie PrP<sup>Sc</sup>. PK treated scrapie strain Chandler PrP<sup>Sc</sup> (generated in C57Bl/6 mice) (2) was detected by mab 3B5, while BSE-PrP<sup>Sc</sup> derived from C57Bl/6 (3) or tga20 (4) mice remained unstained. However, BSE-PrP<sup>Sc</sup> derived from VM95 mice (5) was detected when using mab 3B5 was used. 1 was loaded with a preparation of scrapie-associated fibrils from a non-infected C57Bl/6 control mouse. Immunoblots were incubated using **A** polyclonal rabbit serum Ra5/7 (raised against amino acids 98–115) or **B** mab 3B5 (raised against amino acids 57–72. – indicates untreated samples, + indicates the treatment with 50 µg/ml PK at 37 °C

For these studies, the above mentioned strains and isolates as well as hamster scrapie strain 263 K and two more mouse passaged German field scrapie isolates were propagated in the inbred mouse lines C57BL/6, VM95, CD1 or in murine PrP overexpressing transgenic mice (tga20 mice). Incubation times and brain lesion profiles in the animals were monitored and found similar to those described in literature. In order to investigate the sensitivity of scrapie and BSE strains/isolates to proteinase K digestion, standardized (in respect to protein concentration) PrP<sup>Sc</sup> rods purified from brain pools of at least four mice each were digested with 50 µg/ml proteinase K for 1 h, 3 h, 6 h, 24 h and 48 h at 37 °C. The reaction was stopped by addition of phenylmethylsulfonyl fluoride (to 5 mM) followed by heating (95 °C for 15 min). PrP<sup>Sc</sup> was visualized by immunoblot and again quantified electronically. Residual PrP<sup>Sc</sup> antigens were calculated as arithmetical means from repeated runs (minimum 4 runs). PrP<sup>Sc</sup> banding signals after 1 h proteinase K treatment served as a reference (100%).

Under these conditions, PrP<sup>Sc</sup> from different experimental BSE and scrapie strains/isolates displayed rather non-uniform degradation kinetics. While more than 80% of PrP<sup>Sc</sup> from almost all strains were degraded after 48 h of proteinase K exposure, immunoblot signals referring to residual PrP<sup>Sc</sup> after 6 h treatment varied widely from less than 20% up to more than 80% of the respective reference values. For example, more than 80% of PrP<sup>Sc</sup> of strains 87V and ME7 resisted proteolysis, while less than 20% of PrP<sup>Sc</sup> of strain Chandler survived this procedure. Strain 22A PrP<sup>Sc</sup> displayed an intermediate proteinase K resistance. In comparison, PrP<sup>Sc</sup> isolated from BSE cases from Germany or the United Kingdom and passaged in mice had also an intermediate to low resistance to proteinase K treatment (20–40%). Hence, by long-term proteinase K resistance (LTPKR) analysis of PrP<sup>Sc</sup> it became possible to distinguish the previously undistinguishable 87V and BSE strains/isolates on the basis of physico-chemical criteria. The LTPKR analysis of the three German field scrapie isolates revealed a highly resistant, an intermediate and a very proteinase K sensitive PrP<sup>Sc</sup>.

In further experiments, the influence of different mouse lines used for the propagation of TSE agents was analysed. C57BL/6, CD1 and tga20 carry the sinc s7s7 allele in homozygous form, while VM95 mice harbour the sinc p7p7 allele. No effect of the mouse line used for propagation was observed for the German BSE isolate, nor for the scrapie strain Chandler. However, a slight, yet statistically significant difference in the LTPKR analysis was found for PrP<sup>Sc</sup> of scrapie strain 22A if propagated in VM95 or C57BL/6 mice. Thus, depending on the prion strain, the mouse line used as PrP<sup>Sc</sup> source may have a minor effect on its long-term proteinase K stability.

### **PrP<sup>Sc</sup> ‘glycotyping’ and LTPKR analysis on field scrapie cases**

Concerns have been raised about the possibility of an accidental transmission of the BSE agent to sheep as experimental studies have revealed that following oral infection with BSE sheep develop clinical signs that are indistinguishable from conventional scrapie [12]. Efforts have therefore been intensified in the European Union to characterize sheep scrapie cases in order to exclude the possibility of underlying BSE infections. The question whether such infections can be detected in sheep scrapie cases by use of the above criteria for the molecular characterization of PrP<sup>Sc</sup> was therefore addressed [28]. Samples from the central nervous system (thalamus, mediobasal hypothalamus, medulla, cortex, thoracic cord and basal ganglia) were collected from 16 scrapie infected sheep which had shown a wide variety of clinical signs and which were carrying the following PrP genotypes: AARRQH, AARRQQ; VARRQQ; VARRQH. Cerebellar and brain stem samples were also collected from BSE infected cattle and homogenates as well as scrapie-associated fibrils were prepared from these

tissues. Molecular characteristics of PrP<sup>Sc</sup> from Irish ovine scrapie samples clearly differed from those of PrP<sup>Sc</sup> derived from bovine BSE samples when using a monoclonal antibody (mab p4) directed to positions 89–104 (GGGGWGQGGSQWQNK) of ovine PrP [17]. Similar results were obtained using either brain homogenates or SAFs. No differences in PrP<sup>Sc</sup> glycotype profiles were detected in the six investigated CNS regions. Sheep scrapie PrP<sup>Sc</sup> was generally characterized by less than 55% diglycosylated PrP compounds in immunoblot, while in BSE PrP<sup>Sc</sup> about 65% diglycosylated proteins were detected. It is noteworthy that the molecular masses of proteinase K treated nonglycosylated PrP<sup>Sc</sup> as well as the glycoprofiles obtained were overall uniform. However, when another monoclonal antibody designated L42 which was raised against amino acid positions 145–163 (GNDYEDRYRMYRYPNQ) was used for the immunochemical staining of sheep PrP<sup>Sc</sup>, diglycosylated PrP<sup>Sc</sup> bands were as strongly stained as in BSE PrP<sup>Sc</sup> making a discrimination between both impossible (Fig. 2). The issue of distinguishing scrapie and BSE glycotyping patterns was overcome by the LTPKR analysis. Proteinase K resistance after 6 h treatment was lower in cattle derived BSE PrP<sup>Sc</sup> (43%) than in sheep derived scrapie PrP<sup>Sc</sup> (60–95%) (Fig. 3). The major advantage of this assay is that the results were independent of the monoclonal antibody used. It must be noted, however, that for a final characterization of scrapie cases, a mouse lesion profile scoring of these samples will be analysed.

Three other studies on the molecular characteristics of PrP<sup>Sc</sup> from field scrapie cases have been published to date. Two research groups have reported a considerable degree of variation in PrP<sup>Sc</sup> from British scrapie cases which was assumed to reflect the diversity of different strain types in the country [18, 19]. In contrast to these results French scientists found little

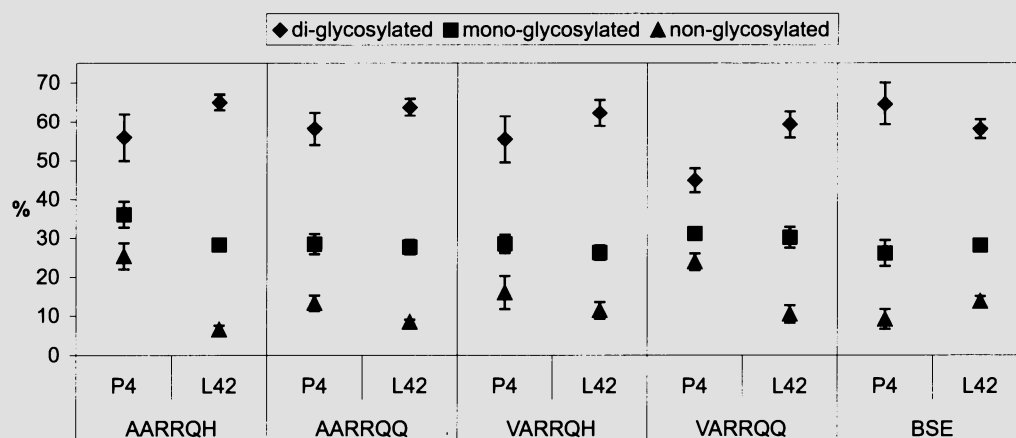


**Fig. 2.** PrP<sup>Sc</sup> glycotyping patterns of scrapie cases in sheep carrying allelic variations at codons 136, 154 and 171 illustrate the impact of the antibody (mab P4 and mab L42) on the results. The contribution (in percent) of the non-, mono- and diglycosylated PrP<sup>Sc</sup> bands to the combined signals (set as 100%) are shown

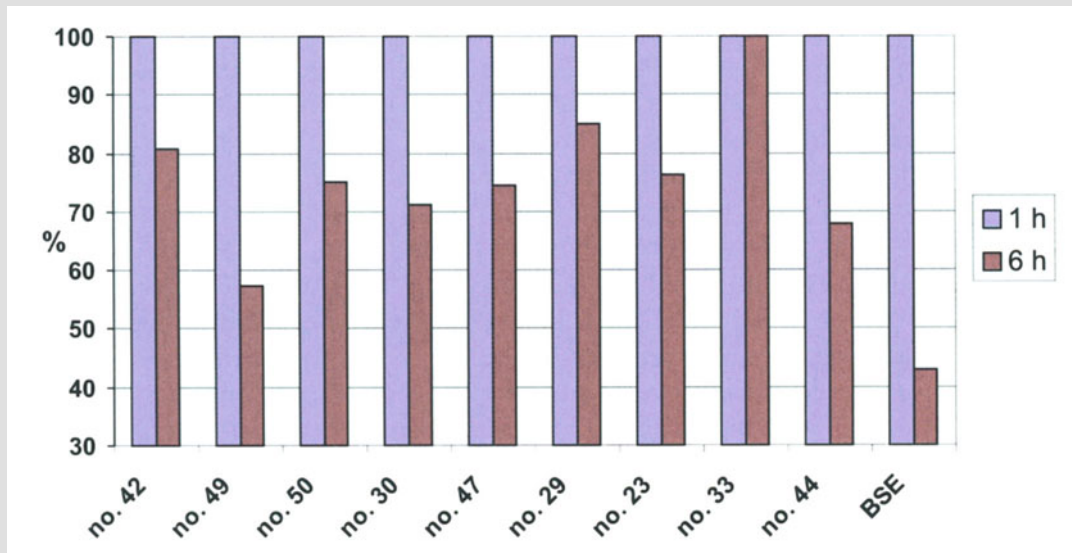


**Fig. 3.** Long-term proteinase K resistance analysis on PrP<sup>Sc</sup> derived from nine sheep scrapie cases as well as from a BSE diseased cow. PrP<sup>Sc</sup> signal intensities were determined electronically by recording immunoblot signals and 1 h signals set as 100% values. After 6 h of proteinase K digestion significantly lower BSE PrP<sup>Sc</sup> signals were retained as compared to PrP<sup>Sc</sup> signals from sheep scrapie cases. Immunoblots were developed using mab L42

diversity in French sheep scrapie cases, but glycotyping patterns which closely resembled BSE patterns [1].

Given the variation in glycosylation patterns using different antibodies, a standardization of methodology and antibodies seems to be crucial for the applicability of the molecular analysis to distinguish strains of ruminant TSEs. A comparison of results between laboratories may only be possible if exactly the same experimental conditions are used.

#### Acknowledgements

We are indebted to Moira Bruce (Edinburgh) and Charles Weissmann (London) for supplying us with the inbred and transgenic mouse lines. Sandra Schädler, Roswitha Fischer and Dan Balkema are acknowledged for their excellent technical assistance. This work was supported in parts by grants from the German 'Bundesministerium für Ernährung, Landwirtschaft und Forste', the German 'Bundesministerium für Bildung, Wissenschaft und Technologie' as well as by grants from the EU commission.

#### References

1. Baron TG, Madec JY, Calavas D (1999) Similar signature of the prion protein in natural sheep scrapie and bovine spongiform encephalopathy-linked diseases. *J Clin Microbiol* 37: 3701–3704
2. Bessen RA, Marsh RF (1992) Biochemical and physical properties of the prion protein from two strains of the transmissible mink encephalopathy agent. *J Virol* 66: 2096–2101

3. Bruce M, Chree A, McConnell I, Brown K, Fraser H (1996) Transmission and strain typing studies of scrapie and bovine spongiform encephalopathy. In: Court L, Dodet B (eds) *Transmissible subacute spongiform encephalopathies: prion diseases*. Elsevier, Paris, pp 259–262
4. Bruce ME (1996) Strain Typing Studies of Scrapie and BSE. In: Baker HF, Ridley RM (eds) *Prion diseases*. Humana Press Inc., Totowa, New Jersey, pp 223–236
5. Bruce ME, McBride PA, Jeffrey M, Scott JR (1994) PrP in pathology and pathogenesis in scrapie-infected mice. *Mol Neurobiol* 8: 105–112
6. Buschmann A, Kuczius T, Bodemer W, Groschup MH (1998) Cellular prion proteins of mammalian species display an intrinsic partial proteinase K resistance. *Biochem Biophys Res Commun* 253: 693–702
7. Cardone F, Liu QG, Petraroli R, Ladogana A, D'Alessandro M, Arpino C, Di Bari M, Macchi G, Pocchiari M (1999) Prion protein glyco-type analysis in familial and sporadic Creutzfeldt-Jakob disease patients. *Brain Res Bull* 49: 429–433
8. Carp RI, Callahan SM, Sersen EA, Moretz RC (1984) Preclinical changes in weight of scrapie-infected mice as a function of scrapie agent-mouse strain combination. *Intervirology* 21: 61–69
9. Collinge J, Sidle KC, Meads J, Ironside J, Hill AF (1996) Molecular analysis of prion strain variation and the aetiology of 'new variant' CJD. *Nature* 383: 685–690
10. Dickinson AG, Meikle VM (1969) A comparison of some biological characteristics of the mouse-passaged scrapie agents, 22A and ME7. *Gene Res* 13: 213–225
11. Endo T, Groth D, Prusiner SB, Kobata A (1989) Diversity of oligosaccharide structures linked to asparagines of the scrapie prion protein. *Biochemistry* 28: 8380–8388
12. Foster JD, Hope J, Fraser H (1993) Transmission of bovine spongiform encephalopathy to sheep and goats. *Vet Rec* 133: 339–341
13. Fraser H (1976) The pathology of a natural and experimental scrapie. *Frontiers Biol* 44: 267–305
14. Fraser H, Bruce ME, McConnell I (1991) Murine scrapie strains, BSE models and genetics. In: Bradley R, Savey M, Marchant B (eds) *Sub-acute spongiform encephalopathies*. Kluwer, Dordrecht, pp 131–136
15. Fraser H, Dickinson AG (1973) Scrapie in mice. Agent-strain differences in the distribution and intensity of grey matter vacuolation. *J Comp Pathol* 83: 29–40
16. Groschup MH, Pfaff E (1993) Studies on a species-specific epitope in murine, ovine and bovine prion protein. *J Gen Virol* 74: 451–456
17. Harmeyer S, Pfaff E, Groschup MH (1998) Synthetic peptide vaccines yield monoclonal antibodies to cellular and pathological prion proteins of ruminants. *J Gen Virol* 79: 937–945
18. Hill AF, Sidle KCL, Joiner S, Keyes P, Martin TC, Dawson M, Collinge J (1998) Molecular screening of sheep for bovine spongiform encephalopathy. *Neurosci Lett* 255: 159–162
19. Hope J, Wood SC, Birkett CR, Chong A, Bruce ME, Cairns D, Goldmann W, Hunter N, Bostock CJ (1999) Molecular Analysis of ovine prion protein identifies similarities between BSE and an experimental isolate of natural scrapie, CH 1641. *J Gen Virol* 80: 1–4
20. Kascsak RJ, Rubenstein R, Merz PA, Carp RI, Wisniewski HM, Diring H (1985) Biochemical differences among scrapie-associated fibrils support the biological diversity of scrapie agents. *J Gen Virol* 66: 1715–1722

21. Kascsak RJ, Rubenstein R, Merz PA, Tonna-DeMasi M, Fersko R, Carp RI, Wisniewski HM, Diringer H (1987) Mouse polyclonal and monoclonal antibody to scrapie-associated fibril proteins. *J Virol* 61: 3688–3693
22. Kimberlin RH, Walker CA, Millson GC, Taylor DM, Robertson PA, Tomlinson AH, Dickinson AG (1983) Disinfection studies with two strains of mouse-passaged scrapie agent. Guidelines for Creutzfeldt–Jakob and related agents. *J Neurol Sci* 59: 355–369
23. Kuczius T, Groschup MH (1999) Differences in proteinase K resistance and neuronal deposition of abnormal prion proteins characterize bovine spongiform encephalopathy (BSE) and scrapie strains. *Mol Med* 5: 406–418
24. Kuczius T, Haist I, Groschup MH (1998) Molecular analysis of bovine spongiform encephalopathy and scrapie strain variation. *J Infect Dis* 178: 693–699
25. Marsh RF, Bessen RA (1994) Physicochemical and biological characterizations of distinct strains of the transmissible mink encephalopathy agent. *Philos Trans R Soc London Ser B*: 343: 413–414
26. Parchi P, Capellari S, Chen SG, Petersen RB, Gambetti P, Kopp N, Brown P, Kitamoto T, Tateishi J, Giese A, Kretzschmar H (1997) Typing prion isoforms. *Nature* 386: 232–234
27. Somerville RA, Chong A, Mulqueen OU, Birkett CR, Wood SC, Hope J (1997) Biochemical typing of scrapie strains. *Nature* 386: 564
28. Sweeney T, Kuczius T, McElroy M, Gomerez-Parada M, Groschup MH (2000) Molecular analysis of Irish scrapie cases. *J Gen Virol* 81: 1621–1627
29. Tagliavini F, Prelli F, Ghiso J, Bugiani O, Serban D, Prusiner SB, Farlow MR, Ghetti B, Frangione B (1991) Amyloid protein of Gerstmann–Straussler–Scheinker disease (Indiana kindred) is an 11 kd fragment of prion protein with an N-terminal glycine at codon 58. *EMBO J* 10: 513–519
30. Wadsworth JD, Hill AF, Joiner S, Jackson GS, Clarke AR, Collinge J (1999) Strain-specific prion-protein conformation determined by metal ions. *Nat Cell Biol* 1: 55–59

Authors' address: Dr. M. H. Groschup, Federal Research Centre for Virus Diseases of Animals, Paul-Ehrlich Straße 28, D-72076 Tübingen, Germany.

## Quantitative traits of prion strains are enciphered in the conformation of the prion protein

J. Safar<sup>1,2</sup>, F. E. Cohen<sup>1,3,4,5</sup>, and S. B. Prusiner<sup>1,2,3</sup>

<sup>1</sup>Institute for Neurodegenerative Diseases,  
Departments of <sup>2</sup>Neurology,  
<sup>3</sup>Biochemistry and Biophysics,  
<sup>4</sup>Medicine, and <sup>5</sup>Cellular and Molecular Pharmacology,  
University of California, San Francisco, California, U.S.A.

**Summary.** Variations in prions, which cause different disease phenotypes, are often referred to as strains. Strains replicate with a high degree of fidelity, which demands a mechanism that can account for this phenomenon. Prion strains differ by qualitative characteristics such as clinical symptoms, brain pathology, topology of accumulated PrP<sup>Sc</sup>, and Western blot patterns of glycosylated or deglycosylated PrP<sup>Sc</sup>. Since none of these qualitative features can directly explain quantitative strain traits such as incubation time or dose response, we analyzed conformational parameters of PrP<sup>Sc</sup> and the rate of accumulation in different prion strains. Using the conformation-dependent immunoassay (CDI), we were able to discriminate among PrP<sup>Sc</sup> molecules from eight different prion strains propagated in Syrian hamsters. CDI quantifies PrP isoforms by simultaneously following antibody binding to both the denatured and native forms of a protein. In a plot of the ratio of antibody binding to denatured/native PrP graphed as a function of the concentration of PrP<sup>Sc</sup>, each strain occupied a unique position, indicating that each strain accumulated different concentrations of particular PrP<sup>Sc</sup> conformers. This conclusion was supported by a unique pattern of equilibrium unfolding of PrP<sup>Sc</sup> found within each strain. By comparing the PrP<sup>Sc</sup> levels before and after limited proteinase K digestion, we found that each strain produces a substantial fraction of protease-sensitive PrP<sup>Sc</sup>. We asked whether this fraction of PrP<sup>Sc</sup> might reflect those PrP<sup>Sc</sup> molecules that are most readily cleared by cellular proteases. When the protease-sensitive PrP<sup>Sc</sup> fraction was plotted as a function of the incubation time, a linear relationship was found with an excellent correlation coefficient ( $r = 0.94$ ). Combined with the data on time courses of prion infection in Tg(MHu2M) and Tg(SHaPrP) mice, the results argue that different incubation times of various prion strains may arise predominantly from distinct rates of PrP<sup>Sc</sup> clearance rather than from different rates of PrP<sup>Sc</sup> formation.

### Prion diversity

Unique characteristics of prion isolates, which cause different disease phenotypes, are often referred to as strains. Prion strains were initially isolated based on different clinical syndromes in goats with scrapie [22]; subsequently, strains were isolated in rodents based on different incubation times and neuropathologic profiles [11, 14]. New strains have been produced upon passage from one species to another [18] or passage from non-Tg mice to mice expressing a foreign or artificial PrP transgene [29].

For several decades, the existence of multiple prion strains was offered as an argument for the existence of a scrapie-specific nucleic acid [6, 12]. Despite numerous attempts to find such a nucleic acid by a multitude of approaches and mounting evidence against the existence of a polynucleotide [16, 17, 20], an explanation for strains of prions remained a formidable conundrum [25]. The parameters distinguishing distinct prion isolates fell into qualitative or quantitative categories:

#### A. Qualitative traits

1. Clinical symptoms [22]
2. Anatomical distribution and characteristics of brain lesions [11, 14]
3. Topology of PrP<sup>Sc</sup> accumulation on histoblots [30]
4.  $M_r$  of un- or deglycosylated PrP 27–30 on Western blots [4, 21]
5. Glycoform pattern of PrP 27–30 on Western blots [9]
6. Conformational characteristics of PrP<sup>Sc</sup> in CDI [28]

#### B. Quantitative traits

1. Incubation time [22]
2. Dose response curve in endpoint titration [19]
3. Susceptibility of PrP<sup>Sc</sup> to proteases (clearance) [28]

Despite the fact that qualitative features of prion isolates have been known for such a long time, the mechanisms responsible for them are poorly understood. Some of the traits, such as clinical symptoms, pathology, and CNS distribution of converted PrP<sup>Sc</sup>, may be evidence of differential prion targeting [10]. Some authors studying Western blot patterns of PrP 27–30 also proposed that the observed differences reflect differences in glycosylation and that Asn-linked CHOs specify prion strains [9]. However, there are not yet any direct data on amino sugar analysis or sugar chain sequencing supporting this proposal. This proposal is also difficult to reconcile with the addition of high mannose oligosaccharides to Asn-linked consensus sites on PrP in the ER and subsequent remodeling of the sugar chains in the Golgi [13]. Modification of the complex CHOs attached to PrP<sup>C</sup> is clearly completed prior to the PrP<sup>C</sup> trafficking to the cell surface [5, 7], which indicates that the Asn-linked CHOs of PrP<sup>Sc</sup> do not instruct the addition of such complex-type sugars to PrP<sup>C</sup>.

Mutagenesis of the complex-type sugar attachment sites seemed to increase PrP<sup>Sc</sup> formation in cultured cells [31] but resulted in prolonged

incubation times in Tg mice and differences in the patterns of PrP<sup>C</sup> distribution and PrP<sup>Sc</sup> deposition in mice expressing mutant PrPs [10]. Taken together, all these studies suggest that Asn-linked glycosylation might alter the stability of PrP and in particular PrP<sup>Sc</sup>, which results in various patterns of PrP<sup>Sc</sup> deposition.

Although it was hypothesized that different conformers of PrP<sup>Sc</sup> might be responsible for particular prion strains [23], there was no evidence to support such an assertion until analysis of two isolates labeled DY and HY from mink that had been passaged in Syrian hamsters [3, 4]. However, the HY strain was indistinguishable from the Sc237, SHa(Me7), and MT-C5 strains with respect to incubation times and the size of PrP 27–30 fragments on SDS-PAGE. Moreover, the diminished resistance of DY to limited proteinase K digestion did not correlate with other isolates that produced similar incubation times such as 139H and SHa(RML) [29]. While these studies were of considerable interest, the obscure origin of HY and DY in mink and a lack of correlation with the properties of other biologically similar strains made these mink strains difficult to reconcile. Only when prion strains generated *de novo* in humans with inherited prion diseases were passaged in Tg(MHu2M) mice could a strong case be made for the deciphering of the biological properties of prion strains in the conformation of PrP<sup>Sc</sup> [24, 32]. These studies were fortuitous in the sense that fCJD(E200K) and FFI gave different sizes of PrP 27–30 fragments after limited proteinase K digestion. However, the limited digestion by proteinase K resulting in either 19 or 21 kDa bands after deglycosylation of PrP 27–30 could not explain strain diversity observed in bioassays.

#### **Many conformations of PrP<sup>Sc</sup> detected by conformation-dependent immunoassay (CDI) *in situ***

In our recent study, a conformation-dependent immunoassay (CDI) allowed us to distinguish all eight strains examined by plotting the ratio of denatured/native PrP as a function of PrP<sup>Sc</sup> concentration before and after limited digestion with proteinase K (Fig. 1). Only the DY strain could be distinguished from the other seven strains by Western blotting after limited proteolysis; moreover, the relatively increased protease sensitivity of PrP<sup>Sc</sup> in DY prions can lead to an underestimation of its level by immunoblotting [29]. Only the Me7-H strain exhibited a unique incubation time while the remaining seven strains clustered into two groups.

Our data provide compelling evidence that eight different strains possess at least eight different conformations. In fact, our data argue that each strain is composed of a spectrum of conformations as revealed by limited protease digestion and GdnHCl denaturation studies [28]. How many conformations can PrP<sup>Sc</sup> adopt? The conformation-dependent immunoassay provides a rapid tool capable of discriminating the secondary and tertiary

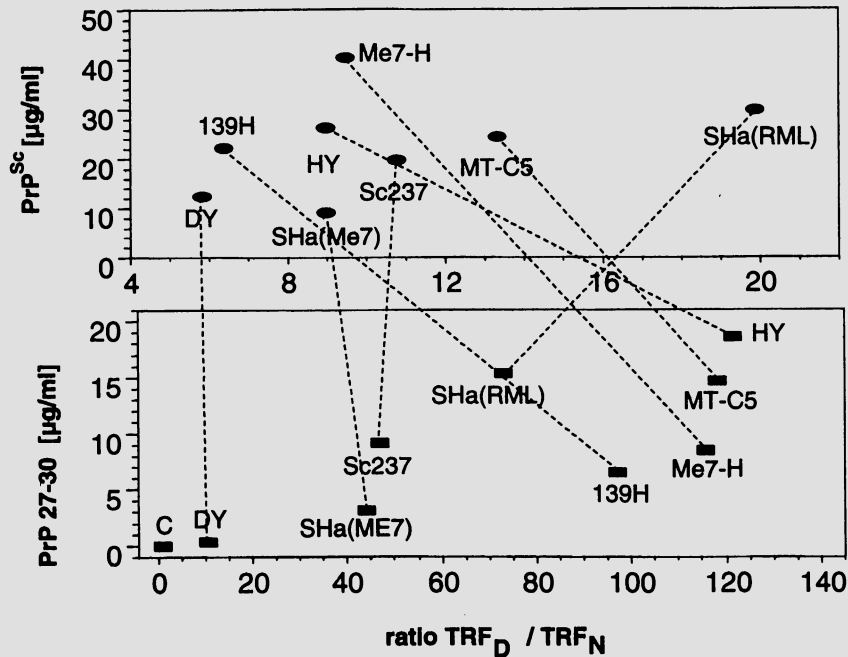


**Fig. 1.** Conformation-dependent immunoassay (CDI) discriminates up to eight Syrian hamster-adapted scrapie strains. By plotting the ratio of denatured/native PrP as a function of PrP<sup>Sc</sup> concentration before and after limited digestion with proteinase K, each strain assumed unique coordinates. Note that the strain relationship changed with proteinase K treatment

structures of a substantial number of PrP<sup>Sc</sup> molecules in crude brain homogenates.

The differences in conformation of PrP<sup>Sc</sup> detected by CDI in different prion strains in situ may suggest two distinctly different conformational mechanisms responsible for propagation of different prion characteristics. In the first scenario, each strain is enciphered by the PrP<sup>Sc</sup> molecules in a definite number of conformations and a specific mixture (ratio) of the same building blocs will replicate itself in the next passage. The second possibility is that each strain characteristic is enciphered in a unique conformer of PrP<sup>Sc</sup>, which then replicates with a high degree of fidelity and thus, reproduces the strain characteristics. Both possibilities can now be tested directly in brain homogenates by CDI.

Thus, in addition to a structure for PrP<sup>C</sup> that is distinct from PrP<sup>Sc</sup>, our data on prion strains argue that there may be multiple, approximately isoenergetic PrP<sup>Sc</sup> conformers. This is an obvious point of departure from earlier work demonstrating that for most proteins there was a single folded structure that was uniquely encoded in the sequence [1]. What is the structural basis of these alternative PrP<sup>Sc</sup> conformers? Work on diphtheria toxin identified distinct crystal forms that displayed different tertiary and quaternary structures for a single polypeptide sequence [2]. To describe this

observation, the notion of domain swapping was introduced whereby a region of one monomer displaced the corresponding region in another monomer to create an interlocking molecular handshake [8]. This phenomenon has now been observed in a variety of other protein structures with the swapped elements as small as an isolated  $\alpha$ -helix or  $\beta$ -strand and as large as an entire folded domain. We suspect that a similar phenomenon may be responsible for prion strains.

The data also argue that  $\text{PrP}^{\text{Sc}}$  must act as a template in the replication of nascent  $\text{PrP}^{\text{Sc}}$  molecules. It seems likely that the binding of  $\text{PrP}^{\text{C}}$  or a metastable intermediate,  $\text{PrP}^*$ , [27] to protein X is the initial step in  $\text{PrP}^{\text{Sc}}$  formation and that this is also the rate-limiting step in prion replication [8, 15, 26].  $\text{PrP}^{\text{Sc}}$  interacts with  $\text{PrP}^{\text{C}}$  but not protein X in the  $\text{PrP}^{\text{C}}$ /protein X complex. When  $\text{PrP}^{\text{C}}$  or  $\text{PrP}^*$  is converted into a nascent  $\text{PrP}^{\text{Sc}}$  molecule, protein X is released. Presumably, protein X functions as a molecular chaperone in the formation of  $\text{PrP}^{\text{Sc}}$  (Fig. 2).

Within this concept of prion replication, the critical constants in the  $\text{PrP}^{\text{C}} \rightarrow \text{PrP}^{\text{Sc}}$  transition are the conversion rate and degradation of the converted  $\text{PrP}^{\text{Sc}}$ . Assuming that concentration and activity of protein X will not change during prion infection with different strains, the different incubation times of various prion strains should arise predominantly from distinct rates of  $\text{PrP}^{\text{Sc}}$  clearance rather than from different rates of  $\text{PrP}^{\text{Sc}}$  formation [26]. Thus, prion strains that are readily cleared should have prolonged incubation times while those that are poorly cleared should

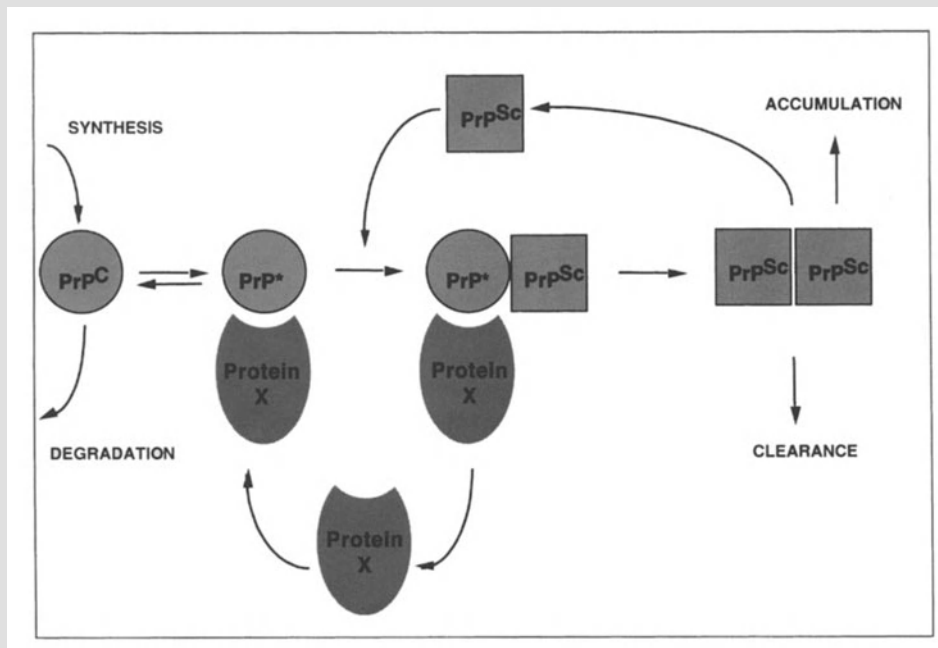


**Fig. 2.** Reaction coordinates of  $\text{PrP}^{\text{Sc}}$  formation and accumulation. Different conversion and clearance rates of  $\text{PrP}^{\text{Sc}}$  dictate the speed of accumulation and thus incubation time in particular prion isolates

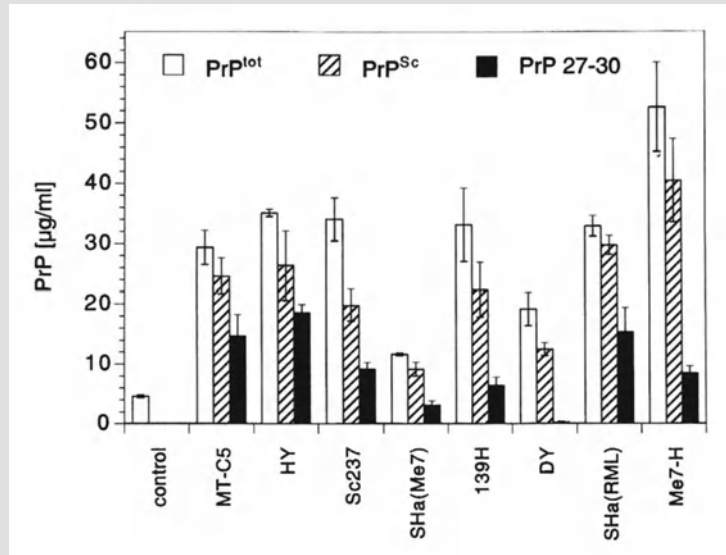


**Fig. 3.** Concentration of total PrP, PrP<sup>Sc</sup>, and PrP 27–30 in eight prion strains and in uninoculated controls distinguished by the conformation-dependent immunoassay (CDI). The columns and bars represent the average  $\pm$  SEM obtained from three different brains of LVG/LAK Syrian hamsters infected with different prion strains and measured in three independent experiments. Concentrations of PrP<sup>Sc</sup> and PrP 27–30 were calculated from CDI

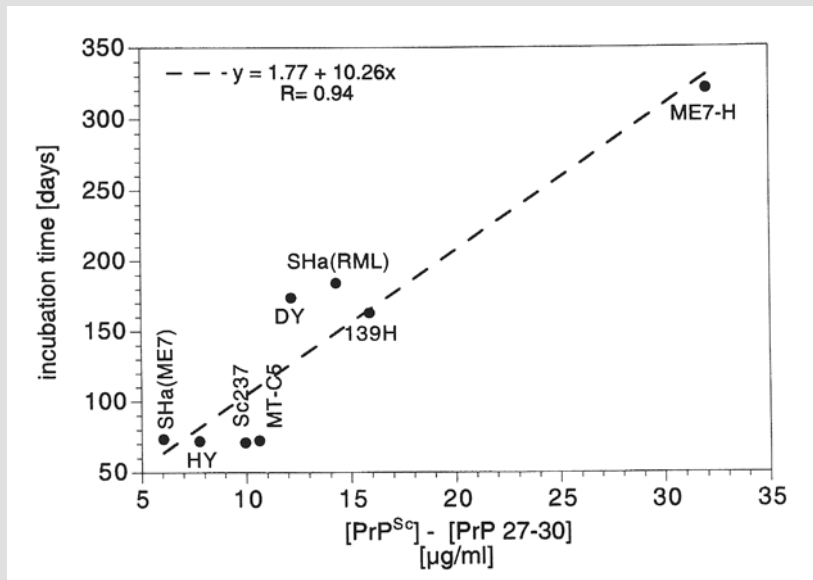


**Fig. 4.** Incubation time plotted as a function of the concentration of the proteinase K-sensitive fraction of PrP<sup>Sc</sup> ([PrP<sup>Sc</sup>] – [PrP 27–30]). Concentrations of PrP<sup>Sc</sup> and PrP 27–30 were calculated from conformation-dependent immunoassay (CDI). Brain homogenates of Syrian hamsters inoculated with different scrapie strains and uninoculated controls, denoted C, were digested with 50  $\mu$ g/ml of proteinase K for 2 h at 37  $^{\circ}$ C prior to the conformation-dependent immunoassay

display abbreviated incubation periods. We investigated this hypothesis by relying upon the difference in brain PrP<sup>Sc</sup> concentrations before and after proteinase K treatment as a surrogate for in vivo clearance of each prion strain (Fig. 3). When clearance as approximated by [PrP<sup>Sc</sup>] – [PrP 27–30] was plotted as a function of the incubation time for eight strains, a linear relationship was found (Fig. 4). It is important to recognize that proteinase K sensitivity is an imperfect model for in vivo clearance and that only one strain with a long incubation time exceeding 300 days has been studied.

### **New approaches arising from this research**

The conformation-dependent immunoassay for PrP<sup>Sc</sup> described recently not only discriminates among a wide variety of prion strains but it is also capable of measuring very low levels of PrP<sup>Sc</sup>. This immunoassay provides important information about the tertiary and secondary structure of PrP<sup>Sc</sup>, which is strain dependent. It will be of interest to correlate results from this conformation-dependent immunoassay with those from optical spectroscopic techniques such as FTIR and CD. The ability to assay features of the tertiary and secondary structure of PrP<sup>Sc</sup> in crude homogenates opens several new avenues of investigation including determinations of the structure of PrP<sup>Sc</sup> in various tissues as well as in different regions of the CNS for a variety of prion strains.

### **Acknowledgements**

The authors thank H. Baron and F. Feldman for encouragement and stimulating discussions. This work was supported by grants from the National Institutes of Health (AG02132, AG010770, NS22786, and NS14069) as well as by gifts from the Leila G. and Harold Mathers Foundation and Centeon.

### **References**

1. Anfinsen CB (1973) Principles that govern the folding of protein chains. *Science* 181: 223–230
2. Bennett MJ, Schlunegger MP, Eisenberg D (1995) 3D domain swapping: a mechanism for oligomer assembly. *Protein Sci* 4: 2455–2468
3. Bessen RA, Marsh RF (1992) Biochemical and physical properties of the prion protein from two strains of the transmissible mink encephalopathy agent. *J Virol* 66: 2096–2101
4. Bessen RA, Marsh RF (1994) Distinct PrP properties suggest the molecular basis of strain variation in transmissible mink encephalopathy. *J Virol* 68: 7859–7868
5. Borchelt DR, Scott M, Taraboulos A, Stahl N, Prusiner SB (1990) Scrapie and cellular prion proteins differ in their kinetics of synthesis and topology in cultured cells. *J Cell Biol* 110: 743–752
6. Bruce ME, Dickinson AG (1987) Biological evidence that the scrapie agent has an independent genome. *J Gen Virol* 68: 79–89
7. Caughey B, Raymond GJ (1991) The scrapie-associated form of PrP is made from a cell surface precursor that is both protease- and phospholipase-sensitive. *J Biol Chem* 266: 18217–18223

8. Cohen FE, Prusiner SB (1998) Pathologic conformations of prion proteins. *Annu Rev Biochem* 67: 793–819
9. Collinge J, Sidle KCL, Meads J, Ironside J, Hill AF (1996) Molecular analysis of prion strain variation and the aetiology of “new variant” CJD. *Nature* 383: 685–690
10. DeArmond SJ, Sánchez H, Yehiely F, Qiu Y, Ninchak-Casey A, Daggett V, Camerino AP, Cayetano J, Rogers M, Groth D, Torchia M, Tremblay P, Scott MR, Cohen FE, Prusiner SB (1997) Selective neuronal targeting in prion disease. *Neuron* 19: 1337–1348
11. Dickinson AG, Fraser HG (1977) Scrapie: pathogenesis in inbred mice: an assessment of host control and response involving many strains of agent. In: ter Meulen V, Katz M (eds) *Slow virus infections of the central nervous system*. Springer, New York, pp 3–14
12. Dickinson AG, Outram GW (1988) Genetic aspects of unconventional virus infections: the basis of the virino hypothesis. In: Bock G, Marsh J (eds) *Novel infectious agents and the central nervous system*. J Wiley, Chichester, pp 63–83 (Ciba Foundation Symposium 135)
13. Endo T, Groth D, Prusiner SB, Kobata A (1989) Diversity of oligosaccharide structures linked to asparagines of the scrapie prion protein. *Biochemistry* 28: 8380–8388
14. Fraser H, Dickinson AG (1973) Scrapie in mice. Agent-strain differences in the distribution and intensity of grey matter vacuolation. *J Comp Pathol* 83: 29–40
15. Kaneko K, Zulianello L, Scott M, Cooper CM, Wallace AC, James TL, Cohen FE, Prusiner SB (1997) Evidence for protein X binding to a discontinuous epitope on the cellular prion protein during scrapie prion propagation. *Proc Natl Acad Sci USA* 94: 10069–10074
16. Kellings K, Meyer N, Miranda C, Prusiner SB, Riesner D (1992) Further analysis of nucleic acids in purified scrapie prion preparations by improved return refocussing gel electrophoresis (RRGE). *J Gen Virol* 73: 1025–1029
17. Kellings K, Prusiner SB, Riesner D (1994) Nucleic acids in prion preparations: unspecific background or essential component? *Phil Trans R Soc London Ser B* 343: 425–430
18. Kimberlin RH, Cole S, Walker CA (1987) Temporary and permanent modifications to a single strain of mouse scrapie on transmission to rats and hamsters. *J Gen Virol* 68: 1875–1881
19. Kimberlin RH, Walker CA (1978) Pathogenesis of mouse scrapie: effect of route of inoculation on infectivity titres and dose-response curves. *J Comp Pathol* 88: 39–47
20. Meyer N, Rosenbaum V, Schmidt B, Gilles K, Miranda C, Groth D, Prusiner SB, Riesner D (1991) Search for a putative scrapie genome in purified prion fractions reveals a paucity of nucleic acids. *J Gen Virol* 72: 37–49
21. Parchi P, Castellani R, Capellari S, Ghetti B, Young K, Chen SG, Farlow M, Dickson DW, Sima AAF, Trojanowski JQ, Petersen RB, Gambetti P (1996) Molecular basis of phenotypic variability in sporadic Creutzfeldt–Jakob disease. *Ann Neurol* 39: 767–778
22. Pattison IH, Millson GC (1961) Scrapie produced experimentally in goats with special reference to the clinical syndrome. *J Comp Pathol* 71: 101–108
23. Prusiner SB (1991) Molecular biology of prion diseases. *Science* 252: 1515–1522
24. Prusiner SB (1997) Prion diseases and the BSE crisis. *Science* 278: 245–251

25. Prusiner SB (1998) Prions (Les Prix Nobel Lecture). In: T. Frängsmyr (ed) Les Prix Nobel. Almqvist & Wiksell International, Stockholm, pp 268–323
26. Prusiner SB, Scott MR, DeArmond SJ, Cohen FE (1998) Prion protein biology. *Cell* 93: 337–348
27. Safar J, Roller PP, Gajdusek DC, Gibbs CJ Jr (1994) Scrapie amyloid (prion) protein has the conformational characteristics of an aggregated molten globule folding intermediate. *Biochemistry* 33: 8375–8383
28. Safar J, Wille H, Itri V, Groth D, Serban H, Torchia M, Cohen FE, Prusiner SB (1998) Eight prion strains have PrP<sup>Sc</sup> molecules with different conformations. *Nature Med* 4: 1157–1165
29. Scott MR, Groth D, Tatzelt J, Torchia M, Tremblay P, DeArmond SJ, Prusiner SB (1997) Propagation of prion strains through specific conformers of the prion protein. *J Virol* 71: 9032–9044
30. Taraboulos A, Jendroska K, Serban D, Yang S-L, DeArmond SJ, Prusiner SB (1992) Regional mapping of prion proteins in brains. *Proc Natl Acad Sci USA* 89: 7620–7624
31. Taraboulos A, Rogers M, Borchelt DR, McKinley MP, Scott M, Serban D, Prusiner SB (1990) Acquisition of protease resistance by prion proteins in scrapie-infected cells does not require asparagine-linked glycosylation. *Proc Natl Acad Sci USA* 87: 8262–8266
32. Telling GC, Parchi P, DeArmond SJ, Cortelli P, Montagna P, Gabizon R, Mastrianni J, Lugaresi E, Gambetti P, Prusiner SB (1996) Evidence for the conformation of the pathologic isoform of the prion protein enciphering and propagating prion diversity. *Science* 274: 2079–2082

Authors' address: Dr. S. B. Prusiner, Institute for Neurodegenerative Diseases, University of California, Box 0518, San Francisco, CA 94143-0518, U.S.A.

## **Structure and Function of PrP**

## Function of PrP<sup>C</sup> as a copper-binding protein at the synapse

H. A. Kretzschmar\*, T. Tings, A. Madlung, A. Giese, and J. Herms

Institute of Neuropathology, University of Göttingen, Göttingen, Germany

**Summary.** The prion protein (PrP<sup>C</sup>) shows cooperative copper binding of the N-terminal octarepeat (PHGGGWGO) ×4. In brain homogenates, PrP<sup>C</sup> is found in highest concentration in synaptosomal fractions. Mice devoid of PrP<sup>C</sup> (Prnp<sup>0/0</sup> mice) show synaptosomal copper concentrations diminished by 50% as compared to normal mice. PrP<sup>C</sup> in the synaptic cleft may serve as a copper buffer. Alternatively it may play a role in the re-uptake of copper into the presynapse or may be of structural importance for the N-terminus and thus may influence binding of PrP<sup>C</sup> to other proteins.

\*

Various approaches have been used to study the function of prion proteins. Biochemical methods were applied to search for a binding partner of PrP<sup>C</sup> which is attached to the cell surface by a GPI anchor [45]. The glial fibrillary acidic protein (GFAP) was one of the first possible binding partners to be described [36] followed by bcl-2 [22, 23], molecular chaperones [10], amyloid precursor-like protein 1 (APLP1) [53], the 37-kDa laminin receptor [39] and a 66-kDa membrane protein which has not been characterized in more detail [29]. However, it has not been possible to show any biological significance of PrP<sup>C</sup> binding of these proteins. Based on biochemical analyses of chicken PrP<sup>C</sup>, Harris et al. [13] hypothesized that PrP<sup>C</sup> might play a role in the regulation of the expression of cholinergic receptors at the neuromuscular end-plate. Biochemical, morphological and electrophysiological studies of the first PrP gene (Prnp) knockout mouse (Prnp<sup>0/0</sup> mouse), which was generated by Büeler et al. [5], showed a regular expression of the acetylcholine receptor [1]. Save for changes in its circadian rhythm [46, 47] and increased sensitivity to seizures [50], this Prnp<sup>0/0</sup> mouse showed no developmental or behavioral changes [5]. These findings were confirmed in studies of another Prnp<sup>0/0</sup> line generated by Manson et al. [26]. The lack of severe defects in these two lines of Prnp<sup>0/0</sup> mice was

\*Present address: Department of Neuropathology, University of Munich, Marchioninstr. 17, D-81377 München, Germany.

ascribed to adaptation, since PrP<sup>C</sup> was absent throughout embryogenesis. However, transgenic mice expressing inducible PrP<sup>C</sup> transgenes that were rendered PrP<sup>C</sup>-deficient as adults by administration of doxycycline have remained healthy for more than 1.5 years [48]. A third Prnp<sup>0/0</sup> mouse generated by Sakaguchi et al. [40] showed progressive ataxia and loss of Purkinje cells in mice aged more than 70 weeks. Also, a fourth independently generated Prnp<sup>0/0</sup> mouse [32, 35] exhibits ataxia and Purkinje cell degeneration. Weissmann [51] suggested that additional deletions of intronic sequences of the Prnp might play a role in this knockout line. Most recently the upregulation of a novel PrP<sup>C</sup>-like protein designated doppel (Dpl), whose gene is located 16 kb downstream of the mouse Prnp, has been speculated to be the cause of Purkinje cell degeneration observed in two of the Prnp<sup>0/0</sup> mouse lines [33]. Even though the hypothesis of the interaction of prion proteins with cholinergic receptors thus could not be confirmed, the studies of Harris et al. [13] indicated that PrP<sup>C</sup> is enriched at the neuromuscular end-plate, i.e., at synaptic endings. Indeed immunohistochemistry of PrP<sup>C</sup>-overexpressing transgenic mice revealed a synaptic expression pattern of PrP<sup>C</sup> [6, 15]. Further evidence for a preferentially synaptic location of the prion protein in the CNS was shown in immunoelectron microscopic studies by Fournier et al. [12] and Salès et al. [41]. Electron microscopic evidence for a synaptic location of PrP<sup>C</sup> has proven very difficult, however. Thus it was necessary to use embedding techniques leading to destruction of the cell membranes. As a consequence, the electron microscopic evidence for PrP<sup>C</sup> location in synaptic vesicles has been disputed. Biochemical studies showed that the prion protein is located predominantly in the synaptic plasma membrane [15] and, to a lesser extent, in the synaptic vesicle fraction. Figure 1 shows a Western blot analysis of PrP<sup>C</sup> expression in various synaptic fractions. The enrichment of PrP<sup>C</sup> in the synaptic plasma membrane fraction is evident (Fig. 1A, lane 4).

Furthermore, electrophysiological studies in Prnp<sup>0/0</sup> mice have been used to identify the function of PrP<sup>C</sup> in neurons. Collinge et al. [8] were the first to describe a change in long-term potentiation (LTP), i.e., a change of synaptic transmission after repetitive stimulation in the Prnp<sup>0/0</sup> mouse generated by Büeler et al. [5]. This finding was confirmed in a second Prnp<sup>0/0</sup> mouse generated by Manson et al. [27]. However, Lledo et al. [25] did not observe LTP changes in the knockout line of Büeler et al. [5].

In addition, Collinge et al. [8] found changed kinetics of the inhibitory postsynaptic currents (IPSCs), i.e., a prolongation of the rise time of GABA<sub>A</sub> receptor-mediated IPSCs in hippocampal neurons of Prnp<sup>0/0</sup> mice. The authors argue that this may be caused by changes in the GABA<sub>A</sub> receptor on the postsynaptic membrane, since a decrease of the amplitude of stimulated inhibitory postsynaptic currents and a shift of the reverse potential of GABA<sub>A</sub> receptor-mediated chloride currents were also observed. Lledo et al. [25] did not confirm this finding for hippocampal neurons of the same knockout line. Also a more detailed analysis of the

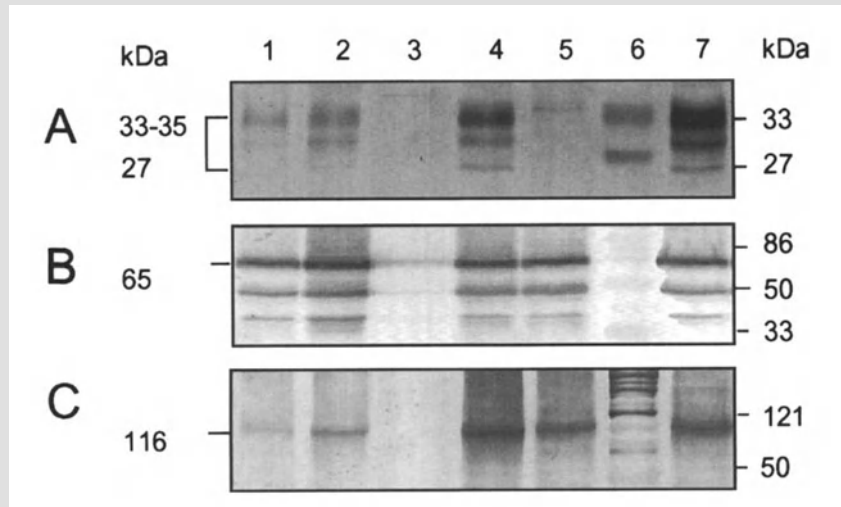


**Fig. 1.** Enrichment of PrP<sup>C</sup> in the synaptic plasma membrane fraction. Preparations of the synaptic plasma membrane and synaptic vesicle fractions from synaptosomes [19]. Equal amounts (100  $\mu$ g per lane) of brain homogenate and various subcellular fractions from wildtype (WT, 1–4), Prnp<sup>0/0</sup> (5) and tg35 (7) mice were investigated in Western blots. The monoclonal antibody 3B5 (A; hybridome supernatant 1:50) [21] was used to identify PrP<sup>C</sup>. A polyclonal antiserum (1:2000) was used to identify the synaptic vesicle protein synaptotagmin (B) [3]. The NMDA receptor subunit R1 was shown using the monoclonal antibody (C; 1:2000) [2]. Subcellular fractions are designated as follows: 1 WT homogenate; 2 WT crude synaptic vesicle fraction; 3 WT cytosolic synaptic fraction; 4 WT synaptic plasma membrane fraction; 5 synaptic plasma membrane fraction from Prnp<sup>0/0</sup> mouse brains; 6 molecular weight standards; 7 tg35 synaptic plasma membrane fraction. An enrichment of PrP<sup>C</sup> (A) is noted in the synaptic plasma membrane fraction of wildtype mice (4) in analogy to the subunit R1 of the NMDA receptor in (C). In contrast to synaptotagmin, (B) a protein that is predominantly localized to the membranes of synaptic vesicles, PrP<sup>C</sup> is not enriched in the synaptic vesicle fraction (2), although it may be found in this location in low concentration

kinetic of GABA<sub>A</sub>-induced currents in outside-out patches from cerebellar Purkinje cells of Prnp<sup>0/0</sup> mice did not reveal significant deviations from control cells [16]. Moreover, studies on the kinetics of spontaneous inhibitory postsynaptic currents (sIPSCs) in cerebellar Purkinje cells of Prnp<sup>0/0</sup> mice initially did not show significant differences between the rise time of wildtype and that of Prnp<sup>0/0</sup> Purkinje cells [16]. Further experiments with Purkinje cells of younger animals with a better voltage clamp (and consequently a more exact estimation of the rise time [24]) showed a significant increase in the rise time from 1.9 ms in wildtype to 2.81 ms in Prnp<sup>0/0</sup> mouse Purkinje cells (Fig. 2D;  $p = 0.001$ ). No differences were found in the decay time (Fig. 2E). Evidence for the hypothesis that the increased rise time is caused by loss of PrP<sup>C</sup> was found in studies on the rise time in Prnp<sup>0/0</sup> mice that were Prnp reconstituted (Fig. 2D; tg35; [11]). The IPSC rise time in Purkinje cells of these animals corresponds to the rise time in wildtype animals. To clarify the question of whether the increase in rise

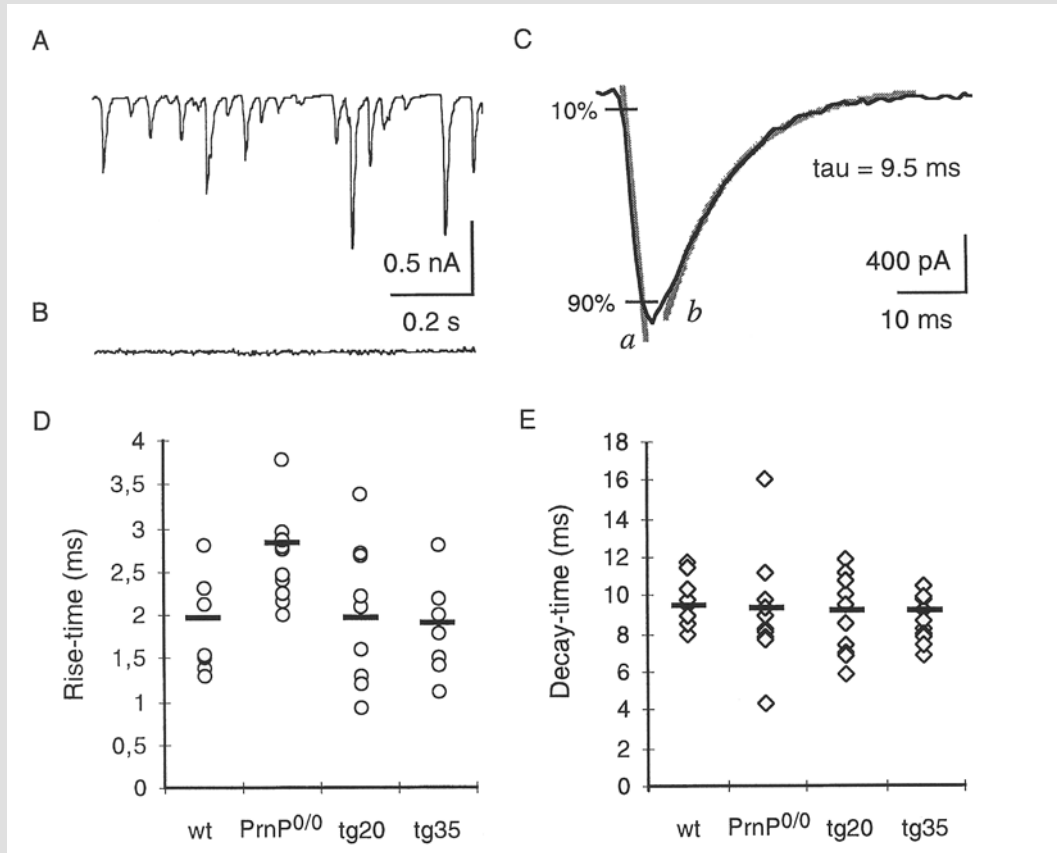


**Fig. 2.** Presynaptic PrP<sup>C</sup> expression modulates the kinetics of inhibitory postsynaptic currents (IPSC). **A** Spontaneous IPSCs from a Purkinje cell of a 10-day-old wildtype mouse using the patch-clamp technique as described [16]. **B** Using the effect of 10 μM bicucullin, a GABA<sub>A</sub> receptor blocker, it is shown that the synaptic currents are inhibitory GABA<sub>A</sub> receptor-mediated conductances. **C** Rise time and decay time in wildtype IPSCs. During rise time, there is a linear increase of GABA<sub>A</sub> receptor-mediated current from 10% to 90% of the maximum (gray line *a*). The decay time ( $\tau$ ) is calculated from the kinetics of an exponential function (gray line *b*) that shows the best fit to the actual decay of the current. **D** Rise time in wildtype, Prnp<sup>0/0</sup>, tg20 and tg35. Shown is the mean of results from each of 10 measurements in Purkinje cells of 9- to 12-day-old animals. Each point corresponds to the rise time of inhibitory postsynaptic currents of a Purkinje cell (mean of the rise time of 20 consecutive IPSCs for each cell). The mean of all measurements is shown as a black line. The IPSC rise time is significantly prolonged in Prnp<sup>0/0</sup> mice compared to wildtype mice ( $p = 0.001$ , t-test according to Welch). No significant differences were found between the rise time of wildtype, tg20 and tg35 cells. **E** Means of the decay time of IPSCs in wildtype, Prnp<sup>0/0</sup>, tg20 and tg35 cells. There are no differences between these mouse lines

time in Prnp<sup>0/0</sup> mice is caused by the loss of PrP<sup>C</sup> expression in the presynapse or postsynapse, an additional transgenic line which expresses PrP<sup>C</sup> only at the presynapse (tg20 [11]) was examined. In this line, rise times corresponding to the wildtype were found (Fig. 2D). Thus it appears that

the loss of the presynaptic PrP<sup>C</sup> expression at the inhibitory synapse is responsible for the prolongation of the rise time of inhibitory postsynaptic currents in Prnp<sup>0/0</sup> mice.

Independent of the findings at inhibitory synapses, Colling et al. [7] described an additional electrophysiological phenotype in Prnp<sup>0/0</sup> mice, i.e., a disturbance of the late after-hyperpolarisation current, I<sub>AHP</sub>. This current is involved in action-potential repolarization and therefore influences the frequency of action potentials. Colling et al. [7] reasoned that the disturbed I<sub>AHP</sub> in Prnp<sup>0/0</sup> mice is caused by a decreased conductance of calcium-activated potassium channels, which may be related to a disturbed intracellular calcium homeostasis. This concept is based on findings by Whatley et al. [52], that indicated an effect of recombinant PrP<sup>C</sup> on the intracellular calcium concentration in synaptosomes.

The cause of the observed electrophysiological alterations in Prnp<sup>0/0</sup> mice is not yet known. They may be related to the decreased copper concentration in synaptic membrane fractions of Prnp<sup>0/0</sup> mice (Fig. 3; [15]). The N-terminus of PrP<sup>C</sup> has a highly conserved octapeptide repeat sequence (PHGGGWGQ) ×4 [42] whose possible copper-binding properties were first shown by Hornshaw et al. [17, 18] and later by Miura et al. [31]. The recombinant N-terminus of PrP<sup>C</sup> from amino acid 23 to 98 (PrP 23–98) shows a cooperative binding of 5 to 6 copper ions [4]. Half-maximal cooperative copper binding of PrP 23–98 is in the micromolar range (5.9 μM).

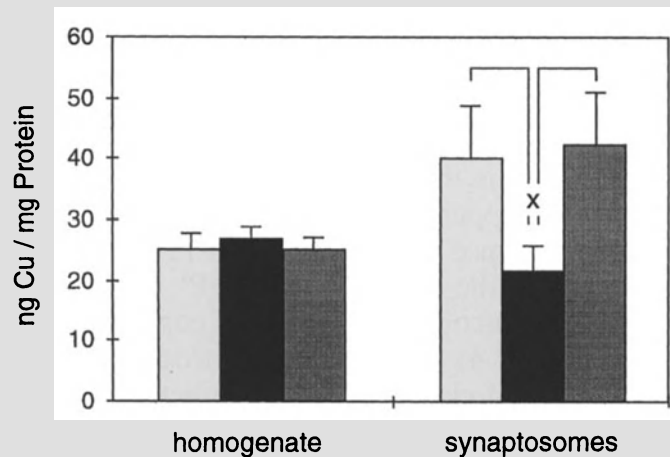


**Fig. 3.** Copper concentration in synaptosomes correlates with PrP<sup>C</sup> expression. The copper concentrations in whole-brain homogenates and synaptosomal fractions from wildtype (WT, open columns), Prnp<sup>0/0</sup> (black columns) and tg20 (gray columns) mice were studied by atomic absorption spectroscopy. Shown are the mean and SE of the arithmetic mean of 3 to 7 preparations from each of 5 brains of age-matched (2 ± 0.4 months) female animals of various lines. Whilst the copper concentration related to protein concentration in whole-brain homogenates shows no significant differences between wildtype, Prnp<sup>0/0</sup> and tg20 mice the synaptosomal fraction shows a significant reduction of copper in Prnp<sup>0/0</sup> mice as compared to wildtype and tg20 mice ( $p = 0.03$ ; t-test)

Further investigations using synthetic octapeptides [49] confirmed cooperative copper binding by PrP<sup>C</sup>.

The significant decrease of synaptosomal copper concentration in Prnp<sup>0/0</sup> mouse synaptosomes (Fig. 3) may be caused by a decreased re-uptake of copper released into the synaptic cleft during synaptic vesicle release, since the difference in the synaptosomal copper concentration between Prnp<sup>0/0</sup> mice and wildtype mice seems to be too large to be explained solely by the loss of copper bound to PrP<sup>C</sup>. In addition, one would then also expect differences in the copper concentration of the crude homogenate in wildtype, tg20 and Prnp<sup>0/0</sup> mice (Fig. 3). The findings may therefore be explained by a dysregulation of the copper concentration in the brains of Prnp<sup>0/0</sup> mice caused by loss of PrP<sup>C</sup>.

In addition to the decreased synaptosomal copper concentration, a number of further changes were observed that indicated a biological function of copper binding by PrP<sup>C</sup>. Thus significant differences between Prnp<sup>0/0</sup> mice and wildtype mice were found in inhibitory synaptic transmission in the presence of copper [4]. The application of copper elicited a significant reduction of the mean amplitude of spontaneous inhibitory postsynaptic GABA<sub>A</sub> receptor-mediated currents in Purkinje cells of Prnp<sup>0/0</sup> mice at a concentration of 2 μM Cu<sup>2+</sup>, whereas this concentration showed no effect on the IPSCs of wildtype mice. Since it is well known that the GABA<sub>A</sub> receptor is functionally disturbed at a concentration of copper in the range 1 μM [43] this finding indicates that differences between Prnp<sup>0/0</sup> and wildtype mice may be caused by the absence of copper buffering in the synaptic cleft by PrP<sup>C</sup>.

It remains to be shown whether buffering of copper released during synaptic vesicle release, which prevents or minimizes unspecific binding of copper to other proteins, is the primary function of PrP<sup>C</sup> (Fig. 4). Alternatively, the binding of copper to PrP<sup>C</sup> might primarily serve the re-uptake of copper into the presynapse by endocytosis of PrP<sup>C</sup> [38, 44] or may be of structural importance for the N-terminus of PrP<sup>C</sup> [28].

The hypothesis of a functional re-uptake of copper in the synaptic cleft by the prion protein (Fig. 4) may explain electrophysiological findings in Prnp<sup>0/0</sup> mice which, on first glance, seem contradictory. A slight increase of extracellular copper concentration caused by decreased or missing copper buffering in the synaptic cleft in Prnp<sup>0/0</sup> mice may cause a decrease in the conductance of voltage-activated calcium channels and a change in the kinetics of the GABA<sub>A</sub> receptor. Thus the conductance of the GABA<sub>A</sub> receptor and voltage-activated calcium channels which modulate intracellular calcium homeostasis is clearly disturbed by copper concentrations of 1 to 10 μM [34, 43]. This would explain the alteration of the intracellular calcium homeostasis in Prnp<sup>0/0</sup> mice, changes in the conductance of calcium-related ion currents as well as changes in GABA<sub>A</sub> receptor-related inhibitory postsynaptic currents observed under certain conditions [8]. Reduced LTP

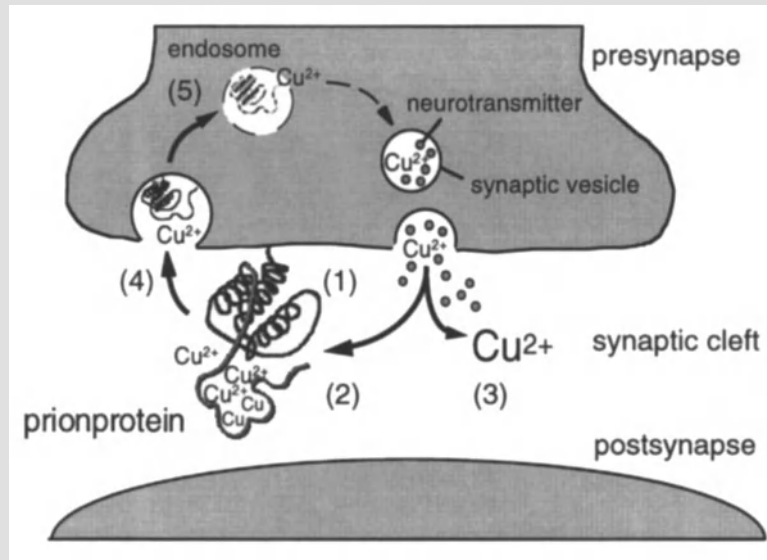


**Fig. 4.** Hypothetical model showing a possible function of copper binding by PrP<sup>C</sup> at the synaptic plasma membrane. The prion protein is attached to the presynaptic plasma membrane (1) [15] where its N-terminal moiety (2) binds free copper that is released, into the synaptic cleft with synaptic vesicle release (3) [14, 20]. There is an endocytotic uptake of PrP<sup>C</sup> into the presynapse (4) [38, 44] where PrP<sup>C</sup>-bound copper is released, possibly induced by endosomal pH changes (5) [49]. Thus PrP<sup>C</sup> serves to keep the copper concentration in the presynaptic cytosol and the synaptic cleft constant in spite of copper losses during synaptic vesicle release (3)

in Prnp<sup>0/0</sup> mice may be explained by this hypothesis as well. As shown by Doreulee et al. [9], LTP is blocked by concentrations of free copper as low as 1  $\mu$ M. Changes in the circadian rhythm observed by Tobler et al. [46, 47] in Prnp<sup>0/0</sup> mice could be related to a disturbed copper uptake and a decreased activity of copper-dependent enzymes, since the synthesis of melatonin, which is important in the regulation of circadian rhythms [30], is regulated by the copper-dependent enzyme monamine oxidase [37].

In summary, our studies have shown that PrP<sup>C</sup> binds copper cooperatively and with high affinity. In the brain highest concentrations of PrP<sup>C</sup> are found at synapses. Synaptosomes of Prnp<sup>0/0</sup> mice demonstrate a strong reduction of copper concentration. Copper binding by PrP<sup>C</sup> in the synaptic cleft has a significant influence on synaptic transmission. It remains to be shown whether additional phenotypes observed in Prnp<sup>0/0</sup> mice are due to decreased copper binding or a disturbance of copper distribution in the absence of PrP<sup>C</sup>.

#### Acknowledgements

This work was supported by the BMBF (German Federal Ministry of Science and Technology) grant KI9461/8, the Deutsche Forschungsgemeinschaft (grant Kr. 1561/21) and Sonderforschungsbereich 406, as well as the Wilhelm-Sander-Stiftung (grant

9343008). We thank Charles Weissmann (University of Zürich) for Prnp<sup>0/0</sup>, tg35 and tg20 mice.

### References

1. Brenner HR, Herczeg A, Oesch B (1992) Normal development of nerve-muscle synapses in mice lacking the prion protein gene. *Proc R Soc London* 250: 151–156
2. Brose N, Huntley GW, Stern-Bach A, Sharma G, Morrison JH, Heinemann SF (1994) Differential assembly of coexpressed glutamate receptor subunits in neurons of rat cerebral cortex. *J Biol Chem* 269: 16780–16784
3. Brose N, Petrenko AG, Südhof TC, Jahn R (1992) Synaptotagmin: a calcium sensor on the synaptic vesicle surface. *Science* 256: 1021–1025
4. Brown DR, Qin K, Herms JW, Madlung A, Manson J, Strome R, Fraser P, Kruck T, von Bohlen A, Schulz-Schaeffer W, Giese A, Westaway D, Kretzschmar H (1997) The cellular prion protein binds copper in vivo. *Nature* 390: 684–687
5. Büeler H, Fischer M, Lang Y, Bluethmann H, Lipp HP, DeArmond SJ, Prusiner SB, Aguett M, Weissmann C (1992) Normal development and behaviour of mice lacking the neuronal cell-surface PrP protein. *Nature* 356: 577–582
6. Chishti MA, Strome R, Carlson GA, Westaway D (1997) Syrian hamster prion protein (PrP<sup>C</sup>) is expressed in photoreceptor cells of the adult retina. *Neurosci Lett* 234: 11–14
7. Colling SB, Collinge J, Jefferys JGR (1996) Hippocampal slices from prion protein null mice: disrupted Ca<sup>2+</sup> activated K<sup>+</sup> currents. *Neurosci Lett* 209: 49–52
8. Collinge J, Whittington MA, Sidle KCL, Smith CJ, Palmer MS, Clarke AR, Jefferys JGR (1994) Prion protein is necessary for normal synaptic function. *Nature* 370: 295–297
9. Doreulee N, Yanovsky A, Haas HL (1997) Suppression of long-term potentiation in hippocampal slices by copper. *Hippocampus* 7: 666–669
10. Edenhofer F, Rieger R, Famulok M, Wendler W, Weiss S, Winnacker E-L (1996) Prion protein PrP<sup>C</sup> interacts with molecular chaperones of the Hsp60 family. *J Virol* 70: 4724–4728
11. Fischer M, Rüllicke T, Raeber A, Sailer A, Moser M, Oesch B, Brandner S, Aguzzi A, Weissmann C (1996) Prion protein (PrP) with amino-proximal deletions restoring susceptibility of PrP knockout mice to scrapie. *EMBO J* 15: 1255–1264
12. Fournier J-G, Escaig-Haye F, De Villemeur TB, Robain O (1995) Ultrastructural localization of cellular prion protein (PrP<sup>C</sup>) in synaptic boutons of normal hamster hippocampus. *C R Acad Sci Paris* 318: 339–344
13. Harris DA, Falls DL, Johnson FA, Fischbach GD (1991) A prion-like protein from chicken brain copurifies with an acetylcholin receptor-inducing activity. *Proc Natl Acad Sci USA* 88: 7664–7668
14. Hartter DE, Barnea A (1988) Evidence for release of copper in the brain: depolarisation-induced release of newly taken-up 67 copper. *Synapse* 2: 412–415
15. Herms J, Tings T, Gall S, Madlung A, Giese A, Siebert H, Schurmann P, Windl O, Brose N, Kretzschmar H (1999) Evidence of presynaptic location and function of the prion protein. *J Neurosci* 19: 8866–8875

16. Herms JW, Kretzschmar HA, Titz S, Keller BU (1995) Patch-clamp analysis of synaptic transmission to cerebellar Purkinje cells of prion protein knockout mice. *Eur J Neurosci* 7: 2508–2512
17. Hornshaw MP, McDermott JR, Candy JM (1995) Copper binding to the N-terminal tandem repeat regions of mammalian and avian prion protein. *Biochem Biophys Res Commun* 207: 621–629
18. Hornshaw MP, McDermott JR, Candy JM, Lakey JH (1995) Copper binding to the N-terminal tandem repeat region of mammalian and avian prion protein: Structural studies using synthetic peptides. *Biochem Biophys Res Commun* 214: 993–999
19. Huttner WB, Schiebler W, Greengard P, De Camilli P (1983) Synapsin I (protein I), a nerve terminal-specific phosphoprotein. III. Its association with synaptic vesicles studied in a highly purified synaptic vesicle preparation. *J Cell Biol* 96: 1374–1388
20. Kardos J, Kovács I, Hajós F, Kálmán M, Simonyi M (1989) Nerve endings from rat brain tissue release copper upon depolarization. A possible role in regulating neuronal excitability. *Neurosci Lett* 103: 139–144
21. Krasemann S, Groschup MH, Harmeyer S, Hunsmann G, Bodemer W (1996) Generation of monoclonal antibodies against human prion proteins in PrP<sup>0/0</sup> mice. *Mol Med* 2: 725–734
22. Kurschner C, Morgan JI (1995) The cellular prion protein (PrP) selectively binds to Bcl-2 in the yeast two-hybrid system. *Mol Brain Res* 30: 165–167
23. Kurschner C, Morgan JI (1996) Analysis of interaction sites in homo- and heteromeric complexes containing Bcl-2 family members and the cellular prion protein. *Mol Brain Res* 37: 249–258
24. Llano I, Marty A, Armstrong CM, A Konnerth (1991) Synaptic- and agonist-induced excitatory currents of Purkinje cells in rat cerebellar slices. *J Physiol* 434: 183–213
25. Lledo PM, Tremblay P, DeArmond SJ, Prusiner SB, Nicoll RA (1996) Mice deficient for prion protein exhibit normal neuronal excitability and synaptic transmission in the hippocampus. *Proc Natl Acad Sci USA* 93: 2403–2407
26. Manson JC, Clarke AR, McBride PA, McConnell I, Hope J (1994) PrP gene dosage determines the timing but not the final intensity or distribution of lesions in scrapie pathology. *Neurodegeneration* 3: 331–340
27. Manson JC, Hope J, Clarke AR, Johnston A, Black C, MacLeod N (1995) PrP gene dosage and long term potentiation. *Neurodegeneration* 4: 113–115
28. Marcotte EM, Eisenberg D (1999) Chicken prion tandem repeats form a stable, protease-resistant domain. *Biochemistry* 38: 667–676
29. Martins VR, Graner E, Garcia-Abreu J, deSouza SJ, Mercadante AF, Veiga SS, Zanata SM, Neto VM, Brentani RR (1998) Complementary hydrophathy identifies a cellular prion protein receptor. *Nature Med* 3: 1376–1382
30. McArthur AJ, Gillette MU, Prosser RA (1991) Melatonin directly resets the rat suprachiasmatic circadian clock in vitro. *Brain Res* 565: 158–161
31. Miura T, Hori-i A, Takeuchi H (1996) Metal-dependent  $\alpha$ -helix formation promoted by the glycine-rich octapeptide region of prion protein. *FEBS Lett* 396: 248–252
32. Moore RC, Hope J, McBride PA, McConnell I, Selfridge J, Melton DW, Manson JC (1998) Mice with gene targeted prion protein alterations show that Prnp, Sinc and Prni are congruent. *Nature Genet* 18: 118–125

33. Moore RC, Lee IY, Silverman GL, Harrison PM, Strome R, Heinrich C, Karunaratne A, Pasternak SH, Chishti MA, Liang Y, Mastrangelo P, Wang K, Smit AFA, Katamine S, Carlson GA, Cohen FE, Prusiner SB, Melton DW, Tremblay P, Hood LE, Westaway D (1999) Ataxia in prion protein (PrP)-deficient mice is associated with upregulation of the novel PrP-like protein doppel. *J Mol Biol* 292: 797–818
34. Nam SC, Hockberger PE (1992) Divalent ions released from stainless steel hypodermic needles reduce neuronal calcium currents. *Pflugers Arch* 420: 106–108
35. Nishida N, Tremblay P, Sugimoto T, Shigematsu K, Shirabe S, Petromilli C, Erpel SP, Nakaoke R, Atarashi R, Houtani T, Torchia M, Sakaguchi S, De Armond S, Prusiner SB, Katamine S (1999) A mouse prion protein transgene rescues mice deficient for the prion protein gene from Purkinje cell degeneration and demyelination. *Lab Invest* 79: 689–697
36. Oesch B, Teplow TB, Stahl N, Serban D, Hood LE, Prusiner SB (1990) Identification of cellular proteins binding to the scrapie prion protein. *Biochemistry* 29: 5848–5855
37. Oxenkrug GF, Requintina P (1998) The effect of MAO-A inhibition and cold-immobilization stress on N-acetylserotonin and melatonin in SHR and WKY rats. *J Neural Transm [Suppl]* 52: 333–336
38. Pauly PC, Harris DA (1998) Copper stimulates endocytosis of the prion protein. *J Biol Chem* 273: 33107–33110
39. Rieger R, Edenhofer F, Lasmézas CI, Weiss S (1998) The human 37-kDa laminin receptor precursor interacts with the prion protein in eukaryotic cells. *Nature Med* 3: 1383–1388
40. Sakaguchi S, Katamine S, Nishida N, Moriuchi R, Shigematsu K, Sugimoto T, Nakatani A, Kataoka Y, Houtani T, Shirabe S, Okada H, Hasegawa S, Miyamoto T, Noda T (1996) Loss of cerebellar Purkinje cells in aged mice homozygous for a disrupted PrP gene. *Nature* 380: 528–531
41. Salès N, Rodolfo K, Hässig R, Faucheux B, Di Giamberardino L, Moya KL (1998). Cellular prion protein localization in rodent and primate brain. *Eur J Neurosci* 10: 2464–2471
42. Schätzl HM, Da Costa M, Taylor L, Cohen FE, Prusiner SB (1995) Prion protein gene variation among primates. *J Mol Biol* 245: 362–374
43. Sharonova IN, Vorobjev VS, Haas HL (1998) High-affinity copper block of GABA<sub>A</sub>-receptor-mediated currents in acutely isolated cerebellar Purkinje cells of the rat. *Eur J Neurosci* 10: 522–528
44. Shyng SL, Heuser JE, Harris DA (1994) A glycolipid-anchored prion protein is endocytosed via clathrin-coated pits. *J Cell Biol* 125: 1239–1250
45. Stahl N, Borchelt DR, Hsiao K, Prusiner SB (1987) Scrapie prion protein contains a phosphatidylinositol glycolipid. *Cell* 51: 229–240
46. Tobler I, Deboer T, Fischer M (1997) Sleep and sleep regulation in normal and prion protein-deficient mice. *J Neurosci* 17: 1869–1879
47. Tobler I, Gaus SE, Deboer T, Achermann P, Fischer M, Rülicke T, Moser M, Oesch B, McBride PA, Manson JC (1996) Altered circadian activity rhythms and sleep in mice devoid of prion protein. *Nature* 380: 639–642
48. Tremblay P, Meiner Z, Galou M, Heinrich C, Petromilli C, Lisse T, Cayetano J, Torchia M, Mobley W, Bujard H, De Armond S, Prusiner SB (1998) Doxycycline control of prion protein transgene expression modulates prion disease in mice. *Proc Natl Acad Sci USA* 95: 12580–12585

49. Viles JH, Cohen FE, Prusiner SB, Goodin DB, Wright PE, Dyson HJ (1999) Copper binding to the prion protein: structural implications of four identical cooperative binding sites. *Proc Natl Acad Sci USA* 96: 2042–2047
50. Walz W, Amaral OB, Rockenback IC, Roesler R, Izquierdo I, Cavalheiro EA, Martins VR, Brentani RR (1999) Increased sensitivity to seizures in mice lacking cellular prion protein. *Epilepsis* 40: 1679–1682
51. Weissmann C (1996) PrP effects clarified. *Curr Biol* 6: 1369
52. Whatley SA, Powell JF, Politopoulou G, Campbell IC, Brammer MJ, Percy NS (1995) Regulation of intracellular free calcium levels by the cellular prion protein. *Neuroreport* 6: 2333–2337
53. Yehiely F, Bamborough P, DaCosta M, Perry BJ, Thinakaran G, Cohen FE, Carlson GA, Prusiner SB (1997) Identification of candidate proteins binding to prion protein. *Neurobiol Dis* 3: 339–355

Authors' address: Prof. Dr. H. A. Kretzschmar, Institute of Neuropathology, Klinikum Großhadern, Marchioninstr. 15, D-81377 München.

# The prion protein globular domain and disease-related mutants studied by molecular dynamics simulations

M. Billeter<sup>1</sup> and K. Wüthrich<sup>2</sup>

<sup>1</sup>Biochemistry and Biophysics, Lundberg Laboratory,  
Göteborg University, Göteborg, Sweden

<sup>2</sup>Institut für Molekularbiologie und Biophysik, Eidgenössische  
Technische Hochschule, Zürich, Switzerland

**Summary.** In humans, familial forms of transmissible spongiform encephalopathies (TSE; “prion diseases”) have been shown to segregate with the exchange of individual amino acids in the prion protein (PrP) sequence. We used the NMR structure of the globular domain of mouse PrP in the cellular form (PrP<sup>C</sup>) as a starting point for investigations by long-time molecular dynamics (MD) simulations at ambient temperature of likely impacts of such mutations on the PrP<sup>C</sup> structure, making use of the fact that species-related amino acid replacements between mouse PrP and human PrP are spatially well separated from the disease-related mutations in human PrP. In the MD simulations these amino acid substitutions were found to have a variety of different effects on the protein structure, with some species showing altered packing of regular secondary structure elements, while other mutants showed no or only strictly localized changes of the structure near the variant amino acid. The fact that some of the disease-related amino acid exchanges cause no measurable change of the PrP<sup>C</sup> structure indicates that their influence on the conformational transition to the scrapie form of PrP may be due to modified intermolecular interactions during the aggregation process.

## Introduction

Prion proteins in healthy mammalian systems are located in a membrane-anchored monomeric form on the cell surface, whereas aggregates of prion proteins with increased proteinase resistance are typically observed in individuals affected by transmissible spongiform encephalopathies (TSEs) [1, 15]. TSEs occur as sporadic diseases, can be spread by infections, and inherited human TSEs have been related with mutations in the protein sequence that were detected in the affected families [14]. The familial human TSEs are classified by their clinical symptoms into Creutzfeldt–Jakob

disease (CJD), Gerstmann–Sträussler–Scheinker syndrome (GSS) and fatal familial insomnia (FFI).

The human prion protein in its mature form consists of 208 residues (numbered 23–230). The C-terminal half of the polypeptide chain with residues 124–226 forms a compact globular domain whereas the N-terminal part is unstructured in aqueous solution at pH5 [6, 17]. The NMR structure of the C-terminal of mouse prion protein fragment of residues 121–231, mPrP(121–231), consists of three helices with residues 144–154, 175–193 and 200–219, a short antiparallel  $\beta$ -sheet with residues 128–131, and 161–164, and connecting loops of which the one formed by residues 167–171 shows an outstandingly high degree of disorder [16, 18].

With the availability of the NMR structure of the C-terminal domain of the mouse prion protein it is possible to study the intramolecular environment of eight of the eleven amino acid replacements that have been associated with human familial TSEs [12, 18], since these are not near any of the sequence differences among mammalian species [3, 20]. For some of the disease-related sequence variations, conformational consequences are strongly indicated. For example, a structurally important hydrogen bond is removed in one of the variant proteins, and in a different mutant protein an aromatic ring is replaced by a much smaller, polar side chain. On the other hand there are some conservative disease-related mutations for which an impact on the three-dimensional structure or on the stability of PrP<sup>C</sup> would not necessarily be expected. This paper complements the analysis of the NMR structure [18] and measurements of the thermal stabilities [12] with molecular dynamics simulations of all eight disease-related mutations that are found in the protein fragment PrP(121–231), in an attempt to identify the spatial regions that are structurally affected by the individual amino acid replacements, and to characterize the nature and extent of likely alterations in the structure.

### **Descriptions of MD calculations and global view of the MD trajectories**

MD runs were performed on the mouse wild type prion protein fragment of residues 124–226, which includes the entire globular domain [17], and on six mutant forms of this polypeptide (Table 1). The starting point for all simulations was the energy-minimized mean structure formed by residues 124–226 in mPrP(121–231) [18] (PDB-code 1AG2). Neutral pH was assumed, i.e., arginines, aspartic and glutamic acids and lysines were charged, while histidines were uncharged. Mutations were introduced into this structure using tools of the program MOLMOL [11]. The MD runs were performed with the program OPAL [13], which uses the AMBER force field [5] and the TIP3P water model [10]. The wild type prion protein, i.e., residues 124–226 of mPrP(121–231), and the different mutant forms (Table 1) were energy-refined and placed in the center of an ellipsoid-shaped water bath [13]. MD runs were started using random velocities corresponding to a temperature

**Table 1.** MD simulations of the fragment 124–226 of the wild type mouse prion protein and mutants thereof <sup>a</sup>

Identification code	Mutation <sup>b</sup> (polymorphism <sup>c</sup> )	Protein charge at pH7	RMSD [Å] <sup>d</sup>
MD0	wild type	−2	2.5; 1.7
MD1	F198S, V210I	−2	2.1; 1.3
MD2	D178N, E200K (M129)	+1	2.5; 1.5
MD3	D178N, E200K (V129)	+1	2.6; 1.4
MD4	T183A	−2	1.8; 1.3
MD5	V180I, Q217R	−1	2.2; 1.3
MD6	R208H, Q217R	−2	2.9; 2.2

<sup>a</sup>The starting structure for each simulation was derived from the energy-minimized mean NMR structure of the fragment comprising residues 124–226 in mouse PrP(121–231) [18], where the variant starting structures for MD1 to MD6 were generated using the program MOLMOL [11]. Each MD simulations included about 1670 protein atoms and 3100 water molecules, with a total number of about 11000 atoms

<sup>b</sup>The diseases related to these mutations are classified as CJD (D178N with V129, T183A, E200K, R208H and V210I), GSS (V180I, F198S and Q217R) and FFI (D178N with M129)

<sup>c</sup>A polymorphism at position 129 (Met or Val) in humans is related to different phenotypes of the prion disease associated with the mutation D178N [7]. Position 129 contains Met in mouse PrP, and all mutation sites considered in this study contain identical residues in the mouse and human wild-type protein. If not indicated explicitly, position 129 was occupied by Met

<sup>d</sup>Two RMSD values are given between the final structure of each MD simulation and the starting structure derived from the energy-minimized mean NMR structure [18]. The first entry is the RMSD calculated for the backbone atoms of residues 124–166 and 172–226, the second one is for the residues 128–131, 161–164, 175–193 and 200–219, which form the two  $\beta$ -strands and the helices 2 and 3 in the wild type protein

of 10 K, but heated rapidly to the reference temperature. The temperature and the pressure were controlled by rescaling of the velocities and coordinates, respectively, as described by Berendsen et al. [2]. Thus, during the entire simulations the following parameters prevailed: a time step of 2 fs, a reference temperature of 293 K, a reference pressure at the ellipsoid wall of 0.9 bar, a constant dielectric of 1, and the use of SHAKE for all bonds [19]. The runs were recorded during simulation times of 700 ps for the wild type domain and 500 ps for each mutant form.

The presently described MD simulations (Table 1) were performed with the goal of characterizing the effect of the selected mutations on the wild type structure of PrP<sup>C</sup>, with the focus on structural changes observed during the simulations rather than on reaching and characterizing equilibrium structures for the mutant proteins. Therefore no attempt is made to obtain quantitative estimates of thermodynamic quantities and to compare

those to corresponding experimental data [12]. Considering that the mutant proteins occur naturally and allow a normal life for the carriers during typically well over 50 years [15], no significant modifications of the tertiary structure such as a different global fold or major alterations in the secondary structures have to be anticipated. Rather, expected changes are limited to local structural rearrangements of which indications may well be detected within the lengths of the present MD simulations of 500–700 ps.

Figure 1a displays the NMR structure of wild type mPrP(121–231) [18] and seven final structures resulting from the MD runs, and indicates with a color code the regions with the largest structural fluctuations during the trajectories. The overall behavior can be characterized as follows: first, the structures show a slight expansion by moving both the first helix (left side in Fig. 1a) and a disordered loop with residues 167–171 (right side in Fig. 1a) away from the core. Second, local mobility during the trajectories occurs mostly at the two chain termini, in the disordered loop of residues 167–171, in the loop leading to the first helix, and in helix 1. The two  $\beta$ -strands and the helices 2 and 3 form a much more rigid scaffold. The RMSD values between the final structures of the MD runs and the NMR-derived starting structure, as calculated for the backbone heavy atoms of the residues 124–166 and 172–226, exceed 2.6 Å in only one case; for the two  $\beta$ -strands and the helices 2 and 3 the corresponding RMSD values are with one exception

---

**Fig. 1. a** Backbone folds of the fragment of residues 124–226 in mPrP and the variant proteins described in Table 1. The NMR structure determined with mPrP(121–231) [18] is shown in light blue. The final structures of the MD simulations MD0 to MD6 (Table 1) were superimposed for best fit of the backbone atoms of residues 124–166 and 172–226 onto the NMR structure and are displayed with a color code that represents the variable local mobility along the backbone during the simulation (yellow, highest mobility, violet, smallest mobility, with orange and red in-between). This and all other color figures were prepared with the program MOLMOL [11]. **b** mPrP globular domain in the same orientation as in **a**. Color code for the backbone: yellow,  $\alpha$ -helices; green:  $\beta$ -sheet; blue: non-regular secondary structure. The amino acid side chains that are drawn as ball and stick models and identified by the one-letter code and the sequence number are preserved in human PrP, where they are involved in amino acid substitutions that segregate with inherited human prion diseases. **c–f** Fragments of mPrP(121–231) that illustrate local structure variations in the MD trajectories due to amino acid exchanges related to human prion diseases. The NMR structure [18] is always shown in light blue, and the structures from the final snapshots of the wild-type protein in MD0 and of the particular mutant protein discussed are shown in dark blue and yellow, respectively. Hydrogen bonds are shown as dotted lines in magenta, and selected residues are identified with the one-letter code, the sequence position and, where applicable, the amino acid replacement studied. **c** D178N. In addition to the NMR structure and the final snapshot of the wild type protein, the end points of two other runs are shown: N178/M129 in MD2 (yellow) and N178/V129 in MD3 (orange). **d** V180I at the end of run MD5. **e** T183A at the end of run MD4; the  $\beta$ -sheet and helix 2 are shown after superposition for minimal RMSD of the backbone heavy atoms of helix 2. **f** F198S at the end of run MD1

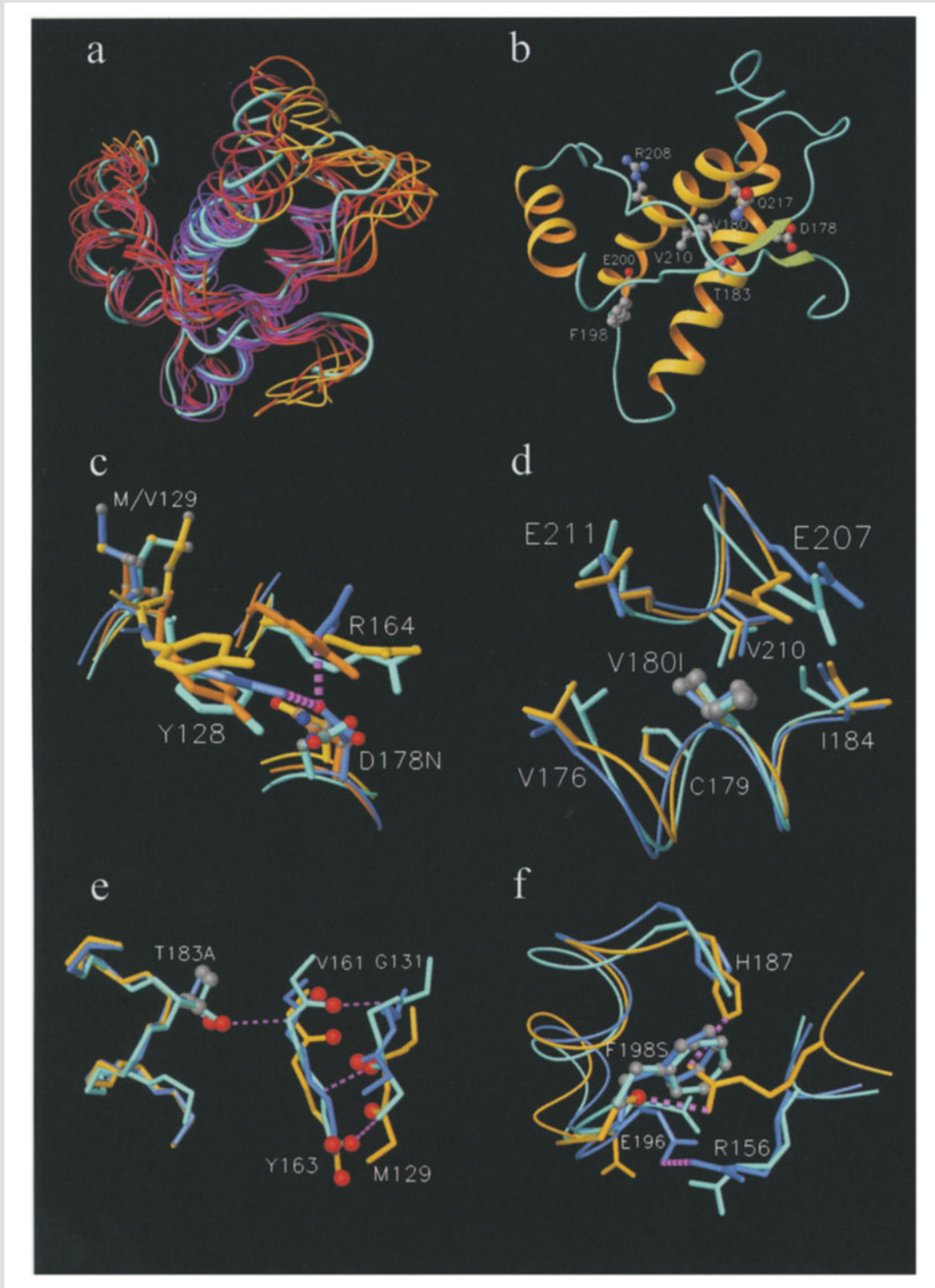


**Table 2.** Percentages of snapshots taken at 1 ps intervals during the MD trajectories<sup>a</sup> that contain individual ones of the  $\beta$ -sheet-associated long-range backbone-backbone hydrogen bonds

Hydrogen bond <sup>b</sup> (HN-O)	MD0	MD1	MD2	MD3	MD4	MD5	MD6
129 – 163 <sup>c</sup>	–	96	79	99	–	97	–
131 – 161*	88	81	91	94	–	78	67
134 – 159	–	–	–	–	–	70	–
161 – 131	–	–	82	–	–	–	–
163 – 129*	96	88	96	89	94	82	91

<sup>a</sup> The notation for the individual trajectories is defined in Table 1

<sup>b</sup> A hydrogen bond is identified if the distance between a donor hydrogen and an acceptor atom shorter than 2.4 Å, and the angle between the N–H bond and the line connecting the donor and acceptor heavy atoms is smaller than 35°. The values indicate the percentages of snapshots, recorded at intervals of 1 ps, for which the individual hydrogen bonds are observed. All long-range backbone-backbone hydrogen bonds that occur with a percentage value  $\geq 67\%$  in at least one of the MD runs are included in this survey

<sup>c</sup> The first number indicates the residue with the donor HN group, the second number the residue with the acceptor O atom. Asterisks identify the hydrogen bonds that were identified in the NMR structure of mPrP(121–231) [18]

below 1.7 Å (Table 1). For both comparisons outstandingly large RMSD values were found for the (R208H, Q217R) double mutant.

Along with the overall fold the pattern of regular secondary structures is largely conserved. Of particular interest is the fate of the  $\beta$ -sheet in the various simulations [9, 15, 16]. Table 2, which surveys the percentage of snapshots with interstrand backbone hydrogen bonds typical for  $\beta$ -sheets in the seven MD simulations, shows that a similar  $\beta$ -sheet to the one described for the NMR structure [18] is preserved during all MD runs except MD4, where the sheet is reduced to a single  $\beta$ -bridge. In MD2 and MD5 the sheet is even extended, with the introduction of a  $\beta$ -bulge in MD5.

The presence of  $\alpha$ -helices for residues 143–151, 172–193 and 199–219 is manifested by hydrogen bonds connecting residues  $i$  and  $i + 4$  in more than 50% of the snapshots for each MD run. In most MD runs a slightly lower percentage of  $\alpha$ -helical hydrogen bonds occurs near the residues 176, 187, 206 and 210, which is paralleled by limited bending motions of the helices 2 and 3. The observation of additional helical hydrogen bonds shows that during the MD simulations all three helices are frequently extended by a few residues at their C-terminus. Compared with the NMR structure [18], the last turn of helix 1 tends to become less regular, whereas helix 2 is transiently extended by almost one turn at its N-terminus. Similar to a feature already seen in the NMR structure, additional helical structure is transiently observed near residue 222.

### Hydrogen bonds formed by amino acid side chains

The NMR structure contains a hydrophobic core surrounded by a network of hydrogen bonds that involve side chain atoms [18]. Table 3 lists all long-range interactions (i.e., those extending over more than four residues along the sequence) that involve side chains and are observed in more than 67% of the snapshots of at least one MD simulation. Nine of the 22 hydrogen bonds listed in Riek et al. [18] are long-range, and they all occur in more than 67% of the snapshots of at least one MD run (normal print in Table 3). Long-range hydrogen bonds of the NMR structure involving residues from helix 1 (144–154) are preserved in most simulations, while those involving the  $\beta$ -sheet (128–131, 161–164) are preserved in about half of the simulations. In the place of the hydrogen bond H $\eta$  157–O 202 found

**Table 3.** Percentages of snapshots taken at 1 ps intervals during the MD trajectories<sup>a</sup> that contain long-range hydrogen bonds involving side chains

Hydrogen bond <sup>b</sup>	MD0	MD1	MD2	MD3	MD4	MD5	MD6
H $\eta$ 128–O $\delta$ 178	100	99	–	–	–	99	–
<b>H<math>\eta</math> 136–O 157</b>	<b>94</b>	<b>97</b>	<b>96</b>	–	<b>97</b>	<b>97</b>	<b>98</b>
H $\eta$ 149–O $\delta$ 202	99	99	98	96	–	99	96
H $\eta$ 150–O 137	99	95	98	99	95	99	–
H $\eta$ 156–O $\epsilon$ 196	94	–	84	–	–	99	84
<b>H<math>\eta</math> 156–O<math>\delta</math> 202</b>	<b>74</b>	–	<b>69</b>	<b>96</b>	<b>98</b>	<b>97</b>	<b>98</b>
H $\eta$ 157–O 202	–	86	–	–	–	–	–
<b>H<math>\eta</math> 157–O<math>\delta</math> 202</b>	<b>70</b>	–	<b>99</b>	–	<b>98</b>	<b>98</b>	<b>98</b>
H $\epsilon$ 160–O 131	77	75	–	72	–	–	–
HN 162–O $\gamma$ 183	–	78	–	96	–	69	–
<b>H<math>\eta</math> 162–O 125</b>	<b>95</b>	–	–	–	<b>89</b>	–	–
<b>H<math>\eta</math> 164–O<math>\delta</math> 174</b>	–	–	<b>85</b>	–	–	–	<b>70</b>
H $\eta$ 164–O $\delta$ 178	89	98	–	–	–	86	–
<b>H<math>\delta</math> 178–O<math>\eta</math> 128</b>	–	–	–	<b>72</b>	–	–	–
<b>H<math>\eta</math> 208–O<math>\epsilon</math> 146</b>	–	<b>85</b>	–	–	–	–	–
H $\epsilon$ 217–O 133	–	–	–	74	72	–	–
<b>H<math>\epsilon</math> 217–O 161</b>	–	–	–	–	<b>81</b>	–	–

<sup>a</sup>The notation for the individual trajectories is defined in Table 1

<sup>b</sup>A hydrogen bond is identified if the distance between a donor hydrogen and an acceptor atom shorter than 2.4 Å, and the angle between the N–H bond and the line connecting the donor and acceptor heavy atoms is smaller than 35°. The values indicate the percentages of snapshots, recorded at intervals of 1 ps, for which the individual hydrogen bonds are observed. Only long-range interactions are listed that involve side chains and occur with a percentage value  $\geq 67\%$  in at least one run. In pairs of atom groups that allow formation of multiple hydrogen bonds (e.g. with each oxygen of a carboxylic group) all snapshots with any of the possible hydrogen bonds are counted. Normal type is used for 9 long-range hydrogen bonds identified in the NMR structure [18], and additional hydrogen bonds seen only in one or several of the MD simulations are shown in bold

in the NMR structure, all but two runs led to structures that contain the interaction H $\eta$  157–O $\delta$  202, and H $\epsilon$  217–O 133 is defined only in two simulations. Additional long-range hydrogen bonds in the simulations that involve side chains (bold print in Table 3) include H $\eta$  136–O 157, which stabilizes the  $\beta$ -sheet, and the above mentioned connectivity H $\eta$  157–O $\delta$  202, and there is also the salt bridge Arg156–Asp202. The hydrogen bond connecting residues 162 and 125 in the runs MD0 and MD4 reinforces the  $\beta$ -sheet. The interaction between Arg164 and Asn174, which is observed in two of the MD runs, connects two surface-exposed side chains. The interactions H $\delta$  178–O $\eta$  128, H $\eta$  208–O $\epsilon$  146 and H $\epsilon$  217–O 161 occur consistently only in one MD run each.

As an illustration, Fig. 2 displays a selection of the long-range hydrogen bond distances observed in the run MD5 as a function of trajectory time. HN 134–O 159 (upper panel; see Table 2), which elongates the  $\beta$ -sheet by a  $\beta$ -bulge, is present during nearly the entire simulation. The  $\beta$ -sheet is further stabilized by the hydrogen bond H $\eta$  136–O 157 (middle panel; Table 3), which was not reported for the NMR structure [18], but is stable throughout the MD5 run. The hydrogen bonds H $\eta$  150–O 137 and H $\epsilon$  160–O 131 have both been reported for the NMR structure, but only the former is conserved during MD5 (lower panel) as well as in all but one of the other simulations (Table 3).

### **Influence of individual amino acid replacements corresponding to human prion disease-related mutations**

In this section the MD simulations are analyzed for structural rearrangements that can be attributed to individual amino acid replacements. To this end, the runs MD1–MD6 are compared to wild-type PrP in MD0, and where a given mutation had been introduced in multiple runs, by comparing these. All mutations sites included in Table 1 reside in a polypeptide fragment formed by the helices 2 and 3 and the connecting loop, which are all part of the stable core identified in Fig. 1 (Fig. 1b). The individual mutations are considered in the order of their sequence locations.

The exchange D178N segregates with two different phenotypes of human prion diseases, depending on the residue type at the polymorphism site 129 [7]. Both combinations have been simulated: N178 with M129 in MD2, and N178 with V129 in MD3. Figure 1c illustrates the results obtained by comparing the NMR structure (light blue) with the final structures obtained from the runs MD0 (dark blue), MD2 (yellow) and MD3 (orange). The electrostatic interaction between Asp178 and Arg164 (Table 3), which is observed in the NMR structure [18], is also found at the end of the simulation of the wild-type protein. Except for the initial 100 ps of the run MD0, the length of the hydrogen bond between these two residues fluctuates in a narrow range around 2.8 Å. In the runs MD2 and MD3 the corresponding distance adopts values between of 4–5 Å. Although the additional inter-

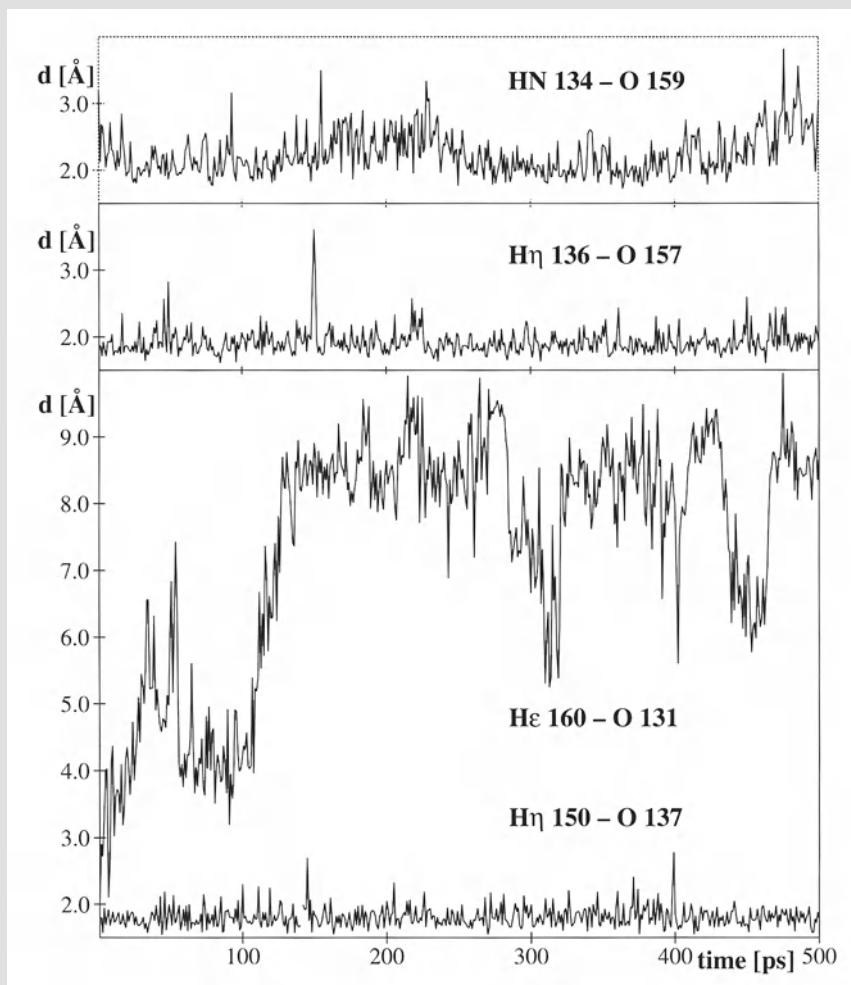


**Fig. 2.** Plot *versus* time of interatomic distances that define selected hydrogen bonds during the simulation MD5. The top panel shows the backbone–backbone interaction HN 134–O 159, which elongates the  $\beta$ -sheet during most of the run (Table 2). The middle panel shows the side chain-to-backbone interaction H $\eta$  136–O 157, which persistently stabilizes the  $\beta$ -sheet. The two hydrogen bonds in the bottom panel, H $\eta$  150–O 137 (lower curve) and H $\epsilon$  160–O 131 (upper curve), have both been reported for the NMR structure, but only the former is maintained during the trajectory

action of residue 178 with Tyr 128 becomes also less frequent in the runs MD2 and MD3 (Table 3), Fig. 1c does not indicate any significant movement of the backbone of the residue 128, 129, 164 or 178. Since the side chain of residue 129 moves sizably in all MD runs, no conclusions emerge regarding the structural role of the polymorphism in position 129 that would cause different phenotypes of prion diseases.

The valine to isoleucine replacements at positions 180 and 210 are in the hydrophobic core. In both MD1 and MD5 the side chain fits well into the structure and the increased size causes no major rearrangements (Fig. 1d). When comparing all heavy atoms in the vicinity of the mutation site,

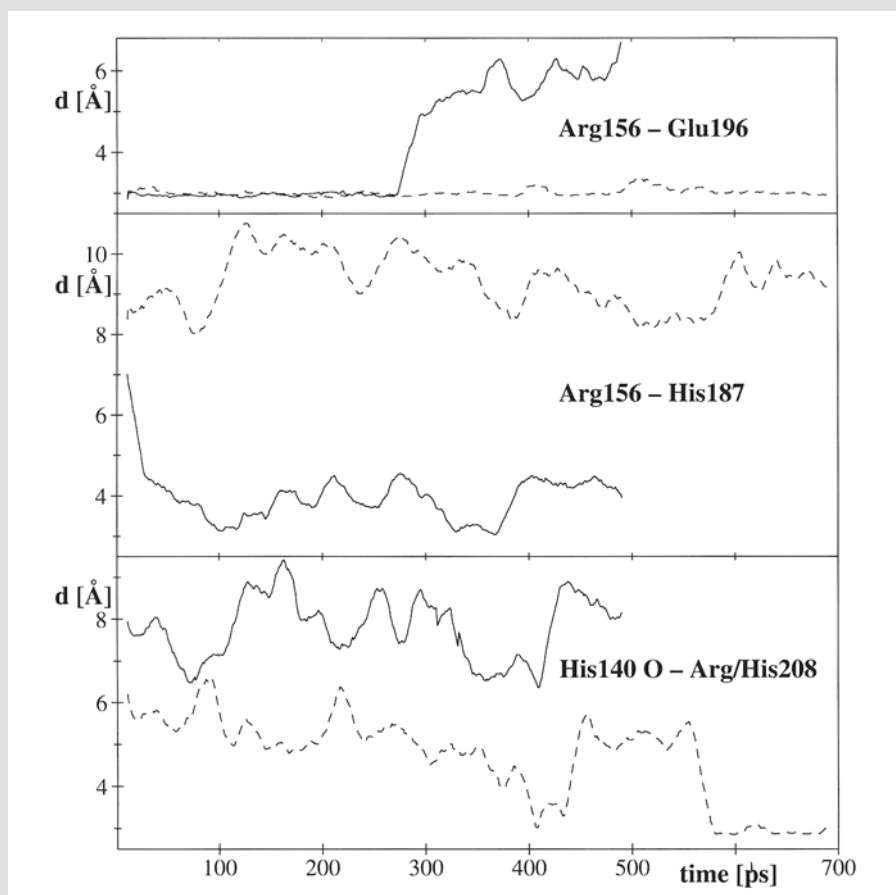
a RMSD of more than 0.6 Å between either MD1 or MD5 and the mean structure in MD0 is observed only in the first 25 ps of the trajectory. Thus, the mutations V180I and V210I have hardly any influence on the structure of PrP<sup>C</sup>.

Figure 1e shows that in the final structure of the run MD4, which contains the amino acid substitution T183A, the  $\beta$ -sheet is displaced relative to the rigid core formed by the helices 2 and 3, when compared to either the NMR structure or the final structure of the run MD0 with the wild type protein. Thus, the attachment of the  $\beta$ -sheet to the helices 2 and 3 is weakened by this amino acid replacement. The structural rearrangement is achieved during the first 150 ps of the run MD4, and it is maintained for the rest of the run. This result can readily be rationalized, since the hydrogen bond HN 162–O $\gamma$  183, which connects the  $\beta$ -sheet with the second helix in the NMR structure [18], cannot be formed in the mutant protein.

In F198S (MD1) a large hydrophobic side chain is replaced by a small hydrophilic one. Figure 1f illustrates likely consequences of this mutation. Ser198 forms new hydrogen bonds, and residues that were separated by the phenylalanine ring can interact with each other in the variant protein. The newly formed hydrogen bonds of Arg156 with His187 and Ser198 pull this residue and the C-terminal end of helix 1 towards the helix 2. Figure 3 indicates the size of the structural rearrangements. In the run MD1, Arg156 soon contacts His187 to form a new hydrogen bond (Fig. 3, middle panel), and after about 300 ps it loses the interaction with Glu196 (Fig. 3, top panel). In contrast, in MD0 the latter interaction is maintained throughout the run. The hydrogen bond between the side chains of Ser198 and Arg156 (Fig. 1f) forms within less than 50 ps in the run MD1 and is preserved for the rest of the simulation (data not shown).

Glutamic acid 200 is the first residue in helix 3, where it is solvent-exposed and does not form any interactions with other parts of the protein [18]. The mutation E200K was investigated in MD2 and MD3, which showed that there is hardly any structural consequence from the exchange of Glu200 by Lys. Since in all simulated structures the side chain of residue 200 reaches out into the solvent in a similar fashion as in the NMR structure, the documented effect of this mutation is most likely due to its impact on intermolecular interactions.

In the simulation MD6 with the mutation R208H the ring of His208 does not form any stable long-range interaction to other parts of the protein. Although Arg208 forms a hydrogen bond to the backbone oxygen of residue 140 toward the end of the run MD0, in the trajectory MD6 the distance between any atom of His208 and the backbone oxygen of residue 140 is always larger than 6.5 Å (Fig. 3, bottom panel). In MD0 the hydrogen bond between residues 140 and 208 connects helix 3 to the loop that leads from the first  $\beta$ -strand to helix 1. Its total time of existence is too short for it to be listed in Table 3, and it was not observed in the NMR structure [18].



**Fig. 3.** Graphs of distances *versus* time which support some observations made in Fig. 1. The selected distances correspond to hydrogen bonds from the runs MD1, with the mutation F198S (solid lines), and MD0 (dashed lines). Shortest side chain heavy atom – side chain heavy atom distances are shown between Arg156 and Glu196 (top panel), and Arg156 and His187 (middle panel). The bottom panel displays the shortest distance between the backbone oxygen of His140 and any heavy atom of residue 208 for the runs MD6, where residue 208 is His, (solid line) and MD0 with Arg208 (dashed line). All distances are smoothed by averaging values over 10 snapshots, i.e., over 10 ps

The mutation Q217R is close to the C-terminus of the third helix. Although a long-range interaction from Gln217 to residue 133 is present in the NMR structure ([18] and Table 3), this interaction to a residue next to the first  $\beta$ -strand as well as an additional one to the second  $\beta$ -strand (Table 3) are observed in only two MD runs. A comparison of the NMR structure and all seven MD runs shows a high degree of mobility in the C-terminal part of helix 3 relative to the  $\beta$ -sheet, and in all instances a wide range of different conformations is adopted by the side chain of residue 217, irrespective of its nature.

Overall, the present MD simulations support the conclusion drawn previously from inspection of the refined NMR structure of mPrP(121–231)

[18], and borne out by measurements of the thermal stabilities [12], that the extent of the structure disruption by the disease-related mutations in human PrP is highly variable. The observation that some amino acid exchanges leave the wild type mPrP(121–231) structure essentially unchanged indicates that their functional impact is limited to intermolecular interactions in the aggregation process leading to PrP<sup>Sc</sup>. A previously advanced hypothesis that familial human prion diseases could be rationalized by reduced stability of the PrP<sup>C</sup> form of the mutant proteins [4, 8] is clearly not compatible either with the results of the present study or with the experimental studies of the stabilities of the variant proteins [12]. For further clarification of possible roles of variant PrP<sup>C</sup> structures in the pathology of inherited human prion diseases, the MD simulations indicate that additional experimental structure determinations might be particularly interesting for the mutant T183A, to check on the predicted shift of the  $\beta$ -sheet relative to the helices 2 and 3, and for the mutant F198S, to characterize the implicated extensive structure rearrangements.

### Acknowledgements

We thank Roland Riek, Gerhard Wider and Rudi Glockshuber for stimulating discussions, the Centro Svizzero di Calcolo Scientifico for use of the NEC SX-4 computer, and Mrs. M. Geier and Mrs. E. Ulrich for the careful processing of the text.

### References

1. Aguzzi A, Weissmann C (1997) Prion research: the next frontiers. *Nature* 389: 795–798
2. Berendsen HJC, Postma JPM, van Gunsteren WF, DiNola A, Haak JR (1984) Molecular dynamics with coupling to an external bath. *J Chem Phys* 81: 3684–3690
3. Billeter M, Riek R, Wider G, Hornemann S, Glockshuber R, Wüthrich K (1997) Prion protein NMR structure and species barrier for prion diseases. *Proc Natl Acad Sci USA* 94: 7281–7285
4. Cohen FE, Pan KM, Huang ZW, Baldwin M, Fletterick RJ, Prusiner SB (1994) Structural clues to prion replication. *Science* 264: 530–531
5. Cornell WD, Cieplak P, Bayly CI, Gould IR, Merz Jr. KM, Ferguson DM, Spellmeyer DC, Fox T, Caldwell JW, Kollman PA (1995) A second generation force field for the simulation of proteins and nucleic acids. *J Am Chem Soc* 117: 5179–5197
6. Donne DG, Viles JH, Groth D, Mehlhorn I, James TL, Cohen FE, Prusiner SB, Wright PE, Dyson HJ (1997) Structure of the recombinant full-length hamster prion protein PrP(29–231): the N-terminus is highly flexible. *Proc Natl Acad Sci USA* 94: 13452–13457
7. Goldfarb LG, Petersen RB, Tabaton M, Brown P, LeBlanc AC, Montagna P, Cortelli P, Julien J, Vital C, Pendelbury WW, Haltia M, Wills PR, Hauw JJ, McKeever PE, Monari L, Schrank B, Swergold GD, Autilio-Gembetti L, Gajdusek DC, Lugaresi E, Gambetti P (1992) Fatal familial insomnia and familial Creutzfeldt–Jakob disease: disease phenotype determined by DNA polymorphism. *Science* 258: 806–808

8. Harrison PM, Bamborough P, Daggett V, Prusiner SB, Cohen FE (1997) The prion folding problem. *Curr Opin Struct Biol* 7: 53–59
9. James TL, Liu H, Ulyanov NB, Farr-Jones S, Zhang H, Donne DG, Kaneko K, Groth D, Mehlhorn I, Prusiner SB, Cohen FE (1997) Solution structure of a 142-residue recombinant prion protein corresponding to the infectious fragment of the scrapie isoform. *Proc Natl Acad Sci USA* 94: 10086–10091
10. Jorgensen WJ, Chandrasekhar J, Madura JD, Impey RW, Klein ML (1983) Comparison of simple potential functions for simulating liquid water. *J Chem Phys* 79: 926–935
11. Koradi R, Billeter M, Wüthrich K (1996) MOLMOL: A program for display and analysis of macromolecular structures. *J Mol Graph* 14: 51–55
12. Liemann S, Glockshuber R (1999) Influence of amino acid substitutions related to inherited human prion diseases on the thermodynamic stability of the cellular prion protein. *Biochemistry*, 38: 3258–3267
13. Luginbühl P, Güntert P, Billeter M, Wüthrich K (1996) The new program OPAL for molecular dynamics simulations and energy refinements of biological macromolecules. *J Biomol NMR* 8: 136–146
14. Prusiner SB (1997) Prion diseases and BSE crisis. *Science* 278: 245–251
15. Prusiner SB (1998) Prions. *Proc Natl Acad Sci USA* 95: 13363–13383
16. Riek R, Hornemann S, Wider G, Billeter M, Glockshuber R, Wüthrich K (1996) NMR structure of the mouse prion protein domain PrP(121–231). *Nature* 382: 180–182
17. Riek R, Hornemann S, Wider G, Glockshuber R, Wüthrich K (1997) NMR characterization of the full length recombinant murine prion protein, mPrP-(23–231). *FEBS Lett* 413: 282–288
18. Riek R, Wider G, Billeter M, Hornemann S, Glockshuber R, Wüthrich K (1998) Prion protein NMR structure and familial human transmissible spongiform encephalopathies. *Proc Natl Acad Sci USA* 95: 11667–11672
19. Ryckaert J, Ciccotti G, Berendsen HCJ (1977) Numerical integration of the Cartesian equations of a system with constraints: molecular dynamics of n-alkanes. *J Comput Phys* 23: 327–341
20. Schätzl HM, DaCosta M, Taylor L, Cohen FE, Prusiner SB (1995) Prion protein gene variation among primates. *J Mol Biol* 245: 362–374

Authors' address: Dr. K. Wüthrich, Institut für Molekularbiologie und Biophysik, Eidgenössische Technische Hochschule, CH-8093 Zürich, Switzerland.

## Neurotoxicity but not infectivity of prion proteins can be induced reversibly in vitro

K. Post<sup>1</sup>, D. R. Brown<sup>2</sup>, M. Groschup<sup>3</sup>, H. A. Kretzschmar<sup>4</sup>, and D. Riesner<sup>1</sup>

<sup>1</sup>Institut für Physikalische Biologie, Heinrich-Heine Universität Düsseldorf, Düsseldorf, Germany

<sup>2</sup>Department of Biochemistry, University of Cambridge, Cambridge, U.K.

<sup>3</sup>Bundesforschungsanstalt für Viruskrankheiten der Tiere, Tübingen, Germany

<sup>4</sup>Department of Neuropathology, Universität Göttingen, Göttingen, Germany

**Summary.** Prion diseases include Creutzfeldt–Jakob disease in humans, scrapie in sheep and bovine spongiform encephalopathy. The hallmark of prion diseases is the accumulation of an abnormal isoform (PrP<sup>Sc</sup>) of the cellular prion protein accompanied by neuronal cell death and astroglial proliferation. To characterize the correlation between PrP secondary and quaternary structure and their biological effects we assayed soluble and aggregated forms of PrP 27–30, the N-terminal truncated form of PrP<sup>Sc</sup>, as well as the corresponding recombinant PrP(90–231) for their neurotoxicity and infectivity. PrP was kept soluble in 0.2% SDS and subsequently re-aggregated either by diluting the SDS or by adding acetonitril. The neurotoxicity of the re-aggregated states were comparable to that of prion rods (PrP 27–30) whereas the soluble forms had no neurotoxic effects. The solubilized PrP 27–30 showed no significant infection upon re-aggregation as determined by bioassays in Syrian golden hamsters. The recombinant PrP did not exhibit infectivity in any state.

### Introduction

Prion diseases are a group of infectious neurodegenerative disorders which include Creutzfeldt–Jakob disease in humans, scrapie in sheep and bovine spongiform encephalopathy. Neither the pathology nor the mode of infectivity are fully understood. An abnormal isoform of the cellular prion protein (PrP<sup>C</sup>) accumulates intracellularly or extracellularly during progression of disease. This abnormal isoform, designated PrP<sup>Sc</sup>, is the main constituent of the “prion”, the agent of prion diseases [15]. The “protein-only-hypothesis” claims that the prion protein is the only component of the agent and that a structural transition of the mainly  $\alpha$ -helical PrP<sup>C</sup> by direct or indirect interaction with PrP<sup>Sc</sup> leads to generation of new PrP<sup>Sc</sup> thereby multiplying the agent. PrP<sup>Sc</sup> is resistant to protease

digestion whereas PrP<sup>C</sup> is sensitive to digestion with proteinase K. Only an “N-terminus” containing 70 amino acids is truncated from PrP<sup>Sc</sup>, leaving a highly resistant core, so-called PrP 27–30. PrP<sup>Sc</sup> and PrP 27–30 contain a high amount of  $\beta$ -sheeted structure. In vitro-conversion of PrP<sup>C</sup> into PrP<sup>Sc</sup> could provide a direct proof for the “protein-only-hypothesis” showing that infectivity of prion diseases is based on the structural transition of a host-encoded protein. Several in vitro-conversion systems have been reported; co-incubation of radiolabeled PrP<sup>C</sup> with purified PrP<sup>Sc</sup> [12] or with an excess of synthetic PrP-peptides [10]. Both systems promote the formation of  $\beta$ -sheeted, protease-resistant PrP aggregates or fibrils, but the generation of infectivity as a consequence of the conversion has failed so far [9, 11].

Another test system using neuronal cell cultures is appropriate to study pathological and in particular neurotoxic effects. Extensive in vitro studies have been performed using the A $\beta$ -peptide characteristic of Alzheimer disease or a synthetic peptide corresponding to amino acid residues 106–126 of human PrP [7]. The neurotoxic effects of the PrP 106–126 in neuronal cell cultures resembled some of the pathological effects of PrP<sup>Sc</sup> in vivo, e.g. by inducing gliosis and apoptotic cell death. The effects depend on the presence of microglia and require the neuronal expression of PrP<sup>C</sup> [4, 5]. It has been shown that PrP106–126 has direct effects on neurons by reducing their cellular resistance to oxidative stress [3]. PrP 106–126 exhibits an increased  $\beta$ -sheet content and forms fibrils in vitro but is not infectious [7]. PrP 27–30 exhibits the same neurotoxic effects in vitro as those described previously for PrP 106–126 [8].

In a study with an alternative approach, we reported the in vitro conversion of PrP where PrP 27–30 first was solubilized in 0.2% SDS (ref. to as sPrP 27–30). Under these conditions PrP 27–30 exhibited a higher  $\alpha$ -helix content, was no longer protease resistant and lost infectivity by at least a factor of  $10^5$  [18]. Incubation of recombinant PrP with 0.2% SDS leads to a stable soluble fraction. Removing the SDS at neutral pH induced a structural transition of the solubilized form of PrP 27–30 as well as of recombinant PrP which was characterized by an increase of the amount of  $\beta$ -sheets and multimerization concomitant with an increased protease resistance [14].

In the present investigation the soluble and aggregated forms of PrP 27–30 from hamster as well as the corresponding recombinant PrP(90–231) were assayed for their neurotoxicity and infectivity. The neurotoxicity of the re-aggregated state either of sPrP 27–30 or rPrP(90–231) was comparable to that of the original PrP 27–30, whereas the soluble forms had no neurotoxic effects. However, the solubilized PrP 27–30 showed a background infectivity which did not increase significantly on account to re-aggregation as determined by bioassays in Syrian golden hamsters. The recombinant PrP did not exhibit infectivity in any state, soluble or insoluble.

## Materials and methods

### *Neuronal cell cultures*

Preparation of cerebellar cells from six-day-old mice (P6) has been described [4]. Briefly, the cerebella were dissociated in Hanks' media (Biochrom) containing 0.5% Trypsin (Biochrom) and plated at  $1-2 \times 10^6$  cells/cm in 24 well trays (Falcon) coated with poly-D-lysine (50  $\mu\text{g}/\text{ml}$ , Sigma). Cultures were maintained in Dulbeccos minimal essential media (Biochrom) supplemented with 10% fetal calf serum, 2 mM glutamine and 1% antibiotics (penicillin, streptomycin). Cultures were maintained at 37 °C with 10% CO<sub>2</sub> for seven days. Protein samples prepared as described below were added at a concentration of 0.01–1  $\mu\text{g}/\text{ml}$  cell culture volume from a PBS/20% sucrose stock solution. After seven days, cell survival was determined by an MTT assay. MTT (3, [4,5 dimethylthiazol-2-yl]-2,5 dimethylphenyl-tetrazolium bromide, Sigma) was diluted to 200  $\mu\text{M}$  in Hanks' solution (Biochrom) and added to cultures for 2 h at 37 °C. The MTT formazan product was released from cells through the addition of demethylsulphoxide (Sigma) and measured at 570 nm in an Ultrospec III spectrophotometer (Pharmacia). Relative survival in comparison to the untreated control could then be determined.

### *Prion proteins*

Preparation of PrP 27–30 from Syrian golden hamster has already been described earlier [17]. Solubilized PrP 27–30 was obtained, as previously published [14], by sonication of 0.33 mg/ml PrP 27–30 in 10 mM sodium phosphate buffer, pH 7.2 (NaPi) and 0.2% sodium dodecylsulfate (SDS). Sonication was carried out in a Labsonic U cup sonicator (B. Braun Diessel Biotech) for 5 min at 70 W and cooled to 4 °C with a water cooling system. To separate the soluble PrP 27–30 from the insoluble pellet fraction, a centrifugation was performed in a TL-100 ultracentrifuge (Beckman Instruments) with swinging bucket rotor TLS-55 for 2.5 h, 50,000 rpm, at 4 °C. Recombinant hamster PrP(90–231) (ref. to as "rPrP") which corresponds to the sequence of PrP 27–30 was prepared as described previously [13].

### *Induction of multimerisation*

Protein samples with 100  $\mu\text{g}/\text{ml}$  PrP in 10 mM NaPi, pH 7.2 or NaH<sub>2</sub>PO<sub>4</sub>, pH 4.3 and 0.2% SDS were diluted 1:20 in PBS and 20% sucrose to a final SDS concentration of 0.01%. In a second approach the samples were adjusted to 25% acetonitril, a  $\beta$ -sheet promoting reagent, in 0.1% SDS/PBS/20% sucrose. The samples were incubated at 37 °C for 24 h in silanized Beckman centrifuge tubes. To induce further aggregation the samples were centrifuged either at 42,000 rpm (100,000  $\times\text{g}$ ) in the TLA-45 rotor for 1 h or 70,000 rpm (250,000  $\times\text{g}$ ) in the TLA-100.3 rotor for 2 h. All centrifugations were carried out in the TL-100 ultracentrifuge (Beckman Instruments) at 20 °C.

### *Bioassays*

Bioassays of scrapie prions were performed in Syrian golden hamsters with an incubation time interval procedure [16]. All samples were adjusted to 1 ml PBS, pH 7.4 and quick-frozen. For each determination six hamsters were inoculated intracerebrally with a 30  $\mu\text{l}$  sample volume. The titers were normalized for log ID<sub>50</sub>/ $\mu\text{g}$  PrP.

## Results and discussion

### *Structure and neurotoxicity*

In this study the relationship between the structure and state of aggregation of the prion protein on one side and neurotoxicity and infectivity on the other were investigated. As reported earlier, PrP 27–30 and the corresponding recombinant PrP(90–231) can be solubilized in 0.2% SDS. Removing the SDS induced structural transitions as characterized by the formation of  $\beta$ -sheets and aggregation up to macroscopic particles [14]. Similar results were obtained by adding 25% acetonitrile to PrP. As a first step of the present studies on in vitro conversion, conditions such as buffer and medium were optimized for cell culture tests. For this reason re-aggregation was performed in the presence of PBS/20% sucrose. Differential ultracentrifugation and further analysis by Western blotting revealed the same results as previously described for aggregation experiments in 10 mM NaPi-buffer [14]: after reducing the SDS concentration to 0.01%, which is equivalent to complete removal or adding 25% acetonitrile/0.1% SDS most of the sPrP 27–30 formed aggregates and pelleted during a 100,000  $\times$ g spin. The acetonitrile-containing samples were either evaporated or the pellet resulting from the centrifugation was resuspended in PBS/20% sucrose to remove acetonitrile. To determine the neurotoxicity of the aggregated and the soluble fractions of PrP 27–30, both were applied to cultures of six-day-old wild-type mouse cerebella. Cells were treated for seven days, then an MTT assay was carried out and the relative survival in comparison to untreated cultures was determined. Prion rods consisting of PrP 27–30 were included in this experiment as a positive control since it had been shown previously that prion rods revealed neurotoxic effects [8]. For all soluble (sPrP 27–30) and aggregated samples the neurotoxicity was determined for three dilution points. The results are shown in Fig. 1. None of the buffers used revealed any cytotoxic effects (data not shown). Prion rods at a concentration of 1  $\mu$ g/ml reduced the cell survival to 55%. After re-aggregation of solubilized PrP 27–30, neurotoxicity was re-introduced and the same concentration-dependent reduction in cell survival as PrP 27–30, regardless of the conditions used, was observed. When, however, solubilized PrP 27–30 which is monomeric or oligomeric and  $\alpha$ -helical, was prepared from prion rods [14, 18] no neurotoxic effects could be found.

In subsequent experiments recombinant PrP of the same sequence was included. The rPrP(90–231), preincubated with 0.2% SDS, and sPrP 27–30 in 0.2% SDS were diluted to 0.01% SDS with PBS/20% sucrose and incubated at 37 °C for 24 h. In these samples the size of the aggregates was enlarged and thereby their protease resistance enhanced by centrifugation at 250,000  $\times$ g for 2 h [14]. The relative survival of cerebella cells treated with 1  $\mu$ g/ml soluble and aggregated forms of recombinant PrP and PrP 27–30 was determined in comparison to untreated control cells. The results are shown in Fig. 2. Again the soluble fractions of either sPrP 27–30 or

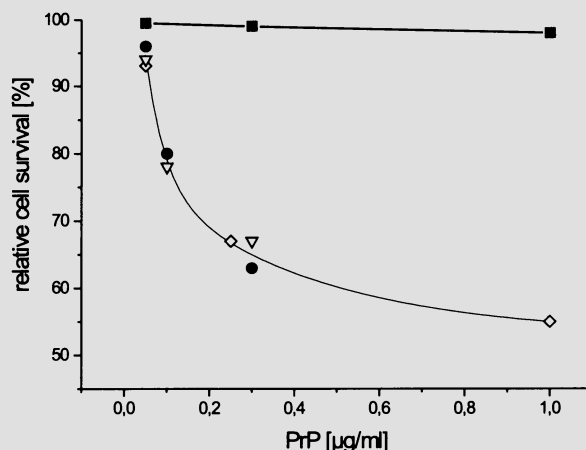


**Fig. 1.** Dose-dependent survival of cerebellar cells after addition of PrP. Cerebellar cells were treated with PrP proteins for seven days; relative survival was determined after that time. The relative cell survival was determined by an MTT assay and the values then related to the untreated control cells as a percentage. Filled squares [■] represent solubilized PrP 27–30 (0.2% SDS); open diamonds [◇] corresponds to PrP 27–30, open triangles [▽] represent re-aggregated sPrP 27–30 after diluting the SDS and filled circles [●] are re-aggregated sPrP 27–30 depending on 25% acetonitrile. Each point represents four experiments with triplicates or duplicates, except sPrP 27–30 (in a concentration of 1 µg/ml) where only three experiments with triplicates were carried out

rPrP(90–231) showed the same survival rates as untreated control cells, whereas the aggregated forms reduced the survival rates to 68% and 67% respectively. These results are in the same scope as previously determined for 1 µg/ml PrP 27–30 with a survival rate of 55% (cf. Fig. 1) or as known for PrP 106–126 [2].

#### *Structure and infectivity*

The infectivity of prion preparations was determined in bioassays. Syrian golden hamsters were inoculated with the soluble and re-aggregated forms of several PrP fractions and the infectivity dose was determined by the incubation time assay. As already published [18], sonication of prion rods in the presence of 0.2% SDS and separation of the soluble fraction decreased the infectivity by  $\approx 4 \log ID_{50}/\mu\text{g PrP}$  (Table 1) in comparison to the starting material (PrP 27–30), i.e. treatment did not abolish infectivity completely. Re-aggregation of sPrP 27–30 either with 25% acetonitrile/0.1% SDS, or by dilution of the initial SDS concentration to 0.01% increased infectivity by 0.83 logarithmic units. However, changes of titers less than one unit are not considered significant. The results are independent of whether the samples were centrifugated after incubation or not. In case re-aggregated PrP had stuck to the surface of the tubes and thus not

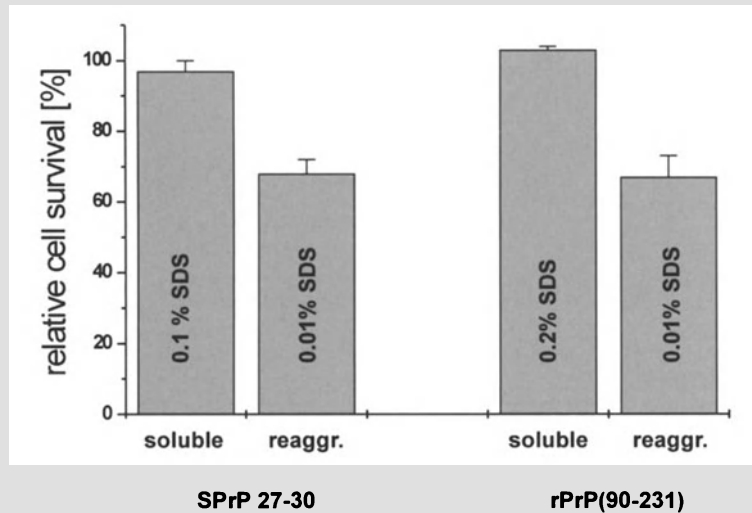


**Fig. 2.** Neurotoxicity test of sPrP 27–30 and rPrP(90–231) of different aggregation states. 1  $\mu$ g/ml of either soluble or re-aggregated forms of sPrP 27–30 and rPrP(90–231) were applied to wild-type cerebellar cells of six-day-old mice. The relative cell survival in percentage of untreated control cells as determined by an MTT assay are depicted. For each point, four experiments with triplicates or duplicates were carried out

**Table 1.** Infectivity assay of sPrP 27–30 in different aggregation states

Sample	Days of incubation [d]	Average	log ID <sub>50</sub> / $\mu$ g PrP
Starting material (PrP27–30)	71, 71, 73, 73, 76, 76	73 $\pm$ 2 d	7.49
sPrP 27–30 (0.2% SDS)	108, 108, 108, 125, 126, 132	118 $\pm$ 11 d	3.82
agg. sPrP 27–30 (25% AcN) <sup>a</sup>	100, 100, 104, 104, 115, 139	110 $\pm$ 15 d	4.3
agg. sPrP 27–30 (0.01% SDS) <sup>a</sup>	94, 94, 94, 100, 104, 139	104 $\pm$ 18 d	4.65
agg. sPrP 27–30 (0.01% SDS) <sup>b</sup>	94, 104, 104, 108, 108, 126	107 $\pm$ 10 d	4.48
agg. sPrP 27–30 (0.01% SDS) <sup>c</sup>	94, 104, 108, 108, 108, 115	106 $\pm$ 7 d	4.54

*agg.* re-aggregated forms

<sup>a</sup>Incubation without further centrifugation

<sup>b</sup>Incubation and 100,000  $\times$ g spin for 1 h in silanized tubes and resuspension in incubation buffer

<sup>c</sup>Incubation and 100,000  $\times$ g spin for 1 h in non-silanized tubes, decantation of the supernatant and resuspension of the pellet in incubation buffer. Animals were observed regularly over a period of 195 days

contributed to infectivity, an extra series with silanized tubes was performed, but no significant change in infectivity was observed.

In a second approach, recombinant PrP(90–231) was included as a control. As previously mentioned, before higher centrifugal forces were applied to determine whether stabilization of the aggregates results not only in an increase of proteinase K resistance [14] but also in an increase of infectivity. The re-aggregated preparations of sPrP 27–30 and rPrP(90–231) were centrifuged at 250,000  $\times$ g for 2 h. But again the re-aggregated fraction of sPrP 27–30 revealed the same background infectivity or even less than that determined for sPrP 27–30 ( $\log ID_{50}/\mu\text{g PrP} = 4.16$ ). This low background infectivity of about 3–4  $\log ID_{50}/\mu\text{g PrP}$  could be due to single, small aggregates present in these fractions as shown by electron microscopy [18]. The rPrP(90–231) did not show any infectivity at all, neither in the presence of 0.2% SDS nor in the aggregated state.

The high molecular weight form of rPrP(90–231) which exhibited marked neurotoxicity revealed amorphous aggregates as shown by electron microscopy [18]. Thus it is obvious that a fibrillar structure is not essential to induce neurotoxic effects. When the toxicity of a segment of PrP, i.e. PrP 106–126 was studied, it was found that PrP106–126 requires the presence of both aggregated and non-aggregated forms [2]. Analysis of variants of PrP 106–126 have shown that the AGAAAAGA palindrome is necessary for the toxicity of the peptide [1]. However, a peptide based on this region forms fibrils but is not toxic. Furthermore, other PrP peptides (PrP106–114, PrP127–147) which are able to adopt fibrillar structures are also not sufficient to induce neurotoxic effects [6]. This means that fibrillar structures themselves are not sufficient to induce neurotoxicity. The relation between the conformation of a particular peptide and neurotoxicity was also studied in the case of the Alzheimer disease-related peptide A $\beta$ . The neurotoxicity of A $\beta$  to neuronal cells has some similarity to that of PrP 106–126; both of them seem to require aggregated states [7]. Recently it was shown by Stege et al. [19] that A $\beta_{1-40}$ -fibrillization can be prevented by  $\alpha$ B crystallin (a molecular chaperone) and that an increased neurotoxicity was observed for the non-fibrillar A $\beta$  fraction. The  $\alpha$ B crystallin-accelerated,  $\beta$ -sheet formation and protein aggregation; however, no fibers could be detected in electron microscopy and shorter, less regular structures were observed instead. It was concluded that A $\beta_{1-40}$  toxicity cannot solely be ascribed to its fibrillar form. The observed structures could be intermediates during fibrillogenesis of A $\beta$  [19] as previously described as protofibrils by Walsh and colleagues [20].

When infectivity was investigated, a unique relation with secondary and quaternary structure could not be found. In the studies of this work, re-aggregation of PrP into a non-fibrillar structure did not result in an increase of infectivity. Several *in vitro* conversion systems lead to the formation of  $\beta$ -sheeted, protease-resistant PrP aggregates or fibrils, but in no case could infectivity be established [9, 11]. Wille et al. [21] concluded from their

experiments that scrapie infectivity and amyloid formation can be distinguished. Both required PrP in a  $\beta$ -sheet-rich structure but infectivity was already lost when amyloid formation as determined by congo red staining and electron microscopy was still conserved [21]. In summary we must conclude that  $\beta$ -sheet secondary structure, proteinase K resistance, a high degree of aggregation, and even fibrillar structure are not sufficient for prion infectivity. In addition, there is no clear-cut relation between fibril formation and neurotoxicity.

### Acknowledgements

This work was supported by grants from the Bundesministerium für Bildung und Forschung, the Ministerium für Wissenschaft und Bildung (NRW) and the Fonds der Chemischen Industrie.

### References

1. Brown DR (2000) Neuronal release of vasoactive intestinal peptide is important to astrocytic protection of neurons from glutamate toxicity. *Mol Cell Neurosci* 15: 465–475
2. Brown DR, Pitschke M, Riesner D, Kretzschmar H (1998) Cellular effects of a neurotoxic prion protein peptide are related to its  $\beta$ -sheet content. *Neurosci Res Commun* 23: 119–128
3. Brown DR, Qin K, Herms JW, Madlung A, Manson J, Strome R, Fraser PE, Kruck T, von-Bohlen A, Schulz-Schaeffer W, Giese A, Westaway D, Kretzschmar H (1997) The cellular prion protein binds copper in vivo. *Nature* 39: 684–687
4. Brown DR, Schmidt B, Kretzschmar HA (1996) A neurotoxic prion protein fragment enhances proliferation of microglia but not astrocytes in culture. *Glia* 18: 59–67
5. Brown DR, Schmidt B, Kretzschmar HA (1996) Role of microglia and host prion protein in neurotoxicity of prion protein fragment. *Nature* 380: 345–347
6. Forloni G, Angretti N, Chiesa R, Monzani E, Samona M, Bugiani O, Tagliavini F (1993) Neurotoxicity of a prion protein fragment. *Nature* 362: 543–546
7. Forloni G, Tagliavini F, Bugiani O, Salmona M (1996) Amyloid in Alzheimer's disease and prion-related encephalopathies: studies with synthetic peptides. *Progr Neurobiol* 49: 287–315
8. Giese A, Brown DR, Groschup MH, Feldmann C, Haist I, Kretzschmar HA (1998) Role of microglia in neuronal cell death in prion disease. *Brain Pathol* 8: 449–457
9. Hill AF, Antoniou M, Collinge J (1999) Protease-resistant prion protein in vitro lacks detectable infectivity. *J Gen Virol* 80: 11–14
10. Kaneko K, Peretz D, Pan K-M, Blochberger TC, Wille H, Gabizon R, Griffith OH, Cohen F, Balwin MA, Prusiner SB (1995) Prion protein (PrP) synthetic peptide induce cellular PrP to acquire properties of the scrapie isoform. *Proc Natl Acad Sci USA* 92: 11160–11164
11. Kaneko K, Wille H, Mehlhorn I, Zhang H, Ball H, Cohen FE, Baldwin MA, Prusiner SB (1997a) Molecular properties of complexes formed between the prion protein and synthetic peptides. *J Mol Biol* 270: 547–586
12. Kocisko DA, Come JH, Priola SA, Chesebro B, Raymond GJ, Lansbury PT, Caughey B (1994) Cell-free formation of protease-resistant prion protein. *Nature* 370: 471–474

13. Mehlhorn I, Groth D, Stöckel J, Moffat B, Reilly D, Yansuro D, Willet WS, Baldwin M, Fletterick R, Cohen FE, Vandlen R, Henner D, Prusiner SB (1996) High-level expression and characterisation of a purified 142-residue polypeptide of the prion protein. *Biochemistry* 35: 5528–5537
14. Post K, Pitschke M, Schäfer O, Wille H, Appel TR, Kirsch D, Mehlhorn I, Serban H, Prusiner SB, Riesner D (1998) Rapid acquisition of  $\beta$ -sheet structure in the prion protein prior to multimer formation. *J Biol Chem* 273: 1307–1317
15. Prusiner SB (1991) Molecular biology of prion diseases. *Science* 252: 1515–1522
16. Prusiner SB, Cochran SP, Groth DF, Downey DE, Bowman KA, Martinez HM (1982) Measurement of the scrapie agent using an incubation time interval assay. *Ann Neurol* 11: 353–358
17. Prusiner SB, Mc Kinley MP, Bowman KA, Bolton DC, Bendheim PE, Groth DF, Glenner GG (1983) Scrapie prions aggregate to form amyloid-like birefringent rods. *Cell* 35: 349–358
18. Riesner D, Kellings K, Post K, Wille H, Serban H, Groth D, Baldwin MB, Prusiner SB (1996) Disruption of prion rods generate 10-nm spherical particles having high  $\alpha$ -helical content and lacking scrapie infectivity. *J Virol* 70: 1714–1722
19. Stege GJJ, Renkawek K, Overkamp PSG, Verschuure P, van Rijk AF, Reijnen-Aalbers A, Boelens WC, Bosman GJGM, DeJong WW (1999) The molecular chaperone  $\alpha$ B-crystallin enhances amyloid  $\beta$  neurotoxicity. *Biochem Biophys Res Commun* 262: 152–156
20. Walsh DM, Hartley DM, Kusumoto Y, Fezoui Y, Condron MM, Lomakin A, Benedek GB, Selkoe DJ, Teplow DB (1999) Amyloid  $\beta$ -protein fibrillogenesis. *J Biol Chem* 274: 25945–25952
21. Wille H, Zhang G-F, Baldwin MA, Cohen FE, Prusiner SB (1996) Separation of scrapie prion infectivity from PrP amyloid polymers. *J Mol Biol* 259: 608–621

Authors' address: Prof. Dr. D. Riesner, Institut für Physikalische Biologie, Heinrich-Heine-Universität Düsseldorf, Universitätsstr. 1, D-40225 Düsseldorf, Germany.

## **PrP Conversion**

## **Inhibition of formation of protease-resistant prion protein by Trypan Blue, Sirius Red and other Congo Red analogs**

**R. Demaimay\*, B. Chesebro, and B. Caughey**

Laboratory of Persistent Viral Diseases, RML, NIAID, NIH, Hamilton, Montana, U.S.A.

**Summary.** Five compounds related to Congo Red were found to inhibit generation of protease-resistant prion protein in a cell-free system. In this assay Trypan Blue, Evans Blue, Sirius Red F3B, Primuline and Thioflavin-S were all more inhibitory than Congo Red itself. In scrapie-infected mouse neuroblastoma cells one compound, Sirius Red F3B, was capable of blocking the formation of protease-resistant prion protein to a similar extent as Congo Red; however, the other four compounds were less effective. Some of these compounds should be considered for testing in TSE disease models in live animals.

\*

The transmissible spongiform encephalopathy (TSE) diseases or prion diseases are a group of fatal neurodegenerative diseases which include scrapie in sheep, bovine spongiform encephalopathy (BSE) in cattle and Creutzfeldt-Jakob disease (CJD) in humans. One of the primary events in the pathogenic process appears to be the conversion of the normal protease-sensitive form of the prion protein ( $\text{PrP}^{\text{sen}}$ ) to an abnormal protease-resistant form ( $\text{PrP}^{\text{res}}$ ) [5, 9, 19]. This abnormal isoform is present in aggregates as well as in amyloid-like fibrils, and can either directly or indirectly initiate the processes of damage leading to neurodegeneration. The conversion of  $\text{PrP}^{\text{sen}}$  to  $\text{PrP}^{\text{res}}$  has been studied in scrapie-infected cell cultures and has also been modeled in a cell-free system in test tubes by mixing of  $\text{PrP}^{\text{sen}}$  and  $\text{PrP}^{\text{res}}$  [1, 12].

The use of cell culture and cell-free systems of  $\text{PrP}^{\text{res}}$  generation has made possible the screening of compounds to search for effective therapeutic agents which might be able to block or reverse the generation of

\*Present address: Laboratory of Secretory Pathways, Imperial Cancer Research Fund, 44 Lincoln's Inn Field, WC2A 3PX London, U.K.

PrP<sup>res</sup> and thus hopefully have a beneficial effect on the disease process. Although there are presently no drugs acceptable for treatment of TSE diseases in humans or domestic animals, several compounds have blocked PrP<sup>res</sup> generation in vitro and/or prolonged the survival time in animal models of TSE diseases. These include Congo Red (CR) and its analogs [2, 7, 10], various sulfated polysaccharides [8, 11, 13], branched polyamines [17], anthracyclines [18], tetrapyrroles [4, 15] and polycyclic compounds related to amphotericin B [6, 14, 20].

In the present work we have used the cell-free conversion system and scrapie-infected mouse neuroblastoma cells to study the effects on PrP<sup>res</sup> generation of five untested compounds related to Congo Red either by their chemical structure or their ability to stain amyloid. Several of these were found to be more effective than Congo Red itself or previously studied analogs. Furthermore, one of these compounds, Sirius Red F3B, was also able to inhibit PrP<sup>res</sup> generation in scrapie infected mouse tissue culture cells.

The structures of CR and four analogs used in these experiments are shown in Fig. 1. CR was purchased from Aldrich. Thioflavine-S (Thio-S) and primuline (Prim) were purchased from Sigma. Sirius red F3B (SR) was purchased from Verona dyes. Trypan Blue (TB) and Evans Blue (EB) were from Allied Chemical Corp. Drugs were stored at  $-20^{\circ}\text{C}$  as 10 mM aqueous solutions.

Cell-free conversion (CFC) was carried out as previously described [7, 12]. PrP<sup>res</sup> was isolated from brain tissue of terminally ill scrapie-infected hamsters. The final PrP<sup>res</sup> pellet was suspended in  $1 \times$  PBS, 0.5% sulfobetaine 3–14. Purity of PrP<sup>res</sup> preparations ranged from 50–70% as determined by standard silver staining. PrP<sup>sen</sup> was isolated from cells expressing hamster PrP lacking the glycoposphatidylinositol anchor sequence. Briefly, cells were grown to 90% confluence and cultivated in methionine-free medium for 1 h. After addition of 1.5 mCi of  $^{35}\text{S}$ -methionine, cells were incubated for 2 h at  $37^{\circ}\text{C}$ . Cells were then lysed in 2 ml of lysis buffer (0.5% sodium deoxycholate; 0.5% triton-X100, 50 mM Tris-HCl pH 7.2), and PrP<sup>sen</sup> was immunoprecipitated by 3F4 monoclonal antibody as previously described. Antibody-PrP<sup>sen</sup> complexes were bound to protein A-Sepharose beads and eluted with 0.1 M acetic acid pH 3.5 in presence of protease inhibitors (Pefabloc, pepstatin, aprotinin, leupeptin). PrP<sup>sen</sup> was stored at  $4^{\circ}\text{C}$  until use. PrP<sup>res</sup> was denatured in 2 M guanidine-HCl for 2 h at  $37^{\circ}\text{C}$ . PrP<sup>sen</sup> was mixed in conversion buffer [(0.5 M citrate pH 6.5, 1 mM cetylpyridiniumchloride (CPC)] with or without drugs to be tested for inhibition. PrP<sup>sen</sup> and denatured PrP<sup>res</sup> were mixed at a final concentration of 0.5 M Gdn-HCl and incubated for two days at  $37^{\circ}\text{C}$ . Samples were then diluted and digested by addition of 80  $\mu\text{g}/\text{ml}$  of PK for 1 h. Undigested and digested samples were run on 14% SDS-PAGE Novex gels, fixed in 10% acetic acid, 50% methanol and dried. Dry gels were exposed and the signals quantified with a STORM-phosphor autoradiographic system (Molecular Dynamics).

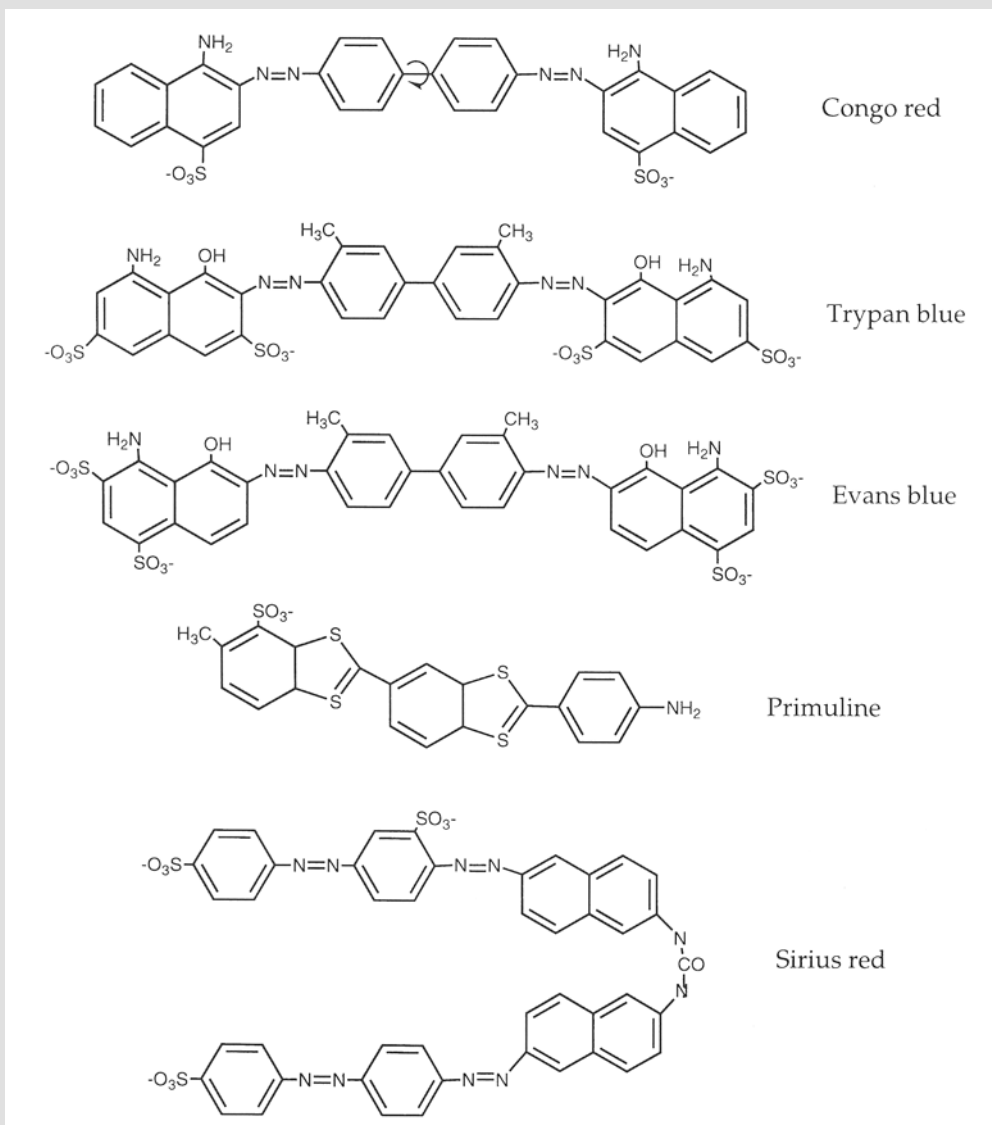


**Fig. 1.** Chemical structures of Congo Red and four related compounds used in the present studies. Trypan Blue and Evans Blue are chemical analogs of Congo Red. Primuline and Sirius Red F3B are less closely related structurally, but nevertheless share the ability to stain amyloid. The precise chemical structure of Thioflavin-S is not known, but it is derived from primuline by methylation and sulfation

Scrapie-infected neuroblastoma cells were described elsewhere [16]. The drugs were added to freshly passaged cells. Cells were cultured several days to confluence and were then lysed by addition into 500  $\mu$ l of lysis buffer (0.5% Triton X-100, 0.5% sodium deoxycholate, 50 mM Tris pH 7.2). Samples were then digested with 20  $\mu$ g/ml of proteinase-K (PK) for 30 min at 37  $^{\circ}$ C. Digestion was stopped on ice by 0.1 mM of Pefabloc (Boehringer Mannheim). Samples were centrifuged at 100,000 rpm for 1 h in a TL-100 Beckman centrifuge. Pellets containing PrP<sup>res</sup> were dissolved in 10  $\mu$ l of

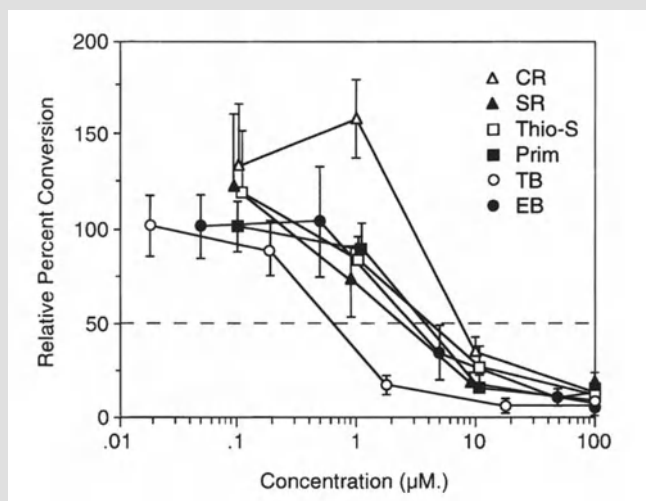


**Fig. 2.** Dose response curves of six compounds for the inhibition of generation of PrP<sup>res</sup> in the cell-free conversion system using hamster PrP<sup>sen</sup> and PrP<sup>res</sup> from scrapie-infected hamster brain. The details are described in the methods section. Results are expressed as the percentage of conversion to PrP<sup>res</sup> relative to control reactions without added drugs

SDS-PAGE loading buffer containing 8 M urea and boiled 5 min before analysis by western-blotting as previously described [3].

In order to search for more effective inhibitors of the formation of protease-resistant PrP five compounds related to Congo Red were tested for ability to inhibit the cell-free conversion of hamster PrP<sup>sen</sup> to PrP<sup>res</sup>. Figure 2 shows a compilation of results from 5 to 8 independent experiments. Dose response curves indicated that Trypan Blue was the most effective inhibitor with an average IC<sub>50</sub> of 0.7 µM (Fig. 2). This was followed by Sirius Red, Thioflavin-S, Primuline, and Evans Blue, which ranged from 2.2 to 4.3 µM. Congo Red was slightly less potent with an IC<sub>50</sub> of 7.5 µM. As has been noted previously [7], at low concentrations CR appeared to enhance the generation of PrP<sup>res</sup>, giving 130–150% relative conversion at 0.1 and 1.0 µM. However, no similar enhancement was produced by any of the other five compounds tested.

These results indicated that several analogs of CR appeared to be more potent than CR itself for the inhibition of the cell-free conversion reaction. As seen in Fig. 1 the ring structures of CR, TB and EB are identical, and the main differences are the presence of two additional sulfonate groups and two hydroxyl groups on the naphthlene rings of TB and EB. These changes appear to have a significant influence on the inhibition of CFC. For primuline, Thioflavin-S and Sirius Red the structures are quite different from CR itself, and therefore it is difficult to draw conclusions as to how or why these compounds might function as inhibitors in these tests.

Because of the effective inhibition of formation of PrP<sup>res</sup> in cell-free conversion reactions, these new compounds were also tested in scrapie-

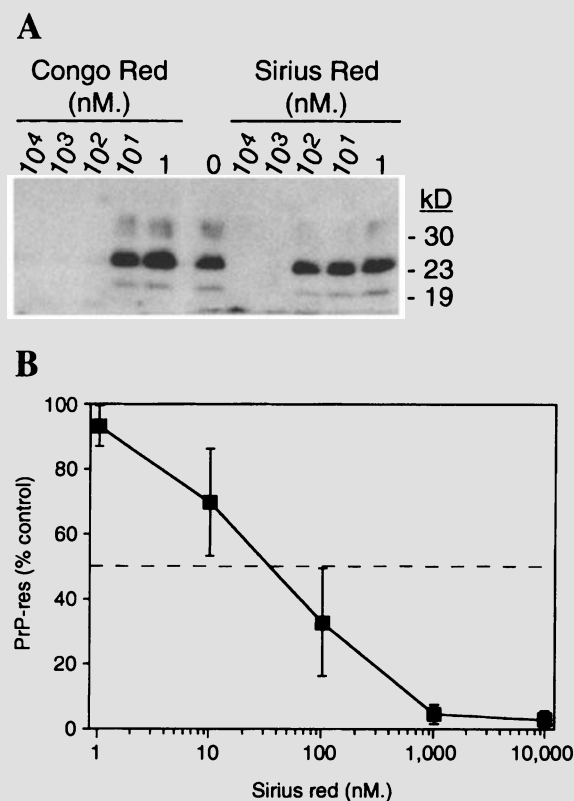


**Fig. 3.** Inhibition of generation of PrP<sup>res</sup> in scrapie-infected mouse neuroblastoma cells by Congo Red and Sirius Red F3B. **A** Western blot analysis of PrP<sup>res</sup> from cultures incubated with or without Congo Red or Sirius Red. Lane labeled 0 has extract from culture with no drugs added. **B** Results for Sirius Red are plotted as the percentage of PrP<sup>res</sup> generated relative to cultures without drugs

infected mouse neuroblastoma cells. Trypan Blue, Evans Blue, Thioflavin-S and Primuline were not as effective as in the cell-free conversion system, having IC<sub>50</sub>'s of greater than 1  $\mu$ M (data not shown). In contrast, Sirius Red was a good inhibitor in this system with an IC<sub>50</sub> of 32 nM (Fig. 3A and 3B), which was similar to the value obtained for Congo Red in control experiments done using these same cells at this same time (Fig. 3A).

Based on the results in these experiments SR appears to merit further testing in some in vivo TSE disease models. Although CR itself has not been very effective in vivo [10], it is possible that SR might show some improvement over CR in certain situations. For example the host and or the TSE strain are both known to be variables which can influence the effectiveness of potential anti-TSE drugs.

The reason for the poor inhibition by TB and EB in the cellular system is not known. However, it is not surprising that there might be discrepancies in the inhibition of PrP<sup>res</sup> formation in the cell-free and the scrapie-infected cell assays because in the cell assays the presence or lack of

interactions of the drugs with cellular molecules or serum proteins in the media such as albumin, might profoundly influence the results. In any case, it is conceivable that suitable chemical modification or alternative routes or delivery, such as via liposomes, might alter the effectiveness of these drugs. Therefore, demonstration of inhibitory potential in any of the available assays for generation of PrP<sup>res</sup> should probably not be ignored in considering the possibilities for development of new drugs in this complex field.

### References

1. Caughey B, Chesebro B (1997) Prion protein and the transmissible spongiform encephalopathies. *Trends Cell Biol* 7: 56–62
2. Caughey B, Race RE (1992) Potent inhibition of scrapie-associated PrP accumulation by Congo red. *J Neurochem* 59: 768–771
3. Caughey B, Raymond GJ (1993) Sulfated polyanion inhibition of scrapie-associated PrP accumulation in cultured cells. *J Virol* 67: 643–650
4. Caughey WS, Raymond LD, Horiuchi M, Caughey B (1998) Inhibition of protease-resistant prion protein formation by porphyrins and phthalocyanines. *Proc Natl Acad Sci USA* 95: 12117–12122
5. Chesebro B (1999) Prion protein and the transmissible spongiform encephalopathy diseases. *Neuron* 24: 503–506
6. Demaimay R, Adjou K, Lasmezas C, Lazarini F, Cherifi K, Seman M, Deslys JP, Dormont D (1994) Pharmacological studies of a new derivative of amphotericin B, MS-8209, in mouse and hamster scrapie. *J Gen Virol* 75: 2499–2503
7. Demaimay R, Harper J, Gordon H, Weaver D, Chesebro B, Caughey B (1998) Structural aspects of Congo red as an inhibitor of protease-resistant prion protein formation. *J Neurochem* 71: 2534–2541
8. Ehlers B, Diringer H (1984) Dextran sulphate 500 delays and prevents mouse scrapie by impairment of agent replication in spleen. *J Gen Virol* 65: 1325–1330
9. Horiuchi M, Caughey B (1999) Prion protein interconversions and the transmissible spongiform encephalopathies. *Structure Fold Des* 7: R231–R240
10. Ingrosso L, Ladogana A, Pocchiari M (1995) Congo red prolongs the incubation period in scrapie-infected hamsters. *J Virol* 69: 506–508
11. Kimberlin RH, Walker CA (1986) Suppression of scrapie infection in mice by heteropolyanion 23, dextran sulfate, and some other polyanions. *Antimicrob Agents Chemother* 3: 409–413
12. Kocisko DA, Come JH, Priola SA, Chesebro B, Raymond GJ, Lansbury PT, Caughey B (1994) Cell-free formation of protease-resistant prion protein. *Nature* 370: 471–474
13. Ladogana A, Casaccia P, Ingrosso L, Cibati M, Salvatore M, Xi YG, Masullo C, Pocchiari M (1992) Sulphate polyanions prolong the incubation period of scrapie-infected hamsters. *J Gen Virol* 73: 661–665
14. Pocchiari M, Schmittinger S, Masullo C (1987) Amphotericin B delays the incubation period of scrapie in intracerebrally inoculated hamsters. *J Gen Virol* 68: 219–223
15. Priola SA, Caughey B, Caughey WS (1999) Novel therapeutic uses for porphyrins and phthalocyanines in the transmissible spongiform encephalopathies. *Curr Opin Microbiol* 2: 563–566

16. Race RE, Fadness LH, Chesebro B (1987) Characterization of scrapie infection in mouse neuroblastoma cells. *J Gen Virol* 68: 1391–1399
17. Supattapone S, Nguyen HO, Cohen FE, Prusiner SB, Scott MR (1999) Elimination of prions by branched polyamines and implications for therapeutics. *Proc Natl Acad Sci USA* 96: 14529–14534
18. Tagliavini F, McArthur RA, Canciani B, Giaccone G, Porro M, Bugiani M, Lievens PM, Bugiani O, Peri E, Dall'Ara P, Rocchi M, Poli G, Forloni G, Bandiera T, Varasi M, Suarato A, Cassutti P, Cervini MA, Lansen J, Salmona M, Post C (1997) Effectiveness of anthracycline against experimental prion disease in Syrian hamsters. *Science* 276: 1119–1122
19. Weissmann C (1999) Molecular genetics of transmissible spongiform encephalopathies. *J Biol Chem* 274: 3–6
20. Xi YG, Ingrosso L, Ladogana A, Masullo C, Pocchiari M (1992) Amphotericin B treatment dissociates in vivo replication of the scrapie agent from PrP accumulation. *Nature* 356: 598–60

Authors' address: Dr. B. Chesebro, Laboratory of Persistent Viral Diseases, RML, NIAID, NIH, 903 South 4th Street, Hamilton, MT 59840, U.S.A.

# The use of monoclonal antibody epitopes for tagging PrP in conversion experiments

I. Vorberg\*, E. Pfaff, and M. H. Groschup

Federal Research Center for Virus Diseases of Animals, Tübingen, Germany

**Summary.** The key event in the pathogenesis of spongiform encephalopathies is a conformational transition of a normal cellular protein, PrP<sup>sen</sup>, to its pathological isoform, PrP<sup>res</sup>. The mechanism of PrP<sup>res</sup> formation is unknown but is likely to involve a direct interaction between PrP<sup>sen</sup> and PrP<sup>res</sup>. The molecular basis of PrP<sup>res</sup> formation has been studied extensively using transgenic mice and scrapie-infected tissue cultures that express heterologous PrP molecules. However, these experiments are dependant on the discrimination of endogenous host PrP and exogenous PrP molecules. Here we give a short review on the PrP-specific epitopes that have been used for tagging exogenous PrP molecules and present a novel PrP-specific epitope that is well suitable for in vivo and in vitro conversion experiments.

## Introduction

Transmissible spongiform encephalopathies (TSE) like Creutzfeldt–Jakob disease in humans and scrapie in sheep and goats are degenerative neurological diseases. In TSE-infected animals, a normal, proteinase K-sensitive host-encoded protein, PrP<sup>sen</sup>, is converted to an abnormal, proteinase K-resistant isoform, PrP<sup>res</sup>, that accumulates in the lymphoid tissues and central nervous system [3, 7]. PrP<sup>res</sup> plays a central role in TSE pathogenesis and is the only known component of TSE infectivity, but the exact nature of the agent is controversial [14, 21]. The conversion of PrP<sup>sen</sup> to PrP<sup>res</sup> is likely to involve a conformational change of PrP<sup>sen</sup> from a predominantly  $\alpha$ -helical form [16] to a structure with a high  $\beta$ -sheet content [4, 11, 18]. PrP<sup>res</sup> is believed to serve as a template for the formation of new PrP<sup>res</sup> via interactions with PrP<sup>sen</sup> [8, 15, 19]. The molecular basis of PrP<sup>res</sup> formation

\*Present Address: Laboratory of Persistent Viral Diseases, NIAID, National Institutes of Health, Rocky Mountain Laboratories, Hamilton, Montana, U.S.A.

has been studied extensively in transgenic mice or scrapie-infected murine tissue cultures that express exogenous PrP molecules as well as by cell-free conversion experiments. These experiments have greatly been facilitated by the availability of antibodies that recognize PrP in a species-specific manner. The insertion of the binding sites of these antibodies into recombinant PrP allows the discrimination of exogenous PrP molecules from endogenous PrP molecules. Here we give a short overview of the commonly used monoclonal antibody epitope tags and present a novel epitope for the discrimination of endogenous and exogenous PrP molecules.

### Expression of PrP molecules with specific epitopes can influence the formation of PrP<sup>res</sup>

The expression of exogenous PrP molecules has usually been assayed by tagging the recombinant PrP molecules with the epitope for the monoclonal

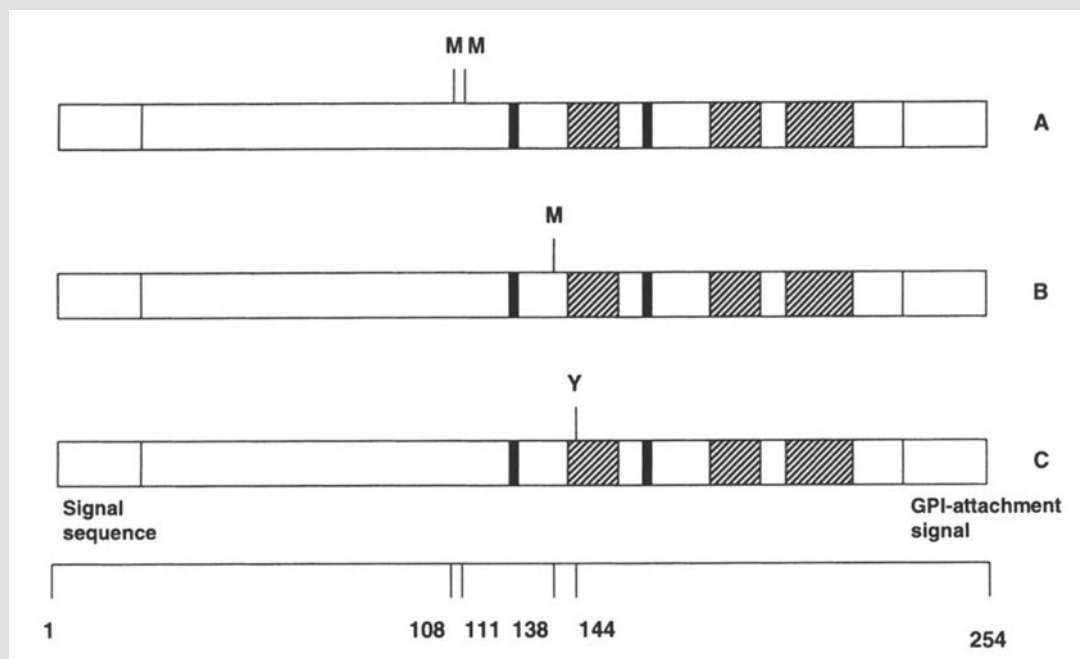


**Fig. 1.** Position of monoclonal antibody epitopes inserted into mouse PrP. The potential secondary structure elements are given. Black bars symbolize  $\beta$ -strands, hatched bars symbolize  $\alpha$ -helices. Amino acid positions are indicated on the bottom line. The 3F4 epitope is located within the N-terminal flexible tail of the PrP molecule. Replacement of Leu (108) and Val (111) with Met introduces the epitope into mouse PrP (A). The binding site for the antibody 13A5 is located within the loop region between the first  $\beta$ -strand and the first  $\alpha$ -helix and is defined by a Met at position 139 in hamster PrP. The epitope can be inserted in mouse PrP by a mutation of residue 138 (Ile to Met) (B). The monoclonal antibody L42 binds to an epitope located in the vicinity of the first  $\alpha$ -helix. The substitution of Tyr for Trp at position 144 inserts the L42 binding site into mouse PrP (C)

antibody 3F4. The antibody has been raised against purified PrP<sup>res</sup> from scrapie-infected hamsters and specifically detects an epitope encompassing residues 106 to 115 within hamster and human PrP [2, 9]. Further studies have demonstrated that the 3F4 epitope can be inserted into mouse PrP by replacing amino acid residues 108 (Leu) and 111 (Val) with Met (Fig. 1A) [17]. Its species-specificity and high affinity to both PrP<sup>sen</sup> and PrP<sup>res</sup> of humans and hamsters as well as its availability have made 3F4 the most common antibody used in the field. However, conversion experiments using scrapie-infected mouse neuroblastoma cells have demonstrated that expression of 3F4 epitope-tagged mouse PrP strongly interferes with the accumulation of endogenous PrP (Fig. 2A) [12]. Interestingly, allelic variation at position 108 in mouse PrP has also been reported to correlate with different scrapie incubation times in inbred mice strains [22].

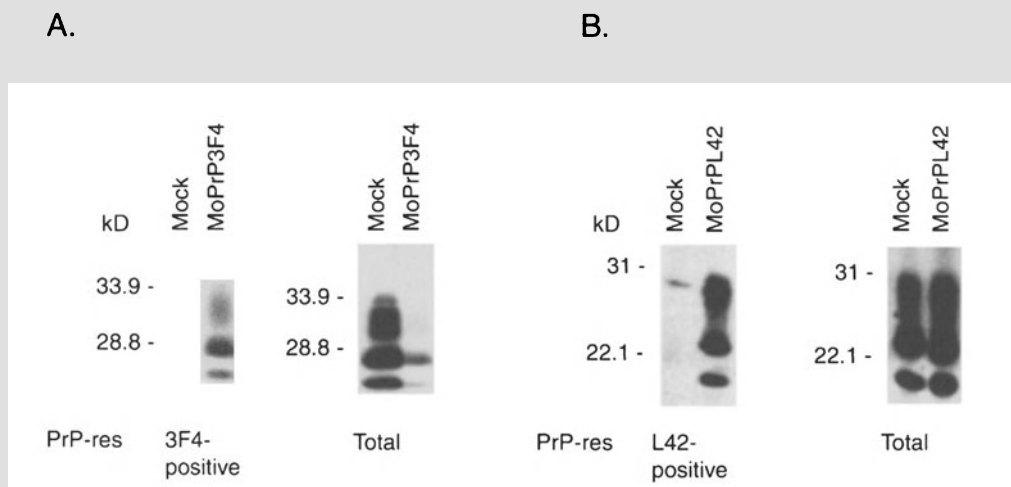


**Fig. 2.** Influence of epitope-tagged PrP molecules on the formation of PrP<sup>res</sup> in scrapie-infected cells. **A** Western blot analysis of proteinase K-treated lysates of normal scrapie-infected cells (Sc<sup>+</sup>-MNB cells) and scrapie-infected cells expressing 3F4 epitope-tagged PrP molecules. While no 3F4-reactive PrP<sup>res</sup> could be detected in normal Sc<sup>+</sup>-MNB cells, 3F4-positive PrP<sup>res</sup> accumulated in Sc<sup>+</sup>-MNB cells expressing the 3F4-epitope-tagged PrP (MoPrP3F4) (left panel). The expression of MoPrP3F4 interfered with the formation of total PrP<sup>res</sup>. This immunoblot was probed with a polyclonal antiserum that detects both mouse PrP and mouse PrP with the 3F4 epitope (right panel). **B** We tested the ability of L42 epitope-tagged mouse PrP<sup>sen</sup> (MoPrPL42) to be converted to PrP<sup>res</sup>. While no L42-reactive PrP<sup>res</sup> could be detected in normal Sc<sup>+</sup>-MNB cells, substantial amounts of L42-positive PrP<sup>res</sup> accumulated in cells expressing L42 epitope-tagged mouse PrP (left panel). L42 epitope-tagged mouse PrP did not interfere with the formation of total mouse PrP<sup>res</sup> in Sc<sup>+</sup>-MNB cells. The increase in PrP<sup>res</sup> accumulation in cells expressing L42 epitope-tagged mouse PrP is probably due to a higher PrP expression level in the cells (right panel). This blot was probed with a polyclonal antiserum Ra5/7 [5] that detects both endogenous mouse PrP and exogenous L42 epitope-tagged mouse PrP

Similar observations have been made when mouse PrP with the binding site for the antibody 13A5 was expressed in scrapie-infected tissue cultures [10]. The epitope is defined by a Met at amino acid 139 in the Syrian hamster PrP sequence (corresponding to position 138 in mouse PrP) and is located within the loop region between the first  $\beta$ -strand and the first  $\alpha$ -helix [1]. By the substitution of Met for Ile at residue 138 the 13A5 binding site can be introduced into mouse PrP [17] (Fig. 1B). However, this epitope has proven to be not suitable for tagging foreign PrP molecules in conversion experiments, since earlier studies already demonstrated that the formation of endogenous and exogenous PrP molecules in scrapie-infected cells is blocked by the expression of mouse PrP with Met at position 138, indicating that this amino acid is critical in the species barrier between hamster and mice [13].

#### **A novel epitope for the discrimination of endogenous and exogenous PrP molecules**

We have recently reported on the generation of a monoclonal antibody that has been raised by immunization with a synthetic peptide spanning amino acid residues 145 to 163 of the sheep PrP sequence [6]. Mapping of the specific epitope revealed that the antibody L42 binds to an epitope that includes a Tyr at position 148 of sheep PrP [20]. The L42 binding site is present in PrP molecules from a wide variety of species including sheep, cows, goats, pigs, dogs, cats, minks, humans, guinea pigs and rabbits. However, the epitope is not present in the PrP sequence of mice and hamster, two commonly used experimental model systems in scrapie research. Therefore, for experiments in scrapie-infected mouse neuroblastoma cells or for studies with transgenic mice, detection of PrP molecules of these species does not require additional tags. The L42 binding site could also be inserted into mouse PrP by a single amino acid mutation from Trp to Tyr at position 144 (which correlates to position 148 in sheep PrP) (Fig. 1C). Recombinant mouse PrP with a L42 epitope tag could thus be used in Sc<sup>+</sup>-MNB cells to distinguish recombinant mouse PrP from endogenous mouse PrP.

When L42 epitope-tagged mouse PrP was expressed in scrapie-infected cells, substantial amounts of L42-reactive PrP<sup>res</sup> could be detected (Fig. 2B, left panel). Furthermore, insertion of the L42 epitope tag into mouse PrP did not interfere with the formation of endogenous PrP<sup>res</sup> (Fig. 2B, right panel). In fact, the level of total PrP<sup>res</sup> increased in cells expressing L42 epitope-tagged PrP molecules when compared with the control. This increase of total PrP<sup>res</sup> is probably due to the increase of PrP<sup>sen</sup> expression. Taken together, the data show that the epitope for the monoclonal antibody L42 is well suited for the discrimination of endogenous and exogenous PrP molecules and could be an invaluable tool for studying PrP<sup>res</sup> formation in transgenic mice, scrapie-infected cells and cell-free conversion studies.

### Acknowledgements

The authors would like to acknowledge S. Priola and B. Chesebro for providing the scrapie-infected cell line Sc<sup>+</sup>-MNB and the retroviral expression system used in this study. This work was supported by the EU Commission.

### References

1. Barry RA, Prusiner SB (1986) Monoclonal antibodies to the cellular and scrapie prion proteins. *J Infect Dis* 154: 518–521
2. Bolton DC, Seligman SJ, Bablanian G, Windsor D, Scala LJ, Kim KS, Chen C-MJ, Kascsak RJ, Bendheim PE (1991) Molecular location of a species-specific epitope on the hamster scrapie agent protein. *J Virol* 65: 3667–3675
3. Caughey B, Raymond GJ (1991) The scrapie-associated form of PrP is made from a cell surface precursor that is both protease- and phospholipase-sensitive. *J Biol Chem* 266: 18217–18223
4. Caughey BW, Dong A, Bhat KS, Ernst D, Hayes SF, Caughey WS (1991) Secondary structure analysis of the scrapie-associated protein PrP 27–30 in water by infrared spectroscopy. *Biochemistry* 30: 7672–7680
5. Groschup MH, Harmeyer S, Pfaff E (1997) Antigenic features of prion proteins of sheep and other mammalian species. *J Immunol Methods* 207: 89–101
6. Harmeyer S, Pfaff E, Groschup MH (1998) Synthetic peptide vaccines yield monoclonal antibodies to cellular or pathological prion proteins of ruminants. *J Gen Virol* 79: 937–945
7. Hope J, Morton LJ, Farquhar CF, Multhaup G, Beyreuther K, Kimberlin RH (1986) The major polypeptide of scrapie-associated fibrils (SAF) has the same size, charge distribution and N-terminal protein sequence as predicted for the normal brain protein (PrP). *EMBO J* 5: 2591–2597
8. Horiuchi M, Caughey B (1999) Specific binding of normal prion protein to the scrapie form via a localized domain initiates its conversion to the protease-resistant state. *EMBO J* 18: 3193–3203
9. Kascsak RJ, Rubenstein R, Merz PA, Tonna-DeMasi M, Fersko R, Carp RI, Wisniewski HM, Diringier H (1987) Mouse polyclonal and monoclonal antibody to scrapie-associated fibril proteins. *J Virol* 61: 3688–3693
10. Muramoto T, Scott M, Cohen FE, Prusiner SB (1996) Recombinant scrapie-like prion protein of 106 amino acids is soluble. *Proc Natl Acad Sci USA* 93: 15457–15462
11. Pan K-M, Baldwin M, Nguyen J, Gasset M, Serban A, Groth D, Mehlhorn I, Huang Z, Fletterick R, Cohen FE, Prusiner SB (1993) Conversion of  $\alpha$ -helices into  $\beta$ -sheets features in the formation of the scrapie prion proteins. *Proc Natl Acad Sci USA* 90: 10962–10966
12. Priola SA, Caughey B, Race RE, Chesebro B (1994) Heterologous PrP molecules interfere with accumulation of protease-resistant PrP in scrapie-infected murine neuroblastoma cells. *J Virol* 68: 4873–4878
13. Priola SA, Chesebro B (1995) A single hamster PrP amino acid blocks conversion to protease-resistant PrP in scrapie-infected mouse neuroblastoma cells. *J Virol* 69: 7754–7758
14. Prusiner SB (1991) Molecular biology of prion diseases. *Science* 252: 1515–1522
15. Prusiner SB, Scott M, Foster D, Pan K-M, Groth D, Mirinda C, Torchia M, Yang S-L, Serban D, Carlson G-A, Hoppe P, Westaway D, DeArmond SJ (1990)

- Transgenic studies implicate interactions between homologous PrP isoforms in scrapie prion replication. *Cell* 63: 673–686
16. Riek R, Hornemann S, Wider G, Billeter M, Glockshuber R, Wuthrich K (1996) NMR structure of the mouse prion protein domain PrP (121–231). *Nature* 382: 180–182
  17. Rogers M, Serban D, Gyuris T, Scott M, Torchia T, Prusiner SB (1991) Epitope mapping of the Syrian hamster prion protein utilizing chimeric and mutant genes in a vaccinia virus expression system. *J Immunol* 147: 3568–3574
  18. Safar J, Roller PP, Gajdusek DC, Gibbs CJ Jr (1993) Conformational transitions, dissociation, and unfolding of scrapie amyloid (prion) protein. *J Biol Chem* 268: 20276–20284
  19. Telling GC, Scott M, Mastrianni J, Gabizon R, Torchia M, Cohen FE, DeArmond SJ, Prusiner SB (1995) Prion propagation in mice expressing human and chimeric PrP transgenes implicates the interaction of cellular PrP with another protein. *Cell* 83: 79–90
  20. Vorberg I, Buschmann A, Harmeyer S, Saalmuller A, Pfaff E, Groschup MH (1999) A novel epitope for the specific detection of exogenous prion proteins in transgenic mice and transfected murine cell lines. *Virology* 255: 26–31
  21. Weissmann C (1996) The ninth Datta lecture. Molecular biology of transmissible spongiform encephalopathies. *FEBS Lett* 389: 3–11
  22. Westaway D, Goodman PA, Mirenda CA, McKinley MP, Carlson GA, Prusiner SB (1987) Distinct prion proteins in short and long scrapie incubation period in mice. *Cell* 51: 651–662

Authors' address: Dr. M.H. Groschup, Institute of Immunology, Federal Research Centre for Virus Diseases of Animals, Paul-Ehrlich-Str. 28, 72076 Tübingen, Germany.

**SpringerLifeSciences**

**Anne A. Gershon,  
Charles Calisher,  
Ann M. Arvin (eds.)**

## **Immunity to and Prevention of Herpes Zoster**

2000. Approx. 240 pages

Hardcover DM 248,-, öS 1736,-

(recommended retail price)

Special edition of "Archives of Virology, Supplement 17"

(Softcover edition of Suppl. 17 only available

for subscribers to "Archives of Virology")

ISBN 3-211-83556-3

Varicella-zoster virus (VZV) causes both chickenpox and zoster. Fundamental to their prevention is an understanding of the natural history of VZV infection. This is a compilation of papers presented in March 1999 in Osaka, Japan, by internationally renowned researchers studying varicella-zoster virus and a vaccine used to prevent disease caused by this virus.

The aim of the meeting was to explore progress made in basic and molecular biology of VZV and current understanding of latent infection and reactivation. Data concerning immune responses to VZV, mechanisms by which virus latency are controlled, and the latest information on vaccination to prevent varicella and zoster are presented and discussed.

Please visit our website: [www.springer.at](http://www.springer.at)



**SpringerWienNewYork**

A-1201 Wien, Sachsenplatz 4-6, P.O. Box 89, Fax +43.1.330 24 26, e-mail: [books@springer.at](mailto:books@springer.at), Internet: [www.springer.at](http://www.springer.at)  
D-69126 Heidelberg, Haberstraße 7, Fax +49.6221.345-229, e-mail: [orders@springer.de](mailto:orders@springer.de)  
USA, Secaucus, NJ 07096-2485, P.O. Box 2485, Fax +1.201.348-4505, e-mail: [orders@springer-ny.com](mailto:orders@springer-ny.com)  
Eastern Book Service, Japan, Tokyo 113, 3-13, Hongo 3-chome, Bunkyo-ku, Fax +81.3.38 18 08 64, e-mail: [orders@svt-eps.co.jp](mailto:orders@svt-eps.co.jp)

**SpringerLifeSciences**

**Philip S. Mellor,  
Matthew Baylis,  
Christopher Hamblin,  
Charles H. Calisher,  
Peter P. C. Mertens (eds.)**

## **African Horse Sickness**

1998. VIII, 342 pages. 86 partly coloured figures.

Hardcover DM 290,-, öS 2030,-

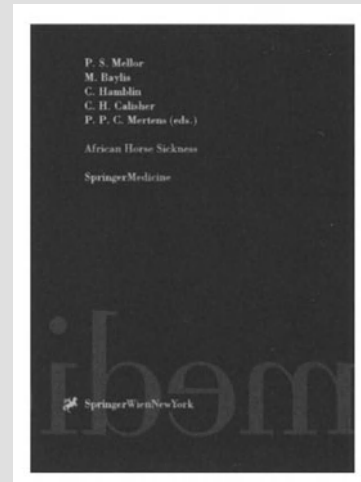
(recommended retail price)

Special edition of "Archives of Virology, Supplement 14"

(Softcover edition of Suppl. 14 only available

for subscribers to "Archives of Virology")

ISBN 3-211-83133-9



African horse sickness virus is a double-stranded RNA virus which causes a non-contagious, infectious arthropod-borne disease of equines and occasionally dogs. Nine distinct, internationally recognised serotypes of the virus have so far been identified. This book is based upon the findings of two programmes funded by the European Commission. It will be of value not only to the specialist research workers but also to veterinary workers dealing with control and to legislators seeking to promote safe international movement of equines. The topics covered include state-of-the-art discussions on diagnostics, vaccines, molecular biology, vector studies, and epidemiology.

"... This splendid and highly entertaining book gives a comprehensive account of the result obtained from those studies. Its contents are organised along disciplinary lines and are divided into sections dealing with epidemiology, entomology, molecular biology, vaccines and diagnosis ..."

The Veterinary Record

Please visit our website: [www.springer.at](http://www.springer.at)

 **SpringerWienNewYork**

A-1201 Wien, Sachsenplatz 4-6, P.O.Box 89, Fax +43.1.330 24 26, e-mail: [books@springer.at](mailto:books@springer.at), Internet: [www.springer.at](http://www.springer.at)  
D-69126 Heidelberg, Haberstraße 7, Fax +49.6221.345-229, e-mail: [orders@springer.de](mailto:orders@springer.de)  
USA, Secaucus, NJ 07096-2485, P.O. Box 2485, Fax +1.201.348-4505, e-mail: [orders@springer-ny.com](mailto:orders@springer-ny.com)  
Eastern Book Service, Japan, Tokyo 113, 3-13, Hongo 3-chome, Bunkyo-ku, Fax +81.3.38 18 08 64, e-mail: [orders@svt-eps.co.jp](mailto:orders@svt-eps.co.jp)

**SpringerLifeSciences**

**Charles H. Calisher,  
M. C. Horzinek (eds.)**

## **100 Years of Virology**

The Birth and Growth of a Discipline

1999. VII, 220 pages. 75 figures.

Hardcover DM 248,-, öS 1736,-

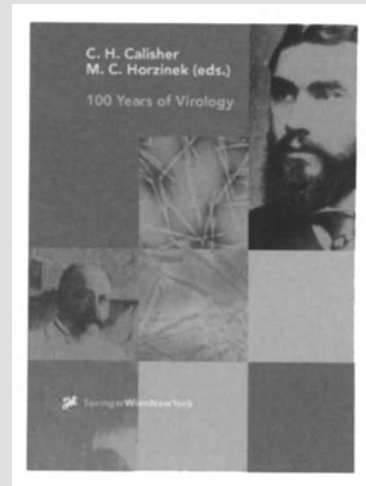
(recommended retail price)

Special edition of "Archives of Virology, Supplement 15"

(Softcover edition of Suppl. 15 only available

for subscribers to "Archives of Virology")

ISBN 3-211-83384-6



One hundred years ago, when Martinus W. Beijerinck in Delft and Friedrich Loeffler on Riems Island discovered a new class of infectious agents in plants and animals, a new discipline was born.

This book, a compilation of papers written by well-recognized scientists, gives an impression of the early days, the pioneer period and the current state of virology. Recent developments and future perspectives of this discipline are sketched against a historic background.

With contributions by A. Alcamì, D. Baulcombe, F. Brown, L. W. Enquist, H. Feldmann, A. Garcia-Sastre, D. Griffiths, M. C. Horzinek, A. van Kammen, H.-D. Klenk, F. A. Murphy, T. Muster, R. O'Neill, P. Palese, C. Patience, R. Rott, H.-P. Schmiedebach, S. Schneider-Schaulies, G. L. Smith, J. A. Symons, Y. Takeuchi, V. ter Meulen, P. J. W. Venables, V. E. Volchkov, V. A. Volchkova, R. A. Weiss, W. Wittmann, H. Zheng

Please visit our website: [www.springer.at](http://www.springer.at)



**SpringerWienNewYork**

A-1201 Wien, Sachsenplatz 4-6, P.O.Box 89, Fax +43.1.330 24 26, e-mail: [books@springer.at](mailto:books@springer.at), Internet: [www.springer.at](http://www.springer.at)

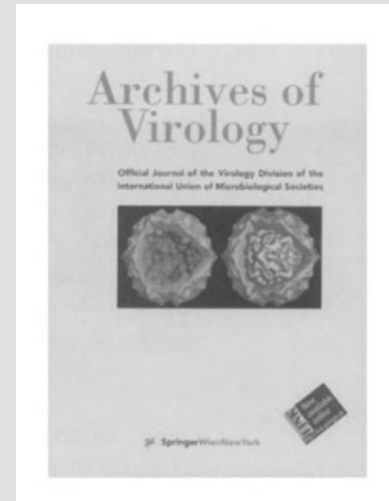
D-69126 Heidelberg, Haberstraße 7, Fax +49.6221.345-229, e-mail: [orders@springer.de](mailto:orders@springer.de)

USA, Secaucus, NJ 07096-2485, P.O. Box 2485, Fax +1.201.348-4505, e-mail: [orders@springer-ny.com](mailto:orders@springer-ny.com)

Eastern Book Service, Japan, Tokyo 113, 3-13, Hongo 3-chome, Bunkyo-ku, Fax +81.3.38 18 08 64, e-mail: [orders@svt-eps.co.jp](mailto:orders@svt-eps.co.jp)

Official Journal of the Virology Division of the  
International Union of Microbiological Societies

**Editor-in-Chief:** M. H. V. Van Regenmortel, Strasbourg  
**Editorial Board:** L. Enjuanes, Madrid  
T. Folks, Atlanta, GA  
T. K. Frey, Atlanta, GA  
I. H. Holmes, Parkville  
R. A. Killington, Leeds  
H.-D. Klenk, Marburg  
E. P. Rybicki, Rondebosch  
E. G. Strauss, Pasadena, CA  
M. Tashiro, Tokyo  
A. Vaheri, Helsinki  
**Virology Division:** M. A. Mayo, Dundee  
**Special Issues Editors:** C. H. Calisher, Fort Collins, CO  
G. Siegl, St. Gallen



**Archives of Virology** publishes original contributions from all branches of research on viruses, virus-like agents, and virus infections of humans, animals, plants, insects, and bacteria. Coverage includes the broadest spectrum of topics, from initial descriptions of newly discovered viruses, to studies of virus structure, composition, and genetics, to studies of virus interactions with host cells, host organisms, and host populations.

Multidisciplinary studies are particularly welcome, as are studies employing molecular biologic, molecular genetics, and modern immunologic and epidemiologic approaches. For example, studies on the molecular pathogenesis, pathophysiology, and genetics of virus infections in individual hosts, and studies on the molecular epidemiology of virus infections in populations, are encouraged. Studies involving applied research, such as diagnostic technology development, monoclonal antibody panel development, vaccine development, and antiviral drug development, are also encouraged. However, such studies are often better presented in the context of a specific application or as they bear upon general principles of interest to many virologists. In all cases, it is the quality of the research work, its significance, and its originality which will decide acceptability.

**Subscription Information**

2001. Vol. 146 (12 issues). Title No. 705  
ISSN 0304-8608 (print), ISSN 1432-8798 (electronic)  
DM 3910.–, ATS 27493.– plus carriage charges  
approx. US \$ 2,369.00 including carriage charges

This journal is included in the program:  
"LINK – Springer Print Journals Go Electronic"  
ISSN (electronic edition): 1432-8798

View table of contents and abstracts online at:  
[www.springer.at/archvirol](http://www.springer.at/archvirol)



**SpringerWienNewYork**

A-1201 Wien, Sachsenplatz 4–6, P.O.Box 89, Fax +43.1.330 24 26-62, e-mail: [journals@springer.at](mailto:journals@springer.at), Internet: [www.springer.at](http://www.springer.at)  
D-69126 Heidelberg, Haberstraße 7, Fax +49.6221.345-229, e-mail: [orders@springer.de](mailto:orders@springer.de)  
USA, Secaucus, NJ 07096-2485, P.O. Box 2485, Fax +1.201.348-4505, e-mail: [orders@springer-ny.com](mailto:orders@springer-ny.com)  
Eastern Book Service, Japan, Tokyo 113, 3–13, Hongo 3-chome, Bunkyo-ku, Fax +81.3.38 18 08 64, e-mail: [orders@svt-eps.co.jp](mailto:orders@svt-eps.co.jp)